UNIVERSITAT ROVIRA I VIRGILI
ORGANIC MOLECULES ON METAL SURFACES: FORECASTING STRUCTURES AND SPECTRA
Benjamí Martorell Masip
ISBN:978-84-691-9747-9 /DL: T-1259-2008

Organic molecules on metal surfaces: Forecasting structures and spectra.

Benjamí Martorell Masip

25th March 2008

UNIVERSITAT ROVIRA I VIRGILI
ORGANIC MOLECULES ON METAL SURFACES: FORECASTING STRUCTURES AND SPECTRA
Benjamí Martorell Masip
ISBN:978-84-691-9747-9 /DL: T-1259-2008

LA RELÍQUIA.

L'UNIVERS VIBRATORI.

"La vibració de l'univers és la que dota de massa a la matèria, és la que li dóna consistència a l'univers esmentat. De la mateixa manera que podem convertir la matèria en energia, si fem vibrar l'energia en la forma adequada, podem crear les partícules que desitgem. L'univers és com un immens estany, un estany sobre el qual cau una fina pluja i els plegaments de l'aigua, les ones són el que percibim com a matèria; però una observació més detallada també ens mostra que tot l'estany és format per la mateixa matèria, encara que en algunes zones no hi hagi ondulacions, segueix éssent part de l'estany."

Francisco Angulo Lafuente

UNIVERSITAT ROVIRA I VIRGILI
ORGANIC MOLECULES ON METAL SURFACES: FORECASTING STRUCTURES AND SPECTRA
Benjamí Martorell Masip
ISBN:978-84-691-9747-9 /DL: T-1259-2008

Contents

UNIVERSITAT ROVIRA I VIRGILI
ORGANIC MOLECULES ON METAL SURFACES: FORECASTING STRUCTURES AND SPECTRA
Benjamí Martorell Masip
ISBN:978-84-691-9747-9 /DL: T-1259-2008

UNIVERSITAT ROVIRA I VIRGILI
ORGANIC MOLECULES ON METAL SURFACES: FORECASTING STRUCTURES AND SPECTRA
Benjamí Martorell Masip
ISBN:978-84-691-9747-9 /DL: T-1259-2008

UNIVERSITAT ROVIRA I VIRGILI
ORGANIC MOLECULES ON METAL SURFACES: FORECASTING STRUCTURES AND SPECTRA
Benjamí Martorell Masip
ISBN:978-84-691-9747-9 /DL: T-1259-2008

UNIVERSITAT ROVIRA I VIRGILI
ORGANIC MOLECULES ON METAL SURFACES: FORECASTING STRUCTURES AND SPECTRA
Benjamí Martorell Masip
ISBN:978-84-691-9747-9 /DL: T-1259-2008

UNIVERSITAT ROVIRA I VIRGILI
ORGANIC MOLECULES ON METAL SURFACES: FORECASTING STRUCTURES AND SPECTRA
Benjamí Martorell Masip
ISBN:978-84-691-9747-9 /DL: T-1259-2008

ACRONYMS

BE: Binding energy.

BP: Becke-Perdew.

CASSCF: Complete active space self-consistent field.

CG: Conjugated gradient.

DFT: Density functional theory.

(P)DOS: (Projected) Density of states.

E_{ads}: Adsorption energy.

ECP: Electronic core potential.

GED: Gas electron diffraction.

GGA: Generalised gradient approximation.

(U)HF: (Unrestricted) Hartree-Fock.

IP: Ionization potential.

IR: Infrared.

KS: Kohn-Sham.

L(S)DA: Local (spin) density approximation.

LEED: Low-energy elecron diffraction.

LYP: Lee-Yang-Parr.

MCSCF: Multi-configurational self-consistent field.

UNIVERSITAT ROVIRA I VIRGILI
ORGANIC MOLECULES ON METAL SURFACES: FORECASTING STRUCTURES AND SPECTRA
Benjamí Martorell Masip
ISBN:978-84-691-9747-9 /DL: T-1259-2008

MD: Molecular dynamics.

MM: Molecular mechanics.

MO: Molecular orbital.

MP2: Second order Moller-Plesset.

NEB: Nudged elastic band.

NEXAFS: Near edge x-ray absorption fine structure.

OMM: Organic molecular materials.

PAW: Projector augmented wave.

(R)PBE: (Revised) Perdew-Burke-Enzerhof.

Pr: Propyne ($HC{\equiv}CCH_3$).

Pr-d1: $DC{\equiv}CCH_3$ specie.

Pr-d3: $HC{\equiv}CCD_3$ specie.

Pr-d4: $DC{\equiv}CCD_3$ specie.

PW: Perdew-Wang.

QC: Quantum chemistry.

RAIR(S): Reflection-absorption infrared (spectroscopy).

RMM: Residual minimisation scheme.

SCF: Self-consistent field.

STM: Scanning tunneling microscope.

StoBe: Stockholm-Berlin.

T_c: Critical temperature.

TP: Slater's transition potential.

TS(T): Transition state (theory).

TSF(-d4): Tetraselenafulvalene (fully deuterated).

UNIVERSITAT ROVIRA I VIRGILI
ORGANIC MOLECULES ON METAL SURFACES: FORECASTING STRUCTURES AND SPECTRA
Benjamí Martorell Masip
ISBN:978-84-691-9747-9 /DL: T-1259-2008

TTF(-d4): Tetrathiafulvalene (fully deuterated).

TZVP: Triple-zeta valence plus polarization.

UHV: Ultra high vacuum.

US: Ultra-soft.

VASP: Vienna ab-initio simulation package.

VC: $CHCHCH_2$ specie.

VC-d1: $CDCHCH_2$ specie.

VC-d3: $CHCDCD_2$ specie.

VC-d4: $CDCDCD_2$ specie.

VNM: Vibrational normal mode.

VWN: Vosko-Wilk-Nusair.

XAS: X-ray absorption spectroscopy.

ZPE: Zero point energy.

UNIVERSITAT ROVIRA I VIRGILI
ORGANIC MOLECULES ON METAL SURFACES: FORECASTING STRUCTURES AND SPECTRA
Benjamí Martorell Masip
ISBN:978-84-691-9747-9 /DL: T-1259-2008

List of Figures

UNIVERSITAT ROVIRA I VIRGILI
ORGANIC MOLECULES ON METAL SURFACES: FORECASTING STRUCTURES AND SPECTRA
Benjamí Martorell Masip
ISBN:978-84-691-9747-9 /DL: T-1259-2008

UNIVERSITAT ROVIRA I VIRGILI
ORGANIC MOLECULES ON METAL SURFACES: FORECASTING STRUCTURES AND SPECTRA
Benjamí Martorell Masip
ISBN:978-84-691-9747-9 /DL: T-1259-2008

UNIVERSITAT ROVIRA I VIRGILI
ORGANIC MOLECULES ON METAL SURFACES: FORECASTING STRUCTURES AND SPECTRA
Benjamí Martorell Masip
ISBN:978-84-691-9747-9 /DL: T-1259-2008

UNIVERSITAT ROVIRA I VIRGILI
ORGANIC MOLECULES ON METAL SURFACES: FORECASTING STRUCTURES AND SPECTRA
Benjamí Martorell Masip
ISBN:978-84-691-9747-9 /DL: T-1259-2008

UNIVERSITAT ROVIRA I VIRGILI
ORGANIC MOLECULES ON METAL SURFACES: FORECASTING STRUCTURES AND SPECTRA
Benjamí Martorell Masip
ISBN:978-84-691-9747-9 /DL: T-1259-2008

List of Tables

UNIVERSITAT ROVIRA I VIRGILI
ORGANIC MOLECULES ON METAL SURFACES: FORECASTING STRUCTURES AND SPECTRA
Benjamí Martorell Masip
ISBN:978-84-691-9747-9 /DL: T-1259-2008

UNIVERSITAT ROVIRA I VIRGILI
ORGANIC MOLECULES ON METAL SURFACES: FORECASTING STRUCTURES AND SPECTRA
Benjamí Martorell Masip
ISBN:978-84-691-9747-9 /DL: T-1259-2008

UNIVERSITAT ROVIRA I VIRGILI
ORGANIC MOLECULES ON METAL SURFACES: FORECASTING STRUCTURES AND SPECTRA
Benjamí Martorell Masip
ISBN:978-84-691-9747-9 /DL: T-1259-2008

UNIVERSITAT ROVIRA I VIRGILI
ORGANIC MOLECULES ON METAL SURFACES: FORECASTING STRUCTURES AND SPECTRA
Benjamí Martorell Masip
ISBN:978-84-691-9747-9 /DL: T-1259-2008

UNIVERSITAT ROVIRA I VIRGILI
ORGANIC MOLECULES ON METAL SURFACES: FORECASTING STRUCTURES AND SPECTRA
Benjamí Martorell Masip
ISBN:978-84-691-9747-9 /DL: T-1259-2008

Chapter 1

Introduction

In this introductory chapter we want to explain the reasons for the research presented in this thesis. Processes on metal surfaces are of great importance, not only for the industry, but also for the daily life. Therefore, it is interesting to increase the knowledge of the molecular processes on the surfaces: Physisorption, chemisorption, diffusion, isomerisation, oxidation and reduction reactions... all of them are possible steps in the reactions of molecules on metals.

In particular, in this thesis we focus on organic molecules. Structures, vibrational and electronic spectra and the reaction profiles are of great importance to understand how processes take place in the macroscopic world from the microscopic point of view. Computational chemistry can be an important support for the experimental researchers, who normally cannot work at molecular level.

Moreover, in this thesis has not only been tackled the heterogeneous catalysis, which is the most commonly studied surface chemistry, but we also have tackled the study of metallic supports for organic molecular materials (OMM).

UNIVERSITAT ROVIRA I VIRGILI
ORGANIC MOLECULES ON METAL SURFACES: FORECASTING STRUCTURES AND SPECTRA
Benjamí Martorell Masip
ISBN:978-84-691-9747-9 /DL: T-1259-2008

1.1 Importance of the surface science.

Nowadays processes on surfaces are unconsciously used for million of people in the world: in the chemical industry, in the cars, in a simple bike, in your room and in the computer I am using to write this thesis.

Lots of efforts in the research of surface science have made their way towards the heterogeneous catalysis, because of importance in industrial processes. Most important industrial reactions that heterogeneous catalysts carry out are presented in table 1.1. We can see in that table most of the actual chemical products are yielded by heterogeneous catalysts, and without them our society would not have reached the present standard of life. In this table are presented applications we use everyday. For example, all current cars wear catalysts in the exhaust pipe to reduce their polluting emissions. This catalyst is known as the threeway catalyst and it is a mixture of platinum, rhodium and palladium [51].

In spite of being less selective for a concret reaction than the homogeneous catalysts, surfaces are used at industry because of the facility to separate the final products (normally gas or liquid phase) from the catalysts (normally solid phase). One example of this is the Haber-Bosch process, where N_2 and H_2 react to yield NH_3 on iron, or the Fischer-Tropsch reaction, where H_2 and CO react to yield methanol or other hydrocarbons on some metallic oxides.

But surface science is not only heterogeneous catalysis [115]. The world of microtechnolgy and nanotechnology has become of particular interest in the last decades. This is of crucial importance for the computer science developing, because the dimensions of chips is everyday smaller, so the properties at molecular scale become everyday more important. Devices such as a single-electron transistor have been built, which is ruled by quantum mechanical effects.

Finally, other very important events (which will not be treated in this thesis) are in the field of surface science: corrosion, adhesion, tribiology, electrochemical reactions...

1.2 Experimental techniques in the surface science.

The knowledge of the behaviour of adsorbed molecules on a surface has a crucial relevance to understand how a process takes place on the surface. In table 1.2 some experimental techniques that allow surface scientists to study the surfaces

UNIVERSITAT ROVIRA I VIRGILI
ORGANIC MOLECULES ON METAL SURFACES: FORECASTING STRUCTURES AND SPECTRA
Benjamí Martorell Masip
ISBN:978-84-691-9747-9 /DL: T-1259-2008

Table 1.1: Developement of important industrial catalytic reactions.

Year	Process / Reaction	Catalysts	Area of interest
1875	Sulfuric acid: $SO_2 + {}^1/_2O_2 \rightarrow SO_3$	Pt, V_2O_5	Chemicals
1903	Nitric acid: $2NH_3 + {}^1/_2O_2 \rightarrow 2NO + 3H_2O$	Pt gauze	Chemicals
1913	Ammonia synthesis: $N_2 + 3H_2 \rightarrow 2NH_3$	$Fe/Al_2O_3/K_2O$	Chemicals, fertilizers
1923	Methanol synthesis: $CO + 2H_2 \rightarrow CH_2OH$	CuZnO	Chemiclas
1930	Fischer-Tropsch: $CO + 2H_2 \rightarrow$ C_1-C_{30} HCs	Fe/K/CuO, Co/Kieselguhr	Petroleous
1920-40	Hydrogenation reactions	Ni/Kisieselguhr, Raney	Petrochemicals, foods
1936-42	Catalytic cracking: C_{20}-$C_{30} \rightarrow$ C_8-C_{16} HCs	SiO_2-Al_2O_3	Petroleum
1937	Ethene oxidation: $C_2H_4 + O_2 \rightarrow C_2H_4O$	Ag/Al_2O_3	Chemicals
1942	Paraffin alkylation: $C_3H_6 + C_4H_{10} \rightarrow C_7H_{16}$	H_2SO_4, HF	Petroleum
1938-46	Oxo process: alekene + $CO/H_2 \rightarrow$ aldehydes	Co carbonyls (homogeneous)	Chemicals
1950	Catalytic naphta reforming	Pt/Al_2O_3	Petroleum
1955	Stereopecific polymerization: $n(C_2H_4) \rightarrow$ polyethylene	$TiCl_3/Al(R)_3$	Chemicals
1960	Wacker process: $C_2H_4 + H_2O \rightarrow CH_2CHO$	$PdCl_2$ (homogeneous)	Chemicals
1963	Ammoxidation: $C_3H_6 + NH_3 + {}^3/_2O_2 \rightarrow CH_2{=}CHCN$	Bismuth phosphomolybdate Sb/U oxide	Chemicals
1964-68	Zeolitic catalytic cracking	Exchanged X, Y zeolites	Petroleum
1967	Multimetallic reforming	Pt-Re, Pt-Ir-Cu	Petroleum
1960s	Hydrodesulphurization: $R\text{-}S + 2H_2 \rightarrow H_2S + RH_2$	$CoMo/Al_2O_3$	Petroleum
1976, 1981	Auto emissions control: CO and CH oxidation, NO reduction	Pt, Pd/Al_2O_3, Rh/Al_2O_3	Automotive environmental control
1980-95	Selective catalytic reduction of NO: $4NH_3 + 4\ NO + O_2 \rightarrow 4N_2 + 6H_2O$	VO_xTiO_2, zeolites	Enviromental control
1980-95	Shape selective reactions	New zeolites, e.g. ZSM-5	Petrochemicals

UNIVERSITAT ROVIRA I VIRGILI
ORGANIC MOLECULES ON METAL SURFACES: FORECASTING STRUCTURES AND SPECTRA
Benjamí Martorell Masip
ISBN:978-84-691-9747-9 /DL: T-1259-2008

Table 1.2: Experimental techniques used in surface science.

Type	Acronym	Name	Obtained information
Scanning Probe techniques	STM	Scanning tunnelling microscopy	Surface images
	AFM	Atomic force microscopy	Surface images
Electron diffraction	LEED	Low-energy electron diffraction	Structure of the surface
Electron spectroscopy	XPS	X-ray photoelectron spectroscopy	Determination of elements
	UPS	Ultraviolet photoelectron spectroscopy	Bonding adsorbate-surface
	PM	Photoelectron microscopy	Surface images
	NEXAFS	Near-edge x-ray absorption fine structure	Structure of the adsorbate
Vibrational spectroscopy	RAIRS	Reflection-absorption infrared spectroscopy	Adsorbate vibrations
	EELS	Electron energy loss spectroscopy	Adsorbate vibrations
Temperature technique	TPD	Temperature programmed desorption	Adsorption energies

and their adsorbed molecules. Some of them provide information mainly about surface (LEED), some of them about adsorbate (RAIRS) and some of them about the surface and the adsorbate (STM).

Some of these techniques have been used during decades, like TPD, because of the simple instruments. Other, like AFM or STM have been developed in the last decades, being very sophisticated devices. We cannot say that new techniques have displaced the existing ones, but they are complementary.

In this thesis two of them have been taken into account: RAIRS and NEXAFS spectroscopy.

RAIR spectroscopy has been used for more than 50 years and it has been one of the most powerful surface techniques. This is a non-destructive technique, with a non-expensive device, and its response is very sensitive to the structure of the adsorbed molecule. Moreover, usually organic molecules are functionalised, and these groups (C=O, N−H, O−H, C≡N...) are highly sensitive to IR spectroscopy.

UNIVERSITAT ROVIRA I VIRGILI
ORGANIC MOLECULES ON METAL SURFACES: FORECASTING STRUCTURES AND SPECTRA
Benjamí Martorell Masip
ISBN:978-84-691-9747-9 /DL: T-1259-2008

On the other hand, NEXAFS spectroscopy is a powerful, non-destructive technique, but its work conditions, in ultra high vacuum (UHV) and the photons source used are difficult to be obtained. Although these inconvenients, the development of new syncrothons has allowed to obtain photons beams that are suitable for this technique. NEXAFS spectroscopy is highly sensitive to the adsorption mode of the molecule and its chemical environment. It has been applied to C atoms, O atoms...

Although the power of these techniques, their results depend on the capability of experimentalists to assign and resolve their spectra. The theoretical simulation of these spectra can be a great help for the assignation of the bands and the interpretation of the results.

1.3 The title of this thesis.

In most thesis and books there is no section explaining the reasons why its own title has been chosen. In this case we have decided to make this section because the title of one thesis is its most visible part. It contains the essence of the work made.

The first part of the title is autoexplanatory: We have focused on the study of adsorbed organic molecules on metal surfaces. In one case the organic molecule is a pure hydrocarbon (i.e. only C and H atoms are present) and in the other organic molecule some S-containing functional groups appear. In all cases the adsorption is carried out on metals, because of the experience of our group on these systems.

An important information must be commented to understand the second part of the title: during the calculation period of this thesis no experimental information about the studied systems was available; only at the final part of this work, experimental data about a particular system (TTF adsorbed on Ag(110), see chapter 3) was obtained. This is the reason why in the title of this thesis appears the verb “forecast”. We have been capable of predicting (forecasting) the geometrical structures, RAIR and NEXAFS spectra of adsorbed molecules on several metals with no previous experimental information.

1.4 Division of this thesis.

This thesis is outlined as follows:

UNIVERSITAT ROVIRA I VIRGILI
ORGANIC MOLECULES ON METAL SURFACES: FORECASTING STRUCTURES AND SPECTRA
Benjamí Martorell Masip
ISBN:978-84-691-9747-9 /DL: T-1259-2008

- In this chapter (chapter 1) we present the thesis, the reasons why every system is studied and the objectives we want to reach at the final of this work.
- Chapter 2 is a summary of the models and methods used for calculations and their foundations.
- In chapter 3 results for the study of the adsorption of tetraselenafulvalene (TTF, $C_6H_4S_4$) and tetraselenafulvalene (TSF, $C_6H_4Se_4$) on metal supports are presented. These molecules belong to the family of precursors for organic molecular materials (OMM).
- The results for the adsorption of $CHCHCH_2$ and $CHCCH_2$ are presented in chapters 4, 5 and 6:
  - The thermodynamic aspects of the adsorption of $CHCHCH_2$ on several metals are presented in chapter 4.
  - In chapter 5 we go beyond, and the kinetic aspects are presented. One new specie ($CHCCH_2$) is important in order to explain the reaction on Cu(111).
  - The collaboration with Pr. Klaus Hermann has allowed us to study NEXAFS spectra of propyne and $CHCHCH_2$ on Cu(111). Results are presented in chapter 6.
- As the closing point of this thesis, a final summary and conclusions are presented chapter 7.

Now we want to present in more detail the central chapters of this thesis, where results for calculations are shown.

1.4.1 Organic molecular materials: TTF and TSF.

An organic molecular material (OMM) is that material of organic base, whose compounds have weak interactions among them (Van der Waals, hydrogen bonds...). Although most OMMs are insulators, 30 years ago were discovered some materials that had properties not typical for organic materials.

In 1973 the first OMM with special features was synthesised: $(TTF)_2$-TCNQ [156] (TCNQ: tetracyanoquinodimethane, $C_{12}H_4N_4$). This is a charge transfer salt (exist a charge donor (TTF) and a charge acceptor (TCNQ)) and it presents

UNIVERSITAT ROVIRA I VIRGILI
ORGANIC MOLECULES ON METAL SURFACES: FORECASTING STRUCTURES AND SPECTRA
Benjamí Martorell Masip
ISBN:978-84-691-9747-9 /DL: T-1259-2008

metallic properties: conductivity. From that moment, more and more OMM have been synthesised with better properties than this salt (and not only charge transfer salt, but also metallic properties have been discovered in polymers and fullerens).

The disposition of the charge donor and the acceptor, the way they pile up and their interactions determine the charge transfer and their electric and magnetic properties. The overlapping of π orbitals in the direction of the piling leads to the charge transfer from cation's HOMO to anion's LUMO. If the overlapping is only made in one direction, the material is anisotropic in that direction. In the case of $(TTF)_2$-TCNQ, TCNQ is reduced in form of $TCNQ^-$ and TTF is $TTF^{+0.5}$, and they pile up in a segregated way [157]. As these salts lie on supports, it is important to know the possible interaction between the support or substrate (metal) and the salt.

$(TTF)_2$-TCNQ was the first charge transfer material with metalic properties, but nowadays new materials have been synthesised. $(TMTSF)_2PF_6$ (tetramethyl-tetraselenafulvalene) was the first salt with superconductivity properties [158, 159]. It has been discovered that the responsible of superconductivity is the cationic part of this salt. Another important cation is BEDT-TTF (bis(etilenditio)-tetrathiafulvalene) because it presents metallic behaviour at normal temperatures. Nowadays, the efforts go to way of finding new material with higher T_c.

It has been commented these materials are prepared on supports, it is interesting to study how is the interaction between the salt and the substrate. When the interaction substrate-adsorbent is strong, the metal and the molecular structure of the salts must clash, otherwise, if the interaction is weak, the growth order of the salt is a long-range effect [160].

Finally, OMM have a wide range of applications in industry:

- Electric switches and memory devices: It has been observed the photoinduced switching between two metastable states in thin films of Cu-TCNQ [161]. BBDN-TCNQ (BBDN: bis(2-butene-2,3-dithia(2-s,s')nickel) presents bistable electronic states with a switching time of 100 ns, which makes it applicable for ROM memories [162].

- Electric capacitors: MnO_2 could be substituted in capacitors by some salts with better properties [163].

- FET (field-electron transistor) and MIS (metal-insulator-semiconductor)

UNIVERSITAT ROVIRA I VIRGILI
ORGANIC MOLECULES ON METAL SURFACES: FORECASTING STRUCTURES AND SPECTRA
Benjamí Martorell Masip
ISBN:978-84-691-9747-9 /DL: T-1259-2008

devices: The photoelectric and rectifying behaviour of some compounds makes them suitable for Schottky barriers. Though most of organic semiconductors are of type p, some of type n have been studied and they can be an alternative to the classical inorganic systems [164, 165].

So, the objective in this part of the thesis will be the study of the interaction between an organic charge donor (in this case will be simplest ones: TTF and TSF) with the metallic supports ((110) surface of Ag and Au).

1.4.2 Studying the intermediates of a heterogeneous catalysis reaction: presenting $CHCHCH_2$ and $CHCCH_2$.

Heterogeneous catalysis is a key step in the industry, as commented in previous sections. Several processes involve organic molecules and metal surfaces. To understand the global reaction it is interesting to know what happens in the microscopic scale.

For example, one specie used in welding and cutting in industrial processes is ethyne (also called acetylene). But it cannot be transported as other gases (for example N_2) at high pressures in one cylinder, because it reacts and can explode. To transport it, two safe alternatives exist: it can be dissolved into an acetone solution, or it can be adsorbed in a porous material (Agamassan). On the other hand, if acetylene is put into contact with metal surface, as Cu(111) or Pd(111) [166], it does not become more stable but it dimerises forming benzene.

The next alkyne in size is propyne. It is also used in welding and cutting processes, but there is an important difference respect to ethyne: when it is compressed it does not explode, making safer its transport and use. Moreover, the behaviour on the metal surfaces above described for ethyne is not the same in the case of propyne. Whereas on Pd(111) it trimerises and yields trimethylbenzene [99], on Cu(111) it dimerises and yields benzene [101]. The difference in reactivity was studied and one reaction intermediate was proposed for the dimerisation: $CHCHCH_2$ [90].

In order to check the effect of the theoretical approach, we summarize the more relevant results obtained with the cluster model in reference [90] for $CHCHCH_2$ intermediate, although those calculations were performed with the B3LYP density functional (different to the one we use). It was used a Cu_{22} cluster model of two layers, centred on a hcp-site. The proposed structure was a $CHCHCH_2$ cis-like structure with the plane of carbon atoms almost perpendicular to the surface. The C1−C2 and C2−C3 distances were 1.36 and 1.51

UNIVERSITAT ROVIRA I VIRGILI
ORGANIC MOLECULES ON METAL SURFACES: FORECASTING STRUCTURES AND SPECTRA
Benjamí Martorell Masip
ISBN:978-84-691-9747-9 /DL: T-1259-2008

Å, respectively (see figure 4.3). The C−C−C angle was 125°. Both C1 and C3 were interacting with the surface, indicating a structure that resembles a 1,3-diradical-like structure more than a carbene one. C1 atom was located on the neighbour fcc site, but the whole molecule did not keep the molecular plane respect to the central hcp-site, i.e. the system lost the C_s symmetry plane, although the C−C−C plane was almost perpendicular to the surface. All hydrogen atoms were placed towards the vacuum, so they did not exhibite any interaction with the surface. The interaction energy with the surface was large, -261 kJ·mol^{-1}, and the interaction energy with respect to gas-phase propyne and the cluster model was -43 kJ·mol^{-1}. Therefore, it could be derived the possibility of a spontaneous isomerization of propyne to adsorbed $CHCHCH_2$ isomer at finite temperatures.

In this part of the thesis we want to study the adsorption of these intermediate on those metal (Cu and Pd) and Pt(111) and Rh(111) [104, 105], where Pr decomposes. During the calculation process we also found another important intermediate for this reaction: $CHCCH_2$, which has been studied on Cu(111).

1.5 Objectives of this thesis.

The aim of this thesis is to study the structure, reactivity and spectra of several organic molecules on metal surfaces using the periodical density functional methodology. We have studied three different systems: TTF and TSF adsorbed on the (110) surface of metal substrates (Ag and Au); $CHCHCH_2$ on the (111) surface of Cu, Pt, Pd, and Rh (where Pr reacts and $CHCHCH_2$ is its isomer); and finally the dehydrogenated product of Pr, $CHCCH_2$ on the (111) surface of Cu.

So, the general objectives of this work are:

- To study the interaction between the adsorbate and the metal. To establish the adsorption modes, the adsorption energies and the adsorption geometries.

- To characterise all obtained structures are minima or saddle points using the vibrational frequencies. To simulate the RAIR spectra for those structures that are minima and assignate their bands. To determine the fingerprints for every structure. To apply ZPE corrections on adsorption energies.

UNIVERSITAT ROVIRA I VIRGILI
ORGANIC MOLECULES ON METAL SURFACES: FORECASTING STRUCTURES AND SPECTRA
Benjamí Martorell Masip
ISBN:978-84-691-9747-9 /DL: T-1259-2008

- To simulate the reactions profiles. To determine the transition states that connect different minima. To try to find out which factors control the reaction process.
- To simulate NEXAFS spectra for gas phase and adsorbed molecules.

In the next chapters, the presented results try to reach the general objectives of this thesis.

UNIVERSITAT ROVIRA I VIRGILI
ORGANIC MOLECULES ON METAL SURFACES: FORECASTING STRUCTURES AND SPECTRA
Benjamí Martorell Masip
ISBN:978-84-691-9747-9 /DL: T-1259-2008

Chapter 2

Methods and models of calculation.

In this chapter we make a look to the theoretical methods and the surface models that are used in this thesis.

All calculations methods used in this thesis are based in the quantum chemistry, where the well-known Schrödinger equation is tried to be solved in the frame of some approaches. In this thesis we have used the density functional theory (DFT), where the Schrödinger equation is solved from the electronic density of the system. DFT has demonstrated to be a reliable and low-time consuming method, which is suitable for surfaces.

Surfaces can be modelled in two different ways. The first one is the cluster model, were a small piece of the surface is modelled as an isolated system of a finite number of atoms (so this model works relatively well for low-coverage systems, where interactions are small). The other model is the slab model, where an unit cell is periodically reproduced in the 3-D space in order to obtain the lateral interactions of the adjacent molecules.

Most calculations carried out in this thesis have been made with the slab model using the VASP code. This method uses plane-waves as the basis for the electronic expansion, which makes the system to be periodic. This modelling way has demonstrated to evaluate properly the adsorption energies, the adsorption geometries, the coverage effects and the vibrational frequencies of adsorbates on metal surfaces.

On the other hand, the cluster calculation is a local calculation, where the

UNIVERSITAT ROVIRA I VIRGILI
ORGANIC MOLECULES ON METAL SURFACES: FORECASTING STRUCTURES AND SPECTRA
Benjamí Martorell Masip
ISBN:978-84-691-9747-9 /DL: T-1259-2008

orbitals are centred in the atoms of the calculation. This local nature allowed us to simulate a type of electronic spectroscopy: NEXAFS.

UNIVERSITAT ROVIRA I VIRGILI
ORGANIC MOLECULES ON METAL SURFACES: FORECASTING STRUCTURES AND SPECTRA
Benjamí Martorell Masip
ISBN:978-84-691-9747-9 /DL: T-1259-2008

2.1 Quantum chemistry and the Schrödinger equation.

In the last years of the XIXth century and in the beginning of the XXth, lots of new experiments were carried out that could not be explained by the classical mechanical laws. Some examples were:

- The radiation of a black body: A black body is an object capable of absorbing and emitting all frequencies of a radiation in a uniform way.
- The dispersion of alpha particles through a metallic film: In 1909 Rutherford, Geiger and Marsden bombarded a metallic film with alpha particles beam. Some of these alpha particles were reflected or dispersed.
- The atomic and molecular spectra: This is a clear quantum effect. The energy in a spectrum is absorbed or emitted at some concrete energies and it is not a continuous band.

A new generation of physics was ready to start explaining all these phenomena. Among them, Albert Einstein, Max Planck, Mr. and Ms. Curie, Ludwig Boltzman, Robert Oppenheimer, Paul Dirac, Enrico Fermi... and Erwin Schrödinger. He proposed the well-known time-independent Scrödinger equation [1]:

$$\hat{H}\,\Psi\left(\vec{r}_1,\vec{R}_1,\ldots,\vec{r}_n,\vec{R}_n\right)=E\,\Psi\left(\vec{r}_1,\vec{R}_1,\ldots,\vec{r}_n,\vec{R}_n\right) \tag{2.1}$$

This equation depends on the position of each nucleus, on the position of each electron, and their derivatives. This makes this equation to be extremely difficult to be solved.

The first approximation is the Born-Oppenheimer's [2] one. It is demonstrated that nuclei move so slow in comparison with electrons, that their movement can be neglected. This makes the equation easier to be solved, because nuclei are frozen, and the number of freedom degrees are decreased in a huge amount. But, even for the smallest polielectronic atoms and molecules, this equation is impossible to be solved, because the potential interaction between two electrons (V_{ee}) is difficult to be evaluated, and other approximations are required. These approximations try to solve this electron-electron interaction, and results depend on the capability of this approximation to describe each term [3, 4, 122]. As all performed calculations in this thesis were carried out in the frame of density functional theory (DFT), I will focus in the description of this

UNIVERSITAT ROVIRA I VIRGILI
ORGANIC MOLECULES ON METAL SURFACES: FORECASTING STRUCTURES AND SPECTRA
Benjamí Martorell Masip
ISBN:978-84-691-9747-9 /DL: T-1259-2008

methodology instead of all methods [3, 122] developed to solve the Schrödinger equation.

2.2 DFT

To solve the Schrödinger equation, one could use wave-function based methods. Although these methods have been demonstrated to be powerful, sometimes they are too expensive and are limited to small or medium size systems. There is an alternative to the wave-function methods: DFT [28, 29], which is based on the electronic density of the system.

In 1964 Hohenberg and Kohn demonstrated that for every chemical system, its energy was a function of its electronic density. Two theorems were enunciated [5, 6]:

> "*Any observable magnitude of a stationary non-degenerated ground-state can be calculated exactly from its electronic density.*"
>
> "*The electronic density of a stationary non-degenerated ground-state can be calculated exactly determining the density that minimises the energy of the ground-state.* "

That allowed them reconstruct the Schrödinger equation, and express the energy of the system as a function of the electronic density [4]:

$$E\left(\rho\right) = T\left(\rho\right) + V\left(\rho\right) + W_{CL}\left(\rho\right) + W_{NCL}\left(\rho\right) \tag{2.2}$$

where T is the kinetic energy, V is the nucleus-electron potential, W is the coulombic (CL) and non-coulombic (NCL) electron-electron potential and ρ is the electronic density. This energy must be minimised, and the expression found is:

$$\mu = \frac{\delta E_v\left(\rho\right)}{\delta\rho\left(\vec{r}\right)} = V_{ext}\left(\vec{r}\right) + \frac{\delta F_{HK}\left(\rho\right)}{\delta\rho\left(\vec{r}\right)} \tag{2.3}$$

$$F_{HK}\left(\rho\right) = T\left(\rho\right) + W_{CL}\left(\rho\right) + W_{NCL}\left(\rho\right) \tag{2.4}$$

2.2.1 Kohn Sham equation

Expression 2.3 is known as the fundamental density equation and allows us to minimise the energy and to find the electronic density of the system. Here two problems are presented. We do not know the exact expression of T and W.

UNIVERSITAT ROVIRA I VIRGILI
ORGANIC MOLECULES ON METAL SURFACES: FORECASTING STRUCTURES AND SPECTRA
Benjamí Martorell Masip
ISBN:978-84-691-9747-9 /DL: T-1259-2008

The first problem was solved by Khon and Sham in 1965 [7]. It is easy to calculate the kinetic energy from the wave function. So they proposed to use a reference system of N electrons that interact with an external potential V_{ext}. This external potential has a special property, the electrons in our V_{ext} create a potential that has the same density as the real system. In this system the electrons do not interact among them but interact with the nuclei. In these terms the energy minimised is:

$$\frac{\delta E_v(\rho)}{\delta \rho(\vec{r})} = \frac{\delta T_s(\rho)}{\delta \rho(\vec{r})} + \int \frac{\rho(\vec{r}_2)}{r_{12}} d\vec{r}_2 + V_{ext}(\vec{r}) + \frac{\delta E_{XC}}{\delta \rho(\vec{r})} = \mu \qquad (2.5)$$

The problem is that the kinetic energy of this reference system $T_s(\rho)$ and the real $T(\rho)$ are not the same. The difference of this expression and the energy of columbic repulsion are joined in one only term, this is the correlation-exchange energy (E_{XC}).

E_{XC} include all terms that are not easily calculated like exchange energy, correlation energy, the difference of the kinetic energies and the correction of the auto-interaction. It makes the equation to be:

$$\hat{h}_{KS}\psi_i = \varepsilon_i \psi_i; \qquad \hat{h}_{KS} = -\frac{1}{2}\bigtriangledown^2 + V_{eff}(\vec{r}) \qquad (2.6)$$

These equations are very similar to the Hartree-Fock (HF) equations, and they are called the Kohn-Sham (KS) equations. Like in HF method, this equation is solved iteratively. From these equations we can calculate KS orbitals. These orbitals and their energies have not a real physical sense, because these orbitals come from the calculation of an external potential were the particles are non-interacting among them.

Another important difference between DFT and the wave-function based methods (for instance HF method), is that for DFT we use an approximated Hamiltonian, but the electronic density for this system is exact. On the other hand, for HF the Hamiltonian is exact, but the wave function is an approximated solution.

2.2.2 Exchange-correlation potential

Now the problem is to calculate the part of the energy that comes from the exchange-correlation potential. Three kind of methods are used to evaluate this term: Local density approximation (LDA), gradient generalised approximation

UNIVERSITAT ROVIRA I VIRGILI
ORGANIC MOLECULES ON METAL SURFACES: FORECASTING STRUCTURES AND SPECTRA
Benjamí Martorell Masip
ISBN:978-84-691-9747-9 /DL: T-1259-2008

(GGA) and hybrid functionals.

2.2.2.1 LDA

Local density approximation was the first way (and the easiest one nowadays) to evaluate the exchange-correlation energy. In this approximation the exchange-correlation energy is evaluated as a function of an uniform gas of electrons. For the exchange part, the model of a homogeneous, constant density gas gives an expression for the energy [4, 5]:

$$E_X^{LDA}(\rho) = -\frac{9}{4}\alpha\left(\frac{3}{8\pi}\right)^{\frac{1}{3}}\int \rho^{\frac{4}{3}}d\vec{r} \tag{2.7}$$

For the exchange part, several possibilities are available. The most famous one is that one, that Vosko, Wilk and Nusair (VWN) [8] developed interpolating a sample of correlation energies values obtained from Monte-Carlo calculations.

The most surprising characteristic of this method are the good results obtained using a very simple model of calculation, because this model does not evaluate accurately the exchange-correlation hole. In special, it works extremely well for systems where the density remains constant, like metals. Geometries, vibrational frequencies and charge densities are very good, but binding energies trend to be too high.

For open shell calculations, the alpha and beta densities must be treated independently and local spin density approximation (LSDA) is used to evaluate independently the alpha and beta equations, like in unrestricted HF calculations.

2.2.2.2 GGA

In LDA the effects of exchange-correlation are local and depend only on the value of the electronic density of a point. The next step is to introduce gradients of the density in the description of the effects of exchange-correlation. This makes that the exchange-correlation potential not only depends on the value of the density on a point, but also how it variates on the near points:

$$V_{XC} = \frac{\delta E_{XC}(\rho)}{\delta\rho(\vec{r})} - \bigtriangledown\cdot\frac{\delta E_{XC}(\rho)}{\delta\left(\bigtriangledown\rho(\vec{r})\right)} \tag{2.8}$$

Several approximations on the gradient have been implemented, and all of them give better results for geometries, vibrational frequencies and charge densities than LDA. However, its computational cost is higher. The main reason

UNIVERSITAT ROVIRA I VIRGILI
ORGANIC MOLECULES ON METAL SURFACES: FORECASTING STRUCTURES AND SPECTRA
Benjamí Martorell Masip
ISBN:978-84-691-9747-9 /DL: T-1259-2008

for using GGA is the increase of the quality of binding energies.

Some implemented functionals are [9, 123, 124, 125, 126, 127, 136]:

- Perdew-Wang 86 (PW86)
- Becke-Perdew (BP)
- Lee-Yang-Parr (LYP)
- Perdew-Wang 91 (PW91)
- Perdew-Burke-Enzerhof (PBE)
- Revised Perdew-Burke-Enzerhof (RPBE)

Most of these functionals contain adjusted experimental parameters to adjust the energies of a series of atoms. The only one that is 100% ab-initio is PW91 functional, which was built using dates of LDA. PBE and RPBE correct PW91 functional to improve results.

In this thesis most of the calculations are made by PW91 functional, which trends to be a good functional for the description of chemical bonds [34, 137, 106].

2.2.2.3 Hybrid Functionals

Even for GGA, some chemical features are still not well described. For example, the gap between the bonding band and the conductive band in semiconductors is too small for GGA calculations. In the case of HF calculations, this gap trends to be too big. These two results give the idea of mixing these two methods to improve the quality of the results. The exchange part of the exchange-correlation potential is in these models the exact exchange of the HF method. The correlation part comes from the DFT treatment. This makes these methods to be a hybrid between DFT and HF.

The problem of this method is that HF exchange potential does not take into account the dynamical correlation, so a new term of dynamical correlation must be added into the functional, and this is made through the adiabatic connection. Depending on how this part is treated, some functionals appear [10, 30]:

- B3LYP
- B3PW91

UNIVERSITAT ROVIRA I VIRGILI
ORGANIC MOLECULES ON METAL SURFACES: FORECASTING STRUCTURES AND SPECTRA
Benjamí Martorell Masip
ISBN:978-84-691-9747-9 /DL: T-1259-2008

These functionals work extremely well for atoms and molecules, but some numerical problems appear for solid state calculation when periodical conditions are required.

2.3 Surface models.

As commented in the introduction of this chapter, two big surface models exist, each one with its advantages and disadvantages. In this section we will explain the features of each one and why they have been chosen for every purpose.

2.3.1 The slab model.

An ideal solid can be observed as the infinite 3-D repetition of a small part of the global system. For example, the copper bulk (Fm3m structure) is the infinite repetition in the three space directions of a cube, where Cu atoms are placed on the vertexes of the cube and on the centre of the cube faces. In this case, the unit cell would be this cube.

In the case of surfaces, it is desired only the repetition of the unit cell in two directions of the space, but not in the third one. In order to avoid the problem of the repetition in the third space direction, one large vacuum region is added in one of the space directions (normally z-direction). This makes a surface to be generated, which is repeated infinitely: this is the slab model. The vacuum region must be large enough to avoid the interaction between consecutive slabs in z-direction [4, 12, 128]. In figure 2.1 is presented the slab model. The biggest problem of the slab method is the use of a vacuum region. Unfortunately, plane-waves have to be combined to simulate no electrons in this vacuum region, and this makes this method to have a high computational cost. Although being so time-consuming, this method has demonstrated to give very good results.

The use of repetitive unit cells allows us to evaluate the lateral interactions and the coverage effects on the system. One can choose the unit cell as big as desired, or even the repetition directions. It makes this method to be so powerful for surfaces.

With the slab model one can obtain the adsorption energies (E_{ads}), which can be calculated as the difference between the energy of total system minus the energy of the parts that form the system:

$$E_{ads} = E_{total} - \left(E_{slab} + E_{adsorbate(g.ph.)}\right) \tag{2.9}$$

UNIVERSITAT ROVIRA I VIRGILI
ORGANIC MOLECULES ON METAL SURFACES: FORECASTING STRUCTURES AND SPECTRA
Benjamí Martorell Masip
ISBN:978-84-691-9747-9 /DL: T-1259-2008

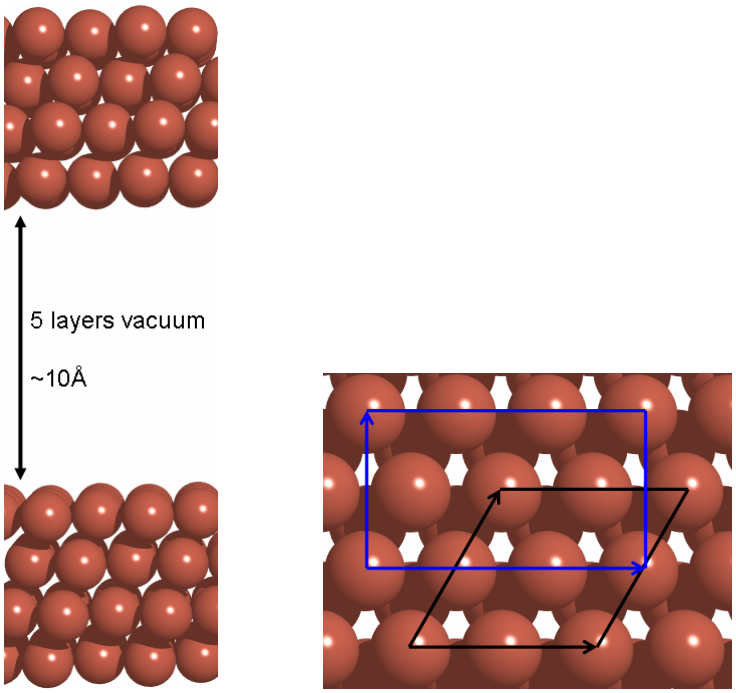

(a) (b)

Figure 2.1: a) four-layers slab and vacuum region. b) two possible unit cells, in black 2×2 unit cell; in blue $3\times\sqrt{3}$ unit cell.

2.3.2 The cluster model.

Another strategy to simulate a surface is to use the cluster model. This is a much simpler method than the slab one. In the cluster model the solid is "cut" and only a small piece of the total system is used for the calculation. In figure 2.2 a cluster of 59 atoms is presented. In this case, all the surface is reduced to only two layers, with 29 and 30 atoms each one.

Although the simplicity of this model, the low-coverage systems can be described well with this model. This model does not take into account the interaction with adjacent molecules, so one could imagine this model to be the limit of the low-coverage regime.

UNIVERSITAT ROVIRA I VIRGILI
ORGANIC MOLECULES ON METAL SURFACES: FORECASTING STRUCTURES AND SPECTRA
Benjamí Martorell Masip
ISBN:978-84-691-9747-9 /DL: T-1259-2008

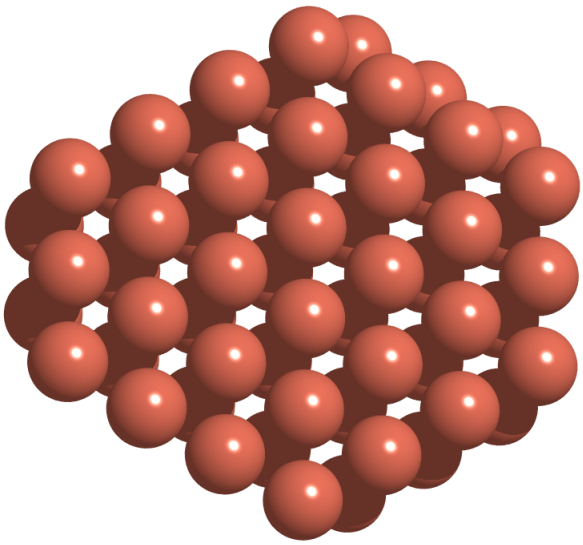

Figure 2.2: Cluster of 59 atoms. 29 atoms are in the first layer and 30 in the second one.

2.4 Slab calculations using VASP.

Vienna Ab-initio Simulation Package (VASP) [11, 19, 22, 130, 131, 132] is a calculation package developed by G. Kresse, J. Furthmüller and J.Hafner, which uses DFT for periodical calculations. Due to the periodicity of the ideal solids, this package is highly efficient for the calculations made in this thesis. Surfaces are simulated by a slab model, which is repeated in the three dimensions of the space. VASP allows calculate adsorption energies, equilibrium geometries of minima and transition states, charge distributions, density of states and projected density of states (DOS and PDOS), vibrational frequencies and dipolar moments

In VASP, the Kohn-Sham equations are solved self-consistently with an iterative matrix diagonalisation combined with the Broyden/Pulie [20, 21] mixing method for charge density. The combination of these two techniques makes the code very efficient, especially for transition metals, which present a complex band structure around Fermi level. The algorithms implemented in VASP are based on a conjugate gradient scheme, the block Davidson scheme or a residual minimisation scheme (RMM). These algorithms work as follows: First they calculate the electronic ground state for a particular geometry, then they evaluate the forces of this geometry, and finally predict a new geometry based on these

UNIVERSITAT ROVIRA I VIRGILI
ORGANIC MOLECULES ON METAL SURFACES: FORECASTING STRUCTURES AND SPECTRA
Benjamí Martorell Masip
ISBN:978-84-691-9747-9 /DL: T-1259-2008

forces[1]. This process is iterative until a convergence parameter is achieved.

Some other algorithms are implemented. Quasi-Newton algorithm allows calcule saddle points on hypersurface of potential energy. NEB algorithm [26] and DIMER algorithm [27] are useful to find transition states. Besides, VASP package permits to evaluate numerically vibrational frequencies using a harmonic approximation by finite displacements of the atoms of a system. A combination of these algorithms must be used to find good descriptions for the hypersurface of potential energy. More information of algorithms used by VASP is available on references [22, 25, 132].

VASP can use several functionals to evaluate the energy of a system. One can choose between LDA and several GGA implementations: PW-B, PW, PW91, PBE, RPBE, LMH.

A special feature of VASP is the use of periodicity. To make easier working with periodicity, the base functions used by VASP are not the typical one for chemistry, which are localised on the atoms, but uses plane-waves, that are not localised on an atom, but they have the periodicity of the supercell used.

VASP code uses pseudopotentials to decrease the number of electrons to be treated, because it is demonstrated that core electrons do not take part in chemical bonds. Projector Augmented Wave-functions (PAW) and ultra-soft (US) pseudopotentials are implemented on VASP package.

2.4.1 Plane-waves and Blöch theorem.

For an ideal surface or solid, the best way to simulate it is to create an unit cell, which is repeated in two or three dimensions respectively. This is still more valid for metallic systems, were valence electrons are delocalised and they form bands. The unit cell is repeated to obtain a perfect periodical system. This means a translation operator is being used, and this operator must commute with the Hamiltonian of the system:

$$\left[\hat{H}, \hat{T}\right] = 0 \tag{2.10}$$

Blöch theorem [14] uses the translational symmetry to reduce the infinite

[1] Three different algorithms are available in VASP to calculate this new geometry:

1. Quasi-Newton calculation.
2. Conjugated gradients (CG) [32].
3. Damped molecular dynamics (MD).

UNIVERSITAT ROVIRA I VIRGILI
ORGANIC MOLECULES ON METAL SURFACES: FORECASTING STRUCTURES AND SPECTRA
Benjamí Martorell Masip
ISBN:978-84-691-9747-9 /DL: T-1259-2008

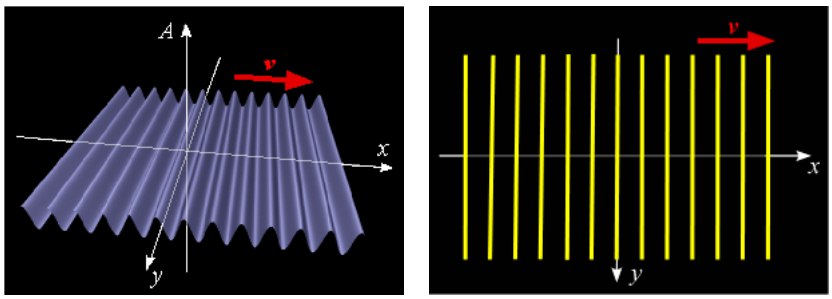

(a) Plane wave. (b) Plane wavefront.

Figure 2.3: Plane-waves images.

number of the one-electron wave functions to be computed to the number of electrons in the unit cell. Then the one-electron wave-functions can be expressed as the product of a cell periodic part and a wave-like part, these are the Blöch functions.

Blöch functions can be chosen as eigenvectors for the Hamiltonian, and Schrödinger equation can be solved from the crystalline orbitals. So, eigenfunctions of Hamiltonian will contain the translational symmetry.

The crystalline orbitals can be expanded using a linear combination of base functions. This expansion can be made with plane-waves. Plane-waves are usual in physics and in electromagnetism fields. In figure 2.3(a) it is shown a plane-wave moving with a $\vec{v}$ velocity and the associated wavefront (b)[2]. Solid state physics uses them to simulate the band structure of solids. Every periodical function can be expanded as an addition of plane-waves, and Blöch functions are expanded as a linear combination of plane-waves:

$$\Psi_{n,\vec{k}}\left(\vec{R}\right) = \sum_{\vec{g}} a_{n,\vec{g},\vec{k}} \exp\left(i\left(\vec{g},+\vec{k}\right)\vec{R}\right) \tag{2.11}$$

The sum runs over all vectors of the reciprocal space, and the wave vector determines one point in the first Brillouin zone. The coefficients of the expansion trend to zero when the kinetic energy of the plane-waves is high enough. This makes possible to cut the energy of the plane-waves, and only use a few of them up to a restricted energy. This makes possible to use a finite base and points to calculate the system. A negative consequence of this method is that the number of plane-waves included in every k-point is different. K-points are those points

[2]These images are taken directly from reference [168]

UNIVERSITAT ROVIRA I VIRGILI
ORGANIC MOLECULES ON METAL SURFACES: FORECASTING STRUCTURES AND SPECTRA
Benjamí Martorell Masip
ISBN:978-84-691-9747-9 /DL: T-1259-2008

in the limit of the Brillouin zone, or alternatively, are the point where one can reach from the origin of the zone crossing no Bragg planes (first Brillouin zone). Of course, it is not possible to calculate for every k-point in the Brillouin zone, but a mesh of k-points can be created and the energy is evaluated on them.

2.4.2 Pseudopotentials. The PAW method

Even using Blöch theorem and calculating only the plane-waves that have up to a certain kinetic energy, to have a good description of the core electrons of an atom would be necessary a huge number of plane-waves, being very time demanding. To solve this problem, pseudopotentials are used.

It is known, core electrons do not take place in chemical bonds, so it is not necessary to describe them explicitly if we only want to deal with chemical processes. This justifies the use of the so-called frozen-core electrons approximation, were core electrons are calculated in a reference configuration and then remain constant in other calculations. Then, the wavefunctions for valence electrons are substituted by pseudowave functions, which reproduce the energetic levels obtained by an all-electron calculation. These pseudowave functions are different from the all-electron wave-functions, because in the inner zone, near the nucleus, are designed not to have any node. This makes that the number of plane-waves required decrease in a substantial way.

Several kinds of pseudopotentials are available, like US pseudopotentials [17], non-conserving pseudopotentials [18]... In this thesis all calculations were made using PAW pseudopotentials [18, 31].

The PAW pseudopotentials have demonstrated to give high quality results in solid state chemistry, so we decided to use them, despite being more time-demanding than other pseudopotentials. The biggest difference between PAW pseudopotentials and the other ones is that PAW pseudopotentials try to reproduce the nodal structure of the zone near the nucleus, so PAW is a frozen-core method, but it tries to introduce the advantages of all-electron calculations in this way:

$$|\Psi\rangle = \left|\tilde{\Psi}\right\rangle - \sum_{N,i} \left|\tilde{\phi}_{N,i}\right\rangle c_{N,i} + \sum_{N,i} |\phi_{N,i}\rangle\, c_{N,i} \tag{2.12}$$

This indicates, for the inner zone the pseudowave function is substituted by the all-electron wave function. For the external zone the pseudofunction is used, because it is identical to the all-electron wave-function. This makes that quality of results improve substantially, and the cases where US pseudopotential fail,

UNIVERSITAT ROVIRA I VIRGILI
ORGANIC MOLECULES ON METAL SURFACES: FORECASTING STRUCTURES AND SPECTRA
Benjamí Martorell Masip
ISBN:978-84-691-9747-9 /DL: T-1259-2008

like for first row atoms, in PAW method are very well described.

2.4.3 Vibrational analysis. Selection rules of RAIR spectra.

Vibrational calculations can be made for two purposes: The first one is to ensure that the optimised stationary point is a minimum on the potential energy surface (or a transition state if it is desired). The other purpose is to simulate the IR spectrum to be compared with the experimental one, and to assignate the bands of the spectra.

It is necessary to remark that vibrational calculations only have sense on the optimised geometries (the forces or first derivatives of the potential energy are zero), because vibrational frequencies are related directly with the force constant, which are the second derivatives of the potential, and mathematical analysis ensures that a stationary point is a minimum if all second derivatives are positive (one negative force constant for TS), and for minima the vibrational frequencies are all real (one imaginary frequency for TS) [25].

To calculate second derivatives of the potential, two mathematical methods are available: the analytical method and the numerical method. The analytical method calculates explicitly the second derivative of the potential. VASP does not work with analytical second derivatives method. The numerical method, which is used by VASP, takes finite displacements for every Cartesian coordinate, and then evaluates the second derivatives from the variation of the energies gradients in these displacements. In the harmonic approximation, these displacements have to be big enough to make a substantial variation of the energy in order to minimise the numerical errors in the calculation of the derivatives, but they have to be small enough to ensure we are in the harmonic zone. We have found that displacements of ± 0.02 Å for each cartesian coordinate give very good results for adsorbed organic molecules. For adsorbates on a surface, another approximation is made. It is considered that phonons of the surface and vibrational frequencies of the adsorbate are decoupled. This decreases the number of steps to calculate and the calculation is faster. When second derivatives are calculated, the Hessian matrix [24] is created:

$$H\,f\,(x_1,\ldots,x_n) = \begin{pmatrix} \frac{\delta^2 f}{\delta x_1^2} & \cdots & \frac{\delta^2 f}{\delta x_1 \delta x_n} \\ \vdots & \ddots & \vdots \\ \frac{\delta^2 f}{\delta x_n \delta x_1} & \cdots & \frac{\delta^2 f}{\delta x_n^2} \end{pmatrix} \tag{2.13}$$

UNIVERSITAT ROVIRA I VIRGILI
ORGANIC MOLECULES ON METAL SURFACES: FORECASTING STRUCTURES AND SPECTRA
Benjamí Martorell Masip
ISBN:978-84-691-9747-9 /DL: T-1259-2008

Once Hessian matrix is created, it is necessary to weight the Hessian up by the mass. Then, the Hessian matrix is diagonalised. The eigenvalues are the vibrational frequencies and the eigenvectors are the VNMs of the system [1].

The other aim to calculate vibrational frequencies is the simulation of IR spectra. Once the intensity is calculated (using equation 2.14), the spectrum can be convoluted by a lorentzian or gaussian approximation.

In the case of surfaces, RAIR spectrum is the most commonly used technique [23, 133, 134, 135, 149]. In gas phase, a sample is bombarded by a beam of IR photons, the photons go through the sample and some of them are absorbed. A detector in the other side of the sample generates a spectrum of absorvance (or transmitance). In the case of solids it is not possible because IR beam cannot pass through the sample. So a reflexion-absorption infra-red spectrum technique is used. In this technique only the changes in the normal direction (respect to the surface) of the dipolar moment are active in the RAIR spectrum, so only is necessary to take into account this directional dipolar moment to simulate the spectrum.

In order to simulate the RAIR spectra, one new code was developed. The VASP code computes the dipole moment components at each nuclear configuration used for the construction of the Hessian matrix. Then, the IRIAN code [121] takes these dipole moment values and estimates the numerical moment derivatives ($^{\delta\mu_z}/_{\delta\Delta r_i}$), on the basis of the atomic cartesian displacements. Finally, the dynamic dipole moments of the vibrational modes are computed to estimate the intensities of the RAIR spectra. Moreover, it allows to make isotopic substitution. During this thesis, it was also implemented the possibility of simulating the IR spectrum of gas phase molecules.

2.4.3.1 The Metal Surface Selection Rule.

The Metal Surface Selection Rule (MSSR) states that only those vibrational modes that significantly change the dipole moment in the direction perpendicular to the surface carry noticeable intensity (it can be directly observed in equation 2.14). Invoking this affirmation, it is often applied to determine whether a given bond of any adsorbed molecule is parallel or not to the surface. If the stretching band of a particular bond is not present on the IR spectrum, one assumes that this bond lies parallel to the surface, whereas if the band appears on the spectrum, the bond is perpendicular to the surface. However, this reading of the MSSR is simple and we will find some examples in this thesis

UNIVERSITAT ROVIRA I VIRGILI
ORGANIC MOLECULES ON METAL SURFACES: FORECASTING STRUCTURES AND SPECTRA
Benjamí Martorell Masip
ISBN:978-84-691-9747-9 /DL: T-1259-2008

that contradict this rule. So, this should be renamed as "*reduced-MSSR*".

The intensity of a fundamental band is proportional to the square of the variation of the dipolar moment in the VNM. VASP does not calculate directly the intensity of the transitions, but does the dipolar moment:

$$I^k \alpha \left(\frac{\delta \mu_z}{\delta Q^k}\right)^2 = \left(\sum_{i=1}^{3N} \frac{P_{ki}}{\sqrt{m_i}} \frac{\delta \mu_z}{\delta \Delta r_i}\right)^2 ; \qquad C_{Ki} = \frac{P_{ki}}{\sqrt{m_i}} \tag{2.14}$$

The intensity depends on the mass-weighted normal mode coefficients and on the dipole moment first derivatives. The z-subindex in the dipolar moment indicates that the intensity in RAIR spectrum is proportional to the variation of the dipolar moment in the z-direction (vector perpendicular to the surface plane).

If one pure A−B bond stretching mode is assumed for a polyatomic molecule adsorbed on the surface, the expression of the intensity of the vibrational mode if the A−B is parallel to surface (will be labelled as "h") or perpendicular to surface (will be labelled as "v") is, respectively, as follows:

$$I(h) = C_{h,A}\mu'_z(\triangle xA) - C_{h,B}\mu'_z(\triangle xB) \tag{2.15}$$

$$I(v) = C_{v,A}\mu'_z(\triangle zA) - C_{v,B}\mu'_z(\triangle zB) \tag{2.16}$$

From equations 2.15 and 2.16, the condition of an inactive stretching mode emerges easily:

$$C_{h,A}\mu'_z(\triangle xA) = C_{h,B}\mu'_z(\triangle xB) \tag{2.17}$$

$$C_{v,A}\mu'_z(\triangle zA) = C_{v,B}\mu'_z(\triangle zB) \tag{2.18}$$

It is important to note that dipole derivatives can be positive or negatives, and conditions 2.17 and 2.18 will only be satisfied when both dipole derivatives will have the same sign (or both have zero value). Obviously, when the centre of a bond of diatomic homonuclear molecule is placed on the centre of a symmetric active centre, the condition 2.17 will always be satisfied because symmetry imposes $C_{h,A} = C_{h,B}$ and $\mu'_z(\triangle xA) = \mu'_z(\triangle xB)$.

If $C_{h,A}$ and $C_{h,B}$ are similar, but $\mu'_z(\triangle xA)$ and $\mu'_z(\triangle xB)$ have opposite sign, the corresponding fundamental stretching band will be infrared active,

UNIVERSITAT ROVIRA I VIRGILI
ORGANIC MOLECULES ON METAL SURFACES: FORECASTING STRUCTURES AND SPECTRA
Benjamí Martorell Masip
ISBN:978-84-691-9747-9 /DL: T-1259-2008

and, the more polarised the bond is, the larger its intensity. This is the case of propyne adsorbed on Cu(111) with its methyl group being deuterated (in order to decouple the C−C stretching mode from the symmetric CH_3 deformation) [96], where the $\mu'_z(\triangle xC1)$ is -0.21 e^- and $\mu'_z(\triangle xC2)$ is 0.28 e^-. When each value is multiplied by the corresponding mass-weighted normal mode coefficients (both coefficients have opposite sign and similar values) the square of this sum of products gives almost the value of the final intensity.

For a bond perpendicular to the surface, symmetry is not able to force a band to be inactive, as we saw above in the case of a bond parallel to the surface, neither on the normal mode coefficients nor on the z-dipole derivatives. Cases where condition 2.18 is satisfied is difficult to be found. Therefore, it is difficult for a perpendicular bond to satisfy this condition, and it is understandable that the "reduced-MSSR" assumes a bond perpendicular to the surface to be IR active. One case where condition 2.18 is accomplished will be presented in chapter 4, section 4.2.3.2, where vinylcarbene in its C1-trans structure presents a perpendicular C−C stretching mode. This is inactive because $\mu'_z(\triangle xC2)$ is -0.20 e^- and $\mu'_z(\triangle xC2)$ is -0.17 e^- and coefficients are similar in value but have different sign, so the intensity of this band will be almost zero.

So only when symmetry restrictions impose that a pure stretching mode is inactive, it can be predicted without mistake that the corresponding pure stretching mode will be inactive.

2.4.4 Projected density of states. Bond analysis.

One of the principal aims of computational chemistry is to understand how chemical bonds are created and how the molecules interact. Density of states (DOS) is the representation of the number of states occupied in a specified energy. The problem is that we do not know whom they belong to. This is a consequence of using plane-waves, that are delocalised and belong to no atom.

This can be solved projecting DOS into the spherical harmonics, which belong to each atom. These spherical harmonics orbitals have a specific radius, called Wigner-Seitz radius. Wigner-Seitz radius depends on the element and the chemical embedding of every atom.

Projected density of states (PDOS) allows us to analyse the bands implied in the bonds. Charge transfers, ionic interactions and covalent interactions can be analysed on the displacement and intensity changes of the bands.

UNIVERSITAT ROVIRA I VIRGILI
ORGANIC MOLECULES ON METAL SURFACES: FORECASTING STRUCTURES AND SPECTRA
Benjamí Martorell Masip
ISBN:978-84-691-9747-9 /DL: T-1259-2008

2.4.5 Computational details.

The results presented in chapters 3, 4 and 5 have been obtained using the VASP code. It has already been commented how VASP works, so in this section only the specific computational details for every system will be commented.

The effect of the core electrons on the valence ones is described by the PAW method. A tight convergence of the plane-wave expansion is obtained with a cut-off of 500 eV in all cases. The GGA was used with the functional PW91. In all calculations, the positions of the ions are relaxed by a conjugate-gradient algorithm or a quasi-newton algorithm until the forces are smaller than 0.02 $^{eV}/_{\text{Å}}$. The electronic energy is reached by an iterative self-consistent field (SCF) method until differences are smaller than 10^{-6} eV. As several unit cells have been used, different girds of Monkhorst-pack special k-points have been used.

Chapter 3. In this chapter, two different unit cells have been used to reproduce the Ag(110) and Au(110) surface: 1×4 and 2×4. The k-points grids used are 12×4×1 and 6×4×1 for both unit cells, respectively. The geometry optimisation includes all degrees of freedom of the adsorbed molecules and the uppermost layer of the metal.

Chapters 4 and 5. In these chapters calculations have been performed on three different unit cells to model the (111) surface of Cu, Pt, Pd, and Rh: 2×2, 3×3, and 4×$\sqrt{3}$. The k-points grids used are 7×7×1 for 2×2 and 3×3 unit cells and 3×7×1 for 4×$\sqrt{3}$ unit cell, respectively. The geometry optimisation includes all degrees of freedom of the adsorbed molecules and the two uppermost layers of the metal.

Once the equilibrium geometry of each system is obtained, the vibrational frequencies and the corresponding normal modes have been calculated using the harmonic approach. The Hessian matrix elements have been obtained by numerical differences of the analytical gradients, with ±0.02 Å displacements for each atomic cartesian coordinate. In order to simplify the treatment, the coupling of the molecular vibrations and the surface phonons was neglected. The IR intensities have been calculated using the IRIAN external code.

The projection of density of states has been carried out for systems of chapter 3. The Wigner-Seitz radii for projections have been reoptimised in order to obtain the best orbital occupation on each atom. The values for these radii are: 1.70 Å for Ag and Au, 1.45 Å for S, 1.5 Å for Se, 1.05 Å for C, and 0.75 Å for

UNIVERSITAT ROVIRA I VIRGILI
ORGANIC MOLECULES ON METAL SURFACES: FORECASTING STRUCTURES AND SPECTRA
Benjamí Martorell Masip
ISBN:978-84-691-9747-9 /DL: T-1259-2008

H.

2.5 Cluster calculations using StoBe. NEXAFS spectra.

StoBe (**Sto**ckholm-**Be**rlin acronym) [33] is a code developed by G.M. Pettersson (Stockholm University, Sweden) and K. Hermann (Fritz-Haber-Institut, Berlin, Germany) from a version of the DeMon package. StoBe is a code to deal with very large molecules and surface clusters with specific implementations for inner-shell spectroscopies and has been used in this thesis to simulate the NEXAFS spectra.

StoBe works in very different way that VASP does, although it uses DFT methodology, like VASP. StoBe does not calculate periodical systems, but it does local calculations (A good comparison of cluster and periodical models can be found in references [34, 106, 137]). Logically, it does not use plane-wave basis set, but it is a realisation of the Linear Combination of Gaussian Type Orbitals to get Molecular Orbitals of the Kohn-Sham DFT equations. NEXAFS spectrum is a characteristic of the core electrons of an atom.

2.5.1 Core level spectroscopies: NEXAFS spectra.

The reason why X-ray Absorption Spectra (XAS, in particular Near-Edge X-ray Absorption Fine Structure or NEXAFS) is collected under the name of core-level spectroscopies is that they involve the creation of a core hole and the measurement of the transitions from it to higher unoccupied energetic levels.

Due to the localised nature of the core-hole, we are capable of investigating the local electronic structure around a specific atom in an element-specific way. It is specially this characteristic, which makes it possible to separate the contributions of adsorbates from their substrates, that has made this technique particularly useful in the study of chemo- and physisorbed molecules on surfaces [35, 138].

The XAS transition is furthermore subjected to the dipole selection rules, so only transitions between states whose angular momentum differ by one unit will have non-zero probability ($\Delta l = \pm 1$); this means that if the initial orbital is the C 1s orbital, only transitions to orbitals with local p-character are allowed. In the case of C 1s orbital, the first x-ray absorptions is around 285 eV if double

UNIVERSITAT ROVIRA I VIRGILI
ORGANIC MOLECULES ON METAL SURFACES: FORECASTING STRUCTURES AND SPECTRA
Benjamí Martorell Masip
ISBN:978-84-691-9747-9 /DL: T-1259-2008

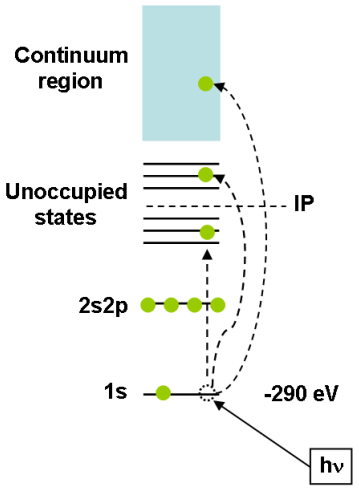

Figure 2.4: Possible electronic transitions of a C 1s electron to higher energetic levels due to the absorption of a photon.

or triple bonds are present in the system and the ionisation potential (IP) is around 290 eV [36, 116, 120]. Above IP value, NEXAFS can become a width, bad-defined spectrum, due to Rydberg orbitals and the continuous states. In figure 2.4 it can be observed the transition of a C 1s electron to unoccupied states, under or above the IP of the C 1s electron.

2.5.2 Core electron excitation energies and NEXAFS intensities calculation: Transition potential approximation.

The first step to calculate the energies of core electrons excitation to molecular orbitals near IP, is to calculate the geometries of the minima on the potential hypersurface. The aim of the use of StoBe is not calculating these minima, but it is to simulate the NEXAFS spectra of the minima obtained by VASP calculations.

The classical way to calculate the energies of XAS would be the calculation of the difference of energies between the final and the initial states. The problem is that a big amount of final states are possible, so the number of calculations would be enormous. Another problem is mathematical, because of the difficulty of convergence of a non-ground state configuration in DFT.

The way to avoid these problems is using the Slater's transition state po-

UNIVERSITAT ROVIRA I VIRGILI
ORGANIC MOLECULES ON METAL SURFACES: FORECASTING STRUCTURES AND SPECTRA
Benjamí Martorell Masip
ISBN:978-84-691-9747-9 /DL: T-1259-2008

tential (TP) [37, 38]. In this approximation an artificial state that is halfway between the groundstate of an atom or molecule and an excited state. In this approximation a half core-hole is created in the inner shell of an atom or molecule. The connection to the orbital binding energy is instead through a derivative of the total energy with respect to changes in orbital occupation numbers, n_i:

$$\varepsilon_i = \frac{\delta E}{\delta n_i} \tag{2.19}$$

This transition potential method has been extensively tested and has demonstrated very good results when they are compared with experiments [36, 116, 120]. In the TP method, the final and initial state contributions are treated in a balanced manner, and it has been proven by Taylor expansion that the final state relaxation effects are taken care of up to the second order for occupation number $n_i = 0.5$.

The DFT TP calculations assume a frozen molecular ion density and thus neglect electronic relaxation on the molecular ion core upon adding the excited electron. Therefore, in a second step the excitations energies are reevaluated by ΔKohn-Sham (ΔKS) DFT calculations [40, 141] to obtain more accurate excitation energies which reflect the correct amount of the electronic relaxation connected with the excitation process. This process corrects the energies by the difference of energy between Ionisation Potential (IP) for TP calculation and the real IP, which is obtained by the difference of energy between the system and the system without the core electron. Further, the excitation spectrum is corrected by a rigid shift of 0.2 eV to higher energies to take into account relativistic effects contributing to core excitation. Recently a review of these relativistic effects has been published, giving a surprising low-value of only 0.08 eV for C 1s core electrons [41].

Once the transition energies are calculated, for generating a spectrum it is necessary to calculate the intensities of the transitions. In the dipole approximation, the intensity of a transition can expressed as [38, 39]:

$$I_{if} = \frac{2}{m\hbar\omega} \left|\langle \Psi_i \left|\bar{e}\cdot\bar{p}\right| \Psi_f\rangle\right|^2 \tag{2.20}$$

Where $\bar{p}$ is the sum of the linear momenta of the electrons and $\bar{e}$ is the polarisation vector. It is also possible rewrite this formula using the transition momentum:

$$I_{if} = \frac{2}{3}\omega_{if} \left|\langle \Psi_i \left|\bar{\mu}\right| \Psi_f\rangle\right|^2 \tag{2.21}$$

UNIVERSITAT ROVIRA I VIRGILI
ORGANIC MOLECULES ON METAL SURFACES: FORECASTING STRUCTURES AND SPECTRA
Benjamí Martorell Masip
ISBN:978-84-691-9747-9 /DL: T-1259-2008

This expression can be simplified when the core-hole is created in the initial 1s orbital, and the final state is an unoccupied state, a Rydberg orbital or the continuous region:

$$I_{if} = \frac{2}{3}\omega_{if} \left|\langle \phi_{1s} \left|\bar{\mu}\right| \phi_f \rangle\right|^2 \tag{2.22}$$

2.5.3 Computational details.

The StoBe package has been used for calculations in chapter 6. Here we apply DFT together with the GGA RPBE exchange-correlation functional. All gas phase molecules and adsorbed propyne have been optimised. In the case of adsorbed $CHCHCH_2$ it was used the geometry obtained in VASP calculations. The cluster atoms were kept fixed at the interatomic distance of 2.56 Å. A two-layers cluster of 59 atoms was our surface model (see figure 2.2(b)). The 30 Cu atoms of the second layer and the 15 atoms of the boundary of the first layer were treated with one-electron electronic core potentials (ECP) describing a Cu 1s-3d core together with appropriate 4s,p valence bases [173]. For the other 14 atoms, which belong to the centre of the first layer, are accounted by all-electron double-zeta valence plus polarisation (DZVP)-type basis sets [172]. The use of one-electron ECP for environmental atoms has been tested extensively and it has been found to permit substantial increase in the size of the cluster without introducing serious artifacts [36, 116, 120]. For carbon atoms no ECP were used for ground-state calculations, using an all-electron triple-zeta valence plus polarisation (TZVP) basis set in a [4s,3p] contraction with one added d and with one p function and contracted to [3s,1p] for hydrogen atoms [169].

The calculation of carbon core electron excitations were carried out using the Slater's transition potential. The orbital basis of the corresponding ionisation centre is of all-electron IGLO-III quality [170], yielding an improved representation of relaxation effects in the inner atomic shells. For the remaining carbon centres ECPs describing the C 1s core and appropriate valence basis sets were applied. The use of ECPs simplified the identification of the core hole orbital while it has only negligible effects on the computed excitation spectrum. Besides, the calculations of carbon core electron excitations include a large diffuse even-tempered [19s,19p,19d] basis set [171] located at the excitation centre which accounts for unbound resonance wave functions within the core electron region.

Then the NEXAFS spectrum was generated by the convolution of all excitations, with a gaussian mode shape. The bandwidth was about 0.8 eV under

UNIVERSITAT ROVIRA I VIRGILI
ORGANIC MOLECULES ON METAL SURFACES: FORECASTING STRUCTURES AND SPECTRA
Benjamí Martorell Masip
ISBN:978-84-691-9747-9 /DL: T-1259-2008

IP and it increased until 5 eV above IP zone.

UNIVERSITAT ROVIRA I VIRGILI
ORGANIC MOLECULES ON METAL SURFACES: FORECASTING STRUCTURES AND SPECTRA
Benjamí Martorell Masip
ISBN:978-84-691-9747-9 /DL: T-1259-2008

Chapter 3

TTF and TSF adsorbed on metal surfaces.

An example of interaction through lone-pair electrons.

As it was explained in chapter 1, tetrathiafulvalene (TTF) is the base of a new generation of materials. Superconductors, semiconductors, molecular switches... can be obtained from the derivatives of this molecule. So it is very interesting to know its molecular and electronic structure and how they can change when derivatives are synthetised.

The aim of this thesis is to study the interaction of different adsorbates on several surfaces. The special features of TTF induced us to study the interaction between it and its experimental supports. In the case of TTF and its derivative tetraselenafulvalene (TSF), it was desired to study their interaction with two inert substrates: Ag and Au. The first system to study was TTF adsorbed on Ag(110) surface. The next one was the adsorption of TTF on Au(110) surface, and finally, to compare with another compound of the same family, we have studied the adsorption of TSF on Ag(110).

The adsorption energy (E_{ads}) was calculated to evaluate the interaction of the adsorbate with the surface. To have a better understand on this interaction, density of states (DOS) and projected density of states (PDOS) were analysed. Besides, vibrational frequencies were calculated to ensure the existence of minima. Changes in structural parameters, vibrational spectra and in electronic

UNIVERSITAT ROVIRA I VIRGILI
ORGANIC MOLECULES ON METAL SURFACES: FORECASTING STRUCTURES AND SPECTRA
Benjamí Martorell Masip
ISBN:978-84-691-9747-9 /DL: T-1259-2008

structure can help us to explain the interaction between the adsorbate and the support.

So, the objectives of this study were:

- *The study of a charge donor with a metallic substrate. The charge donor is one organic, special molecule, TTF, and one of its derivatives, TSF. The substrates chosen are Ag(110) and Au(110), because they are experimentally used to grow the thin films of TTF salts.*
- *To establish the adsorption sites, the adsorption energy and the distortion of the substrate when it is adsorbed.*
- *To study different unit cells and changes of adsorption sites when coverage changes.*
- *To calculate vibrational frequencies and to simulate RAIR spectra.*
- *To discover why Ag(110) and Au(110) are good substrates for TTF.*
- *To simulate theoretical STM images when the molecule is adsorbed.*

This study tries to explain how TTF and TSF interact with the metallic substrate. I introduce now that interaction between adsorbate and substrate is through the lone-pair electrons of sulphur atoms (or selenium atoms).

UNIVERSITAT ROVIRA I VIRGILI
ORGANIC MOLECULES ON METAL SURFACES: FORECASTING STRUCTURES AND SPECTRA
Benjamí Martorell Masip
ISBN:978-84-691-9747-9 /DL: T-1259-2008

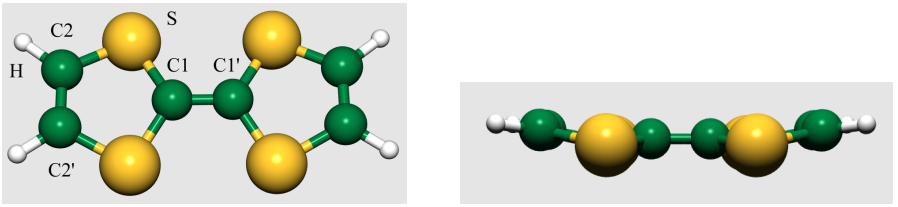

(a) (b)

Figure 3.1: TTF molecule. Every non-equivalent atom is labelled.

3.1 TTF in gas phase.

The aim of this chapter part is not to make a deep study of this molecule in gas phase, because it has already been done in previous works, but the aim is to compare our results with the other ones that are already reported.

3.1.1 Structural parameters.

In the past it was thought TTF was a flat molecule (D_{2h} symmetry). Nowadays a lot of publications have demonstrated TTF is not a flat molecule, but it has a boat-form (C_{2v} symmetry). In figure 3.1, TTF molecule is presented and we can see it is not a flat one. When vibrational frequencies were calculated for flat, optimised TTF, one imaginary frequency appeared, which corresponded to the bending out-of-plane of the molecule. That indicated it was a transition state (TS) between two stable minima. The potential barrier of this TS is 0.3 kcal·mol^{-1}, with an imaginary frequency of 55i cm^{-1}. This value is among all other values already published in literature. In table 3.1 a summary of published values is presented, and it can be observed, our 0.3 kcal·mol^{-1} value is in the range of 0.026 kcal·mol^{-1} for B3LYP [42] calculations and 0.92 for BP [44].

Another important feature of this molecule is that its cation (TTF^{+}) has a D_{2h} geometry. So, flat TTF is not stable, but it is TTF^{+}. This feature is very important, because the bending out-of-plane of the molecule is believed to be related with the conductivity of TTF salts; it has been studied the coupling of the bending movement of two TTF molecules and the electrons transfer between both TTF molecules [46]; they realised that the oxidation of TTF brings to a flat specie, which can be $TTF^{+0.5}$, TTF^{+1} or TTF^{+2}. So there is a direct relationship between the oxidation facility of TTF and the easy path to become flat, because the conformational energy to become flat is almost a non-barrier

UNIVERSITAT ROVIRA I VIRGILI
ORGANIC MOLECULES ON METAL SURFACES: FORECASTING STRUCTURES AND SPECTRA
Benjamí Martorell Masip
ISBN:978-84-691-9747-9 /DL: T-1259-2008

Table 3.1: Structural parameters of TTF in gas phase.

	VASP	B3LYP/MP2[43]	CASSCF[44]	LDA/BP[45]	[e](GED)
[a]d(C1−C1')	1.36	1.35/1.357	1.345	1.345/1.361	1.358
d(C1−S)	1.77	1.788/1.768	1.78	1.733/1.777	1.767
d(S−C2)	1.77	1.764/1.752	1.762	1.721/1.764	1.753
d(C2−H)	1.09	1.04/1.084	1.082	1.095/1.092	1.105
d(C2−C2')	1.34	1.337/1.345	1.36	1.339/1.351	1.348
[b]α(C1'−C1−S)	122.8	123.3/122.9	123.1	122.7/122.4	122.9
α(C1−S−C2)	95.5	94.7/93.9	94.7	94.4/93.6	94.5
α(S−C2−C2')	117.4	118/117.5	117.9	117.2/117.9	117.6
α(S−C2−H)	118.6	117.1/117.8	117.6	117.9/117.5	117.8
[c]θ	14.35	9.9/18.2	10.3	17/15	13.5
[d]ΔE	0.3	0.026/0.53	0.03	0.46/0.92	/

[a]d: distances (Å); [b]α: angles (degrees); [c]θ: bending angle (degrees); [d]ΔE: potential barrier (C_{2v}-D_{2h}; kcal·mol^{-1}); [e]GED: gas electron diffraction.

process.

TTF geometrical parameters are also given in table 3.1. Our results, obtained with VASP code, compare very well with the other previously reported. For C=C bonds, the central is around 1.36 Å, and the C=C bonds in the extreme of TTF are around 1.34 Å. In the case of ethene, C=C bond distance is around 1.34 Å, and for benzene, C=C bond distance is around 1.40 Å. These distances indicate the real double bond character of C=C bonds in TTF. This is coherent with the fact TTF is not flat, so a non-aromatic molecule. We got a C−S distance around 1.77 Å in all cases. It can be compared with C−S bond in the easiest molecule possible $S(CH_3)_2$, which is around 1.75 Å.

As can be seen in table 3.1, all our results compare very well with the previously reported and the experimental ones. Our bending angle is the most similar to the experimental one, and distances and angles are almost equal. For the potential barrier no experimental data was found, but all values are less than 1 kcal·mol^{-1}, indicating the process has no conformational barrier. This can explain why TTF is a great charge donor. *Ersan et al.* have studied the effect of some TTF derivatives and some great electrons acceptors [47]. The electrons transfer must also have a relationship with the TTF electronic structure, as was explained in other publications [44, 48].

UNIVERSITAT ROVIRA I VIRGILI
ORGANIC MOLECULES ON METAL SURFACES: FORECASTING STRUCTURES AND SPECTRA
Benjamí Martorell Masip
ISBN:978-84-691-9747-9 /DL: T-1259-2008

3.1.2 Vibrational frequencies calculation.

The calculation of vibrational frequencies is important to ensure that our structure is a minimum. Besides, we can simulate the IR spectrum and compare it with experimental results. Some papers have already been written about this topic, and most bands have been assigned.

If VNM are decomposed in their irreducible representations (C_{2v}), we get [63]:

$$\Gamma_{TTF} = 10A_1 \oplus 9A_2 \oplus 8B_1 \oplus 9B_2 \tag{3.1}$$

This means TTF has 36 VNM, but those that belong to A_2 symmetry do not produce variation in dipolar moment, so they will not be observed experimentally in IR spectrum (but they will in Raman spectrum). In table 3.2 are presented the results of our frequencies calculations[1]. The values of frequencies previously reported [49] are given in table 3.3. Besides, hessian matrix elements and VNMs were recalculatedfor fully deuterated TTF (TTF-d4) were obtained.

Bozio et al. reported experimental TTF spectrum and the assignation of the bands [49]. Besides, in literature have been found TTF's salts spectra [50]. All them can be compared with figure 3.2, where we present theoretical TTF spectrum in gas phase. The VNM assignation of this last work was not very accurate, and some recent studies, helped by theoretical calculations, have improved the quality of the assignation [42, 43]. *Liu et al.* calculated vibrational frequencies for some derivatives of TTF, among them was TTF-d4 [43]. *Katan* gives the graphical figures of VNM of $TTF^{+0.5}$, which are similar for TTF [42].

In figure 3.3 experimental TTF spectrum is presented [75], but it is in solid phase. Despite being in another phase, we can see that it can be compared quite good with our theoretical TTF spectrum. Around 3000 cm^{-1} there is an intense band, more intense than in our simulated spectrum. Around 1500 cm^{-1} the same effect happens, and for 800 and 500 cm^{-1} two intense bands appear, like in our case. Despite this good agreement, we have to realise some other bands appear due to solid state effects.

C−H stretching modes are obtained at 3141, 3142 and 3161(2) cm^{-1}, which are a bit higher than the experimental values of 3072 (2), 3083 and 3108 cm^{-1}, due to the anharmonicity existing in real molecules. For VNM corresponding to C=C stretching, we obtained the values of 1551, 1528 and 1513 cm^{-1}, which

[1] Terminology used for VNM:
ν: stretching; δ: bending in-plane or scissoring; ρ: rocking; τ: twisting; ω: wagging; γ: bending out-of-plane.
In figure 7.1 on page 277 are presented the vibrational modes.

UNIVERSITAT ROVIRA I VIRGILI
ORGANIC MOLECULES ON METAL SURFACES: FORECASTING STRUCTURES AND SPECTRA
Benjamí Martorell Masip
ISBN:978-84-691-9747-9 /DL: T-1259-2008

Table 3.2: Calculated vibrational frequencies of TTF. Changing VNM for TTF-d4 are in brackets (Symbol A references to assignation for TTF).

Symmetry	TTF	Assignation	TTF-d4
A_1	3161	$\nu_{\text{C-H}}$ asym.	2357
	1551	$\nu_{\text{C=C}}$	1538
	1513	$\nu_{\text{C=C}}$	1492
	1072	$\delta_{\text{C-H}}$	769
	729	$\nu_{\text{C1-S}}$ sym.	713
	613	$\omega_{\text{C-H}}$	480 (A + $\omega_{\text{C-D}}$)
	476	A: $\nu_{\text{C1-S}}$ sym. + $\nu_{\text{C2-S}}$ sym.	463 (A - $\omega_{\text{C-D}}$)
	272	$\omega_{\text{C1-C1'}}$ + $\nu_{\text{C1-S}}$ sym.	271
	228	$\omega_{\text{C1-C1'}}$ - $\nu_{\text{C1-S}}$ sym.	226
	62	$\omega_{\text{C-H group}}$	58
A_2	3141	$\nu_{\text{C-H}}$ asym.	2317
	1236	$\rho_{\text{C-H}}$	1035
	950	$\nu_{\text{C2-S}}$ asym.	935
	826	$\tau_{\text{C-H}}$	652
	786	$\rho_{\text{C-H group}}$ + $\nu_{\text{C1-S}}$	696
	608	$\nu_{\text{C1-S}}$ asym.	591
	419	$\tau_{\text{C-H group}}$	381
	304	$\rho_{\text{half TTF}}$	300
	78	$\tau_{\text{S-C-H group}}$	78
B_1	3142	$\nu_{\text{C-H}}$ sym.	2317
	1232	$\rho_{\text{C-H}}$	1019
	830	$\tau_{\text{C-H}}$ + $\nu_{\text{C1-S}}$ sym.	824 ($\nu_{\text{C1-S}}$ sym.)
	821	$\tau_{\text{C-H}}$ + $\nu_{\text{C1-S}}$ sym.	652 ($\tau_{\text{C-H}}$)
	781	$\rho_{\text{C-H group}}$+ $\nu_{\text{C1-S}}$ asym.	690
	614	$\nu_{\text{C1-S}}$ asym.	596
	422	$\tau_{\text{C-H group}}$	383
	99	$\delta_{\text{half TTF}}$	96
B_2	3161	$\nu_{\text{C-H}}$ asym.	2356
	1528	$\nu_{\text{C=C}}$	1494
	1072	$\delta_{\text{C-H}}$	766
	778	$\nu_{\text{C2-S}}$ sym.	779 ($\delta_{\text{C-H}}$ + $\nu_{\text{C2-S}}$ sym.)
	725	$\nu_{\text{C1-S}}$ sym.	711
	612	$\omega_{\text{C-H}}$	503 ($\omega_{\text{C-H}}$ + $\tau_{\text{C1-C1'}}$)
	498	$\tau_{\text{C1-C1'}}$	464 ($\omega_{\text{C-H}}$)
	417	$\nu_{\text{C1-S}}$ sym. + $\nu_{\text{C2-S}}$ sym.	416
	100	$\omega_{\text{C-H group}}$	95

UNIVERSITAT ROVIRA I VIRGILI
ORGANIC MOLECULES ON METAL SURFACES: FORECASTING STRUCTURES AND SPECTRA
Benjamí Martorell Masip
ISBN:978-84-691-9747-9 /DL: T-1259-2008

Table 3.3: Vibrational frequencies of TTF corresponding to previously reported and experimental values. Values are given in cm^{-1}.

Symmetry	B3LYP[43]	BP-PAW[45]	Exp.[43]	B3LYP[43]	BP-PAW[45]	Exp.[43]
	TTF			TTF-d4		
A_1	3095	3124	3083	2309	2330	2280
	1569	1570	1555	1555	1550	1544
	1524	1523	1528	1502	1500	1504
	1085	1088	1094	778	776	787
	750	755	735	733	739	715
	640	630	639	492	512	492
	478	521	474	474	476	470
	264	284	247	263	281	246
	237	225	244	235	224	229
	30	55	110	28	53	/
A_2	3076	3130	3072	2270	2297	2280
	1249	1237	1258	1058	1061	1057
	987	986	994	968	962	975
	859	843	/	714	711	/
	813	811	800	674	666	715
	620	632	612	604	612	594
	402	422	/	367	383	/
	310	354	308	306	351	305
	80	51	/	80	50	/
B_1	3076	3111	3073	2271	2297	2285
	1246	1243	1254	1037	1045	1040
	860	/	863	853	/	/
	853	834	/	708	706	865
	808	791	794	674	665	703
	630	/	639	612	/	603
	404	423	414	369	380	382
	111	/	110	108	/	108
B_2	3095	3128	3108	2309	2327	2337
	1542	1533	1530	1507	1501	1508
	1084	1080	1090	785	797	758
	785	798	781	776	771	779
	747	755	734	731	738	719
	640	619	/	515	503	/
	507	497	/	482	473	/
	434	450	427	432	449	425
	79	105	/	76	100	/

UNIVERSITAT ROVIRA I VIRGILI
ORGANIC MOLECULES ON METAL SURFACES: FORECASTING STRUCTURES AND SPECTRA
Benjamí Martorell Masip
ISBN:978-84-691-9747-9 /DL: T-1259-2008

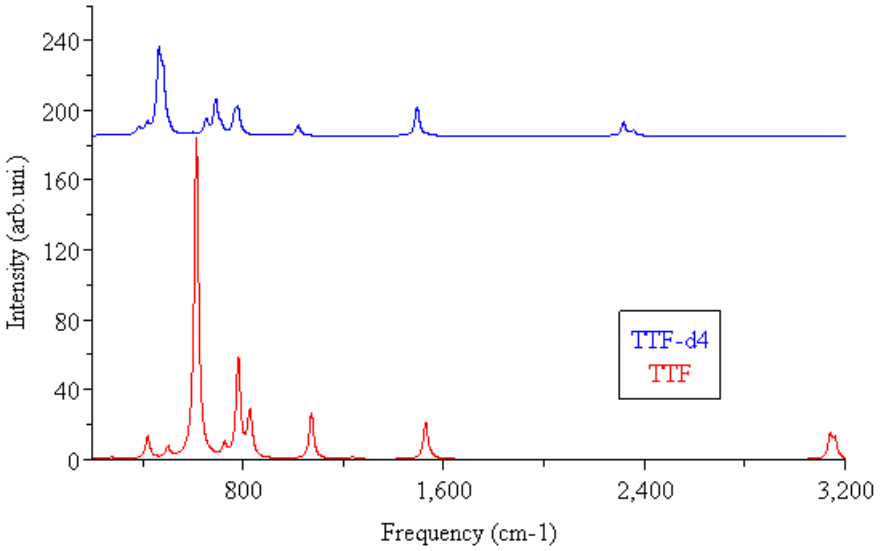

Figure 3.2: Theoretical spectra of TTF and TTF-d4 in gas phase. Red line is TTF spectrum and blue line is for TTF-d4.

approximate very well to the experimental values of 1555, 1542 and 1528 cm^{-1}. Rocking of C−H bonds have values of 1232 and 1236 cm^{-1}, in comparison with experimental values of 1258 and 1254 cm^{-1}. Bending in-plane, also called scissoring, of C−H bonds give values of 1072 (2) cm^{-1}, in front of the experimental values of 1094 and 1080 cm^{-1}. The most intense band in TTF spectrum is the VNM that corresponds to the wagging of C−H group, whose frequency is 613 cm^{-1}, near the experimental value of 639 cm^{-1}.

For TTF-d4 the same analysis is made. The most significant changes respect TTF are those VNM that imply a large displacement of deuterium atoms. C−D stretching modes values decrease to 2317 (2) and 2356 (2) cm^{-1}; experimental values are 2247, 2280 and 2285 cm^{-1}(this means a decrease of 700 cm^{-1} respect to TTF). C=C bond stretching values change in a smaller amount, and 1538, 1494, and 1492 cm^{-1} are obtained in calculations, which compare very well with experimental values of 1544, 1508, and 1504 cm^{-1}. Frequencies of C−D rocking and scissoring are 1035, 1019, 769, and 766 cm^{-1} (this means that they decrease 250 cm^{-1} respect to undeuterated TTF), and the experimental values are 1057, 1040, 787 and 758 cm^{-1}. Waggings of C−D bonds decrease in frequency respect to TTF, and they can couple with the central C=C deformation, so we have two frequencies, one next to the other one that can couple. So we get two frequencies

UNIVERSITAT ROVIRA I VIRGILI
ORGANIC MOLECULES ON METAL SURFACES: FORECASTING STRUCTURES AND SPECTRA
Benjamí Martorell Masip
ISBN:978-84-691-9747-9 /DL: T-1259-2008

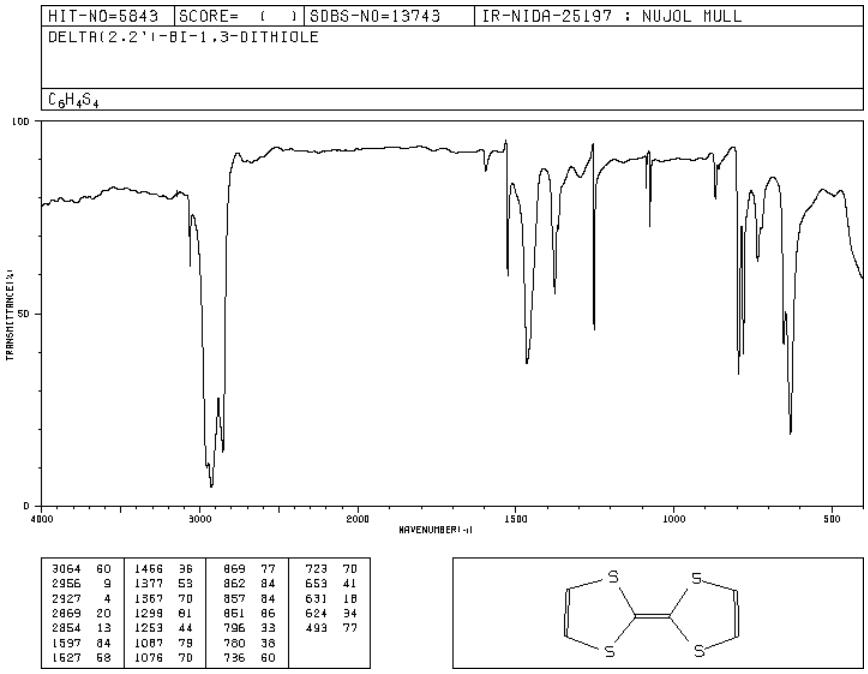

3064	60	1466	36	869	77	723	70
2956	9	1377	53	862	84	653	41
2927	4	1367	70	857	84	631	18
2869	20	1298	81	851	86	624	34
2854	13	1253	44	796	33	493	77
1597	84	1087	78	780	38		
1527	58	1076	70	736	60		

Figure 3.3: Experimental TTF spectrum in solid state.

with high intensity. These are 480 and 463 cm^{-1} for theoretical calculations, and 492 and 470 cm^{-1} for experimental values. We can compare all these values in figures 3.2 and 3.3.

As it can be observed in table 3.3, our results are in good agreement with experimental values. Only C−H (C−D) stretching values are larger than experimental ones, a normal fact when calculations are made in the frame of harmonic approximation. It must be remembered that VNMs with A_2 symmetry are not actives in IR spectrum, but they are in Raman (that is the reason why we have experimental values). If values in table 3.3 are observed, it can be concluded our calculated values are comparable with the other ones previously reported. Theoretical and experimental values compare well with ours, for both the geometrical parameters and the vibrational frequencies.

UNIVERSITAT ROVIRA I VIRGILI
ORGANIC MOLECULES ON METAL SURFACES: FORECASTING STRUCTURES AND SPECTRA
Benjamí Martorell Masip
ISBN:978-84-691-9747-9 /DL: T-1259-2008

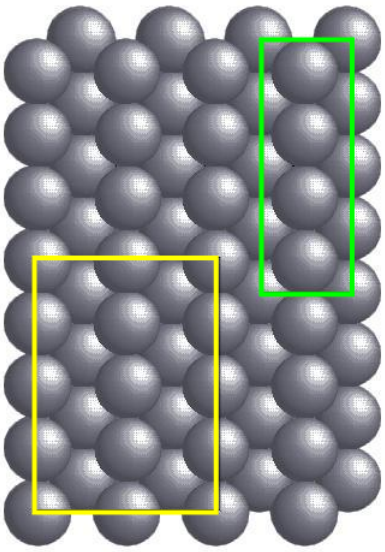

Figure 3.4: Unit cells used to study TTF on Ag(110). In yellow 2×4 unit cell; in green 1×4 unit cell.

3.2 TTF adsorbed on Ag(110).

3.2.1 Geometric parameters.

Silver is a nobel metal that presents a Fm3m structure. Ag(110) surface is presented in figure 3.4. Experimental lattice parameter of silver is 4.0853 Å [61], but we have optimised this value with the same calculation method and have obtained a value of 4.1512 Å, a little bit larger than the experimental one. For our slab model, this value was kept constant, but the uppermost layer of the slab was included in the optimisation.

Several possible geometries and adsorption sites have been computed on Ag(110). For this study two different unit cells have been used, a 1×4 unit cell and a 2×4 unit cell. In figure 3.4 it can be observed both unit cells. For 2×4 unit cell, a coverage of 0.125 is obtained. For 1×4 unit cell, coverage duplicates and becomes 0.25. In the case of 2×4 unit cell the number of possibilities of adsorption are larger than on 1×4 unit cell. On 1×4 unit cell, only possibilities perpendicular to the surface are possible, due to steric effects. In the case of the other unit cell, situations with the adsorbate parallel to the surface are also allowed "*a priori*", due to the major surface area.

UNIVERSITAT ROVIRA I VIRGILI
ORGANIC MOLECULES ON METAL SURFACES: FORECASTING STRUCTURES AND SPECTRA
Benjamí Martorell Masip
ISBN:978-84-691-9747-9 /DL: T-1259-2008

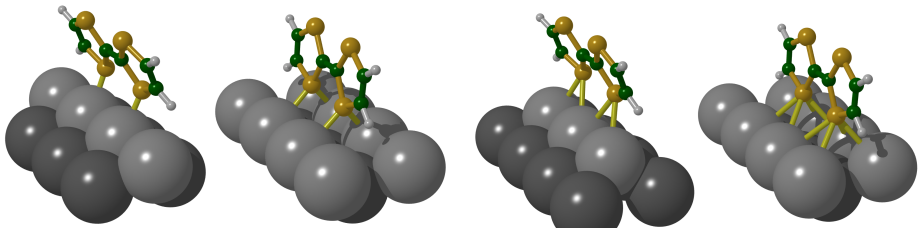

(a) Top site. (b) Long bridge site. (c) Short bridge site. (d) Hollow site.

Figure 3.5: Possible adsorption sites for TTF on Ag(110) 1×4 unit cell.

Now it can be advanced that the stable structures are those that maximises the interaction between sulphur and silver atoms. Lots of possible adsorption sites have been tested. For 1×4 unit cell, four starting adsorbate positions have been computed, which are present in figure 3.5. These adsorption modes can be seen as the interaction of sulphur atoms on top-site (figure 3.5(a)), on large bridge site (figure 3.5(b)), on short bridge site (figure 3.5(c)) and on hollow site (figure 3.5(d)). All these structures present at least a local C_s symmetry.

For 2×4 unit cell these same adsorption modes were also calculated. Moreover, five other adsorption sites parallel to surface were explored, which are presented in figure 3.6. In this case the adsorption sites can be seen as the adsorption of sulphur atoms like in the perpendicular cases. The adsorption of sulphur atoms is on top site (figure 3.6(a)), on large bridge site (figure 3.6(b)), on short bridge site (figure 3.6(c)), on hollow site (figure 3.6(d)), and one special case that is a little bit rotated and cannot be seen as a pure adsorption site (figure 3.6(e)). The adsorption sites (c) and (d) for 2×4 unit cell, can also be seen as the adsorption of a double C=C bond on top or on short bridge sites, respectively. This will be important for the forthcoming discussion in section 3.6.1. Besides, all these structures have a local C_{2v} symmetry (they conserve TTF's local symmetry) except adsorption site 3.6(e), which belongs to a local C_2 symmetry.

Several studies of sulphonated species have been found in literature, being theoretical works less abundant than experimental ones. *Yu et al.* studied the adsorption of H_2S on Ag(111), concluding that this specie adsorbs on the Ag surface, but it is not reactive on it (that's one of the reasons why silver is used as support for sulphonated species when reactivity is not desired) [52]. Other studies have been made on other surfaces, as can be gold (which is also inert for sulphonated species) [53, 54] or copper (which is reactive with sulphonated

UNIVERSITAT ROVIRA I VIRGILI
ORGANIC MOLECULES ON METAL SURFACES: FORECASTING STRUCTURES AND SPECTRA
Benjamí Martorell Masip
ISBN:978-84-691-9747-9 /DL: T-1259-2008

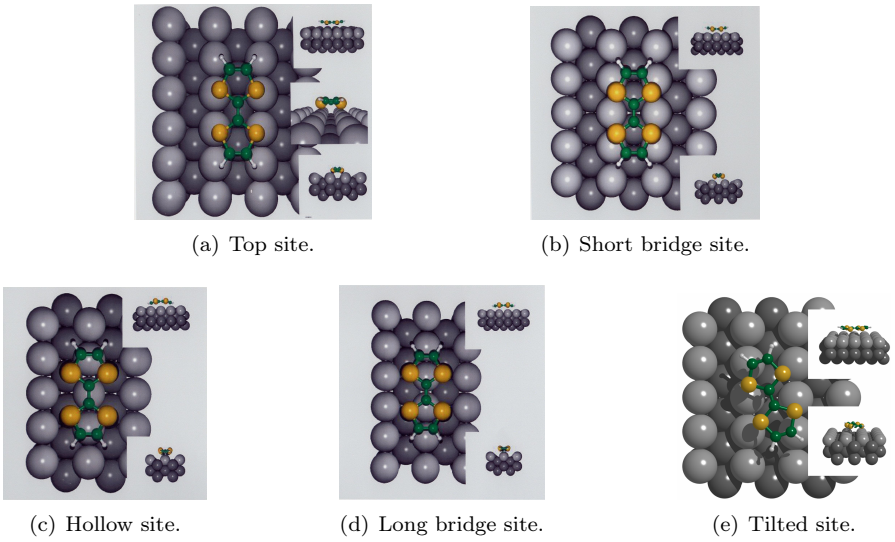

(a) Top site. (b) Short bridge site.

(c) Hollow site. (d) Long bridge site. (e) Tilted site.

Figure 3.6: Possible adsorption sites for TTF on Ag(110) 2×4 unit cell.

species, so would not be a good support for S-containing adsorbates) [55, 56]. A study of TTF adsorbed on silver is available in literature, *Joy et Srinivisan* [57] studied TTF electrochemically deposited on silver (unfortunately they did not work with a specific surface of silver). They reported the FT-SER (Fourier-Transform Surface-Enhanced Raman) spectrum of TTF adsorbed on Ag (the vibrational frequencies could be compared with ours) and they concluded that TTF adsorbs with its sulphur atoms directly bonded to the silver atoms of surface in the regime of high coverage. They also proposed TTF adsorbs on a perpendicular way to surface.

Results for 2×4 unit cell are presented in table 3.4, but only for those structures parallel to surface. For 1×4 unit cell results are presented in table 3.5. Perpendicular species for 2×4 unit cell are not presented because their structures were similar to the 1×4 structures, but none of them was a minimum. At this point, it is also interesting to note that for 2×4 unit cell, only adsorption site (a) is a minimum, the other sites have imaginary frequencies. They are presented in table 3.4 because they are interesting for discussion in section 3.6.1. The adsorption energies in this case go from -6 up to -21 kcal·mol^{-1}. These adsorption energies are big enough to be considered chemisorbed. For this adsorption site (a), four sulphur atoms are interacting with surface, so the real interaction between surface and one sulphur atom is around -5 kcal·mol^{-1}. The

UNIVERSITAT ROVIRA I VIRGILI
ORGANIC MOLECULES ON METAL SURFACES: FORECASTING STRUCTURES AND SPECTRA
Benjamí Martorell Masip
ISBN:978-84-691-9747-9 /DL: T-1259-2008

Table 3.4: Geometrical parameters of adsorbed TTF on Ag(110) using a 2×4 unit cell, corresponding to 5 adsorption sites of figure 3.6. For e) two non-equivalent distances and angles exist.

	Gas phase	3.6(a)	3.6(b)	3.6(c)	3.6(d)	3.6(e)	
[(a)]d(C1-C1')	1.36	1.36	1.36	1.36	1.36	1.36	
d(C1-S)	1.77	1.76	1.76	1.76	1.77	1.76	1.76
d(S-C2)	1.77	1.75	1.75	1.74	1.74	1.75	1.74
d(C2-H)	1.09	1.09	1.09	1.09	1.09	1.09	1.09
d(C2-C2')	1.34	1.34	1.34	1.36	1.36	1.35	
[(b)]α(C1'-C1-S)	122.8	122.6	123.0	123.0	123.0	122.5	122.7
α(C1-S-C2)	95.5	93.9	94.4	93.9	94.9	94.5	94.5
α(S-C2-C2')	117.4	117.4	117.3	117.3	117.6	117.1	118.0
α(S-C2-H)	118.6	117.2	117.3	117.7	117.4	117.7	117.1
[(c)]θ	14.35	10.53	12.74	-17.67	-7.89	7.30	6.00
[(d)]d(S-Ag)	/	2.73	3.18	3.60	3.82	3.02	3.24
[(e)]E_{ads}	/	-20.9	-10.7	-8.6	-6.1	-12.8	

[(a)]d: distances (Å); [(b)]α: angles (degrees); [(c)]θ:bending angle; [(d)]distances to nearest Ag atom; [(e)]E_{ads}: adsorption energy (kcal·mol^{-1}).

most stable site is (a), as it is the one that maximises the interaction between sulphur atoms and Ag surface.

In table 3.4 it can observed that intramolecular distances do not change significantly when TTF is adsorbed respect to gas phase. Central C=C bond and C−H bond distances do not change and remain in values of 1.36 and 1.09 Å after adsorption for all sites. Extreme C=C bonds remain constant at 1.34 Å on adsorption sites (a) and (b), but they increase slightly to 1.35 Å in (d) and (e), and up to 1.36 Å in (c). Those can be compared with C=C bond in ethene that is 1.34 Å, in comparison with benzene that is 1.40 Å. So, C=C bonds in TTF remain as double bonds when it is adsorbed. S−C1 bond always decreases 0.01 or 0.02 Å, except for adsorption site (d) that remains constant at the gas phase value: 1.77 Å. S−C2 bond distance decreases in all cases 0.01 or 0.02 Å respect to the gas phase value, and this decrease makes that S−C distance becomes more similar to that S−C distance of $S(CH_3)_2$ molecule, which is 1.75 Å. Intramolecular angles do not change significantly.

More interesting is the bending angle of TTF. This is the most changing parameter. In the gas phase it has a value of 14.4°. Only for adsorption site (c) this value increases to |17.7°|. For the other adsorption sites this value decreases. This means TTF becomes flatter on surface than in gas phase. The positive or negative value of dihedral angle means about orientation of TTF on

UNIVERSITAT ROVIRA I VIRGILI
ORGANIC MOLECULES ON METAL SURFACES: FORECASTING STRUCTURES AND SPECTRA
Benjamí Martorell Masip
ISBN:978-84-691-9747-9 /DL: T-1259-2008

Table 3.5: Geometrical parameters of adsorbed TTF on Ag(110) on a 1×4 unit cell. For double values, first value is the furthest and the second one is the nearest to the surface.

	Gas phase	3.5(a)		3.5(b)	
d(C1-C1')	1.36	1.36		1.36	
d(C1-S)	1.77	1.76	1.77	1.76	1.77
d(S-C2)	1.77	1.74	1.75	1.74	1.75
d(C2-H)	1.09	1.09	1.09	1.09	1.09
d(C2-C2')	1.34	1.34		1.34	
α(C1'-C1-S)	122.8	123.2	122.1	124.5	120.5
α(C1-S-C2)	95.5	94.8	94.8	94.6	94.4
α(S-C2-C2')	117.4	118.2	117.6	118.5	117.5
α(S-C2-H)	118.6	117.1	116.5	117.2	116.4
θ	14.35	1.3		1.0	
d(S-Ag)	/	2.74		3.03	
E_{ads}	/	-11.1		-8.3	

surface. If it is positive, TTF acquires a boat-like conformation (adsorption site (a), (b) and (e)) on surface, otherwise, if it is negative, it acquires a bridge-like conformation (adsorption site (c) and (d)). These two last adsorption sites are those with a smaller E_{ads}, on the other hand, adsorption sites with a boat-form have the strongest energy adsorption. This can corroborate the study made by *Joy et Srinivisan* [57], because they proposed TTF adsorbs with its sulphur atoms direct to surface, and in the boat-conformation TTF has the smallest Ag−S distances; for bridge-conformation Ag−S distances are longer and TTF interacts with surface through extreme C=C bonds.

For 1×4 unit cell two minima were found. Only these two minima are presented in table 3.5. These minima correspond to figure 3.5(a) and figure 3.5(b).

In table 3.5 adsorption energies for 1×4 unit cell are presented. In the case of adsorption site (a) the E_{ads} is -11.1 kcal·mol^{-1} and for adsorption site (b) -8.3 kcal·mol^{-1}. This means that adsorption site (a), which has a direct interaction between one sulphur atom and one Ag atom, is -3 kcal·mol^{-1} stronger than for adsorption site (b), where every sulphur atom interacts with two Ag atoms. If we take into account that two sulphur atoms interact with surface, the $\frac{E_{ads}}{\text{number sulphur atoms}}$ are around -5.6 and -4.1 kcal·mol^{-1}. These values are similar to the value obtained for 2×4 unit cell, and it seems clear that as more direct is the Ag−S interaction, larger will be the adsorption energy.

As in the case of 2×4 unit cell, intramolecular distances do not change more

UNIVERSITAT ROVIRA I VIRGILI
ORGANIC MOLECULES ON METAL SURFACES: FORECASTING STRUCTURES AND SPECTRA
Benjamí Martorell Masip
ISBN:978-84-691-9747-9 /DL: T-1259-2008

than ±0.02 Å and ±2° respect to the corresponding values in gas phase. This means no significant changes are appreciated in the inner structure of TTF. Only the bending angle changes significantly and decreases down to ∼1°. So, TTF becomes almost flat in this case. This effect has two possible explanations:

1. There is a coverage effect: two near molecules interact themselves and they become flat.

2. TTF gives charge density to surface and becomes a cation, as explained in the section 3.1.1.

These effects can also explain the decrease of this angle on 2×4 unit cell. This fact will be discussed in subsection 3.2.3.

Another important feature of 1×4-top site (3.5(a)) is that it is not strictly perpendicular to surface. If we take the plane of four sulphur atoms, it is 28° tilted respect to surface normal. This can be easily explained on the basis that TTF trends to maximise interaction between lone-pair electrons of sulphur atoms with Ag atoms. The best way to make this interaction stronger is to tilt TTF and move it, because interacting sulphur atoms of TTF are not on a top-site, but they are moved a little bit to a long bridge site, doing this interaction to be stronger.

Finally, S−Ag distances can be a good indicator of the strength of the interaction between S and Ag atom. For 2×4-top and 1×4-top sites this distance is 2.73 and 2.74 Å, indicating a strong interaction between both atoms in both cases, but for 1×4-bridge site this distance increases up to 3.03 Å, indicating that the interaction between both atoms is not as strong as in the case of top sites.

3.2.2 Vibrational frequencies calculations. RAIR spectra simulation.

All vibrational frequencies and their corresponding modes have been computed for all possible adsorption sites to ensure that all obtained adsorption sites were minima on the potential surface. Furthermore, dipolar moments have been computed to evaluate the intensity of fundamental bands in RAIR spectrum, using and external code, IRIAN [121], developed for this purpose. The mass-weighted hessian matrix was recalculated using the IRIAN code to evaluate VNM, vibrational frequencies and intensities of fully deuterated TTF (TTF-d4) adsorbed on Ag(110).

UNIVERSITAT ROVIRA I VIRGILI
ORGANIC MOLECULES ON METAL SURFACES: FORECASTING STRUCTURES AND SPECTRA
Benjamí Martorell Masip
ISBN:978-84-691-9747-9 /DL: T-1259-2008

The most important conclusion that it can be drawn from these calculations is that only three minima for all possible adsorption sites have been found, being the other structures stationary points on the potential surface but not minima. For 2×4 unit cell only one minimum has been found, this can be seen in figure 3.6 (a). For 1×4 unit cell two minima have been found, and they are represented by figure 3.5 (a) and (b), as discussed in section 3.2.1. From here on, in order to simplify nomenclature, we will call them adsorption site 2×4, 1×4-top and 1×4-bridge, respectively. A very important feature is that these three minima are the structures with a lowest energy, and this means we probably have found the absolute minima, because if they were not the most stable ones, that would mean another more stable minimum exists. Only for these three adsorption sites is meaningful to make vibrational analysis.

In table 3.6, the values of vibrational frequencies for TTF when is adsorbed on three different adsorption sites are presented. Instead to give a large number of band intensities, we present the corresponding RAIR spectra of these three minima in figure 3.7. They should be compared with the figure 3.2 and the values of table 3.3 (3.1.2).

It can be observed in table 3.6 that no large changes exist in vibrational frequencies when TTF is adsorbed on Ag(110) (as neither existed for geometrical parameters). Variations are in the range of ± 25 cm^{-1}. For instance, C−H bond stretching frequency decreases from 3161 and 3142 cm^{-1} to 3152 and 3136 cm^{-1} for 2×4, to 3144 and 3110 cm^{-1} for 1×4-top, and to 3145 and 3112 cm^{-1} for 1×4-bridge (this means it decreases $\sim$20 cm^{-1} in all cases). Values for C=C stretching modes decrease from 1551, 1528, and 1513 cm^{-1} to 1525, 1510, and 1484 cm^{-1} for adsorption site 2×4. For other adsorption sites something similar happens. The most important variations in vibrational frequencies belong to the lowest ones, because when TTF adsorbs on Ag(110) its structure, due to an anchorage effect, becomes more rigid, and all these VNM that were very low in frequency, become a little bit stronger.

More important changes are in the intensity of bands. We have to compare figure 3.2 and figure 3.7. The first interesting thing for intensities is that in adsorbed TTF, all intensities decrease respect to gas phase. For adsorption site 2×4 it decreases to half intensity, and for adsorption site 1×4 to tenth. We have to remember that for RAIR spectra only variations in dipolar moment perpendicular to surface produce intensity. For gas phase all directions must be taken into account. This could explain why exists this decrease in the intensity of bands. For adsorption site 2×4, the most intense band is the same as in

UNIVERSITAT ROVIRA I VIRGILI
ORGANIC MOLECULES ON METAL SURFACES: FORECASTING STRUCTURES AND SPECTRA
Benjamí Martorell Masip
ISBN:978-84-691-9747-9 /DL: T-1259-2008

Table 3.6: Vibrational frequencies (cm^{-1}) of TTF in gas phase and adsorbed on the different adsorption sites.

Assignation	TTF gas	2×4	1×4-top	1×4-bridge
$\nu_{\text{C-H}}$ asym.	3161	3152	3144	3145
	3161	3152	3142	3145
$\nu_{\text{C-H}}$ sym.	3142	3136	3113	3113
	3141	3135	3108	3112
$\nu_{\text{C=C}}$	1551	1525	1544	1545
	1528	1510	1528	1530
	1513	1484	1492	1489
$\rho_{\text{C-H}}$	1236	1228	1237	1235
	1232	1226	1234	1233
$\delta_{\text{C-H}}$	1072	1074	1081	1081
	1072	1068	1073	1073
$\nu_{\text{C2-S}}$ asym.	950	953	950	950
$\tau_{\text{C-H}}$ + $\nu_{\text{C1-S}}$ sym.	830	823	831 ($\tau_{\text{C-H}}$)	839($\tau_{\text{C-H}}$)
$\tau_{\text{C-H}}$	826	806	829 ($\tau_{\text{C-H}}$)	837($\tau_{\text{C-H}}$)
$\tau_{\text{C-H}}$ + $\nu_{\text{C1-S}}$ sym.	821	806 ($\tau_{\text{C-H}}$)	821	816
$\rho_{\text{C-H group}}$+ $\nu_{\text{C1-S}}$ asym.	786	787	795	798
	781	782	786	786
$\nu_{\text{C2-S}}$ sym.	778	780	770	767
$\nu_{\text{C2-S}}$ sym.	729	715	731	728
	725	713	727	726
$\nu_{\text{C2-S}}$ asym.	614	602	609	609
$\omega_{\text{C-H}}$	613	613	620	629
	612	607	618	628
$\nu_{\text{C2-S}}$ asym.	608	596	603	603
$\tau_{\text{C1-C1'}}$	498	484	488	489
$\nu_{\text{C1-S}}$ sym. + $\nu_{\text{C2-S}}$ sym.	476	475	460	457
$\tau_{\text{C-H group}}$	422	397	415	419
	419	397	411	414
$\nu_{\text{C1-S}}$ sym. + $\nu_{\text{C2-S}}$ sym.	417	423	421	417
$\rho_{\text{half TTF}}$	304	302	298	302
$\omega_{\text{C1-C1'}}$ + $\nu_{\text{C1-S}}$ sym.	272	289 ($\omega_{\text{C1-C1'}}$)	253 ($\omega_{\text{C1-C1'}}$)	244
$\omega_{\text{C1-C1'}}$ - $\nu_{\text{C1-S}}$ sym.	228	252($\nu_{\text{C1-S}}$ sym.)	242($\nu_{\text{C1-S}}$ sym.)	230
$\omega_{\text{C-H group}}$	100	162	139	122
$\delta_{\text{half TTF}}$	99	119	119	107
$\tau_{\text{S-C-H group}}$	78	135	103	102
$\omega_{\text{C-H group}}$	62	129	100	69
Frustrated trans. and rot.	/	104	74	58
	/	82	62	53
	/	81	44	46
	/	49	35	43
	/	46	23	30
	/	42	14	20

UNIVERSITAT ROVIRA I VIRGILI
ORGANIC MOLECULES ON METAL SURFACES: FORECASTING STRUCTURES AND SPECTRA
Benjamí Martorell Masip
ISBN:978-84-691-9747-9 /DL: T-1259-2008

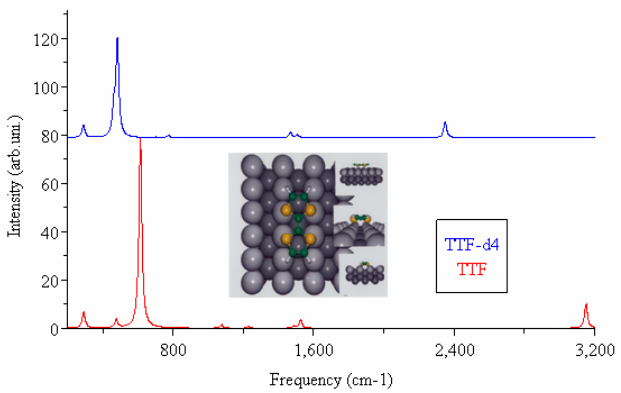

(a) TTF adsorbed on site 2x4.

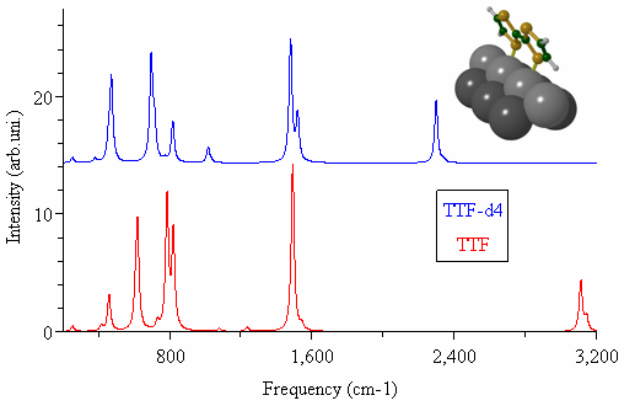

(b) TTF adsorbed on site 1x4-top.

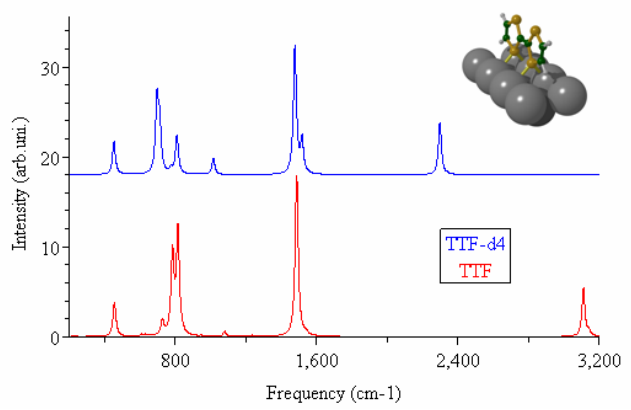

(c) TTF adsorbed on site 1x4-bridge.

Figure 3.7: RAIR spectra of TTF adsorbed on Ag(110). Red line is TTF; blue line is TTF-d4.

UNIVERSITAT ROVIRA I VIRGILI
ORGANIC MOLECULES ON METAL SURFACES: FORECASTING STRUCTURES AND SPECTRA
Benjamí Martorell Masip
ISBN:978-84-691-9747-9 /DL: T-1259-2008

gas phase: the wagging of C−H bond (610 cm^{-1}). Up to 1510 cm^{-1}, no other band remains and all bands present in gas phase, disappear for the adsorption site 2×4. This is because these bands belong to VNM that do not variate the dipolar moment in the normal direction. At 1550 cm^{-1} exists a very weak band, which is associated to the C=C stretching mode. *A priori*, following the surface selection rule, this band should not appear in this spectrum because C=C VNM stretching is parallel to surface. An explanation why this band exists is the coupling with H movements. H moves out of the plane with C=C stretching, so a variation in dipolar moment is generated and the band is visible. More examples about this kind of couplings and variation in dipolar moment will be given in later sections. Around 3150 cm^{-1} C−H stretching are present, but their intensity is quite weak.

A very different situation is found for 1×4 adsorption sites. Both spectra are very similar, but they are really different respect to 2×4-site RAIR spectrum, being the absolute intensities for 2×4-site five times the ones for 1×4 adsorption sites. This is because of the conformational change of TTF when it is adsorbed perpendicular to surface. VNMs that create a variation in dipolar moment are completely different from 2×4-site. The most intense band becomes C=C stretching, around 1550 cm^{-1}. This is not surprising because TTF is perpendicular to surface. No special changes occur around 3150 cm^{-1} (C−H stretching). The second most intense band is around 800 cm^{-1}, and it involves the rocking of C−H group. The biggest difference between 1×4-top and 1×4-bridge, is that 1×4-top is not completely perpendicular to surface, so the most intense band in adsorption site 2×4 still appears at 1×4-top, but not at 1×4-bridge. The way to differentiate their RAIR spectra would be the band around 610 cm^{-1}. If this band were much more intense than all other bands, it could be associated with 2×4 adsorption site. If this band had, more or less, the same intensity as C=C stretching band, it could be proposed 1×4-top, and if no band existed at 610 cm^{-1}, 1×4-bridge would be the adsorption site.

Now we can analyse TTF-d4 when is adsorbed on Ag(110). RAIR spectra are also presented in figures 3.7. Numerical values of vibrational frequencies are presented in table 3.7.

Like for TTF, no big changes are present in vibrational frequencies when TTF-d4 is adsorbed. All changes are in a range of ±25 cm^{-1} once again. For instance, C−D stretching modes decrease from 2357 and 2317 cm^{-1} to 2350 and 2313 in site 2×4, to 2340 and 2298 in site 1×4-top, and to 2341 and 2300 cm^{-1} in site 1×4-bridge. Also C=C stretchings decrease in all cases (only for site 1×4-

UNIVERSITAT ROVIRA I VIRGILI
ORGANIC MOLECULES ON METAL SURFACES: FORECASTING STRUCTURES AND SPECTRA
Benjamí Martorell Masip
ISBN:978-84-691-9747-9 /DL: T-1259-2008

bridge, VNM in gas phase 1494 increase to 1496 cm^{-1}, but it is a meaningless increase).

The most important changes are not about the numerical value of vibrational frequencies, but in the intensity of VNM, like for TTF (see figure 3.7). The analysis is quite similar to the TTF one. For adsorption site 2×4, the most intense band is 480 cm^{-1}, that corresponds to the wagging of C−D bond (as in the case of TTF). Then under 1500 cm^{-1} appears the small band corresponding to C=C stretchings, and finally at 2350 cm^{-1} exist the C−D stretching bands. For 1×4 adsorption sites analysis is also similar to the undeuterated case. On both 1×4 adsorption sites, the most intense band becomes C=C stretching below 1500 cm^{-1}. Around 700 cm^{-1} an intense band appears corresponding to the rocking of C−D bond. The main difference between 1×4-top and 1×4-bridge is the band around 470 cm^{-1}, that corresponds to the wagging of C−D bond. For 1×4-top site, this band is more intense than for 2×4-bridge (around 450 cm^{-1}) and it is not only related to the C−D rocking, but it is a VNM that corresponds to a coupling between the C−D rocking and a movement of sulphur atoms.

It is also interesting to compare adsorbed TTF and TTF-d4. All VNMs that imply a H movement are actually decreased in a numerical value of ∼1.36 approximately when TTF is deuterated, as expected from the mass-weigthed arguments. Moreover, some couplings are broken and other are created, like in case 1×4-bridge band around 450 cm^{-1}.

3.2.3 PDOS analysis and charge transfer. STM images.

In this section an analysis of the density of states (DOS) and its projection on atomic orbitals is made to study the interaction between TTF and the surface, and the possible charge transfer from TTF to surface. In the final part, STM images obtained with a hydrogen-type tip are presented.

Analysing DOS and its variation during adsorption process, it can be seen how the energetic levels of TTF change when it is adsorbed. All properties of a system are described by its electronic structure, in consequence results of DOS analysis must be coherent with results in other sections.

In figure 3.8, the DOS of TTF in gas phase and adsorbed on adsorption site 2×4 are presented. Red line is TTF in gas phase and blue line is adsorbed TTF. As can be observed, TTF in gas phase has clearly defined all energetic levels, it does not have continuous bands of energy. Comparing with some calculations

UNIVERSITAT ROVIRA I VIRGILI
ORGANIC MOLECULES ON METAL SURFACES: FORECASTING STRUCTURES AND SPECTRA
Benjamí Martorell Masip
ISBN:978-84-691-9747-9 /DL: T-1259-2008

Table 3.7: TTF-d4 vibrational frequencies in gas phase and adsorbed on the different adsorption sites.

	Gas	2×4	1×4-top	1×4-bridge
$\nu_{\text{C-D}}$ asym.	2357	2350	2341	2341
	2356	2349	2339	2341
$\nu_{\text{C-D}}$ sym.	2317	2313	2299	2300
	2317	2313	2297	2300
$\nu_{\text{C=C}}$	1538	1506	1520	1519
	1494	1474	1493	1496
	1492	1466	1480	1479
$\nu_{\text{C2-S}}$ asym. + $\rho_{\text{C-D}}$	1035	1025	1034	1033
	1019	1008	1017	1017
$\nu_{\text{C2-S}}$ asym. - $\rho_{\text{C-D}}$	935	938	940	936
$\nu_{\text{C1-S}}$ sym.	824	821	818	811
$\delta_{\text{C-D}}$ + $\nu_{\text{C2-S}}$ sym.	779	780	773	772
$\delta_{\text{C-D}}$	769	771	776	776
	766	765	765	765
$\nu_{\text{C2-S}}$ sym.	713	699	716	713
	711	698	714	712
$\rho_{\text{C-H group}}$+ $\nu_{\text{C2-S}}$ asym.	696	698	702	703
	690	694	697	698
$\tau_{\text{C-D}}$	652	636	653	659
	652	635	652	658
$\nu_{\text{C2-S}}$ asym.	596	585	593	592
	591	581	588	588
$\omega_{\text{C-D}}$ + $\tau_{\text{C1-C1'}}$	503	491	491	493
A + $\omega_{\text{C-D}}$	480	482	457	454
$\omega_{\text{C-D}}$	464	462	473	479
A - $\omega_{\text{C-D}}$	463	460	471	476
A: $\nu_{\text{C1-S}}$ sym. + $\nu_{\text{C1-S}}$ sym.	416	422	419	415
$\tau_{\text{C-H group}}$	383	363	379	382
	381	362	374	377
$\rho_{\text{half TTF}}$	300	298	295	299
$\omega_{\text{C1-C1'}}$ + $\nu_{\text{C1-S}}$ sym.	271	288($\omega_{\text{C1-C1'}}$)	253($\omega_{\text{C1-C1'}}$)	243
$\omega_{\text{C1-C1'}}$ - $\nu_{\text{C1-S}}$ sym.	226	249($\nu_{\text{C1-S}}$ sym.)	240($\nu_{\text{C1-S}}$ sym.)	230
$\omega_{\text{C-H group}}$	96	156	135	119
$\delta_{\text{half TTF}}$	95	117	100	105
$\tau_{\text{S-C-H group}}$	78	133	115	100
$\omega_{\text{C-H group}}$	58	123	70	55
Frustrated trans. and rot.	/	101	99	68
	/	80	61	51
	/	78	43	45
	/	47	34	42
	/	46	23	30
	/	42	14	20

UNIVERSITAT ROVIRA I VIRGILI
ORGANIC MOLECULES ON METAL SURFACES: FORECASTING STRUCTURES AND SPECTRA
Benjamí Martorell Masip
ISBN:978-84-691-9747-9 /DL: T-1259-2008

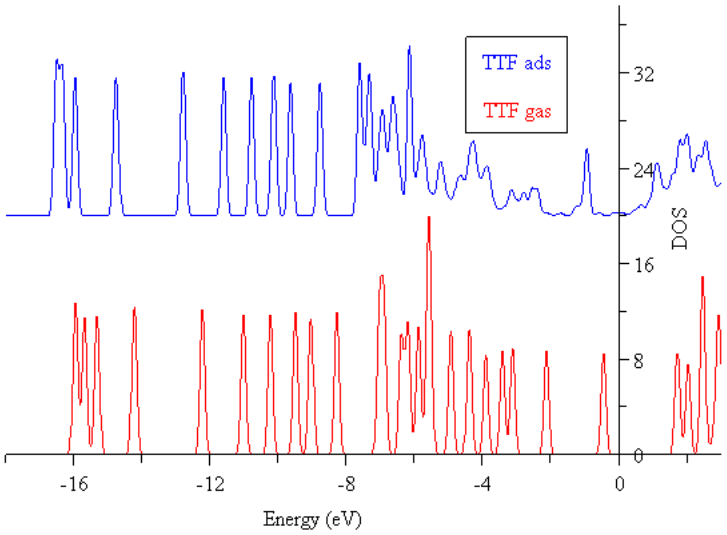

Figure 3.8: DOS of TTF in gas phase (red line) and adsorbed on Ag(110) on adsorption site 2×4 (blue line).

with localised orbitals on atoms, we could distinguish different zones of energy. Bands below -7.5 eV correspond to C−H bonds and σ C−C bonds. Bands in the range -7.5 up to -5 eV correspond to C−S bonds. Finally, zone between -5 and 0 eV (Fermi level) are bands corresponding to lone-pair electrons of sulphur atoms and π C=C bonds. In order to compare with adsorbed TTF, DOS calculation for TTF in gas phase on the adsorbed geometries (so three different calculations) were carried out. No significant changes due to geometrical distortions were observed in DOS (because no significant changes in geometrical structures are present).

When gas phase TTF DOS and adsorbed TTF DOS are compared, the first significant fact is that all bands of adsorbed TTF are stabilised around 1 eV respect to TTF in gas phase (this value is similar to the adsorption energy of 20.9 kcal·mol^{-1}). In other studies it has been proved that the stabilisation of bands is proportional to E_{ads} of the system [60]. This is a consequence of the interaction adsorbate−surface. If DOS of adsorbed molecule is analysed, it can be concluded no significant changes occur below -5 eV, but above it is extremely different. This is the zone of πC=C and lone-pair electrons of sulphur atoms. It is observed a decrease in the intensity of the bands and they widen. Integration of PDOS in gas phase and adsorbed TTF were also made. Both integrated 46.5

UNIVERSITAT ROVIRA I VIRGILI
ORGANIC MOLECULES ON METAL SURFACES: FORECASTING STRUCTURES AND SPECTRA
Benjamí Martorell Masip
ISBN:978-84-691-9747-9 /DL: T-1259-2008

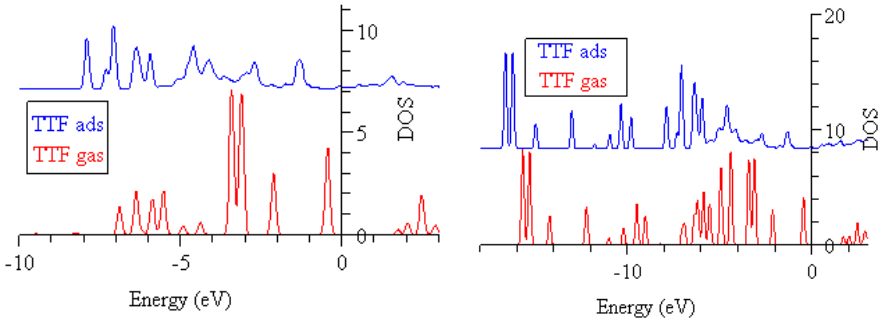

(a) PDOS of pz orbitals on S. (b) PDOS of s+pz+px orbitals on S.

Figure 3.9: PDOS on S atoms for TTF. Red line is for TTF in gas phase and blue line is for TTF adsorbed on Ag(110) 2×4.

electrons. One must care about these integrations because they depend on the Wigner-Seitz radius used in the projection, so the absolute number of integrated electrons is not the real one, but it can serve to evaluate different situations.

To have a better understanding of how adsorption occurs we decided to study the zone in the range from -5 to 0 eV. This means we projected DOS on p_z orbital of carbons and on lone-pairs electrons of sulphur atoms. For p_z orbitals (not presented here) of carbon atoms only the changes described in the last paragraph occurred (that is the bands stabilised, they lost intensity and became wider, but they remained). To simulate the projection on lone-pair electrons of sulphur atoms, PDOS on p_z and on the addition of $s+p_x+p_z$ orbitals of sulphur atoms was made. These projections are presented in figure 3.9.

In figure 3.9(a), we can observe p_z orbital of a sulphur atoms, where there is a big change between gas phase and adsorbed molecule. Intensity of bands decrease and they widen in a big range. This indicates a strong interaction between sulphur atoms and the surface. In figure 3.9(b), it can be seen a representation of S lone-pair energy levels, observing that under -5 eV there is a change in the configuration of bands. The integration of this last PDOS gives a value of 15.35 electrons for gas phase and 15.15 when TTF is adsorbed. This means a charge transfer of 0.2 electrons to the surface.

PDOS on Ag atoms directly bonded to TTF was made for d_{z^2} and p_z orbitals (figure 3.10). A previous study of d band and sp band was not concluding, so we decided to study the orbitals that are normal to surface. In d_{z^2} orbital no significant changes exist, this means we have a decrease in intensity of the

UNIVERSITAT ROVIRA I VIRGILI
ORGANIC MOLECULES ON METAL SURFACES: FORECASTING STRUCTURES AND SPECTRA
Benjamí Martorell Masip
ISBN:978-84-691-9747-9 /DL: T-1259-2008

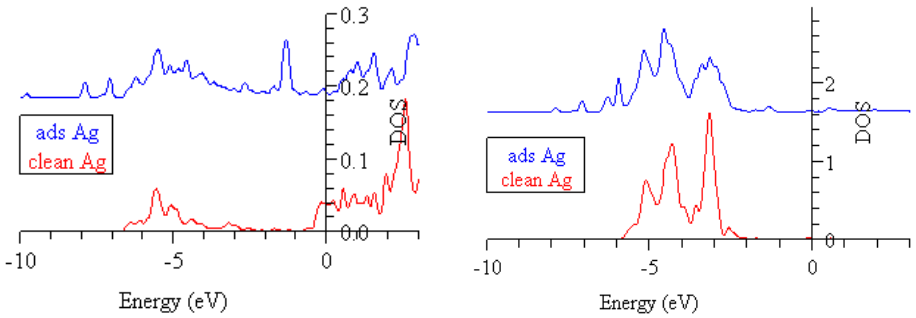

(a) PDOS of Ag on pz orbital.

(b) PDOS of Ag on dz2 orbital.

Figure 3.10: PDOS on Ag atom directly bonded to TTF. Red line is clean surface and blue line is with adsorbed TTF.

band and it widen, but the form remains, and its integration does not change when TTF is adsorbed. But for p_z orbitals a clear band appears around -1 eV, indicating an increase in charge density. The integration of p_z orbitals gives an increase of 0.36 electrons for this orbital. So it seems clear that adsorbed TTF interacts with the sp band of the surface, with a charge transfer around 0.25-0.35 electrons to the surface.

In the case of TTF adsorbed on 1×4-top and 1×4-bridge the analysis is similar. In figure 3.11 we present gas phase TTF DOS compared with the adsorbed TTF on adsorption sites 1×4-top and 1×4-bridge. First of all, there is a stabilisation of bands around -0.5 eV, quite similar to their E_{ads}. Furthermore, the interaction zone (where bands change when TTF is adsorbed), is above -5 eV, like in 2×4 site case. It can be observed that for 1×4-top site DOS is quite similar to 2×4-site, but 1×4-bridge is somewhat different. This can be explained because in 2×4 and 1×4-top sites, every interacting sulphur interacts with only one Ag atom, but in the case of 2×4-bridge site, every interacting atom does with two Ag atom. Of course, changes in DOS are not dramatic. In order to obtain a better understanding how TTF interacts with the surface, PDOS on sulphur atoms that interact with surface and PDOS on silver atoms that interact with TTF are presented in figure 3.12. In these figures it can be observed that PDOS on sulphur atoms of 1×4-bridge site is more different to gas phase than 1×4-top site. The reason seems to be the interaction of every sulphur atom with two Ag atoms. In the case of PDOS on the sp surface band, no clear differences between the two adsorption sites exist.

UNIVERSITAT ROVIRA I VIRGILI
ORGANIC MOLECULES ON METAL SURFACES: FORECASTING STRUCTURES AND SPECTRA
Benjamí Martorell Masip
ISBN:978-84-691-9747-9 /DL: T-1259-2008

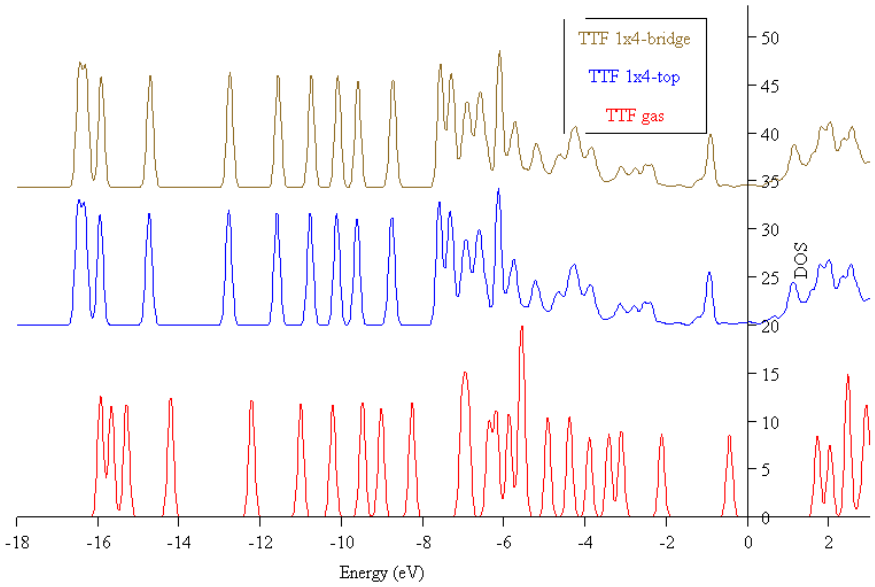

Figure 3.11: DOS of TTF in gas phase (red line) compared with TTF adsorbed 1×4-top site (blue line) and 1×4-bridge site (sienna line).

Variation of charge integration is in all cases less than 0.05 electrons, so in the case that TTF is perpendicularly adsorbed on the surface, no charge transfer to the surface is observed. It is important, because, as commented in section 3.2.1, TTF can become flat for two reasons. One is that TTF becomes a cation, or a partial cation. The second is the coverage effect, i.e., the possible interaction among different adsorbed molecules. In the case of 2×4 site, TTF becomes flatter and it can be due to a charge transfer to the surface. In 1×4 sites, this charge transfer does not occur, and the reason why TTF becomes flat is the interaction with the surface and neighbour TTF molecules.

Finally, we decided to simulate STM images to be compared with experimental STM, which are related with charge distribution on the molecule. When charge density is more intense, there is more tunnelling current, and image become lighter; when there is less charge density, not so many electrons can flow and image is darker. In figure 3.13 we present our simulated images for the most stable minimum found (2×4 site), where the tip variates from 6.0 Å from surface up to 10.0 Å.

UNIVERSITAT ROVIRA I VIRGILI
ORGANIC MOLECULES ON METAL SURFACES: FORECASTING STRUCTURES AND SPECTRA
Benjamí Martorell Masip
ISBN:978-84-691-9747-9 /DL: T-1259-2008

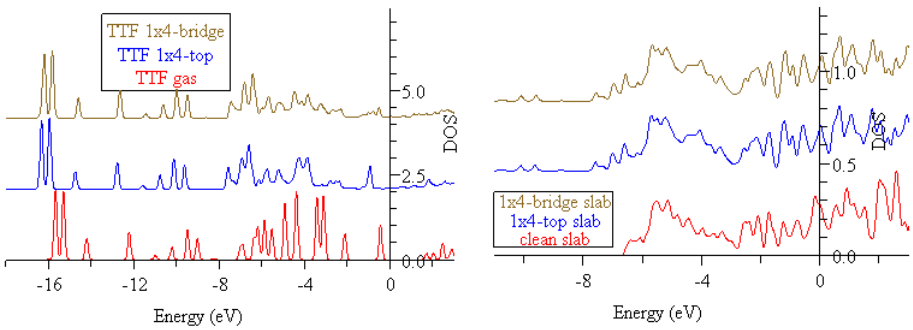

(a) (b)

Figure 3.12: a) PDOS on lone-pair electrons of interacting sulphur atoms. b) PDOS on sp band of interacting Ag atoms. Red line is for clean surface or TTF in gas phase, blue line for 1×4-top site and sienna line for 1×4-bridge.

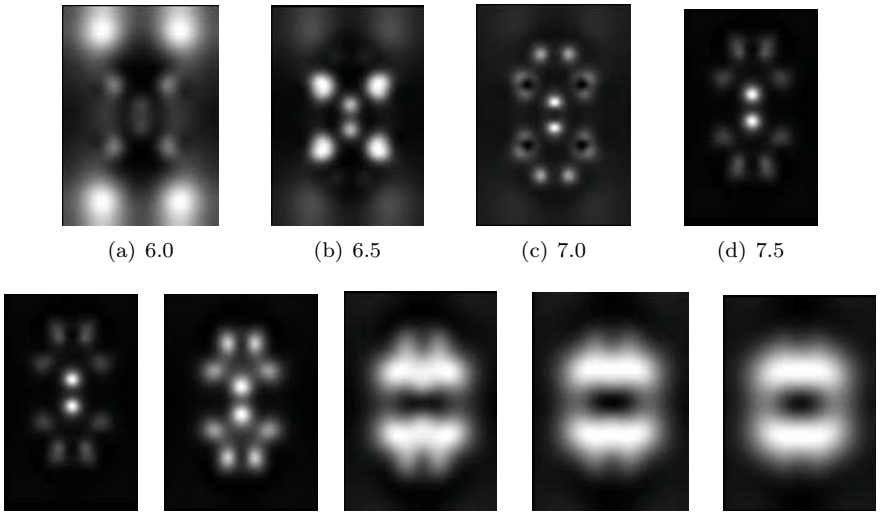

(a) 6.0 (b) 6.5 (c) 7.0 (d) 7.5

(e) 7.5 (f) 8.0 (g) 9.0 (h) 9.5 (i) 10.0

Figure 3.13: STM images for adsorption site 2×4. Tip is moved from 6.0 Å from surface up to 10.0 Å.

UNIVERSITAT ROVIRA I VIRGILI
ORGANIC MOLECULES ON METAL SURFACES: FORECASTING STRUCTURES AND SPECTRA
Benjamí Martorell Masip
ISBN:978-84-691-9747-9 /DL: T-1259-2008

3.3 TTF adsorbed on Au(110).

3.3.1 Geometric parameters.

Gold is a nobel metal that has a Fm3m structure. The Au(110) surface is exactly the same that was presented in figure 3.4 for Ag(110). Experimental lattice parameter of gold is 4.0782 Å [150], but we have recomputed this value, finding a value of 4.1748 Å, very near to the experimental one. It can be seen the effect called "lantanid contraction", that explains why third row transition metals have almost the same radius or lattice parameter as metals that belong to the second row. This is important, because for these studies no real geometric differences exist for Ag and Au. For our slab model, the value of 4.1748 Å remained constant, and only the uppermost layer of the slab was optimised.

As Ag and Au lattice parameters are so similar, it was thought that adsorption sites for TTF on Ag(110) and on Au(110) should be quite similar. So all adsorption modes that were found for TTF on Ag(110), were computed for Au(110), using two different coverages 0.25 and 0.125. They can be seen in figures 3.5 and 3.6. Results were very similar to Ag(110). The main difference was that in this case, with an Au surface, for 1×4 unit cell only one minimum was found, the most stable one for Ag: 1×4-top. So for Au(110) surface only the sites where interaction between TTF and surface is made directly (S adsorbate atom with metal surface atom) are minima. In table 3.8 are presented the geometric parameters of gas phase and adsorbed TTF.

TTF adsorbs parallel to surface on 2×4 site, but it does perpendicular on 1×4 site. Like on Ag(110), TTF on 1×4 is not strictly perpendicular, but it tilts ∼30° respect to the normal surface, due to the same reason stated on Ag(110). If we compare geometrical parameters with those in the gas phase no important changes are observed, like in the case of TTF on Ag(110). All distances variations are in a range of ±0.02 Å and all angles variations are around ±2.5° (but distances C=C increase 0.01 Å respect to gas phase, whereas on Ag(110) they remained constant). The most changing parameter, like on Ag surface, is the bending angle of TTF, that decreases from 14° to 11° on 2×4 site and to 3° (almost flat) on 1×4 site. When we comment DOS, we will associate these bending angles to the charge density lose or to a coverage effect.

The main difference between Ag and Au is the adsorption energy. In the case of gold the adsorption is quite stronger. For 2×4-site E_{ads} increases from -20.9 kcal·mol^{-1} on silver to -35.6 kcal·mol^{-1} on gold and for 1×4 site increases from

UNIVERSITAT ROVIRA I VIRGILI
ORGANIC MOLECULES ON METAL SURFACES: FORECASTING STRUCTURES AND SPECTRA
Benjamí Martorell Masip
ISBN:978-84-691-9747-9 /DL: T-1259-2008

Table 3.8: Geometrical parameters of adsorbed TTF on Au(110) on two different unit cells. For double values, first value is the furthest one and the second is the nearest to the surface.

	Gas phase	2×4	1×4	
[a]d(C1-C1')	1.36	1.37	1.37	
d(C1-S)	1.77	1.75	1.76	1.76
d(S-C2)	1.77	1.75	1.74	1.75
d(C2-H)	1.09	1.09	1.09	1.09
d(C2-C2')	1.34	1.35	1.34	
[b]α(C1'-C1-S)	122.8	122.8	123.1	121.7
α(C1-S-C2)	95.5	93.9	94.6	94.4
α(S-C2-C2')	117.4	117.2	118.2	117.4
α(S-C2-H)	118.6	117.1	117.1	116.1
[c]θ	14.35	10.6	2.9	
[d]d(S-Au)	/	2.57	2.57	
[e]E_{ads}	/	-35.6	-17.6	

[a]d: distances (Å); [b]α: angles (degrees); [c]θ: bending angle; [d]distances to nearest Au atom; [e]E_{ads}: adsorption energy (kcal·mol^{-1})

-11.1 to -17.6 kcal·mol^{-1}. This means that interaction increases a 75 % on Au respect to Ag. Despite interacting stronger, no reactivity of TTF on gold was found, indicating this system could be a good support for TTF and derivatives. If we take into account that for TTF on 2×4 site four sulphur atoms interact, it means an interaction energy of ∼-9 kcal·mol^{-1} for each sulphur atom, being almost the same energy for 1×4 site. As a consequence of a stronger interaction, S−Au distance is shorter than S−Ag distance, that is reduced ∼0.15 Å for both sites. This is quite interesting because one could think that gold should be less reactive (because it is a more noble metal) than silver, but several cases have been found where gold behaves in a non-classical way [62, 142, 143, 144].

3.3.2 Vibrational frequencies calculations. RAIR spectra simulation.

All vibrational frequencies and their corresponding VNM have been computed for all possible adsorption sites to ensure that all obtained adsorption sites were minima on the potential surface. Furthermore, dipolar moments have been calculated to evaluate the intensity of each frequency in RAIR spectrum. We have also obtained the corresponding frequencies and intensities for fully deuterated TTF (TTF-d4) adsorbed on Au(110).

UNIVERSITAT ROVIRA I VIRGILI
ORGANIC MOLECULES ON METAL SURFACES: FORECASTING STRUCTURES AND SPECTRA
Benjamí Martorell Masip
ISBN:978-84-691-9747-9 /DL: T-1259-2008

Only two stable minima have been found on Au(110), one for 2×4 unit cell, and another one for 1×4 unit cell (they will be called 2×4-site and 1×4-site, respectively), as explained in section 3.3.1. In table 3.9 vibrational frequencies for these adsorption sites are presented and compared with gas phase values for TTF and TTF-d4.

C−H stretching modes decrease when it is adsorbed from 3161(2), 3142 and 3141 to 3147, 3146, 3131, and 3130 cm^{-1} on 2×4-site, and to 3144(2), 3099, and 3098 on 1×4-site, being the decrease in this last case larger than on Ag(110) (it was 30 cm^{-1} for Ag(110) and it is 40 cm^{-1} for Au(110)). In the case of C=C stretching modes, they decrease from 1551, 1528 and 1513 cm^{-1} to 1512, 1592 and 1447 cm^{-1} for 2×4-site and to 1535, 1521 and 1469 cm^{-1} for 1×4-site. These values decrease much more than in the case of adsorbed TTF on Ag(110), whose maximum decrease was 30 cm^{-1}. In the case of Au(110) this maximum decrease is up to 60 cm^{-1}. This is a clear consequence of the enlarge of C=C distance, because the longer a bond is, the weaker the bond is, and vibrational frequency decreases. The C−H bonds rocking goes from 1232 and 1236 cm^{-1} down to 1229 and 1226 cm^{-1} on 2×4-site and to 1234 and 1231 cm^{-1} on 1×4-site, so no important changes are observed. Neither the scissorings of C−H bonds suffer any important variation on adsorption process.

TTF-d4 C−D stretching modes decrease in the process of adsorption from 2357, 2356, and 2317(2) cm^{-1} to 2346, 2345, 2310, and 2309 cm^{-1} on 2×4-site, and to 2338(2) and 2292(2) cm^{-1} on 1×4-site. In TTF-d4 the decreases are not as big as in the case of TTF, maximum of 30 cm^{-1}, like TTF-d4 adsorbed on Ag(110). For C=C stretching modes changes are also important, the values decrease from 1538, 1494, and 1492 cm^{-1} to 1481, 1466, and 1442 cm^{-1} on 2×4-site, and to 1505, 1486, and 1463 cm^{-1} on 1×4-site. This implies a decrease of 50 cm^{-1}, which is larger than on Ag(110) (30 cm^{-1}). This is also a consequence of the C=C distance enlarge respect to gas phase. In the case of C−H rocking and scissoring modes, changes are $\leqslant$10 cm^{-1}, so no meaningful changes in these VNMs exist.

Most interesting changes respect to gas phase are not in the vibrational frequencies, but in the intensities, i.e. in the spectrum. In figure 3.14 RAIR spectra of TTF and TTF-d4 on Au(110) are presented. The analysis is similar to the one made with TTF and TTF-d4 on Ag(110).

Like on Ag(110) all bands decrease in intensity respect to gas phase due to the adsorption of the molecule and the changes in selection rules from gas phase IR spectrum to the adsorbed one. For adsorption site 2×4, the most intense

UNIVERSITAT ROVIRA I VIRGILI
ORGANIC MOLECULES ON METAL SURFACES: FORECASTING STRUCTURES AND SPECTRA
Benjamí Martorell Masip
ISBN:978-84-691-9747-9 /DL: T-1259-2008

Table 3.9: Vibrational frequencies for TTF and TTF-d4 in gas phase and adsorbed on Au(110). All values are in cm^{-1}.

Gas phase	2×4	1×4	Gas phase	2×4	1×4
TTF			TTF-d4		
3161	3147	3144	2357	2346	2338
3161	3146	3144	2356	2345	2338
3142	3131	3099	2317	2310	2292
3141	3130	3098	2317	2309	2292
1551	1512	1535	1538	1481	1505
1528	1502	1521	1494	1466	1486
1513	1447	1469	1492	1442	1463
1236	1229	1234	1035	1025	1032
1232	1226	1231	1019	1008	1015
1072	1079	1079	935	944	941
1072	1073	1071	824	828	822
950	959	956	779	786	777
830	829	832	769	775	774
826	803	829	766	769	766
821	802	823	713	698	713
786	791	798	711	696	712
781	789	791	696	703	702
778	786	774	690	699	699
729	714	727	652	632	653
725	710	724	652	631	652
614	600	609	596	584	593
613	622	627	591	578	587
612	615	625	503	494	495
608	593	602	480	488	462
498	485	491	464	463	475
476	477	466	463	466	481
422	407	420	416	431	426
419	401	414	383	372	384
417	433	428	381	366	377
304	302	303	300	298	300
272	322	275	271	320	275
228	255	247	226	252	245
100	197	167	96	119	132
99	121	140	95	188	162
78	159	134	78	157	135
62	160	122	58	152	117
/	143	94	/	141	91
/	111	80	/	109	78
/	111	67	/	107	66
/	53	52	/	52	50
/	46	39	/	45	39
/	44	27	/	44	27

UNIVERSITAT ROVIRA I VIRGILI
ORGANIC MOLECULES ON METAL SURFACES: FORECASTING STRUCTURES AND SPECTRA
Benjamí Martorell Masip
ISBN:978-84-691-9747-9 /DL: T-1259-2008

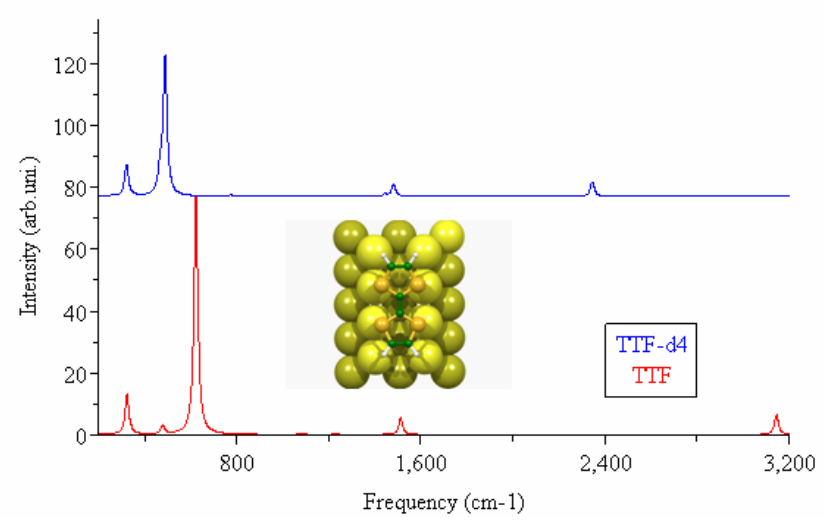

(a) TTF adsorbed on Au(111) on site 2x4.

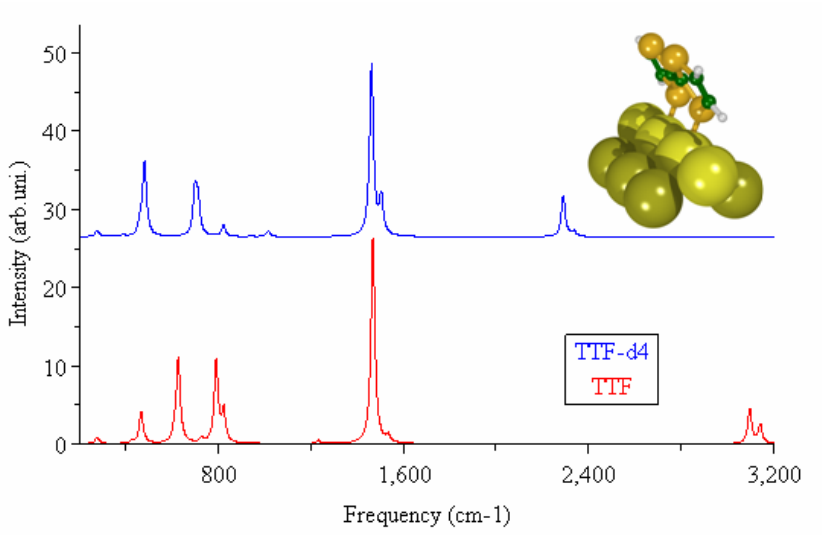

(b) TTF adsorbed on Au(110) on site 1x4.

Figure 3.14: RAIR spectra of TTF adsorbed on Au(110) on both adsorption sites: 2×4 and 1×4.

UNIVERSITAT ROVIRA I VIRGILI
ORGANIC MOLECULES ON METAL SURFACES: FORECASTING STRUCTURES AND SPECTRA
Benjamí Martorell Masip
ISBN:978-84-691-9747-9 /DL: T-1259-2008

band of TTF is the same as on gas phase and on Ag(110), it is the C−H bond wagging around 622 cm^{-1}. Like in case of Ag(110), no other band appears up to 1510 cm^{-1}, which is a small band that corresponds to C=C stretching modes. Finally under 3150 cm^{-1} appears a small band corresponding to C−H stretching modes. Below the most intense band, the second most intense band in the spectrum appears at 320 cm^{-1} and corresponds to the central C=C bond wagging. For adsorption site 1×4, the spectrum has a very different appearance than 2×4 site, like in the case of Ag(110). The most intense band lies above 1450 cm^{-1} , corresponding to C=C stretching modes. This is the same case as on Ag(110). Around 3150 cm^{-1} a small band corresponding to C−H stretching modes appears. Under the most intense band, two bands appear with the same intensity. One lies at 791 cm^{-1} and the other one at 627 cm^{-1}, and they correspond to the rocking of C−H bond coupled with S−C stretching mode and to the C−H groups wagging, respectively (like in case of Ag(110) this band appears because TTF is not perpendicular to surface, but it is tilted almost 30°). Another less intense band appears around 465 cm^{-1} corresponding to the totally symmetric S−C stretching, where sulphur atoms go out of the TTF plane.

So the way to differentiate the two possible adsorption sites of TTF on Au(110) is to observe the band at 622 cm^{-1}, like in case of Ag(110). If this band is the most intense one, the adsorption site will be the 2×4-site, but if this band is not the most intense one, but it is the band above 1450 cm^{-1}, the preferred adsorption site will be the 1×4-site.

Now let's analyse the spectra and vibrational frequencies of TTF-d4 adsorbed on Au(110). Vibrational frequencies of TTF-d4 are presented in table 3.9, together with TTF frequencies. C−D stretching modes decrease when TTF-d4 is adsorbed from 2357(2) and 2317(2) cm^{-1} down to 2346(2) and 2310(2) cm^{-1} on 2×4-site and down to 2338(2) and 2292 (2) cm^{-1} on 1×4-site. C=C stretching modes decrease their frequencies from 1538, 1494, and 1492 cm^{-1} to 1481, 1466, and 1442 cm^{-1} adsorbed on 2×4-site and to 1505, 1486, and 1463 cm^{-1} on 1×4-site, this means a larger decrease than on Ag(110) (∼50 cm^{-1}, like in the case of TTF on Au(110)). The C−D bond rocking decrease a little bit its values from 1035 and 1019 cm^{-1} to 1025 and 1008 cm^{-1} on 2×4-site and to 1032 and 1015 cm^{-1} on 1×4-site. The values of C−D bond scissorings do not almost change, on gas phase values are 769 and 766 cm^{-1}, on 2×4-site 775 and 769 cm^{-1} and on 1×4-site 774 and 766 cm^{-1}.

Major changes in the vibrational features of TTF-d4 respect to the gas phase appear in the spectrum of adsorbed system. The intensities, like in case of

UNIVERSITAT ROVIRA I VIRGILI
ORGANIC MOLECULES ON METAL SURFACES: FORECASTING STRUCTURES AND SPECTRA
Benjamí Martorell Masip
ISBN:978-84-691-9747-9 /DL: T-1259-2008

Ag(110), change. For 2×4-site the most intense band lies at 488 cm^{-1}, which is the C−D bond wagging. The second band in intensity lies at 320 cm^{-1} and corresponds to the wagging of central C=C group, like in the case of free TTF. Two small bands appear at 1481 cm^{-1}, which are the C=C stretching modes, and at 2345 cm^{-1} appears the small band corresponding to the C−D stretchings. For the 1×4-site the most intense band appears at 1463 cm^{-1}, with a shoulder at 1505 cm^{-1}, both correspond to C=C stretching modes. Below this band, two similar bands in intensity appear around 700 and 480 cm^{-1}. The first one is associated to the S−C stretching mode coupled with the C−D group rocking. The second one is the wagging of the C−D bond. Finally, around 2290 cm^{-1} appears the band corresponding to C−D stretching modes.

It is also interesting to compare the spectra of TTF and TTF-d4 adsorbed on Ag(110) and Au(110). The most interesting conclusion is that for 2×4-site, for TTF and TTF-d4, the spectra on Ag(110) and Au(110) are almost equal. This indicates that the structure of TTF on Ag(110) and Au(110) is similar, and no big differences exist among them. In the case of 1×4-site the spectra are also similar, but not equal, because for TTF intensities of bands between 400 and 800 cm^{-1} are bigger on Ag(110) than on Au(110). For TTF-d4 the same happens, above 800 cm^{-1} appear no bands in the case of Au(110), but do on Ag(110) (they actually appear on TTF-d4, but are so low in intensity that they are not visible, because intensity depends inversaly on the square root of the reduced mass of the system). So it would be impossible to distinguish one RAIR spectrum on Ag(110) from one on Au(110) if the adsorption site is 2×4, and would be quite difficult for 1×4-site.

3.3.3 PDOS analysis and charge transfer.

As in the case of TTF adsorbed on Ag(110), PDOS was simulated for several atomic orbitals to analyse the bond between TTF and the surface. As the behaviour of the geometry and vibrational frequencies do not change meaningfully respect to Ag(110), it is supposed that DOS and PDOS have to bring the same conclusions as for adsorbed TTF on Ag(110).

In figure 3.15 PDOS of TTF in gas phase and compared with PDOS of TTF adsorbed on Au(110) for both adsorption sites are presented. All bands are stabilised when TTF is adsorbed, about 0.5 eV in 2×4-site and around 0.25 eV in 1×4-site. This is due to the effect of the interaction between surface and TTF, making all bands to become stabilised (like in case of Ag(110)). Bands

UNIVERSITAT ROVIRA I VIRGILI
ORGANIC MOLECULES ON METAL SURFACES: FORECASTING STRUCTURES AND SPECTRA
Benjamí Martorell Masip
ISBN:978-84-691-9747-9 /DL: T-1259-2008

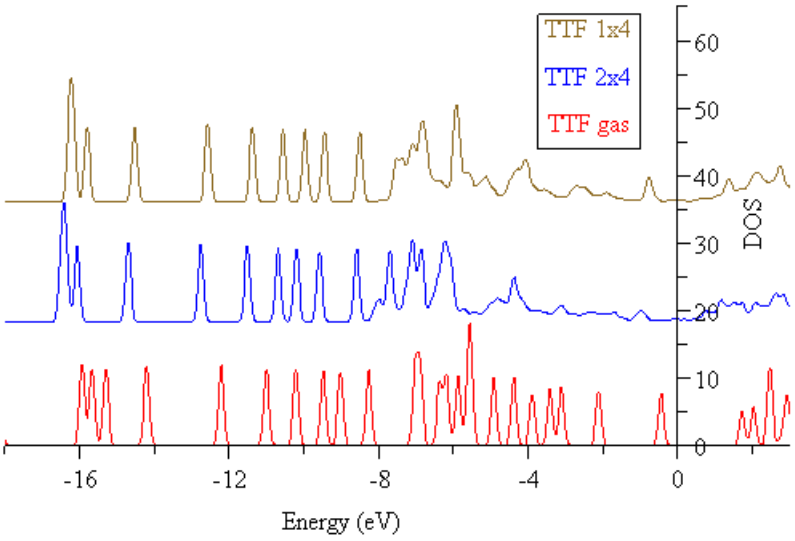

Figure 3.15: PDOS of TTF in gas phase (red line) and adsorbed on Au(110). In blue line the adsorption site 2×4; in sienna line the 1×4 one.

below -8 eV in gas phase do not suffer any change, apart from the stabilisation before commented. All important changes lie above -8 eV. It is the interaction zone with surface, which is made in the zone of sulphur lone-pair electrons and in the zone of C=C bonds.

The integration of electrons over all TTF molecule shows TTF is a good electron-donor. In the case of the adsorption site 2×4, TTF loses 0.15 electrons and in the case of adsorption site 1×4 the lose is smaller, 0.1 electrons. This can explain why TTF becomes flatter on 2×4-site respect to gas phase (the bending angle changes from 14° to 11°), but the charge transfer for 1×4-site seems to be too small to explain the change in the bending angle (it becomes almost flat, only 3°). The next step is to analyse the lone-pair electrons of sulphur atoms and the sp band of the surface, which are the interacting ones (the analysis is very similar to the one made on Ag(110)).

In figure 3.16(a) it can be observed PDOS on lone-pair electrons of S atoms of TTF in gas phase (red line) and when TTF is adsorbed on 2×4-site (blue line) and on 1×4-site (sienna line). It can be observed that interaction with the surface is strong in the zone above -8 eV because bands widen and lose their intensity for both adsorption sites. The integration of charges in this case discovers that TTF loses 0.3 electrons on 2×4-site and only 0.1 electrons on

UNIVERSITAT ROVIRA I VIRGILI
ORGANIC MOLECULES ON METAL SURFACES: FORECASTING STRUCTURES AND SPECTRA
Benjamí Martorell Masip
ISBN:978-84-691-9747-9 /DL: T-1259-2008

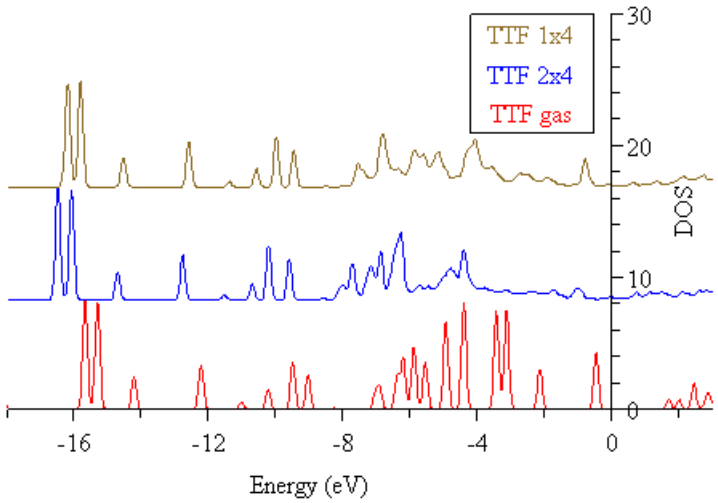

(a) PDOS on lone-pair electrons of S atoms of TTF.

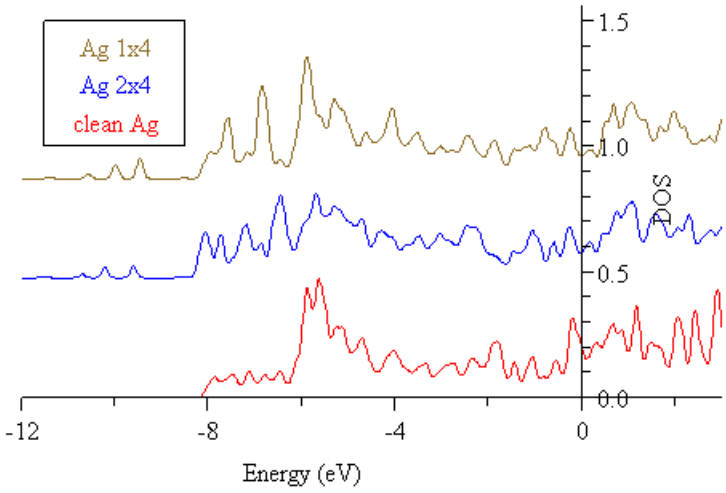

(b) PDOS on sp band of Au(110).

Figure 3.16: a) Lone-pair electrons of sulphur atoms. b) sp band of Au(110).

UNIVERSITAT ROVIRA I VIRGILI
ORGANIC MOLECULES ON METAL SURFACES: FORECASTING STRUCTURES AND SPECTRA
Benjamí Martorell Masip
ISBN:978-84-691-9747-9 /DL: T-1259-2008

1×4-site, indicating a similar behaviour to Ag(110).

In figure 3.16(b) the changes in the sp band of Au can be observed. The zone between -6 and -8 eV becomes populated when TTF is adsorbed and some bands appear on 2×4-site and 1×4-site in this zone. Also changes in the band at -5.5 eV can be observed. The integration of PDOS on the 2×4-site gives an increase of 0.65 electrons (similar to the case of Ag(110)), and on the 1×4-site the integration of this band also gives a big increase of electrons, 0.6, indicating that TTF is a better donor on Au(110) than on Ag(110) for this adsorption mode. Despite this value, the integration on sulphur lone-pair electrons and on TTF seems to indicate that TTF is not as charged on 1×4-site as on 2×4-site, like in the case of Ag(110).

3.4 TSF in gas phase.

3.4.1 Structural parameters.

Tetraselenafulvalene (TSF or TSeF) is a homologous molecule to TTF. The four sulphur atoms are replaced by four selenium atoms. This molecule and its derivatives are important because they are really good superconductors, as explained in section 1.4.1. TSF molecule has not been studied so widely like TTF, and very few results have been found in literature. *Demiralp et Goddard* have reported a study of TTF and its derivatives [47]. They reported that for HF level calculation TTF and TSF are flat, but adding correlation effects, using MP2 calculations or DFT methods, they found TTF and TSF to be in a boat-like conformation. Unfortunately, they do not report TSF geometry obtained with DFT and MP2 methods, and the only value they give is the angle C1−Se−C2, 93.2°, which was obtained with HF method.

In table 3.10 structural parameters of TSF are presented. The C1−Se−C2 angle obtained with our methods is a little bit smaller than the other one reported, $<\sim$1.3°. C=C bond distances are, like in TTF case, around 1.34 or 1.35 Å, indicating no aromaticity for this molecule. Selenium atoms are bigger than sulphur atoms and, as a logic consequence, C−Se distances are $\sim$0.15 Å larger than the corresponding distances on TTF. No big changes are observed in the case of molecular angles, all changes are <2° respect to TTF, being the angle C1−Se−C2 the most changing one. For TTF it has a value of 96° and for TSF it is 92°. It is logic because of the increase of C−Se distances, which makes the angle to decrease.

UNIVERSITAT ROVIRA I VIRGILI
ORGANIC MOLECULES ON METAL SURFACES: FORECASTING STRUCTURES AND SPECTRA
Benjamí Martorell Masip
ISBN:978-84-691-9747-9 /DL: T-1259-2008

Table 3.10: Structural parameters of TSF in gas phase.

	VASP
[a]d(C1-C1')	1.35
d(C1-Se)	1.92
d(Se-C2)	1.90
d(C2-H)	1.09
d(C2-C2')	1.34
[b]α(C1'-C1-Se)	123.1
α(C1-Se-C2)	91.9
α(Se-C2-C2')	119.5
α(Se-C2-H)	116.3
[c]θ	21.9

[a]d: distances (Å); [b]α: angles (degrees); [c]θ: bending angle (degrees)

The other parameter that changes respect to TTF is the bending angle. For TTF it was 14°, whereas for TSF it is 22°. *Demiralp et Goddard* [47] have explained this effect because TTF or TSF, if they were flat, they should have an angle C1−Se−C2 around 105°, but sulphur and selenium form angles only of 90°. The way to avoid an internal stress in the molecule is to bend itself, and the bigger the atom, the bigger the bending angle of the molecule.

3.4.2 Vibrational frequencies calculation.

Vibrational frequencies calculation was carried out to ensure that the structure found was a minimum. In literature it was not found works that reported the frequencies of TSF or the assignation of its spectrum bands.

TSF has the same number of atoms as TTF and, consequently, it presents the same number of fundamental vibrational frequencies: 36. Only those ones that belong to symmetry A_2 will not present variations of the dipolar moment, and, as consequence, will not be observed in IR spectrum. In table 3.11 vibrational frequencies of TSF and TSF-d4 are presented. As no other data was available, no comparison can be made with other theoretical or experimental values. However, vibrational frequencies of TSF can be compared with the corresponding ones of TTF. As expected, VNMs that do not imply any selenium movement have similar frequency to the homologous TTF frequency. One example of this are C−H stretching modes. The decrease in TSF is only 30 cm^{-1} respect to TTF. On the other hand, if vibrational modes implies a selenium movement, the frequency decreases and it can become coupled with another functional group.

UNIVERSITAT ROVIRA I VIRGILI
ORGANIC MOLECULES ON METAL SURFACES: FORECASTING STRUCTURES AND SPECTRA
Benjamí Martorell Masip
ISBN:978-84-691-9747-9 /DL: T-1259-2008

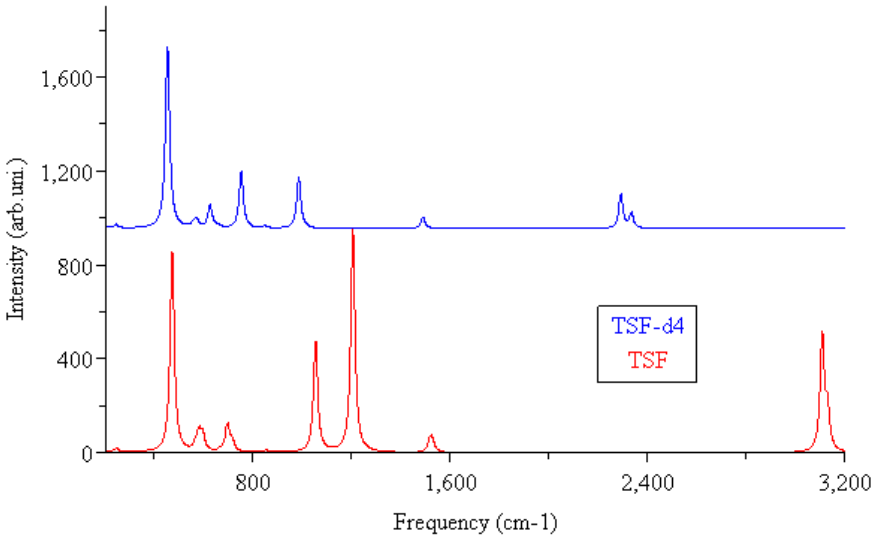

Figure 3.17: Infrared spectrum of TSF (red line) and TSF-d4 (blue line).

For instance, asymmetric C1−S(Se) stretching mode of TTF is around 624 cm^{-1}, whereas it decreases to 475 $cm^{-1}$for TSF.

Comparison between the values of TSF and TSF-d4 do not bring unexpected results. The most changing frequencies are those that involve an important displacement of hydrogen (deuterium) atoms. For example, C−H stretching decrease from 3134 and 3112 cm^{-1} to 2337 and 2294 cm^{-1} (-800 cm^{-1}), or C−H scissoring decrease from 1056 cm^{-1} to 752 cm^{-1} (more than 300 cm^{-1}). On the other hand, C=C stretching modes do not imply important hydrogens movement and vibrational frequencies remain almost constant, only a small decrease between 15-30 cm^{-1} can be observed in table 3.11, indicating a certain degree of coupling.

In figure 3.17 the infrared spectra of TSF and TSF-d4 are presented. The most intense peak in the spectrum of TSF is around 1200 cm^{-1} and corresponds to the C−H bond rocking. The second most intense band is located at 470 cm^{-1}, corresponding to the asymmetric C2−Se stretching, and this vibrational mode can also be seen as the translation of all H−C=C−H group in the plane of the molecule in the direction of the C=C bond. The third band in intensity is the one that corresponds to the C−H stretching modes above 3110 cm^{-1}. The next band in intensity lies at 1050 cm^{-1}, and corresponds to the C−H bond

UNIVERSITAT ROVIRA I VIRGILI
ORGANIC MOLECULES ON METAL SURFACES: FORECASTING STRUCTURES AND SPECTRA
Benjamí Martorell Masip
ISBN:978-84-691-9747-9 /DL: T-1259-2008

Table 3.11: TSF vibrational frequencies and their assignations. No assignation means it is the same as the above one, but couplings between two parts of TSF are different. Changing VNM for TSF-d4 are in brackets.

TSF		TSF-d4
Frequencies	Assignation	Frequencies
3134	$\nu_{\text{C-H}}$ asym.	2337
3134		2337
3112	$\nu_{\text{C-H}}$ sym.	2294
3112		2294
1532	$\nu_{\text{C=C}}$	1517
1521		1492
1510		1489
1206	$\rho_{\text{C-H}}$	986
1206		982
1055	$\delta_{\text{C-H}}$	753
1054		752
853	$\nu_{\text{C1-Se}}$ asym.	847
822	$\tau_{\text{C-H}}$	645
822		645
717	$\nu_{\text{C1-Se}}$ sym. + $\rho_{\text{C-H group}}$	710 ($\nu_{\text{C1-Se}}$ sym.)
703	$\rho_{\text{C-H group}}$ + $\nu_{\text{C2-Se}}$	628
695	$\rho_{\text{C-H group}}$ + $\nu_{\text{C2-Se}}$+ $\nu_{\text{C1-Se}}$ sym.	625($\rho_{\text{C-H group}}$ + $\nu_{\text{C2-Se}}$)
664	$\nu_{\text{C1-Se}}$ sym. + $\nu_{\text{C2-Se}}$ sym.	660
597	$\omega_{\text{C-H}}$	458($\omega_{\text{C-D}}$+$\tau_{\text{C1-C1'}}$)
588		454
580	$\omega_{\text{C-H}}$ + $\nu_{\text{C1-Se}}$ sym.	571($\nu_{\text{C1-Se}}$ sym.)
566	$\omega_{\text{C-H}}$ + $\nu_{\text{C2-Se}}$ sym.	557($\nu_{\text{C1-Se}}$ sym.)
475	$\nu_{\text{C2-Se}}$ asym.	456
472		453
440	$\tau_{\text{C1-C1'}}$	430($\omega_{\text{C-D}}$+$\tau_{\text{C1-C1'}}$)
382	$\tau_{\text{C-H group}}$	348
375		341
282	$\nu_{\text{C1-Se}}$ sym. + $\nu_{\text{C2-Se}}$ sym.	282
244		244
225	$\omega_{\text{C1-C1'}}$	225
183	$\rho_{\text{half TSF}}$	183
142	$\omega_{\text{C1-C1'}}$ + $\nu_{\text{C1-Se}}$ sym.	142
63	$\delta_{\text{half TSF}}$	57
60	$\omega_{\text{C-H group}}$	48
51		36
37	$\tau_{\text{Se-C-H group}}$	63

UNIVERSITAT ROVIRA I VIRGILI
ORGANIC MOLECULES ON METAL SURFACES: FORECASTING STRUCTURES AND SPECTRA
Benjamí Martorell Masip
ISBN:978-84-691-9747-9 /DL: T-1259-2008

scissoring. These four bands are the main fingerprints of this spectrum. The C=C stretching modes, the C−H group rocking, and the C−H bond wagging present low intensity bands at 1520, 695 and 580 cm^{-1} respectively.

The comparison of TSF and TTF spectra shows differences arising from bands intensities. Whereas vibrational frequencies were very similar, the intensity of bands changes a lot, and the most intense bands in TTF are not the most intense ones in TSF. This fact can be related with the different charge distribution, because intensities are associated with dipole moment first derivatives. For example, the wagging of C−H bond was the most intense band in TTF, but in TSF it is a weak band. On the other hand, the rocking of C−H bond was not visible for TTF and in TSF is the most intense band.

In the spectrum of TSF-d4 the most intense band lies at 453 cm^{-1} and corresponds to the asymmetric C2−Se stretching, which was the second most intense band in TSF. Two very similar bands in intensity are at 750 and 985 cm^{-1}. Respectively, they correspond to the scissoring and the rocking of the C−D bond. So, the most intense band of TSF becomes the second most intense band because the change of hydrogen by deuterium makes the intensities of these bands decrease respect the band at 450 cm^{-1}, that is not so affected. The next band in intensity lies at ∼2300 cm^{-1} and are C−D stretching modes. The C=C stretching modes and to the rocking of C−D group present weak intensity bands at 1490 and 625 cm^{-1}.

3.5 TSF adsorbed on Ag(110).

3.5.1 Geometric parameters.

TSF is a molecule very similar to TTF. TTF is 7.98 Å long per 2.96 Å wide and TSF is 8.21 Å long per 3.21 Å wide. Although being a little bit bigger (∼ 0.25 Å), TSF is very similar to TTF, so it is logic to imagine that properties of adsorption will be homologous to the ones of TTF. The unit cell chosen to adsorb TSF was the biggest one used for TTF: 2×4 unit cell. This unit cell is the minimum cell to adsorb TSF parallel to surface. So calculations were also made using a 2×4 unit cell. No calculations with 1×4 unit cell were carried out because it was desired to compare the adsorption of TTF and TSF on the most stable adsorption site, and this is that one that maximises interaction between four sulphur (or selenium) atoms with four surface atoms (in this case silver atoms).

UNIVERSITAT ROVIRA I VIRGILI
ORGANIC MOLECULES ON METAL SURFACES: FORECASTING STRUCTURES AND SPECTRA
Benjamí Martorell Masip
ISBN:978-84-691-9747-9 /DL: T-1259-2008

Table 3.12: Structural parameters and adsorption energy of TSF in gas phase and adsorbed on Ag(110).

	Gas phase	TSF adsorbed on Ag(110)
[(a)]d(C1-C1')	1.35	1.35
d(C1-Se)	1.92	1.92
d(Se-C2)	1.90	1.91
d(C2-H)	1.09	1.09
d(C2-C2')	1.34	1.34
[(b)]α(C1'-C1-Se)	123.1	122.4
α(C1-Se-C2)	91.9	91.7
α(Se-C2-C2')	119.5	119.6
α(Se-C2-H)	116.3	115.7
[(c)]θ	21.9	10.6
[(d)]d(Se-Ag)	/	2.76
[(e)]E_{ads}	/	-24.7

[(a)]d: distances (Å); [(b)]α: angles (degrees); [(c)]θ: bending angle; [(d)]distances to nearest Ag atom; [(e)]E_{ads}: adsorption energy (kcal·mol^{-1}).

Several adsorption sites were tested, like in the case of TTF on Ag. The adsorption sites studied are presented in figure 3.6. Also frequencies were computed to ensure that all obtained structures were minima on the potential energy surface. Only one of the tested adsorption sites was found to be a minimum. It corresponds to figure 3.6(a), that is the same one as for TTF adsorbed on Ag(110).

On table 3.12 structural parameters and the adsorption energy of TSF on Ag(110) are presented. The comparison of structural parameters of TSF in gas phase and adsorbed on Ag(110) finds out that the structure of adsorbed TSF is not altered respect to gas phase. Distances are almost invariable, and variations in angles are $<\pm 1°$. The only parameter that changes, like in the case of TTF on Ag(110), is the bending angle of TSF, that decrease from 22° in gas phase to 11° adsorbed on Ag(110). This fact is related with the charge transfer from molecule to surface, and it will be discussed in section 3.5.3.

TSF adsorbs on Ag(110) with an adsorption energy of -24.7 kcal·mol^{-1}, only -4 kcal·mol^{-1} stronger than TTF on Ag(110). Ag−Se distance is slightly increased respect TTF, from 2.73 up to 2.76 Å. This increase is small if we compare the increase of Se−C distances when S is substituted by one Se atom ($\sim$0.16Å), with the increase of Se−Ag distance when S is substituted by Se (0.03 Å). This fact can be due to the adsorption energy of TSF, which is stronger than the one of

UNIVERSITAT ROVIRA I VIRGILI
ORGANIC MOLECULES ON METAL SURFACES: FORECASTING STRUCTURES AND SPECTRA
Benjamí Martorell Masip
ISBN:978-84-691-9747-9 /DL: T-1259-2008

TTF, and it makes the distance not to be so long as one could be expect. This also happened with TTF adsorbed on Au(110), where distance S−Au was very short, only 2.56 Å, due to the large E_{ads}, -35.6 kcal·mol^{-1}. All this indicates that TTF and TSF have a very similar behaviour in the adsorption process.

3.5.2 Vibrational frequencies calculations. RAIR spectra simulation.

Vibrational frequencies and their corresponding vibrational modes have been calculated for all possible adsorption sites to ensure that all obtained species were minima in the potential surface. Furthermore, dipolar moment at each displacement have been computed to evaluate the intensity of he fundamental bands. Also hessian matrix has been recalculated to evaluate VNM, frequencies and intensities of deuterated TSF (TSF-d4) when it is adsorbed on Ag(110).

Only one stable minimum was found on Ag(110) for a 2×4 unit cell, as was explained in section 3.5.1. In table 3.13 vibrational frequencies for this adsorption site are presented and compared with the corresponding values on the gas phase. Results for TSF-d4 are also presented.

C−H stretching modes remain constant when TSF is adsorbed around 3132 and 3112 cm^{-1} (in the case of TTF there was a decrease in these values that is not present now). In the case of C=C stretching modes, they decrease from 1532, 1521, and 1510 to 1517, 1513, and 1477 cm^{-1}. The decrease is around 30 cm^{-1}, the same value as in TTF on Ag(110), indicating that C=C double bonds seem to behave very similar in both adsorption processes. The C−H bonds rocking and scissoring do not suffer important changes in adsorption process (variations are $<$10 cm^{-1}).

In the case of TSF-d4 results are very similar to TSF. C−D stretching modes do not variate and remain at 2335 and 2294 cm^{-1}, like in the gas phase. C=C stretching modes decrease from 1517, 1492, and 1489 cm^{-1} in gas phase to 1488, 1480, and 1473 cm^{-1} when TSF-d4 is adsorbed. This is a decrease similar to TTF-d4 adsorbed on Ag(110)-2×4 site (around 30 cm^{-1}). The C−D bonds rocking and scissoring neither in this case suffer important variations, being the biggest variation 13 cm^{-1}.

Most interesting changes respect to gas phase are not in the numeric values of vibrational frequencies, but in the intensities of the bands.

The most intense band for TSF adsorbed on Ag(110) lies at 586 cm^{-1} and corresponds to C−H wagging. This is different respect to gas phase, because this

UNIVERSITAT ROVIRA I VIRGILI
ORGANIC MOLECULES ON METAL SURFACES: FORECASTING STRUCTURES AND SPECTRA
Benjamí Martorell Masip
ISBN:978-84-691-9747-9 /DL: T-1259-2008

Table 3.13: Vibrational frequencies for TSF and TSF-d4 in gas phase and adsorbed on Ag(110).

TSF (frequencies)			TSF-d4 (frequencies)	
Gas phase	Adsorbed	Assignation	Adsorbed	Gas phase
3134	3132	$\nu_{\text{C-H}}$ asym.	2335	2337
3134	3131		2335	2337
3112	3113	$\nu_{\text{C-H}}$ sym.	2294	2294
3112	3112		2294	2294
1532	1517	$\nu_{\text{C=C}}$	1488	1517
1521	1513		1480	1492
1510	1477		1473	1489
1206	1198	$\rho_{\text{C-H}}$	973	986
1206	1197		970	982
1055	1061	$\delta_{\text{C-H}}$	756	753
1054	1052		751	752
853	846	$\nu_{\text{C1-Se}}$ asym.	842	847
822	805	$\tau_{\text{C-H}}$	628	645
822	802		627	645
717	702	$\nu_{\text{C1-Se}}$ sym. + $\rho_{\text{C-H group}}$	677	710
703	698	$\rho_{\text{C-H group}}$ + $\nu_{\text{C2-Se}}$	624	628
695	672	$\rho_{\text{C-H group}}$ + $\nu_{\text{C1-Se}}$ sym.	623	625
664	654	$\nu_{\text{C1-Se}}$ sym. + $\nu_{\text{C2-Se}}$ sym.	650	660
597	586	$\omega_{\text{C-H}}$	450	458
588	579		449	454
580	566	$\nu_{\text{C2-Se}}$ sym.	552	571
566	553		541	557
475	460	$\nu_{\text{C2-Se}}$ sym.	443	456
442	459		442	453
440	429	$\tau_{\text{C1-C1'}}(\omega_{\text{C-D}}+\tau_{\text{C1-C1'}})$	425	430
382	351	$\tau_{\text{C-H group}}$	320	348
275	347		317	341
282	277	$\nu_{\text{C1-Se}}$ sym. + $\nu_{\text{C2-Se}}$ sym.	277	282
244	242		244	244
225	220	$\omega_{\text{C1-C1'}}$	220	225
183	174	$\rho_{\text{half TSF}}$	173	183
142	152	$\nu_{\text{C1-Se}}$ sym.	151	142
60	115	$\omega_{\text{C-H group}}$	108	57
51	100		93	48
37	82	$\tau_{\text{Se-C-H group}}$	82	36
63	67	$\delta_{\text{half TSF}}$	66	63

UNIVERSITAT ROVIRA I VIRGILI
ORGANIC MOLECULES ON METAL SURFACES: FORECASTING STRUCTURES AND SPECTRA
Benjamí Martorell Masip
ISBN:978-84-691-9747-9 /DL: T-1259-2008

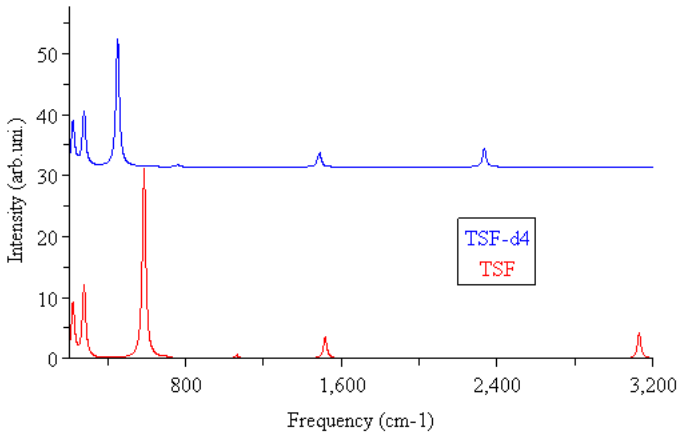

Figure 3.18: RAIR spectrum of TSF and TSF-d4 adsorbed on Ag(110).

was the second most intense band, being the most intense that one around 1200 cm^{-1} corresponding to the C−H rocking (when TSF is adsorbed, selection rules change, and this band becomes forbidden). Above this intense band, almost all other peaks become weaker, and only C=C stretching mode and C−H stretching mode are visible, but their intensity respect to gas phase is strongly decreased.

For TSF-d4 the analysis is similar to the one made for TSF. The most intense band lies at 450 cm^{-1}, corresponding to C−D wagging, but in this case, this also corresponds to the same peak as was the most intense one in gas phase (see section 3.4.2). Above this peak, all other peaks almost disappear, they do not produce a big change in the dipolar moment perpendicular to surface, and only tiny bands corresponding to C=C and C−D stretching modes are visible.

3.5.3 PDOS analysis and charge transfer.

The analysis of the DOS and PDOS is very similar to the one made for TTF adsorbed on Ag(110) and TTF adsorbed on Au(110). In the case of TSF, only the adsorption site where four selenium atoms are directly bonded to four atoms of the surface has been determined.

In figure 3.19 the PDOS of TSF in gas phase is presented and compared with the PDOS of adsorbed TSF on Ag(110). For DOS in gas phase, the graphic can be divided in several zones, like in the case of TTF. The bands below -7.5 eV correspond to C−H bonds and to σ C−C bonds. Bands in the range between -7.5 eV and -5 eV correspond to C−Se bonds. Bands above this limit

UNIVERSITAT ROVIRA I VIRGILI
ORGANIC MOLECULES ON METAL SURFACES: FORECASTING STRUCTURES AND SPECTRA
Benjamí Martorell Masip
ISBN:978-84-691-9747-9 /DL: T-1259-2008

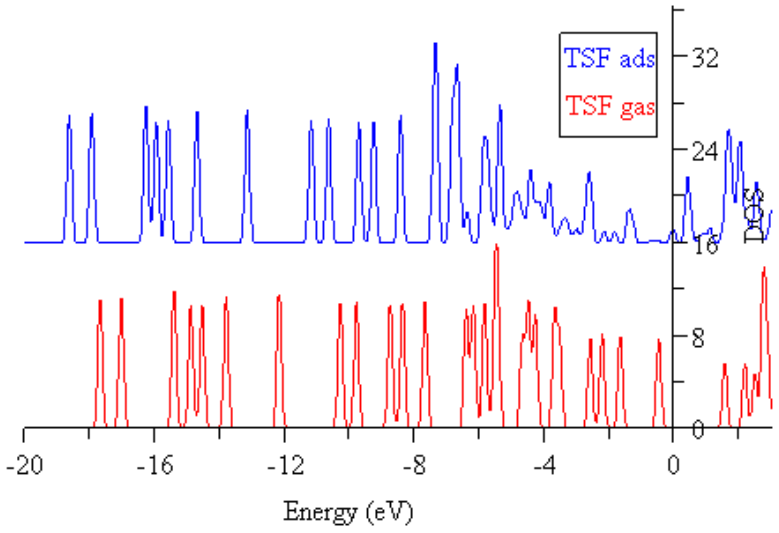

Figure 3.19: PDOS for TSF in gas phase (red line) and adsorbed on Ag(110) (blue line).

are the selenium lone-pair electrons and π C=C bonds. This is similar to the results obtained for TTF, indicating that the behaviour of TTF and TSF must be similar when they are adsorbed.

Comparison of PDOS of free and adsorbed TSF shows the interaction between TSF and surface, because all TSF bands go down in energy (it means they stabilise) around 1 eV. The bands below -5 eV in TSF do not suffer any considerable change in intensity or shape (apart from the translation to lower energies). Main changes appear above this value. Above -5 eV bands lose their intensity and become really wider, indicating a direct interaction between lone-pair electrons (or π C=C, if we only look at the zone and do not have into account any posterior analysis or the results for TTF) and the surface. To improve the understanding of the interaction of TSF with the surface, PDOS on lone-pair electrons of selenium atoms and on surface sp band was carried out.

In figure 3.20 (a), PDOS on lone-pair electrons of TSF in gas phase and adsorbed on Ag(110) are presented. Under -7 eV small changes are present, being the main one the translation of all bands to lower energies due to the interaction between TSF and surface, and the consequent stabilisation of all molecular orbitals in TSF. Main changes appear above -7 eV, where bands lose their intensity and become wider, indicating a direct interaction with the surface.

UNIVERSITAT ROVIRA I VIRGILI
ORGANIC MOLECULES ON METAL SURFACES: FORECASTING STRUCTURES AND SPECTRA
Benjamí Martorell Masip
ISBN:978-84-691-9747-9 /DL: T-1259-2008

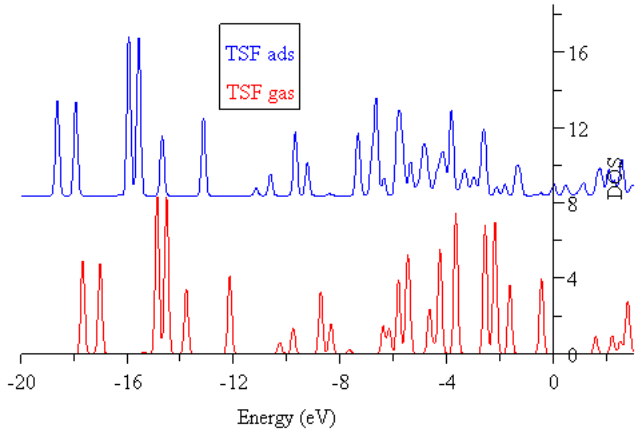

(a) PDOS on lone-pair electrons of Se

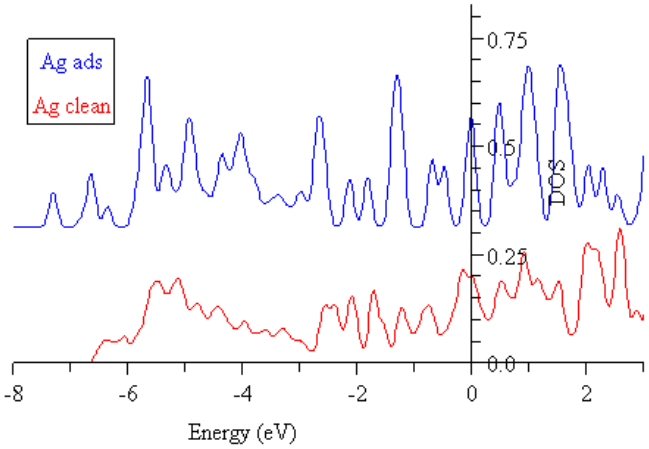

(b) PDOS on surface sp band.

Figure 3.20: a) PDOS on the lone-pair electrons of TSF. b) The sp band of Ag(110).

If the charge integration is made, a decrease of 0.7 electrons is observed for TSF when it is adsorbed on the surface, indicating that it is a good charge donor, even better than TTF.

In figure 3.20 (b) PDOS on the sp band of the surface is presented, for clean and TSF covered Ag surface. In the case of the interaction with TSF, it is clearly observed that some peaks appear in the interacting zone, even under -6 eV. In this case the integration of charge density gives an increase of 0.3 electrons.

UNIVERSITAT ROVIRA I VIRGILI
ORGANIC MOLECULES ON METAL SURFACES: FORECASTING STRUCTURES AND SPECTRA
Benjamí Martorell Masip
ISBN:978-84-691-9747-9 /DL: T-1259-2008

So the interaction between TSF and surface is made through the lone-pair electrons of TSF and the sp surface band. This result is coherent and similar to the one obtained for TTF on Ag(110) and on Au(110). This interaction takes place transferring some charge density from TSF to surface, in the range from 0.3 up to 0.7 electrons a TSF molecule.

3.6 Discussion of results.

3.6.1 Interaction between the surface and TTF (TSF). The most stable structures.

For TTF (and for TSF) all obtained minima (except the adsorption site 1×4-bridge for TTF on Ag(110)) are those structures that maximise the interaction between one sulphur atom (or selenium atom) with one silver atom (or gold atom). From this point of the discussion, only will be take into account the case of TTF adsorbed on Ag(110), but results and arguments used here are valid for discussions of TTF adsorbed on Au(110) or TSF adsorbed on Ag(110).

First of all, the case of 2×4 unit cell is explained, and later, and as a consequence of this, the case of 1×4 unit cell is commented. For 2×4 unit cell only one minimum is obtained (figure 3.6(a)), and the easiest way to discover why this structure is a minimum and not the others is explaining why the other structures are not minima. As commented in section 3.2.1, for adsorption modes shown on figures 3.6 (c) and (d), TTF adopts a bridge-like conformation, and for the other structures, the conformation is boat-like. For bridge-like conformation, the interaction between TTF and surface is made through double C=C bonds. Looking external C=C distances for sites (c) and (d) in table 3.4 in page 65, no meaningful changes are observed respect to gas phase. If interaction between surface and C=C bond were strong, double bond would transfer π electron density to surface and C=C bond should enlarge, but this does not happen and C=C distance remain constant. The same analysis can be made with vibrational frequencies. For sites (c) and (d), no vibrational frequencies are presented, but are presented here for our discussion. For adsorption site (c), C=C stretching frequencies are 1518, 1474, and 1469 cm^{-1} and for site (d) frequencies are 1531, 1509, and 1484 cm^{-1}. If a strong interaction between surface and double bond existed, C=C bond would lose its double bond feature, and C=C stretching frequency should decrease (1500 cm^{-1} is the value of C=C stretching for TTF in gas phase). The experimental value of the vibrational

UNIVERSITAT ROVIRA I VIRGILI
ORGANIC MOLECULES ON METAL SURFACES: FORECASTING STRUCTURES AND SPECTRA
Benjamí Martorell Masip
ISBN:978-84-691-9747-9 /DL: T-1259-2008

frequency of ethene adsorbed on Pt(111), whose interaction is strong, is around 1210 cm^{-1}. On the other hand, the frequency of ethene adsorbed on silver, which presents a very weak interaction, is 1660 cm^{-1} [64]. The adsorption site (c) has a larger decrease in vibrational frequencies of C=C stretching modes respect to gas phase than site (d), which can be related with the fact that TTF has a larger adsorption energy on site (c) than (d) (table 3.4). This is not a great interaction, because frequencies only decrease 50 cm^{-1}, a weak decrease if it is compared with the decrease of ethene when it is adsorbed on Pt (the interaction energy is around 45 kcal·mol^{-1}). So, a conclusion is that C=C double bonds do not interact efficiently with the surface Ag(110). This can be the easiest explanation why adsorption sites (c) and (d) are not minima, because the interaction of S atoms with surface is much more efficient. *Lambert et al.* have reported an experimental study where species with terminal C=C bonds where used, but with heavy substitutes because C=C double bonds adsorb very weak on silver surfaces [65]. If interaction between C=C bond and surface were strong, the possibility of reactivity would increase, and this does not interest because silver is used as a support for OMM. On the other hand, there are metals commonly used in the reactivity of double bonds as Cu or Ni [66, 67].

Previous studies of several sulphonated species adsorbed on metals reveal us important features. First of all, metals can be divided in two groups: those that present reactivity with sulphonated species and those that are inactive. In the first group are present metals like copper and platinum [55, 56, 68, 71]. In the second group, gold and silver are present [56, 71, 72, 73, 74]. Several studies of sulphonated species on silver and gold have been made, and adsorption energies of these species have been calculated. For methanethiol adsorbed on Ag(110), the adsorption energy is -11.3 kcal·mol^{-1} [56]. For H_2S adsorbed on Au(110), several adsorption energies are given, in the range from -7.7 to -10.8 kcal·mol^{-1} [72], and for this molecule adsorbed on Ag(111) the adsorption energy is -5.7 kcal·mol^{-1} [74]. These adsorption energies are much lower than the adsorption energy of TTF adsorbed on Ag(110) (-20.9 kcal·mol^{-1}), but it must be reminded that TTF has four interacting atoms, and the previous species only one. So all these values must be multiplied by four (or the value of TTF divided by four) in order to compare our adsorption energies with those other values. Four times the adsorption energy of H_2S adsorbed on Ag(111) is -22.8 kcal·mol^{-1}, very similar to the value of TTF on Ag(110), and this could be explained by an adsorption mechanism that is similar to the interaction mechanism of TTF with this metal surface.

UNIVERSITAT ROVIRA I VIRGILI
ORGANIC MOLECULES ON METAL SURFACES: FORECASTING STRUCTURES AND SPECTRA
Benjamí Martorell Masip
ISBN:978-84-691-9747-9 /DL: T-1259-2008

Analysing C−S distances, it can be observed that they almost do not change, only one or two hundredth of Å. Besides, no distance changes in the structures where interaction is boat-like, and vibrational frequencies neither change meaningfully, only the lowest ones increase their values due to the interaction with the surface. RAIR spectrum of site (a) and IR spectrum of gas phase for TTF and TTF-d4 are also very similar, as commented in section 3.2.2. This fact can be easily explained if we take into account how TTF interacts with surface.

This is confirmed by the analysis of PDOS. Important changes are present in the zone of lone-pair electrons, but PDOS on C=C double bonds do not change so much like lone-pair electrons do. More details about this are present in section 3.2.3. With the analysis of PDOS, we can also explain why the bending angle decreases when TTF is adsorbed. Charge transfer seems to be the responsible, and a transfer of 0.25-0.35 electrons exist from TTF to the surface.

For 2×4 unit cell is also interesting explaining why no perpendicular adsorption site of TTF is found to be a minimum. It is easy explained if we take into account that TTF trends to maximise the interaction of every sulphur atom with surface. If a perpendicular adsorption mode of TTF were adopted, only two sulphur atoms should interact with surface and the adsorption energy would be the half that the obtained with TTF parallel to surface, consequently, no perpendicular adsorption modes have been found for TTF on 2×4 unit cell.

For 1×4 unit cell no possible interaction between surface and C=C double bond can take place because the unit cell is too small. If TTF interacts with surface via double C=C bonds, it must be parallel to the surface, but this conformation is not possible on this unit cell due to steric effects, so no possible discussion about this interaction can take place for this unit cell. The only possible interaction with this unit cell is through sulphur atoms via their lone-pair electrons. This explains why only the adsorption sites corresponding to figures 3.5 (a) and (b) are minima, because they maximise the interaction of lone-pair electrons with the surface sp band. The adsorption energy for the adsorption site 1×4-top is -11.1 kcal·mol^{-1}, two times the adsorption energy of H_2S on Ag(111) [74], but the adsorption energy on site 2×4-bridge is smaller, indicating that the adsorption process is different to that one that involves H_2S on Ag(111).

Everything explained in this section can also be extended to the case of TTF adsorbed on Au(110) and TSF on Ag(110). TTF can be compared with H_2S adsorbed on Au(111), that is also here presented. Unfortunately no adsorption data of H_2Se specie were found in literature on Au or Ag.

UNIVERSITAT ROVIRA I VIRGILI
ORGANIC MOLECULES ON METAL SURFACES: FORECASTING STRUCTURES AND SPECTRA
Benjamí Martorell Masip
ISBN:978-84-691-9747-9 /DL: T-1259-2008

3.6.2 Comparison of TTF adsorbed on Ag(110) and on Au(110).

Ag(110) and Au(110) surfaces are very similar. Ag and Au are isoelectronic in their valence orbitals, both are $d^{10}s^1$, so their chemical, electronic behaviour can be very similar. Besides, structural parameters are almost equal for Ag and Au. They have very similar lattice parameters due to the effect of the lantanid contraction. All this can explain why Ag and Au behave very similar in front the adsorption of TTF. In both cases no reaction is detected and the adsorption energy is high enough for TTF becoming chemically adsorbed on surface. However, some differences are also present for these metals.

In the case of TTF adsorbed on Ag(110) three minima have been found, but only two for Au(110). In the 2×4 unit cell, both metals only present one minimum, and in both cases is the same, as commented in section 3.6.1. The adsorption energy of TTF on Ag(110) is -21 kcal·mol^{-1} and on Au(110) is -36 kcal·mol^{-1}. It means that interaction between sulphur atoms and Au atoms is stronger than the interaction with Ag atoms. This behaviour is similar to the values of adsorption energy of H_2S adsorbed on Au(110) and on Ag(111). No important differences in geometrical parameters or vibrational frequencies exist in the case of TTF adsorbed on both metals on a 2×4 unit cell.

In the case of TTF adsorbed on 1×4 unit cell, two minima exist for Ag(110), but only one for Au(110). This cannot be explained easily, because differences between Ag and Au are not so significative to ensure the reason of the appearance of this minimum on Ag(110) but not on Au(110). Adsorption energies for TTF on Ag(110) are -11 for site 1×4-top and -8 for site 1×4-bridge, and it is bigger in the case of Au(110), -18 kcal·mol^{-1}. No other changes in geometric parameters or vibrational frequencies seem outstanding.

3.6.3 Comparison of TTF and TSF adsorbed on Ag(110).

Results of sections 3.2 and 3.5 demonstrate that TTF and TSF belong to the same family of charge donor molecules. The adsorption energy of both species on Ag(110) is very similar, -21 kcal·mol^{-1} in the case of TTF and -25 kcal·mol^{-1} in the case of TSF. This indicates that both species chemisorbe on Ag(110), and S−Ag and Se−Ag distances are 2.73 and 2.76 Å, that are almost equal (in section 3.5.1 has been discussed why for TSF this distance is small compared with TTF). Another important geometric parameter is the bending angle of TTF and TSF

UNIVERSITAT ROVIRA I VIRGILI
ORGANIC MOLECULES ON METAL SURFACES: FORECASTING STRUCTURES AND SPECTRA
Benjamí Martorell Masip
ISBN:978-84-691-9747-9 /DL: T-1259-2008

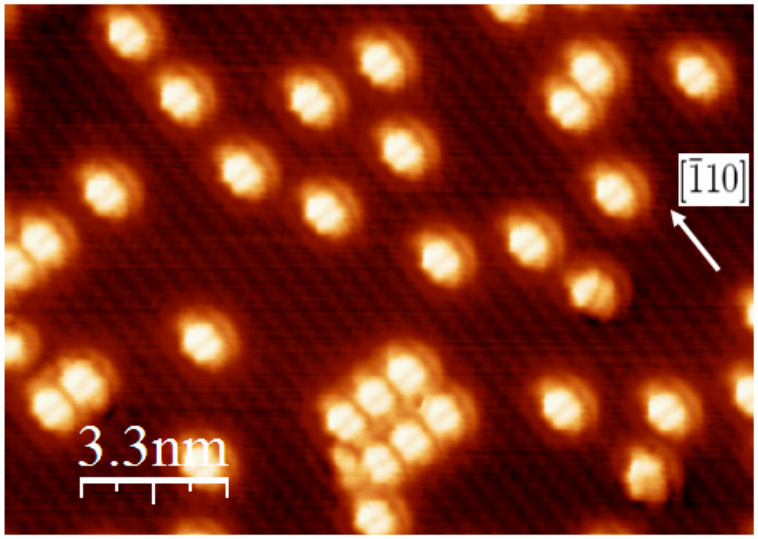

Figure 3.21: Experimental STM image of TTF adsorbed on Ag(110)

when they are adsorbed, being for both species ∼11°. This indicates that both are charge donors on this surfaces, being the charge transfer around 0.25-0.35 electrons for TTF and 0.3-0.7 for TSF (this explains the experimental fact that TSF is a better charge transfering molecule than TTF).

If vibrational spectra of both species are compared (figure 3.7(a) and figure 3.18), both are really similar, and hardly would be find out which spectrum corresponds to each specie. The reason is that all visible bands do not involve displacements of S or Se with an important weight, so the bands that are visible in RAIRS are the same for TTF and TSF. The same happens in the case of TTF-d4 and TSF-d4.

3.6.4 Comparison of theoretical calculations with experimental results: TTF on Ag(110).

In figure 3.21 experimental STM image of TTF adsorbed on Ag(110) is presented. This image was taken by J. Fraxedas & I. Pascual the last year (still not published). This can be compared with those images we presented in section 3.2.3. For a better comparison with theoretical STM images, we present in figure 3.22 a 2×2 STM image, where four TTF molecules are visible.

This experimental image is very important because this image agrees with

UNIVERSITAT ROVIRA I VIRGILI
ORGANIC MOLECULES ON METAL SURFACES: FORECASTING STRUCTURES AND SPECTRA
Benjamí Martorell Masip
ISBN:978-84-691-9747-9 /DL: T-1259-2008

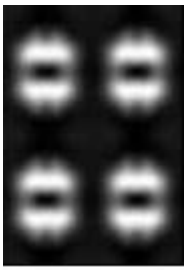

Figure 3.22: Theoretical STM image, where 4 TTF molecules are visible.

our theoretical results, which were obtained three years before this image was available. The agreement between experimental and theoretical results is very good.

We can consider that the coverage used in the experimental image is low and it is comparable with the one we obtain for 2×4-unit cell. The comparison of theoretical and experimental images indicates that the choice of this unit cell is correct. Besides crystallographic direction of adsorption, $[\bar{1}10]$, is the same we used in the theoretical calculations. This corroborates that the only minimum we found for this unit cell was the correct one, which is obtained in the experiments.

Unfortunately, no results about geometric parameters of TTF or vibrational spectrum are still available, and no possible comparison with our results can be made.

3.7 Final summary

In this chapter we have studied the adsorption of some representative molecules of a family of compounds very interesting in new technologies. The interaction of TTF on Ag(110), TTF on Au(110) and TSF on Ag(110) has been studied by means of DFT and compared with the experimental results. With all these results we have been capable of answering questions that were raised at the beginning of this chapter:

- TTF and TSF have been studied in gas phase and compared with results previously reported.
- The adsorption of TTF on Ag(110), TTF on Au(110) and TSF on Ag(110), has been studied, using for TTF 2×4 and 1×4 unit cells and only 2×4 unit

UNIVERSITAT ROVIRA I VIRGILI
ORGANIC MOLECULES ON METAL SURFACES: FORECASTING STRUCTURES AND SPECTRA
Benjamí Martorell Masip
ISBN:978-84-691-9747-9 /DL: T-1259-2008

cell for TSF.

- The study revealed 3 minima for TTF on Ag(110), 2 minima for TTF on Au(110) and only one for TSF on Ag(110).
- The most stable sites for every system were those on 2×4 unit cell (where TTF or TSF adsorbs parallel to the surface), being the adsorption energies -21, -36, and -25 kcal·mol^{-1}, respectively for each system.
- In the adsorption site 2×4, the interaction is made through the lone-pair electrons of four sulphur (or selenium) atoms and four surface atoms.
- RAIR spectra were simulated for every minimum. It has been simulated for TTF and TTF-d4 (TSF and TSF-d4).
- In all spectra of 2×4 unit cells, the most intense band was the one corresponding to C−H wagging (∼600 cm^{-1}).
- The other unit cell studied for TTF, 1×4 unit cell, does not allow a parallel adsorption. TTF on Ag(110) adsorbs perpendicular or tilted 28° respect to the normal of the surface, being E_{ads} -8 and -11 kcal·mol^{-1}, respectively. TTF on Au(110) adsorbs only tilted 30° respect to the surface and E_{ads} is -18 kcal·mol^{-1}.
- RAIR spectra on the 1×4 unit cell are very different of RAIR spectra on the 2×4 unit cell, because the orientation of TTF is completely different, and VNM that are active are really different respect to the ones actives in the other unit cell.
- TTF and TSF suffer a charge transfer to the surface when are adsorbed on the 2×4 unit cell, demonstrating they are good charge donors.
- On the 1×4 unit cell the charge transfer is smaller due to coverage effects.
- An important parameter is the bending angle of TTF (or TSF). It decreases down to ∼10° when it is adsorbed on the 2×4 unit cell, and becomes practically 0° on the 1×4 unit cell. This parameter is related with charge transfer on the 2×4 unit cell, but not in the case of 1×4 unit cell.
- Theoretical STM images have been simulated and compared with the experimental ones.

UNIVERSITAT ROVIRA I VIRGILI
ORGANIC MOLECULES ON METAL SURFACES: FORECASTING STRUCTURES AND SPECTRA
Benjamí Martorell Masip
ISBN:978-84-691-9747-9 /DL: T-1259-2008

Chapter 4

Adsorption of $CHCHCH_2$ on M(111).

C_3H_4 unsaturated hydrocarbons present three stable isomers in the gas phase: propyne ($CH_3C{\equiv}CH$), propadiene ($CH_2{=}C{=}CH_2$) and cyclopropene. The conversion of an isomer into another has attracted the attention of experimentalists and theoreticians in the last decades [76, 77, 78, 80, 81, 85]. This set of unimolecular reactions involves in general radicallary species as intermediates or transition states. In figure 4.1 we can observe the possible isomers.

A very important role is played by the central isomer $CHCHCH_2$, which can be regarded as a carbene or a 1,3-diradical, as a function of where the unbounded electrons are placed on. Consequently, $CHCHCH_2$ can be called vinylcarbene or propene-1,3-diyl.

The work of this chapter is placed in the project of understanding the different reactivity that propyne exhibits on Cu(111) respect to ethyne on the same metal. Whereas ethyne trimerises to form benzene, propyne does not, but it dimerises to the same aromatic specie (Figure 4.2). Moreover, the study involves also more metals: Pt(111), Pd(111) and Rh(111). The catalytic coupling of propyne on Cu(111) was studied in our group from a theoretical point of view, and the main conclusion that emerged from this previous study was the proposal of $CHCHCH_2$ as the key intermediate to explain such reaction [90]. However, propyne presents very different reactivity on other metals. On Pt(111) and Rh(111) propyne decomposes to hydrogen and a carbidic layer. On Pd(111) its behaviour is similar to the ethyne's and trimerises to form trimethylbenzene.

UNIVERSITAT ROVIRA I VIRGILI
ORGANIC MOLECULES ON METAL SURFACES: FORECASTING STRUCTURES AND SPECTRA
Benjamí Martorell Masip
ISBN:978-84-691-9747-9 /DL: T-1259-2008

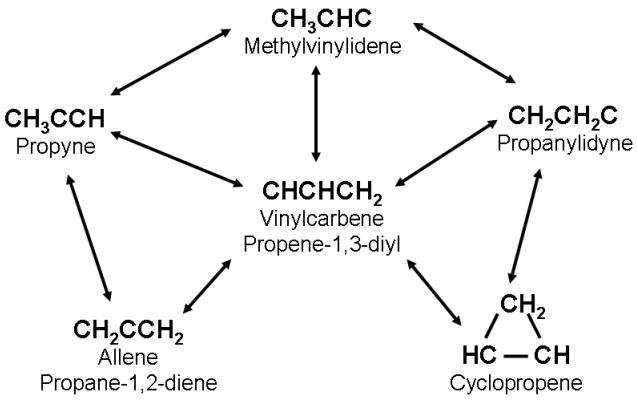

Figure 4.1: Scheme of all possible C_3H_4 isomers.

That is the reason why in this chapter the adsorption of $CHCHCH_2$ is studied. Principal objectives of this chapter are:

- *The study of $CHCHCH_2$ in gas phase and comparison with literature previously reported.*
- *To establish the adsorption modes of $CHCHCH_2$ on Cu(111) on different unit cells.*
- *The evaluation of coverage effects on Cu(111).*
- *To simulate RAIR spectra of $CHCHCH_2$ on Cu(111).*
- *The evaluation of zero point energy (ZPE) correction for $CHCHCH_2$ on Cu(111).*
- *To establish the adsorption modes of $CHCHCH_2$ on Pt(111), Pd(111) and Rh(111).*
- *To evaluate ZPE correction for $CHCHCH_2$ on Pt(111), Pd(111) and Rh(111).*
- *To simulate RAIR spectra of $CHCHCH_2$ on Pt(111), Pd(111) and Rh(111).*
- *To search differences in the adsorption modes on every metal to try to explain differences in reactivity.*

This study is the continuation of our group project, which is the study of the coupling reaction of propyne. For this reason, some data of other previous studies have been used. It would be interesting for a better understanding of this

UNIVERSITAT ROVIRA I VIRGILI
ORGANIC MOLECULES ON METAL SURFACES: FORECASTING STRUCTURES AND SPECTRA
Benjamí Martorell Masip
ISBN:978-84-691-9747-9 /DL: T-1259-2008

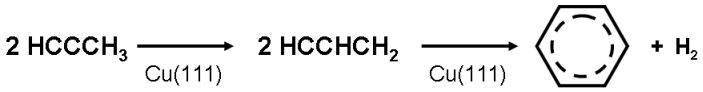

Figure 4.2: Propyne coupling or dimerisation on Cu(111).

chapter and the next one to read previous studies concerning propyne [60, 96, 97, 106, 107].

UNIVERSITAT ROVIRA I VIRGILI
ORGANIC MOLECULES ON METAL SURFACES: FORECASTING STRUCTURES AND SPECTRA
Benjamí Martorell Masip
ISBN:978-84-691-9747-9 /DL: T-1259-2008

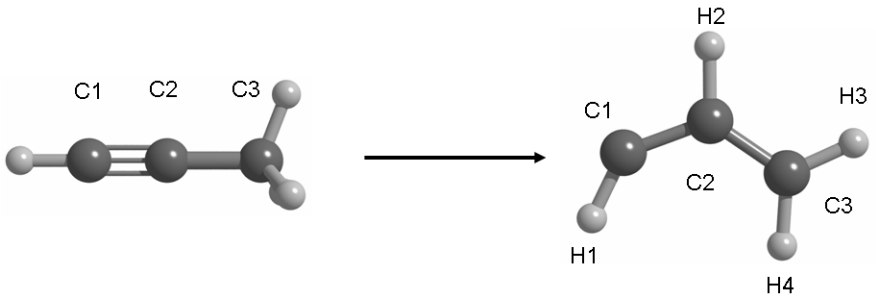

Figure 4.3: Labels of propyne and $CHCHCH_2$ carbons.

4.1 C_3H_4 isomers in the gas phase.

As section 3.1, this section does not pretend to make any discover, but it wants to collect the information already available in literature and to compare this with our results. Because of our objectives, it is not desired to make a complete study of C_3H_4 energetic surface; the only interesting isomers for us are those isomers that are involved in the reaction in Figure 4.2, i.e. propyne and the specie $CHCHCH_2$. Although this, a general overview of C_3H_4 isomers is made. In figure 4.1 a scheme of the interconversion of C_3H_4 isomers is presented, and as a link, $CHCHCH_2$ connects all them [80].

First of all let's focus in $CHCHCH_2$ isomer, and then a general comment of other important species will be made. From here on, to designate the three different carbons of propyne and $CHCHCH_2$, we will use the nomenclature that is shown in figure 4.3. For propyne, the acetylenic carbon is C1, the carbon in the middle is C2 and the methylenic carbon is C3. $CHCHCH_2$ can be seen as the isomerisation product of propyne when one hydrogen goes from C3 to C2, so it is logic to think about C3 to be the carbon with two H atoms, C2 the carbon of the middle and the other carbon comes from the propyne's acetylenic carbon, so it is C1.

Honjou et al. have studied the structure and stability of C_3H_4 isomers, and in particular, $CHCHCH_2$ specie [76, 80, 81]. They have used SCF and MCSCF with CI methodology to study the set of isomers. $CHCHCH_2$ exists in two structures: cis and trans. The difference between cis and trans structures is the relative position of hydrogen in C1 respect to hydrogen in C2. No important differences in energies or in electronic structure exist among them, so all values that will be compared will be refered to trans structure (see $CHCHCH_2$

UNIVERSITAT ROVIRA I VIRGILI
ORGANIC MOLECULES ON METAL SURFACES: FORECASTING STRUCTURES AND SPECTRA
Benjamí Martorell Masip
ISBN:978-84-691-9747-9 /DL: T-1259-2008

Table 4.1: Geometrical parameters of $CHCHCH_2$ in gas phase.

	MCSCF [76]		B3LYP [79]	[e]VASP	
	(^{3}A")	(^{1}A')	(^{3}A")	(^{3}A")	(^{1}A')
[a]d(C1-C2)	1.39	1.47	1.36	1.37	1.44
d(C2-C3)	1.39	1.35	1.38	1.39	1.36
[b]α(C1-C2-C3)	124.6	118.2	126.3	125.2	116.0
α(H1-C1-C2)	135.1	108.8	136.6	136.2	106.4
[c]ΔE (^{3}A"-^{1}A')	50.2		/	54.7	
[d]ΔE (Pr-^{3}A")	192.1		/	214.2	

[a]d: distances (Å); [b]α: angles (degrees); [c]ΔE: difference of energy between propene-1,3-diyl and vinylcarbene(kJ·mol^{-1}); [d]ΔE: difference of energy between propyne and propene-1,3-diyl (kJ·mol^{-1}); [e]VASP: PW91-PW, plane-waves.

molecule in figure 4.3) . The most stable $CHCHCH_2$ structure at SCF level is ^{3}A" with these two electrons localised on C1, and only 2 kcal·mol^{-1} above lies ^{3}A" with the two electrons localised one on C1 and the other one on C3. When MCSCF method is used, this two possible electronic structures are resonant and, consequently, we can call this structure propene-1,3-diyl. 9.7 kcal·mol^{-1} above triplet structure exist one ^{1}A' structure, where two unpaired electrons lie on C1, so this singlet structure can be called vinylcarbene. Before *Honjou et al.* made this study, *Feller et al.* and *Davis et al.* had also studied vinylcarbene [77, 78], but the theory level used was lower than the used by *Honjou et al.*, so no references to their values will be made. Not only theoretical studies are made about $CHCHCH_2$, but also experimental evidences have been found this is a key intermediate in the interconversion of C_3H_4 isomers [85].

From here on, to simplify nomenclature of $CHCHCH_2$ isomer, it will be called VC (vinylcarbene's acronym) for both electronic structures. If it is necessary to differentiate between both electronic structures, no acronym will be used and "vinylcarbene" and "propene-1,3-diyl" words will be the used ones.

Another important feature of $CHCHCH_2$ is its geometry, because depending on its electronic structure, geometry changes. As commented before, for vinylcarbene, two unpaired electrons are localised on C1, and one double C=C bond exists between C2 and C3. In the case of propene-1,3-diyl, two resonant structures exist between diradical, whose two unpaired electrons are localised on C1 and C3, and carbene, whose two unpaired electrons are localised on C1; as a consequence in this case both C−C bonds must be very similar. In table 4.1 geometrical parameters of VC in gas phase are presented. *Honjou et al.* have

UNIVERSITAT ROVIRA I VIRGILI
ORGANIC MOLECULES ON METAL SURFACES: FORECASTING STRUCTURES AND SPECTRA
Benjamí Martorell Masip
ISBN:978-84-691-9747-9 /DL: T-1259-2008

used wave-functions based methods and in a recent study *Le et al.* have used DFT methods to study reactivity on the triplet state electronic surface of C_3H_4 isomers. For propene-1,3-diyl, C1−C2 and C2−C3 distances are very similar in all cases, being 1.39 and 1.39 Å using MCSCF method, 1.36 and 1.38 Å using B3LYP method and 1.37 and 1.39 Å with our calculation method (PW91-PW; plane-waves). It can be observed that both DFT methods produce very similar results and being C2−C3 distance a bit larger than C1−C2, being the contrary case for MCSCF method. The angle between three carbon atoms is around 125° in all cases, being 124.6° for MCSCF, 126.3° for B3LYP and 125.2° for PW91-PW and plane-waves. Thereafter, in the case of vinylcarbene, only the values reported by *Honjou et al.* have been found in literature. In this case both distances are different, indicating C1−C2 bond is a single bond and C2−C3 bond a double bond. Using MCSCF method, distances are, respectively, 1.47 and 1.35 Å, and using PW91-PW are 1.44 and 1.36 Å. Differences are around ±0.02 Å. Another important parameter is the carbonated structure angle. In the case of MCSCF methods it is 118.2° and in PW91-PW it is 116.0°, being in good agreement. It can be observed that this angle is around 8° smaller in vinylcarbene than in propene-1,3-diyl due to the different electronic structure, but both are close to 120°, which is the angle in a sp^2 hybridisation, indicating a double C=C bond exists. Besides, it is clear that propene-1,3-diyl is the most stable electronic structure, lieing 50.2 kJ·mol^{-1} or 54.7 kJ/ml (MCSCF or PW91-PW respectively) under vinylcarbene.

The aim of this chapter is to study the adsorption of VC on (111) surface of several metals, and in the next chapter it is desired to study the isomerisation from propyne (from here on Pr) to VC on these same surfaces, so it is logic to think about how this process takes place in gas phase. In table 4.1 difference of energies between Pr and propene-1,3-diyl is around 200 kJ·mol^{-1} (192.1 kJ·mol^{-1} for MCSCF calculations and 214.2 for PW91-PW calculations). What is more, propene-1,3-diyl is a triplet state, and propyne in gas phase is a singlet, this means that a conical intersection exists and this isomerisation is not possible termically. It is possible to isomerisate to vinylcarbene, which is even higher in energy, around 250 kJ·mol^{-1}. This big thermodynamic difference could explain why propyne does not dimerise in gas phase and becomes benzene, the intermediate is too high in energy.

Honjou et al. studied the thermal interconversion of all C_3H_4 isomers, and they reported an activation energy of 334.0 kJ·mol^{-1} in the isomerisation of propyne to vinylcarbene [81]. This is a very high barrier and explains why no

UNIVERSITAT ROVIRA I VIRGILI
ORGANIC MOLECULES ON METAL SURFACES: FORECASTING STRUCTURES AND SPECTRA
Benjamí Martorell Masip
ISBN:978-84-691-9747-9 /DL: T-1259-2008

isomerisation exists among C_3H_4 isomers or why propyne does not dimerise in gas phase. It has also been reported a scheme of all possible termal interconversions in C_3H_4 surface, being propyne and propadiene the most stable structures, and cyclopropene lieing at 94.9 kJ·mol^{-1}.

More recently, *Kakkar et al.* have reported two studies about C_3H_4 surface by means of DFT [82, 83]. They report that vinylcarbene lies 247.9 kJ·mol^{-1} higher in energy than propyne, but no geometrical values of VC are given. Although the lack of geometrical data for VC, a deep study of propyne, allene and cyclopropene is made, giving results of geometries, vibrational frequencies and charge distribution on these molecules. Moreover, they calculate interconversion rates among all C_3H_4 isomers, and in the case that propyne isomerises to vinylcarbene, the activation energy to the transition state is 331.5 kJ·mol^{-1}, in good agreement with the value reported by *Honjou et al.* that was 334.0 kJ·mol^{-1}, and the rate constant is calculated to be 1.1E10 at 1500 K and 1 atm of pressure.

Finally, *Miller et al.* have gone further and they have calculated possible dehydrogenation paths to study other ways to obtain benzene, phenyl and fulvene in gas phase, calculating rate constants and relative energies to form C_3H_4 species [84].

4.2 VC adsorbed on Cu(111).

Copper is a metallic element that belongs to the first row of the transition metals. Its electronic valence structure is $d^{10}s^1$, being isoelectronic to Ag [154], Au [155] and Rg [155]. Copper has a crystallographic Fm3m structure, and the lattice parameter is 3.6147 Å (atomic radius of 1.2780 Å) [151].

Cu surface (and all other metals) is modelled using a slab model with four layers, whose two uppermost ones are relaxed. Five layers of vacuum are placed between consecutive slabs. All atoms of VC molecule are allowed to relax. Plane-waves basis set cut-off is in all cases 500 eV, and the inner-shell electrons are modelled by PAW pseudo-potentials. The density functional used for calculations is PW91-PW.

4.2.1 Adsorption modes.

It has been commented that propyne reacts on copper to yield benzene (and other subproducts) [101]. In this section it is studied the behaviour of VC

UNIVERSITAT ROVIRA I VIRGILI
ORGANIC MOLECULES ON METAL SURFACES: FORECASTING STRUCTURES AND SPECTRA
Benjamí Martorell Masip
ISBN:978-84-691-9747-9 /DL: T-1259-2008

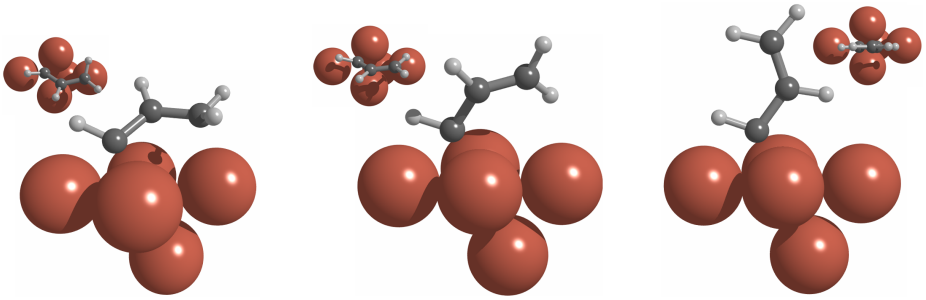

(a) C1-fcc-C3-top (b) C1-fcc-cis (c) C1-fcc-trans

Figure 4.4: Different adsorption modes of VC on Cu(111) on a 2×2 unit cell.

adsorbed on Cu(111), which is the intermediate purposed for this reaction [90].

In this point it is recommended to see figure 4.26 on page 191, where a summary of all VC structures that we have found in this chapter is presented.

4.2.1.1 2×2 unit cell.

We consider first the adsorption of VC on the 2×2 unit cell (i.e., a molecular coverage of 0.25). This unit cell should describe the high coverage regime. Several adsorption modes and starting geometries were explored. We found six stable surface structures characterised as minima. Three of them have the C1 atom placed on fcc site, while the other on hcp site. In figure 4.4 those corresponding to C1 on fcc site are presented. Nomenclature used in figure 4.4 is the one used from this point of discussion (for hcp structures "fcc" will be substituted by "hcp"). The C1-fcc-trans and the C1-hcp-trans structures (in general, C1-trans structures) have a molecular plane perpendicular to the surface, and only C1 atom interacts with the surface. The molecular plane is lacked by the other four structures. In the C1-fcc-cis and C1-hcp-cis structures (in general, C1-cis structures) only C1 atom interacts with surface, being C2 and C3 closer to surface than in C1-trans structures. In the C1-fcc-C3-top and the C1-hcp-C3-top structures (in general, C3-top structures), all carbon atoms interact with the surface, being C3 atom placed almost above a metal atom (top position).

The adsorption energies (E_{ads}) respect to gas phase propyne are showed in table 4.2. The ZPE corrected and uncorrected values are shown in different columns in order to check ZPE effects on energy differences. For sakes of com-

UNIVERSITAT ROVIRA I VIRGILI
ORGANIC MOLECULES ON METAL SURFACES: FORECASTING STRUCTURES AND SPECTRA
Benjamí Martorell Masip
ISBN:978-84-691-9747-9 /DL: T-1259-2008

Table 4.2: Relative adsorption energies respect to propyne in gas phase on Cu on the 2×2 unit cell. All values are given in kJ·mol^{-1}.

	E_{ads}				
	No ZPE	ZPE	ZPE-d1	ZPE-d3	ZPE-d4
Propyne C1-fcc	-79.0	-74.7	-75.1	-75.2	-75.6
Propyne C1-hcp	-79.4	-75.1	-75.4	-75.6	-75.9
VC C1-fcc-trans	-25.7	-22.8	-23.0	-23.0	-23.2
VC C1-hcp-trans	-20.2	-17.6	-17.8	-17.7	-18.0
VC C1-fcc-cis	-20.7	-17.7	-17.9	-17.8	-18.0
VC C1-hcp-cis	-15.9	-13.0	-13.2	-13.2	-13.4
VC C1-fcc-C3-top	-17.8	-13.5	-14.1	-13.6	-14.2
VC C1-hcp-C3-top	-18.6	-14.2	-15.1	-14.0	-15.0

parison, energies of adsorbed propyne are also included (in fact, propyne structures and energies were recomputed to exclude variations coming from small differences on computational details between this work and the other previously reported [60, 96, 97, 106]).

The relative energies among adsorbed VC structures are in a range of 10 kJ·mol^{-1}, being the C1-fcc-trans the most stable one. Both C1-trans structures are slightly more stabilised on the surface than the other structures. The difference of energy for C1-fcc-cis and C1-fcc-C3-top structures are 5.0 and 7.9 kJ·mol^{-1} respect to C1-fcc-trans, and for hcp structures are 4.3 and 1.6 kJ·mol^{-1}, respectively. When ZPE is taken into account, four different possibilities can take place. All VC structures come from the isomerisation of propyne: if the acetylenic hydrogen is substituted by deuterium is obtained DC≡CCH$_3$ (Pr-d1), if the three methylenic hydrogens are substituted by deuterium it is obtained HC≡CCD$_3$ (Pr-d3), and if all H atoms are substituted by deuterium, we obtain DC≡CCD$_3$ (Pr-d4). When isomerisation takes place, we yield CDCHCH$_2$ (VC-d1), CHCDCD$_2$ (VC-d3) and CDCDCD$_2$ (VC-d4), respectively. In general, when ZPE is taken into account, differences of energy respect to the C1-trans structures, do not vary meaningfully for C1-cis structures, but differences of energy are slightly enlarged for C3-top structures because ZPE correction is larger for these structures. For C1-trans and C1-cis structures, fcc sites are slightly more stabilised than hcp sites (∼5 and ∼4 kJ·mol^{-1}, respectively), whereas the differences in energy of both C3-top structures is in the limit of the energy accuracy in the calculation.

All VC structures are less stable than adsorbed propyne by ∼50 or ∼60 kJ·mol^{-1}. When ZPE corrections are included, these differences do not change

UNIVERSITAT ROVIRA I VIRGILI
ORGANIC MOLECULES ON METAL SURFACES: FORECASTING STRUCTURES AND SPECTRA
Benjamí Martorell Masip
ISBN:978-84-691-9747-9 /DL: T-1259-2008

meaningfully because ZPE have the same order of magnitude. This is specially true between C3-top structures and adsorbed Pr, whose ZPE correction is about 4 kJ·mol^{-1} in both cases. In the case of adsorbed Pr, the lowering of the C−H stretching frequency of acetylenic H and the loss of the triple C≡C bond character is almost compensated by the inclusion of the whole molecule against surface vibrations. The major ZPE correction for the adsorbed Pr could be ascribed to the major frequency values of adsorbed molecule in the region between 600 and 1000 cm^{-1}. In the case of C3-top structures, all frequencies above 600 up to 3000 cm^{-1} decrease respect to the corresponding Pr values, whereas the other frequencies outside this range increase in the same amount, so ZPE correction of C3-top structures have the same value than adsorbed Pr.

All VC structures become stable respect to gas phase Pr and the surface (from -18 to -26 kJ·mol^{-1}). When ZPE corrections are included all values are lower in absolute value (from -13 to -22 kJ·mol^{-1}), because ZPE is larger for adsorbed structures than for gas phase propyne. This is a very important aspect, because VC structures in gas phase were much more unstable than propyne in gas phase, in this case, adsorbed VC is more favourable than propyne in gas phase, and only ∼50 kJ·mol^{-1} above adsorbed Pr.

Finally, in this point it is interesting to explain why the two uppermost layers of the slab have been relaxed. For C1-trans structure, if this relaxation is not taken into account the no-ZPE corrected E_{ads} is -20.7 kJ·mol^{-1} and for C3-top it is -11.3 kJ·mol^{-1}. The addition of the this effect stabilises in both cases around 5 kJ·mol^{-1} (E_{ads} is -25.7 and -17.8 kJ·mol^{-1}, respectively). This contribution is of the same order as the ZPE correction, so it must be taken into account. Moreover, the atoms in the first layer of the slab suffer some displacement from their ideal site. For C1-trans site, this displacement is up to ±0.11 Å and in C3-top ±0.09 Å.

4.2.1.2 3×3 unit cell.

In order to check coverage effects, the size of the unit cell was increased to 3×3, which corresponds to a molecular coverage of 1/9. This unit cell should depict the low (or medium) coverage regime, or situations where repulsions among adsorbed molecules are minimised. We found four structures that were present on the 2×2 unit cell (C1-fcc-trans, C1-hcp-trans, C1-fcc-C3-top and C1-hcp-C3-top), but two new minima are obtained in this case. Both new structures are like C3-top structures, but in this case the main difference is that C3 is placed

UNIVERSITAT ROVIRA I VIRGILI
ORGANIC MOLECULES ON METAL SURFACES: FORECASTING STRUCTURES AND SPECTRA
Benjamí Martorell Masip
ISBN:978-84-691-9747-9 /DL: T-1259-2008

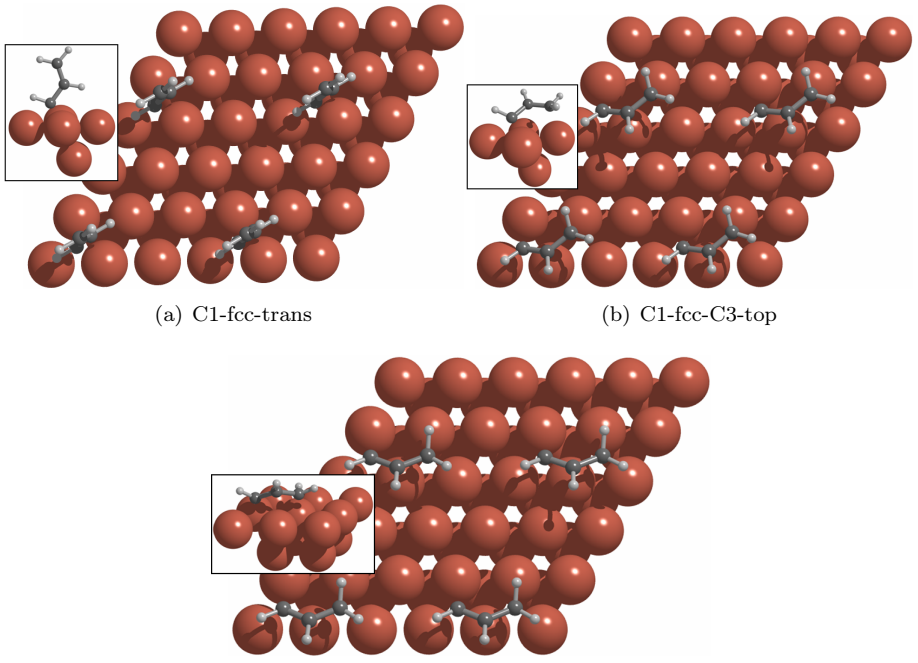

(a) C1-fcc-trans (b) C1-fcc-C3-top

(c) C1-fcc-C3-fcc

Figure 4.5: Adsorption modes of VC on Cu(111)on the 3×3 unit cell.

on the nearest three-hollow site of the same type as C1, obtaining in this case C1-fcc-C3-fcc and C1-hcp-C3-hcp structures (in general, C3-hollow structures). The C1-fcc-cis and C1-hcp-cis structures were not found on this unit cell. In figure 4.5 all structures with C1 on fcc for 3×3 unit cell are presented. In this case unit cell is duplicated to have a better view of structures and the coverage.

When ZPE corrections are not taken into account, the most stable structure is C1-fcc-C3-fcc. Adsorption energies of all structures are shown in table 4.3. The corresponding hcp structures is almost degenerate. Energy difference between C3-top structures and C3-hollow structures is only ∼4 kJ·mol^{-1} with no ZPE correction. ZPE correction is larger for C3-hollow structures than for C3-top structures, and when ZPE correction is included, C1-fcc-C3-top structure is slightly favoured, but energy differences are bellow the energy accuracy, so we can conclude that these four structures (C3-top and C3-hollow) become degenerated.

The most important coverage effects are the appearance of a new adsorption mode and the stabilisation of C3-top structures in front of C1-trans structures.

UNIVERSITAT ROVIRA I VIRGILI
ORGANIC MOLECULES ON METAL SURFACES: FORECASTING STRUCTURES AND SPECTRA
Benjamí Martorell Masip
ISBN:978-84-691-9747-9 /DL: T-1259-2008

Table 4.3: Relative adsorption energies respect to propyne in gas phase on Cu on the 3×3 unit cell. All values are given in kJ·mol^{-1}.

	E_{ads}				
	No ZPE	ZPE	ZPE-d1	ZPE-d3	ZPE-d4
Propyne C1-fcc	-98.9	-93.9	-94.3	-94.2	-94.6
Propyne C1-hcp	-98.9	-93.5	-93.9	-94.0	-94.4
VC C1-fcc-trans	-36.4	-33.4	-33.7	-33.7	-34.0
VC C1-hcp-trans	-34.8	-31.9	-32.1	-32.1	-32.4
VC C1-fcc-C3-fcc	-60.4	-54.0	-54.5	-54.0	-54.5
VC C1-hcp-C3-hcp	-59.9	-53.3	-53.8	-53.4	-53.9
VC C1-fcc-C3-top	-56.6	-54.1	-54.6	-54.1	-54.7
VC C1-hcp-C3-top	-56.0	-53.6	-54.1	-53.6	-54.1

One can imagine that if three carbon atoms are interacting with surface, the E_{ads} must be larger than if only one C atom is interacting with surface. In the case of 2×2 unit cell it did not happen because C3-top structure had too much repulsion with adjacent adsorbed VC molecules. As the coverage decreases, C3-top modes of adsorption become more stable than the C1-trans structures because C3-top structures need a major surface area to be located, so when coverage decreases, the repulsion between adjacent molecules is reduced. The energy difference between C1-trans and C3-top structures is around 25 kJ·mol^{-1} (20 with ZPE corrections).

As in the case of propyne molecule, another coverage effect is the larger adsorption energy of all structures respect to gas phase Pr in the larger unit cell, which is from -56 to -61 kJ·mol^{-1}. The inclusion of ZPE correction decreases the E_{ads}, as expected.

As in the case of 2×2 unit cell, adsorbed VC species are not more stable than adsorbed Pr. A coverage reduction does not change the stabilisation order of propyne versus VC moieties. For C1-trans structures this energy difference slightly increases as coverage is reduced by 8 or 4 kJ·mol^{-1} (for C1-fcc-trans and C1-hcp-trans, respectively). For C3-top structures the energy difference respect to adsorbed Pr decreases much more, from ∼60 to ∼40 kJ·mol^{-1} when coverage is reduced. So, C1-trans and C3-top structures behave different when coverage decreases. Besides, one adsorption mode disappears and another new appears (C1-cis and C3-hollow, respectively) when the unit cell is increased.

UNIVERSITAT ROVIRA I VIRGILI
ORGANIC MOLECULES ON METAL SURFACES: FORECASTING STRUCTURES AND SPECTRA
Benjamí Martorell Masip
ISBN:978-84-691-9747-9 /DL: T-1259-2008

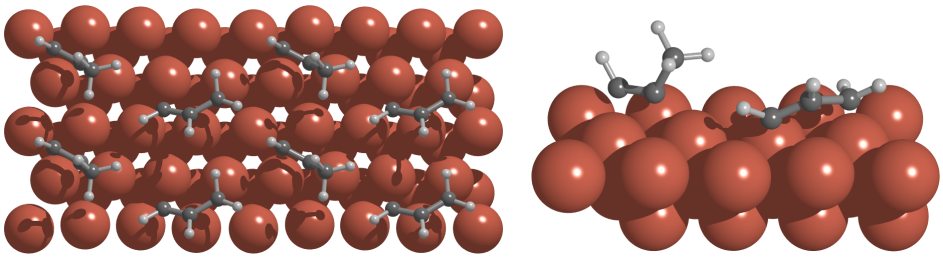

(a) Top view, duplicated unit cell. (b) Front view.

Figure 4.6: Coadsorption of one propyne molecule and one VC molecule on a $4\times\sqrt{3}$ unit cell.

4.2.1.3 $4\times\sqrt{3}$ unit cell.

Finally, some test calculations with $4\times\sqrt{3}$ unit cell have been performed. This unit cell with two adsorbed propyne molecules was proposed from LEED experiments [104, 105]. A model to reproduce this surface order consists of two adsorbed propyne molecules per unit cell in a criss-cross fashion. The extra stabilisation of this system could be computed as the difference between the adsorption energy of both Pr molecules adsorbed simultaneous on this unit cell and the sum of the E_{ads} of both orientations computed each one in the 2×2 unit cell. This stabilisation is only of 2.5 kJ·mol^{-1} (2.9 with ZPE correction).

However, one could compute the whole process of the adsorption of both molecules in two steps. First, one propyne molecule is adsorbed on the $4\times\sqrt{3}$ unit cell, whose E_{ads} is -69 kJ·mol^{-1}. Then, the second propyne molecule is added to the surface, obtaining the whole E_{ads}, -161 kJ·mol^{-1}. The energy difference between both steps (-91 kJ·mol^{-1}) gives the stabilisation of the second molecule from gas phase in the presence of another molecule on the unit cell. This fact can justify the election of a 3×3 unit cell to study the conversion from propyne to VC species, without considering two adsorbed Pr molecules in the unit cell. To this purpose, it has been considered on this unit cell the coadsorption of one Pr molecule and one VC isomer. Among all possibilities, the most stable structure for each isomer on the 3×3 unit cell has been chosen as the starting point of the optimisation process, i.e. propyne C1-fcc and VC C1-fcc-C3-fcc. The E_{ads} of this system is -115 kJ·mol^{-1}, so the isomerisation energy, from Pr to VC is endothermic, by 46 kJ·mol^{-1}, when one Pr molecule is present on the surface. The isomerisation energy, from Pr to VC, was 37 kJ·mol^{-1} on the 3×3 unit cell. So, coadsorbed Pr increases in some extent the endothermicity of the

UNIVERSITAT ROVIRA I VIRGILI
ORGANIC MOLECULES ON METAL SURFACES: FORECASTING STRUCTURES AND SPECTRA
Benjamí Martorell Masip
ISBN:978-84-691-9747-9 /DL: T-1259-2008

Table 4.4: Adsorption energies for propyne and VC on Cu(111) using a $4\times\sqrt{3}$ unit cell. The second value in first column is the energy of the system respect to 1 adsorbed propyne (1 ads. Pr). All values are in kJ·mol^{-1}.

	E_{ads} / ΔE (1 ads. Pr)				
	No ZPE	ZPE	ZPE-d1	ZPE-d3	ZPE-d4
1 ads. Pr	-69.8 / 0.0	-65.5	-65.8	-65.9	-66.3
2 coads. Pr	-161.1 / -91.3	-152.7	-153.4	-153.5	-154.2
1 ads. VC	-32.0 / 37.8	-29.1	-29.7	-29.1	-29.7
coads. Pr & VC	-115.6 / -45.8	-107.7	-108.5	-108.2	-109.1

isomerisation process. Note that the position of C3 atom of VC is between the hollow-site and the top-site (see figure 4.6), similar to the 2×2 unit cell. This is another effect of repulsion between adjacent molecules as coverage increases. Finally, the C1-fcc-C3-fcc structure was also computed alone on this unit cell. In this case, the structure retains the position of both C1 and C3 atoms. The energy difference between adsorbed propyne and VC is around 38 kJ·mol^{-1}. As a result of these test calculations, one could argue the use of 2×2 and 3×3 unit cells to study the isomerisation from Pr to VC as representative situations of high and low coverage regimes, respectively. So, the study of kinetics of this reaction (chapter 5) will be done without considering the $4\times\sqrt{3}$ unit cell, i.e. avoiding the coadsorbed Pr molecule in the determination of transition states structures.

4.2.2 Adsorption geometries.

As in the case of propyne adsorption on Cu(111), the position of C1 on the fcc or on the hcp site does not introduce any relevant change on adsorption geometry [106]. The comparison of adsorption geometry between fcc and hcp site for the same kind of adsorbed structure indicates that all distances do not change more than ±0.02 Å, and all bond angles do not differ more than ±1°. So, in order to reduce such amount of information, we have only reported in table 4.5 geometric parameters of C1-fcc structures, which are slightly more stable than the corresponding hcp structures. Some differences take place when the unit cell changes. So, it has been chosen to display geometrical parameters obtained with 3×3 unit cell, or with 2×2 unit cell if structure does not exist for 3×3 unit cell. Values for other unit cells are reported in brackets, but only when differences are larger than ±0.02 Å or ±1°. C−H distances are not shown in this

UNIVERSITAT ROVIRA I VIRGILI
ORGANIC MOLECULES ON METAL SURFACES: FORECASTING STRUCTURES AND SPECTRA
Benjamí Martorell Masip
ISBN:978-84-691-9747-9 /DL: T-1259-2008

Table 4.5: Geometrical parameters of VC adsorbed on Cu(111). A slash ("/") means meaningless value in the case of C1-trans dihedral angle (structure is flat) or meaningless change in the case of C3-hollow. In brackets changing parameters more than ±0.02 Å or ±1°.

	C1-trans	C1-cis	C3-top	C3-hollow
	3×3 (2×2)	2×2	3×3 (2×2)	3×3 (4×$\sqrt{3}$; 4×$\sqrt{3}$&Pr)
[(a)]d(C1-C2)	1.45	1.45	1.41	1.40
d(C2-C3)	1.36	1.36	1.44	1.45
[(b)]α(C1-C2-C3)	125.3	127.5	124.9 (122.3)	124.1
α(H1-C1-C2)	106.6	106.8	112.0	112.5
α(H2-C2-C1)	117.1	115.8	118.6	119.2
α(H2-C2-C3)	117.7	116.7	116.3 (118.2)	116.7
α(H3-C3-H4)	117.3	117.3	112.2	110.0 (/ ; 111.2)
α(H3-C3-C2)	121.1	121.3	116.3 (117.4)	115.9
α(H4-C3-C2)	121.6	121.3	114.5	113.2
[(c)]tilt	0	30.6	46.1	45.7 (/ ; 42.9)
[(d)]θ(H1-C1-C2-C3)	/	-148.7	-159.1 (-155.4)	-166.7 (/ ; -165.0)
θ(H3-C3-C2-C1)	/	-179.9	-177.6	-179.1 (/ ; 177.5)
θ(H4-C3-C2-C1)	/	8.1	48.9	52.5 (/ ; 50.7)
θ(H1-C1-C2-H2)	/	28.6	16.4 (19.3)	12.9
θ(H2-C2-C3-H3)	/	2.9	6.8	1.3 (/ ; 4.5)
θ(H2-C2-C3-H4)	/	-174.1	-126.7	-128.8 (-125.7 ; /)
[(e)]d(C1-M)	2.04	1.98	2.00	1.99
d(C2-M)	/	/	2.27 (2.34)	2.17 (/ ; 2.25)
d(C3-M)	/	/	2.10	2.26 (2.19 ; 2.13)
d(H1-M)	1.97	1.92	2.16 (2.08)	2.23 (/ ; 2.17)
d(H2-M)	2.72	/	2.87 (2.94)	2.88 (/ ; 2.94)
d(H3-M)	/	/	2.77	2.47 (2.53 ; 2.83)
d(H4-M)	/	2.45	2.23 (2.35)	1.97 (2.00 ; 2.05)

[(a)]d: distances (Å); [(b)]α: angles (degrees); [(c)] tilt: angle between C1-C2-C3 plane and the normal vector of surface; [(d)]θ: dihedral angles (degrees); [(e)] distances to nearest surface atom.

table as all distances are between 1.09 and 1.12 Å, so they do not contribute to give information about VC adsorption. Also the distances of carbon atoms respect to the position of the relaxed surface atoms are presented. See figure 4.3 to remember nomenclature.

Observing the coordination mode, one expects structures that are linked only by C1 to surface (C1-fcc-trans, C1-hcp-trans, C1-fcc-cis and C1-fcc-cis) to be a carbene-like structures, in particular, C1-trans structures retain the molecular plane. The C2−C3 distance in C1-trans structure is 1.36 Å, whereas

UNIVERSITAT ROVIRA I VIRGILI
ORGANIC MOLECULES ON METAL SURFACES: FORECASTING STRUCTURES AND SPECTRA
Benjamí Martorell Masip
ISBN:978-84-691-9747-9 /DL: T-1259-2008

C1−C2 distance is 1.45 Å, indicating the existence of a double C=C bond and a short C−C single bond, respectively, which is an evidence of the carbene-like structure (look at table 4.1 to compare geometric parameters with VC in gas phase in singlet (carbene-like) and triplet state (resonant)). The most changing angle between vinylcarbene and propene-1,3-diyl is H1−C1−C2 (107.0° when molecule is adsorbed), indicating a sp^3-like hybridisation of C1, like vinylcarbene in gas phase. For C1-trans structures no differences appear neither for fcc or hcp structures nor for 2×2 and 3×3 unit cells.

Finally, it is important to note that for C1-trans structures H1 and H2 atoms are near the surface (H−M distance of 1.95 and 2.51 Å, respectively). In fact, adsorbed C1-trans structure is similar, in some sense, to that proposed as an agostic intermediate in the conversion (β-H elimination) of adsorbed allyl to allene on Ag(111), despite the allyl moiety has an extra hydrogen atom on the interacting carbon atom [86]. β-H elimination is one of the most important and favourable process of hydrocarbon conversion on metal surfaces [87, 88]. Accordingly, the possibility of the existing of allenyl (CH_2=C=CH) structures on the surface should be taken into account. So, in the study of the conversion from Pr to VC (see chapter 5), not only the direct 3,2-H shift mechanism will be determined, but also the dehydrogenation-hydrogenation pathway following the Horiuti-Polanyi mechanism [89].

C1-cis structures appear only when a 2×2 unit cell is modelled, indicating this structure is only stable in the high coverage regime. These structures lack of the molecular plane that VC posses in gas phase, because H1 tilts out the molecular plane 28.6°, remaining H2, H3 and H4 in the same plane as the C1−C2−C3 plane, which is tilted ∼30° respect to the surface normal. In C1-cis structures H2 lies at the same site as H1 respect to C1−C2 bond, whereas in C1-trans structures H1 and H2 are placed on the opposite site of the C1−C2 bond (as commented in section 4.1). The C1−C2 distance is 1.45 Å, whereas C2−C3 distance is 1.36 Å, indicating, as in the case of C1-trans structures, that a double C=C bond exists between C2 and C3, and that this is a carbene-like structure. The H1−C1−C2 angle is 106.8°, that agrees with the fact that this structures is a carbene-like structure (vinylcarbene), because propene-1,3-diyl angle is more opened in gas phase (around 130°). Another important fact is that H1 and H4 have agostic interactions with the surface and β-H elimination could be possible. The H1−M distance is 1.92 Å, being the H4−M rather larger, 2.45 Å. The C1-M distance is a bit shorter than in C1-trans structures, which was only 1.98 Å. Finally, no important differences exist between C1-fcc-cis and

UNIVERSITAT ROVIRA I VIRGILI
ORGANIC MOLECULES ON METAL SURFACES: FORECASTING STRUCTURES AND SPECTRA
Benjamí Martorell Masip
ISBN:978-84-691-9747-9 /DL: T-1259-2008

C1-hcp-cis structures, not existing this structure on the 3×3 unit cell.

C3-top and C3-hollow structures have a very different adsorption geometry than C1-trans and C1-cis structures. First, these structures do not retain the molecular plane, like C1-trans structure did. Then, the coordination mode to the surface, which is the more important variation, is very different: in this case, all carbon atoms interact with the surface. The shorter M−C distances of each C atom are in the range from 2.0 to 2.3 Å. Consequently, they show an allylic structure, being C1−C2 and C2−C3 distances for C3-hollow structures 1.40 and 1.45 Å, and distances for C3-top are 1.41 and 1.44 Å, respectively, so no localised double bond persists upon adsorption, and being these distances much larger than propene-1,3-diyl's in gas phase, indication that double C=C bond interacts with the surface. The mode of coordination is an important difference respect to previous cluster calculations carried out by *Clotet et al.* [90], where only C1 and C3 interacted with the surface, therefore exhibiting a bisected 1,3-diradical structure and localised double and simple C−C bonds. In all structures, C1 interacts with the three Cu atoms of the hollow site, showing the typical coordination of an acetylenic unit on copper like the case of propyne [91] and acetylene [92] on Cu(111), i.e. the typical coordination mode of C2C1H1 proposed by *Sheppard*, though distorted [93].

Bond and dihedral angles reveal the quasi-planarity of the H3C3C2H2 unit. In fact, C2 seems to retain sp^2 hybridisation, so it interacts with the surface via the π orbitals. Due to this extra π-bond, the C1−C2−C3 plane is tilted away from the surface normal 46°. In hcp structures this tilting is somewhat larger, 49°. This is the unique influence of the second layer in molecular geometry. The main difference between C3-top and C3-hollow structures is the position of C3. The coordination of the CH_2CH unit in C3-top structure resembles the di-σ coordination of the same unit of propylene on Pt(111) surface [94, 95], where the C=C bond is aligned along a M−M bond and almost parallel to the metal. Obviously, the presence of two hydrogen atoms more on the other C atom of propylene makes the whole coordination mode different. In our case, the interaction of C1H1 unit with the surface makes the C2−C3 bond not to be aligned with the corresponding Cu−Cu bond.

H atoms in C3-top and C3-hollow structures are also activated (like in the case of C1-trans and C1-cis structures). In these structures, H−M distances are always under 3 Å. On both types of structures H2 atom is the one more distant to the surface (distances of ∼2.88 Å for C3-top and C3-hollow structures), followed by H3 atom (distances of 2.47 and 2.77 Å for C3-hollow and

UNIVERSITAT ROVIRA I VIRGILI
ORGANIC MOLECULES ON METAL SURFACES: FORECASTING STRUCTURES AND SPECTRA
Benjamí Martorell Masip
ISBN:978-84-691-9747-9 /DL: T-1259-2008

C3-top structures, respectively). Consequently, H1 and H4 are the nearest to the surface, being the order different depending on the C3 atom position. For the C3-top structures, the nearest atom is H1, despite being the difference small (distances of 2.16 and 2.23 Å for H1 and H4, respectively), whereas for C3-hollow structure H4 atom shows a major agostic interaction (2.23 and 1.97 Å for H1 and H4, respectively). Therefore, the possibility of H-elimination in C3-top and C3-hollow structures before the coupling reaction, i.e. dimerisation of CHCHCH, should also be taken into account (the first proposal [90] was the coupling of two $CHCHCH_2$ units to yield cyclohexadiene followed by the H_2 elimination to yield benzene). Moreover, the hydrogenation of $CHCHCH_2$ should also explain the production of some amount of propene (another product of the catalytic coupling of propyne on Cu(111), ∼5%).

To end this section, some comments about coverage effects should be done. First, neither C3-hollow minima exist on the 2×2 unit cell, nor C1-cis exist for 3×3 unit cell. C3-top and C3-hollow structures are almost degenerated in energy in the low coverage regime. In fact, adsorption geometry of C3-top structure in high coverage situation, represented here by slab calculation on the 2×2 unit cell, shows some differences respect to the low regime situation. On the 2×2 unit cell, the repulsion between adjacent molecules causes a shorter C2−C3 distance and a closer C1−C2−C3 angle (1.41 Å and 122° for 2×2 unit cell, 1.45 Å and 125° for 3×3 one). The position of H atoms (minor values of H4−C3−C2 angle, major dihedral angles of H1−C3−C2−H2 and H3−C3−C2−H2 units) and the major C2−Cu distance make also a more compacted structure at high coverage. Finally, for C3-hollow structures one can regard to compare the effect of coverage in the results obtained on the 3×3 unit cell (low coverage, low repulsion) with those obtained on the $4\times\sqrt{3}$ unit cell, when the molecule is adsorbed alone (low coverage but major repulsion), as well as when coadsorbed propyne molecule is present on the surface (high coverage).

4.2.3 IR spectra.

The simulated spectra and assignments of VC structures adsorbed on Cu(111) are summarised in the tables of next subsections. In these tables only results for 3×3 unit cell (not for C1-cis structure, of course) and for C1-fcc structures are displayed. The simulated RAIR spectra are also showed in the next subsections, which also include the spectra derived from partial deuteration, $CDCHCH_2$ (VC-d1) and $CHCDCD_2$ (VC-d3), and total deuteration, $CDCDCD_2$ (VC-d4),

UNIVERSITAT ROVIRA I VIRGILI
ORGANIC MOLECULES ON METAL SURFACES: FORECASTING STRUCTURES AND SPECTRA
Benjamí Martorell Masip
ISBN:978-84-691-9747-9 /DL: T-1259-2008

for each structure. All simulated spectra have been obtained using Lorentzian functions, with a bandwidth of 20 cm^{-1} and a resolution of 0.5 cm^{-1}. When significant differences arise from coverage or from the position of C1 atom, those results will be explicitly commented.

To the best of our knowledge there is no vibrational information of these structures adsorbed on metals. The good agreement between the theoretical frequencies and intensities with experimental data available enabled us to predict the vibrational spectra for some adsorbed molecules on metals [58, 60, 95, 96, 97, 98], mainly hydrocarbons, so it is supposed a similar accord in this study. Therefore, the useful of the computed spectra to identify these structures and band assignments is expected, as in previous works in our group. Concerning band assignments, our aim is to express the normal modes into the usual "functional group" modes, like it was made in chapter 3 for TTF. In the forthcoming discussion, first the RAIR spectrum of each type of structure and the effect of deuteration will be commented separately. After that, it will be tried to find out which are the fingerprints of each type of structure necessary to identify their presence on Cu(111).

4.2.3.1 C1-cis structure.

This system lacks of the symmetry respect to the gas phase, but only because H1 is out of the molecular plane, all other atoms remain almost in the molecular plane, as dihedral angles indicate (see table 4.5). It is important to take this into account for the forthcoming discussion. In some cases, the couplings among functional groups[1] can be achieved to this structural feature.

All frequencies and intensities are presented in table 4.6 and the simulated RAIR spectrum in figure 4.7. In the C−H stretching region, the computed frequencies lie at 3142, 3026, 3013, and 2709 cm^{-1}. When VNMs are examined it can be observed that the two highest frequencies are the asymmetric and symmetric ν $C3H_2$. Then appears the most intense band in the C−H region corresponding to ν C2−H. Finally, the lowest frequency corresponds to ν C1−H, which lies 300 cm^{-1} down the other ν C−H frequencies, because the M−H1 distance is really short making C1−H distance to be long, being this the most activated C−H bond. When H1 is deuterated (VC-d1) no important changes in spectrum appear at this region, decreasing the frequency of ν C1−D down to

[1] Terminology used for VNM:
ν: stretching; δ: bending in-plane or scissoring; ρ: rocking; τ: twisting; ω: wagging; γ: bending out-of-plane.

UNIVERSITAT ROVIRA I VIRGILI
ORGANIC MOLECULES ON METAL SURFACES: FORECASTING STRUCTURES AND SPECTRA
Benjamí Martorell Masip
ISBN:978-84-691-9747-9 /DL: T-1259-2008

Table 4.6: Vibrational frequencies for C1-fcc-cis on the 2×2 unit cell. All frequencies are given in cm^{-1}.

	C1-fcc-cis 2×2	
Vibrational mode	$\bar{\nu}_e$	I (km/mol)
asym. ν $C3H_2$	3142	0.75
sym. ν $C3H_2$	3026	2.37
ν C2−H	3013	4.47
ν C1−H	2709	1.23
ν C2=C3 - δ $C3H_2$ + δ C2−H + δ C1−H	1539	0.03
$\delta C3H_2$ + δ C2−H	1379	1.12
δ C2−H + δ C3−H4	1277	0.56
δ C1−H	1225	0.16
(δ C2−H - δ C2−H) + ν C1−C2	1084	0.82
γ C2−H + τ $C3H_2$	963	0.79
γ C2−H - τ $C3H_2$	934	0.21
$\omega C3H_2$	840	9.18
γ C1−H + τ $C3H_2$	647	3.6
γ C1−H - τ $C3H_2$	596	2.7
δ C1−C2−C3	494	2.25
ν VC−surf	367	0.01

1993 cm^{-1} (very low intensity at the spectrum). In VC-d3 ν C1−H remains like in VC, but the other ν C−D decrease to 2344, 2234, and 2208, corresponding to the asymmetric ν CD_2, and the positive and the negative coupling of both the symmetric ν CD_2 and the ν C2−D, respectively, and being this last one the most intense band of this region. VC-d4 behaves like the deuterated modes of VC-d1 and VC-d3.

The frequencies range from 1000 to 1600 cm^{-1} is the one that contains ν C−C and δ C−H, being these bands very low in intensity (<10 % of the most intense band in the spectrum). ν C2−C3 is coupled with δ C−H of all H atoms in the molecule, which has a frequency value of 1539 cm^{-1}, and ν C1−C2 is coupled with δ C1−H and δ C2−H, whose frequency value is 1084 cm^{-1}. This indicates the clear existence of a double and a simple C−C bond. Among these two values appear three VNM at 1379, 1277, and 1225 cm^{-1}, which correspond to the positive and negative coupling of δ $C3H_2$ with δ C2−H, and δ C1−H, respectively (in this case geometry plays an important role in the coupling of the functional groups). In VC-d1 only VNM that correspond to ν C1−C2 and to δ C1−D are affected. The first one because δ C1−D decouples from ν C1−C2, increasing the frequency from 1084 to 1121 cm^{-1}. Moreover, δ C1−D decreases

UNIVERSITAT ROVIRA I VIRGILI
ORGANIC MOLECULES ON METAL SURFACES: FORECASTING STRUCTURES AND SPECTRA
Benjamí Martorell Masip
ISBN:978-84-691-9747-9 /DL: T-1259-2008

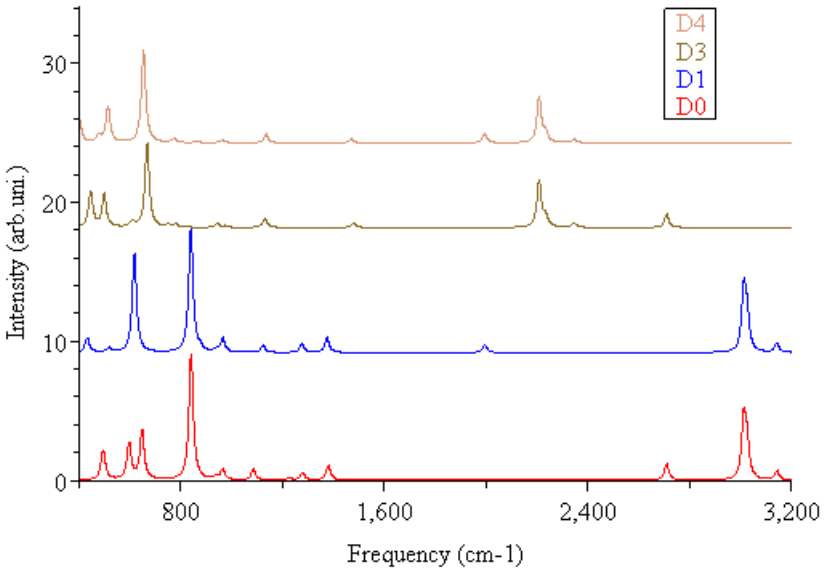

Figure 4.7: Simulated RAIR spectrum for VC adsorbed in C1-cis structures. From bottom to top spectra of VC, VC-d1, VC-d3, and VC-d4.

in frequency and couples with γ C2−H, lieing at 876 cm^{-1}. In VC-d3 a strong coupling between ν C−C and δ C−D exists, lieing ν C2−C3 and ν C1−C2 at 1478 and 1129 cm^{-1}, respectively. VC-d4 behaves similar to VC-d3.

Going to a lower region of the spectrum, γ C−H and δ C1−C2−C3 modes appear. The most intense band of the spectrum lies at this region, it is the ω $C3H_2$, which is not coupled with any other vibrational mode and has a vibrational frequency of 840 cm^{-1}. Above this band appear two weak bands at 963 and 934 cm^{-1}, corresponding to the positive and negative coupling of γ C2−H and τ $C3H_2$. Under the ω $C3H_2$ band, appear the bands corresponding to the positive and negative coupling of γ C1−H and τ $C3H_2$, at 647 and 596 cm^{-1}. Finally, a small band corresponding to δ C1−C2−C3 is present at 494 cm^{-1}. When C1 is deuterated, the main difference respect to VC is that τ $C3H_2$ is decoupled from γ C1−D, lieing τ $C3H_2$ at 617 cm^{-1}, which is a band almost so intense like the most intense one (ω $C3H_2$); and γ C1−D couples with δ C1−C2−C3 and two new small bands appear at 515 and 431 cm^{-1}. In the case of VC-d3 and VC-d4 a new set of couplings are obtained, but the most important feature is that ω $C3D_2$ mode is always the most intense band in the spectrum, in the case of VC-d3 it is coupled with γ C1−H at 667 cm^{-1} and in the case of VC-d4 it is

UNIVERSITAT ROVIRA I VIRGILI
ORGANIC MOLECULES ON METAL SURFACES: FORECASTING STRUCTURES AND SPECTRA
Benjamí Martorell Masip
ISBN:978-84-691-9747-9 /DL: T-1259-2008

Table 4.7: Vibrational frequencies for C1-fcc-trans on the 3×3 unit cell. All frequencies are given in cm^{-1}.

	C1-fcc-trans 3×3	
Vibrational mode	$\bar{\nu}_e$	I (km/mol)
asym. ν $C3H_2$	3160	0.2
sym. ν $C3H_2$	3064	1.4
ν C2−H	3021	0.2
ν C1−H	2737	0.8
ν C2=C3 - δ $C3H_2$ + δ C2−H	1537	4.5
$\delta C3H_2$ + δ C2−H	1393	32.6
δ C2−H	1280	5.4
δ C1−H	1249	0.6
ν C1−C2 - δC1−H	1097	0.0
γ C2−H	964	0.1
ρ $C3H_2$	951	1.2
ω $C3H_2$	865	0.4
γ C1−H	668	0.0
τ $C3H_2$	578	0.1
δ C1−C2−C3	537	12.6
ν VC−surf	265	0.6

coupled with γ C2−D, lieing at 653 cm^{-1}.

Finally, ν VC−M appears around 350 cm^{-1}, being few affected by deuteration of molecule (from 367 cm^{-1} in VC down to 339 cm^{-1} in VC-d4).

The spectra of C1-fcc-cis and C1-hcp-cis exhibit no differences neither in frequencies nor in intensities. This system is only present on the 2×2 unit cell, so no comparison with 3×3 unit cell is possible.

4.2.3.2 C1-trans structure.

The spectrum (figure 4.8) presents four transitions in the C−H stretching region (3160, 3064, 3021 and 2737 cm^{-1}). As expected, the more intense band (3064 cm^{-1}) corresponds to the symmetric $C3H_2$ stretching mode, although its intensity is very weak. The asymmetric counterpart is not forbidden because the height of both hydrogen atoms are not the same. Both C1−H and C2−H stretching modes have a very low intensity due to the low values of z-dipole derivatives of both H atoms. The very low frequency value, 2737 cm^{-1}, indicates that C1−H bond is the most activated C−H one in this structure. The deuteration of this hydrogen atom causes a decrease of 724 cm^{-1} and its intensity also decreases. In VC-d3 and VC-d4, C−D frequencies decrease is somewhat

UNIVERSITAT ROVIRA I VIRGILI
ORGANIC MOLECULES ON METAL SURFACES: FORECASTING STRUCTURES AND SPECTRA
Benjamí Martorell Masip
ISBN:978-84-691-9747-9 /DL: T-1259-2008

larger, ∼800 cm^{-1}, following also the typical 1.36 factor that could be derived from simple reduced mass arguments. However, symmetric ν $C3D_2$ and ν C2−D are strongly coupled in this deuterated system, whose negative coupling mode is the more intense band in this zone of the spectrum (but few relative intensity respect to the most intense band, δ $C3D_2$ + δ C2−D), whereas the positive coupling appears as a shoulder at somewhat higher frequencies.

In the range between 1275 and 1600 cm^{-1} three fundamental transitions at 1537, 1392 and 1280 cm^{-1} appear. These bands are mainly related to ν C2=C3 , δ $C3H_2$ and δ C2−H , respectively, but all of them exhibit some degree of coupling. The band at 1392 cm^{-1} is the most intense band of the spectrum and corresponds to the positive coupling of this three functional group modes. The band at 1537 cm^{-1} corresponds to the coupling of ν C2=C3 mode with the δ $C3H_2$. The intensity of this band is only due to the negative coupling with the δ $C3H_2$ mode, as ν C2=C3 is practically not active. The movement of C2 and C3 on the z-direction causes a z-dipole derivative positive for both C atoms. As the mass-weighted normal mode coefficients of these carbon atoms are similar and have opposite sign, the corresponding intensity is almost zero. The transitions corresponding to δ C1−H , ν C1−C2 and ρ $C3H_2$ lie at lower frequencies and they are very weak. These modes are also strongly coupled. Regarding z-dipole derivatives of C1 and C2 atoms, which are of opposite sign, one expects the ν C1−C2 (1907 cm^{-1}) to have a somewhat large intensity. The coupling with ρ $C3H_2$ neglects its intensity in favour of this mode (950 cm^{-1}), which a priory should have an almost zero intensity. Finally, as the overall system has a C_s symmetry, all bendings out-of-plane modes have intensity zero.

The deuteration of C1 does not cause important differences in this IR region. The deuteration on C2 and C3 breaks (or weakens) the coupling between ν C2=C3 and deformation modes. For VC-d3, these bands move to 1464 (ν C2=C3 is almost inappreciable in the spectrum), 990 (δ $C3D_2$ is less intense as the mass-weighted normal mode coefficients of the D atoms are smaller than the corresponding H ones) and 940 cm^{-1} (δ C2−D is not observed in the spectrum). The band at 1137 cm^{-1} is assigned to ν C1−C2 , which is now coupled with the δ $C3D_2$ mode and decoupled of the rocking mode. The deuteration of all H atoms (VC-d4) does not introduce important changes in this IR region respect to VC-d3. Only the band that emerges at 942 cm^{-1} in the fully deuterated case could be assigned to the coupling of both δ C1−D and δ C2−D . Below 600 cm^{-1}, only a band has an appreciable intensity. It is assigned to the δ C1−C2−C3. This band moves from 537 to 506, 490, and 467 cm^{-1} in progressive deuteration

UNIVERSITAT ROVIRA I VIRGILI
ORGANIC MOLECULES ON METAL SURFACES: FORECASTING STRUCTURES AND SPECTRA
Benjamí Martorell Masip
ISBN:978-84-691-9747-9 /DL: T-1259-2008

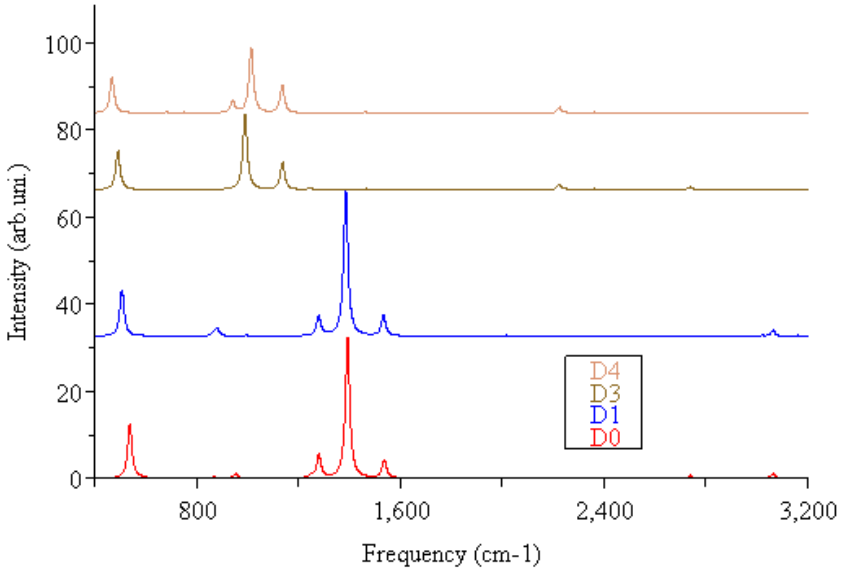

Figure 4.8: Simulated RAIR spectrum for VC adsorbed in C1-trans structures. From bottom to top spectra of VC, VC-d1, VC-d3, and VC-d4.

of H atoms, as all H atoms move in this normal mode.

For this structure no differences appear between C1-fcc and C1-hcp coordination modes. The effect of coverage does not cause significant differences neither on frequency values nor in the VNM, but reduces almost all the corresponding associate intensities due to the minor values of some dipole derivatives. In fact, when dipole derivatives of 3×3 unit cell are used to compute intensities of the 2×2 unit cell, (or viceversa) there is no difference in intensity of both spectra. So differences appear as a consequence of small differences on dynamic electronic distribution in z-direction, as neither geometry nor frequencies change with coverage.

4.2.3.3 C3-hollow structure.

This system has no symmetry, so all normal modes can be IR active *a priori*. Due to the low z-dipole derivatives, specially of the H atoms, the intensities of the overall spectrum are lower than the ones of the spectrum of C1-trans structure (note the different scale range in intensities in table 4.7 and table 4.8). Among all H atoms, the H atom bonded to C2 has the major contributions of z-dipole derivatives, thus the bands concerning the movement of this atom should

UNIVERSITAT ROVIRA I VIRGILI
ORGANIC MOLECULES ON METAL SURFACES: FORECASTING STRUCTURES AND SPECTRA
Benjamí Martorell Masip
ISBN:978-84-691-9747-9 /DL: T-1259-2008

Table 4.8: Vibrational frequencies for C1-fcc-C3-fcc structure on the 3×3 unit cell. All frequencies are given in cm^{-1}.

	C1-fcc-C3-fcc 3×3	
Vibrational mode	$\bar{\nu}_e$	I (km/mol)
ν C3−H3	3054	0.00
ν C2−H	3007	3.15
ν C1−H	2926	0.47
ν C3−H4	2818	0.43
(ν C1−C2 - ν C2−C3) + δ C3H$_2$	1388	1.34
δ C3H$_2$ + (ν C1−C2 - ν C2−C3)	1364	0.05
δ C2−H	1229	1.29
δ C1−H + δ C2−H + δ C3−H4 - ω C2−C3	1165	0.37
ρ C3H$_2$ - δ C1−H	1031	0.00
(ν C1−C2 + ν C2−C3) + ρ C3H$_2$	976	0.19
ω C3H$_2$ - γ C2−H	945	0.93
ω C3H$_2$ + γ C2−H	832	0.00
γ C1−H + m γ C2−H	724	6.81
τ C3H$_2$ + δ C1−C2−C3	636	0.44
δ C1−C2−C3 - τ C3H$_2$	516	1.66
ν C1−surf	377	1.69
ν C2−surf	329	0.99
ν C3−surf	244	1.53

m : medium.

be the most intense ones. For the forthcoming discussion, it is important to state that C1−C2−C3 plane is tilted, H1, H2 and H3 atoms remain approximately in this plane and H4 is clearly out this plane. Thus, concerning C3H$_2$ unit, the contributions of both H atoms sometimes are coupled as usual although not in a symmetrical way, but in some VNM they are absolutely decoupled.

In table 4.8 vibrational frequencies and intensities are presented. In figure 4.9, the RAIR spectra for C1-fcc-C3-fcc adsorption mode is presented for VC, VC-d1, VC-d3 and VC-d4. In the C−H stretching region, the computed bands appear at 3054, 3007, 2926, and 2818 cm^{-1}. The first conclusion that arises from the examination of the normal modes is the decoupling of all ν C−H modes (the coupling do not go beyond the 3% in terms of squared normal mode coefficients). The bands correspond to the stretching of H3, H2 (the most intense, following the above arguments), H1 and H4. The major agostic interaction of H1 and H4 causes the lower frequency of the corresponding stretching mode, being the H4 atom the most activated one of the adsorbed molecule. Deuteration do not cause any coupling. The position of bands goes to 2260, 2223, 2155, and 2066

UNIVERSITAT ROVIRA I VIRGILI
ORGANIC MOLECULES ON METAL SURFACES: FORECASTING STRUCTURES AND SPECTRA
Benjamí Martorell Masip
ISBN:978-84-691-9747-9 /DL: T-1259-2008

cm^{-1}, following the typical factor of ∼1.36 and exhibiting lower intensities due to the smaller vibrational mode coefficients.

The wavenumbers ranged between 975 and 1400 cm^{-1} contain modes related to ν C−C and δ C−H. All this modes are strongly coupled. An assignment of these features is provided in table 4.8. Modes at 1388 and 1364 cm^{-1} are essentially characterised by the negative coupling of both ν C−C coupled with δ $C3H_2$. The central part of this region is predominantly associated with δ C1−H and δ C2−H modes (1229 and 1165 cm^{-1}), whereas the low part is mainly linked to ρ $C3H_2$ (1031 and 975 cm^{-1}). In all modes, C atoms move from their equilibrium position in some extent. Only the fundamental vibrations at 1388 and 1229 cm^{-1} have some intensity, which is almost equal. The isotopic substitution of H1 does not change appreciably this region (the position of δ C1−D will be commented below). The deuteration on C2 and C3 modifies this region (see figure VC-d3 and VC-d4) and it rules out one of the bands. The feature observed in the spectra is attributed to the negative coupling of both ν C−C mode as δ $C3D_2$ goes to lower frequencies. The decoupling of δ $C3D_2$ is consistent with a lower frequency (∼55 cm^{-1}) and an increase of the band intensity. An analysis of the atomic contributions to the final intensity unravels that the main contribution could be ascribed to the movement of C2 on its own plane, which implies a variation of the dipole moment on the z-direction (the contribution of C1 cancels the one of C3). The weak band at 1064 cm^{-1} in the VC-d3 spectrum is assigned to the δ C1−H coupled with ν C2−C3 and δ $C3D_2$, although δ C1−H also participates in the unobserved transition at 1190 cm^{-1}, in this case coupled with the positive coupling of both ν C−C, which also could be mainly associated to the very weak feature at 1139 cm^{-1} in the VC-d4 spectrum.

Next region going to lower frequencies are related to γ C−H and δ C1−C2−C3 modes. Note that, though the molecular plane is lost in this adsorption mode, the bending in-plane (δ) and out-of-plane (γ) modes remain well separated. The ω $C3H_2$ is coupled with the γ C2−H mode. The negative coupling appears at 945 cm^{-1} (weak) whereas the positive coupling at 832 cm^{-1} has zero intensity. The following band at 724 cm^{-1} is the most intense one in the spectrum and it is assigned to the positive coupling of γ C1−H and γ C2−H. The τ $C3H_2$ mode is coupled with δ C1−C2−C3 mode, being the positive coupling at 636 cm^{-1} and the negative one, more intense, at 516 cm^{-1}. The deuteration on C1 breaks the coupling between γ C1−D and γ C2−H, so the band at 724 cm^{-1} splits into two components. The γ C1−D appears at 566 cm^{-1} and decreases in intensity. This band is located between the positive and negative counterparts

UNIVERSITAT ROVIRA I VIRGILI
ORGANIC MOLECULES ON METAL SURFACES: FORECASTING STRUCTURES AND SPECTRA
Benjamí Martorell Masip
ISBN:978-84-691-9747-9 /DL: T-1259-2008

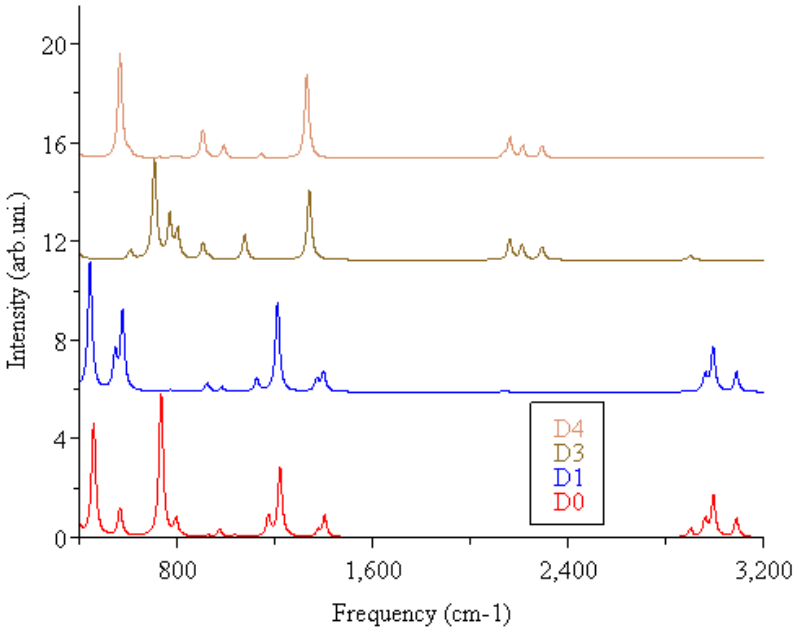

Figure 4.9: Simulated RAIR spectrum for VC adsorbed in C3-hollow structures. From bottom to top spectra of VC, VC-d1, VC-d3, and VC-d4.

of τ $C3H_2$ and δ C1−C2−C3 modes, which also go to lower frequencies when C1 is deuterated, because this H(D) atom moves in the δ C1−C2−C3 mode. The γ C2−H mode seems to go to higher frequencies when C1 is deuterated, indicating a low coupling between them. On one hand, the band at 822 cm^{-1} corresponds to the coupling of γ C2−H mode with ω $C3H_2$. On the other hand, it mixes with the corresponding δ C1−D mode (804 cm^{-1}). So, the separation of in-plane and out-of-plane is partially lost when deuteration takes place. This fact is reinforced when the number of D atoms increases. The band at 621 cm^{-1} in VC-d3 spectrum is purely a γ mode (positive coupling of ω $C3D_2$, γ C2−D and γ C1−H), whereas the upper bands at 709, 775, and the shoulder at 805 cm^{-1} implies both δ C1−H and γ C1−H modes (and also ω $C3D_2$, δ C2−D, and ρ $C3D_2$ modes). Similar effect is observed in full deuterated system. The band at 558 cm^{-1} is mainly characterised by the γ C1−D and, in some extent, by the γ C2−D, and ω $C3D_2$ modes. The major contribution (around 85%) of the γ C1−D mode makes the band more intense than the corresponding band of VC-d3 (band at 709 cm^{-1}, ∼60%). The other upper bands in VC-d4 remain very weak due to the minor mass-weighted mode coefficients and also to different

UNIVERSITAT ROVIRA I VIRGILI
ORGANIC MOLECULES ON METAL SURFACES: FORECASTING STRUCTURES AND SPECTRA
Benjamí Martorell Masip
ISBN:978-84-691-9747-9 /DL: T-1259-2008

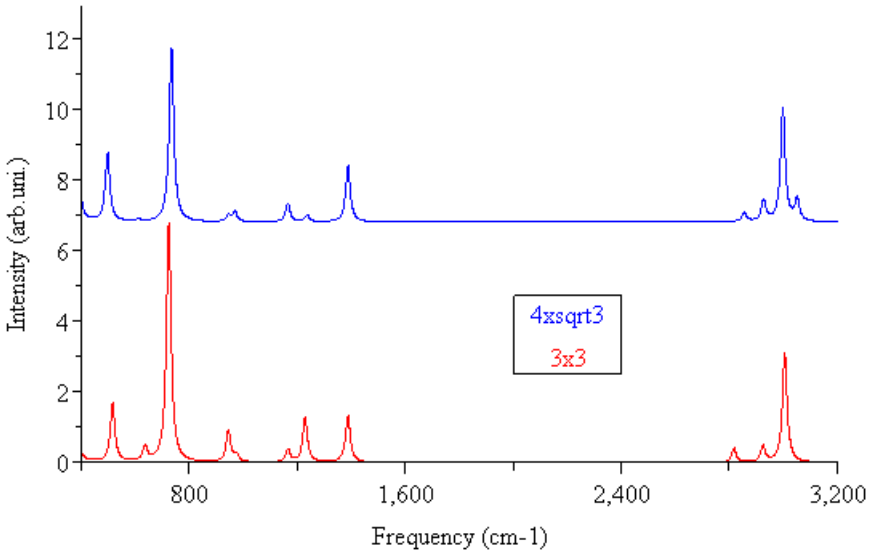

Figure 4.10: Comparison of RAIR spectra of VC adsorbed in C1-fcc-C3-fcc mode. In red 3×3 unit cell; in blue $4\times\sqrt{3}$ unit cell.

couplings between ν C−C and δ C−D modes.

Finally, three weak bands at 377, 329, and 244 cm^{-1} are assigned to ν C−surface modes (C1, C2 and C3, respectively). These modes are coupled with the γ C1−C2−C3 in some extent, specially the one related to C2 atom.

Comparing 3×3 and $4\times\sqrt{3}$ unit cells for C1-fcc-C3-fcc structure (figure 4.10), some small differences emerge in band position and intensity, although spectra assignations are the same. In the ν C−H region two differences can be observed. First, the ν C3−H3 band has the same frequency value in both unit cells, but only is observed on the $4\times\sqrt{3}$ unit cell (weak). On the 3×3 unit cell it is not observed because the contribution of each cartesian coordinate of H3 atom cancel each other, but not on the $4\times\sqrt{3}$ unit cell. Second, the ν C3−H4 band moves to higher frequencies (∼40 cm^{-1}) when surface coverage slightly increases as the distance of this H atom to the surface also increases, showing a minor agostic interaction and in consequence a less activated C−H bond. In the middle IR zone, several bands (1229, 945 and 724 cm^{-1}) lose part of the intensity for the $4\times\sqrt{3}$ unit cell. The analysis of atomic contributions to the final intensity indicates the main differences arise from H1 and H2 contributions. Finally, in the γ C−H and δ C1−C2−C3 zone, some frequencies change from 10 to -26

UNIVERSITAT ROVIRA I VIRGILI
ORGANIC MOLECULES ON METAL SURFACES: FORECASTING STRUCTURES AND SPECTRA
Benjamí Martorell Masip
ISBN:978-84-691-9747-9 /DL: T-1259-2008

cm^{-1}. This is due in part to the minor degree of coupling of some modes and to the major H−surface distance in the case of the $4\times\sqrt{3}$ unit cell.

The spectra of C1-fcc-C3-fcc and C1-hcp-C3-hcp do not exhibit any difference neither in frequency values nor in intensities, so it is not presented here.

4.2.3.4 C3-top structure.

As in the case of C3-hollow structure, the C3-top structure lacks of the molecular plane too, and the C1−C2−C3 plane is tilted respect to the surface normal with a similar value as C3-hollow specie (see table 4.5). H3 has a dihedral angle minor than in the corresponding C3-hollow structure, whereas the H1 angle is major in this case. The intensities of the overall spectrum are in the same range of C3-hollow type structure. In figure 4.11 RAIR spectra for VC and its deuterated isomers are presented for C3-top structure.

In the ν C−H region (see table 4.9), the bands at 3090, 2996, 2962, and 2901 cm^{-1} are assigned mainly to ν C3−H3, C2−H, C3−H4, and C1−H, respectively. For this structure both stretching modes associated to the $C3H_2$ unit are mixed by ∼10%. When C3 interacts directly only with a surface Cu atom, H4 loses part of the agostic interaction, so ν C3−H4 mode goes to higher frequencies and couples, in a small amount, with ν C3−H3. When the degree of coupling increases, the asymmetric coupling of both C3−H3 and C3−H4, which is the major frequency of the spectrum, increases its frequency (compare the values of C1-trans, C3-top, and C3-hollow structures). It is important to note that C1−H is the most activated C−H bond in this structure. Deuteration of C1 affects only to the corresponding stretching mode, with the typical 1.36 factor. However, deuteration of C2 and C3 introduces changes in the intensities due to a major (∼20%) coupling of ν C3−D3 and ν C3−D4 modes, and decreases the intensity of the ν C2−D mode, because of the coupling of this mode with ν C1−H(D) and ν C3−D4 ones.

The region corresponding to δ C−H and ν C−C modes has similar bands positions and assignments as the C3-hollow structure. However, some band intensities are different due to small variations in the degree of coupling among the functional group modes. The intensity of the upper band in the region decreases, but the intensity of the band at 1229 cm^{-1} increases, consequently, the overall aspect of the spectrum seems unlike. Note that deuteration on C2 and C3 (VC-d3 and VC-d4 spectra) causes the same effects as in C3-hollow structure, showing a very similar aspect (frequencies around 10 cm^{-1} higher and

UNIVERSITAT ROVIRA I VIRGILI
ORGANIC MOLECULES ON METAL SURFACES: FORECASTING STRUCTURES AND SPECTRA
Benjamí Martorell Masip
ISBN:978-84-691-9747-9 /DL: T-1259-2008

Table 4.9: Vibrational frequencies for C1-fcc-C3-top on the 3×3 unit cell. All frequencies are given in cm^{-1}.

	C1-fcc-C3-top 3×3	
Vibrational mode	$\bar{\nu}_e$	I (km/mol)
ν C3−H3	3090	0.80
ν C2−H	2996	1.70
ν C3−H4	2962	0.72
ν C1−H	2901	0.36
δ $C3H_2$+ (ν C1−C2 - ν C2−C3)	1404	0.87
δ $C3H_2$ - (ν C1−C2 - ν C2−C3)	1377	0.25
δ C2−H + ν C1−C2	1222	2.86
δ C1−H + δ C2−H - δ C3−H4	1174	0.84
ρ $C3H_2$ - δ C1−H	1034	0.13
(ν C1−C2 + ν C2−C3) - ρ $C3H_2$	973	0.36
γ $C3H_2$ - δ C1−H	927	0.08
ω $C3H_2$	796	0.69
γ C1−H	735	5.89
δ C1−C2−C3 + τ $C3H_2$	567	1.19
τ $C3H_2$ - δ C1−C2−C3	459	4.66
ν C1H−surf	384	1.86
ν C2H−surf - ν $C3H_2$−surf	311	0.37
ν $C3H_2$−surf + ν C2H−surf	277	0.02

somewhat more intense). In VC-d1, this region of the spectrum is very similar to the one of VC. The main difference is that δ C1−D decreases to 823 cm^{-1}, breaking some couplings. In VC-d3, the couplings between ν C−C and δ C−H change because the decrease in the frequency value of some δ C−D, appearingν C−C at 1342 cm^{-1}, somewhat lower than in VC, but much more intense than in VC and VC-d1. The band at 1222 cm^{-1} in VC corresponding to the coupling of ν C1−C2 and δ C1−Hdisappears in VC-d3. In VC-d4 something similar to VC-d3 happens.

The fundamental transitions at 927 (I≈0), 796 (weak), and 735 (the most intense band of the spectrum) cm^{-1} are assigned to the coupling of γ C2−H, ω $C3H_2$, and γ C1−H. The minor contribution of H1 atom to the VNM for those at 927 and 735 cm^{-1} explains the minor intensity of them respect to the C3-hollow structure, while the band at 796 cm^{-1} has a major contribution of H1 atom, which enhances its intensity. The minor role of the γ C1−H mode also explains the major grouping of these three frequencies (82 cm^{-1} for C3-top in front of 121 cm^{-1} for C3-hollow). In VC-d1 the most intense band corresponds

UNIVERSITAT ROVIRA I VIRGILI
ORGANIC MOLECULES ON METAL SURFACES: FORECASTING STRUCTURES AND SPECTRA
Benjamí Martorell Masip
ISBN:978-84-691-9747-9 /DL: T-1259-2008

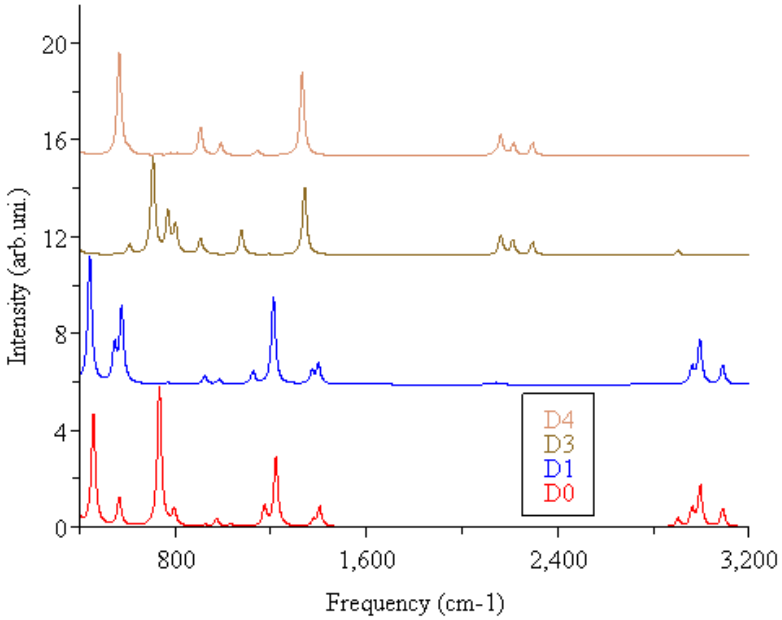

Figure 4.11: Simulated RAIR spectrum for VC adsorbed in C3-top structures in a 3×3 unit cell. From bottom to top spectra of VC, VC-d1, VC-d3, and VC-d4.

to the coupling of γ C1−D with τ $C3H_2$ lieing at 444 cm^{-1}, and being at 577 cm^{-1} γ C1−D that is also a very intense band. In VC-d3 the coupling of γ C1−H, γ C2−D and γ C3−D is the most intense band at 708 cm^{-1}, being the same VNM for VC-d4 the most intense band, but in this case, the deuteration of H1 makes the frequency to decrease down to 567 cm^{-1}.

The bands at 567 and 459 cm^{-1} correspond to the positive and negative coupling of δ C1−C2−C3 and τ $C3H_2$ modes. Two differences respect to C3-hollow structure can be observed: a displacement of both bands to lower frequencies and a major intensity of both bands for C3-top structure, and the band at lower frequencies (negative coupling) has a major contribution of the twisting mode. The contribution of H4 to the twisting mode is major for the C3-top structure, and, moreover, the corresponding z-dipole derivative of this atom moving along the z-direction is higher than the corresponding value in the C3-hollow structure.

Finally, the lowest region of the spectrum is for C−surface stretching modes. In this case only ν C1−surf has an appreciable intensity for this structure. These VNMs are not affected by deuteration and remain almost constant for all

UNIVERSITAT ROVIRA I VIRGILI
ORGANIC MOLECULES ON METAL SURFACES: FORECASTING STRUCTURES AND SPECTRA
Benjamí Martorell Masip
ISBN:978-84-691-9747-9 /DL: T-1259-2008

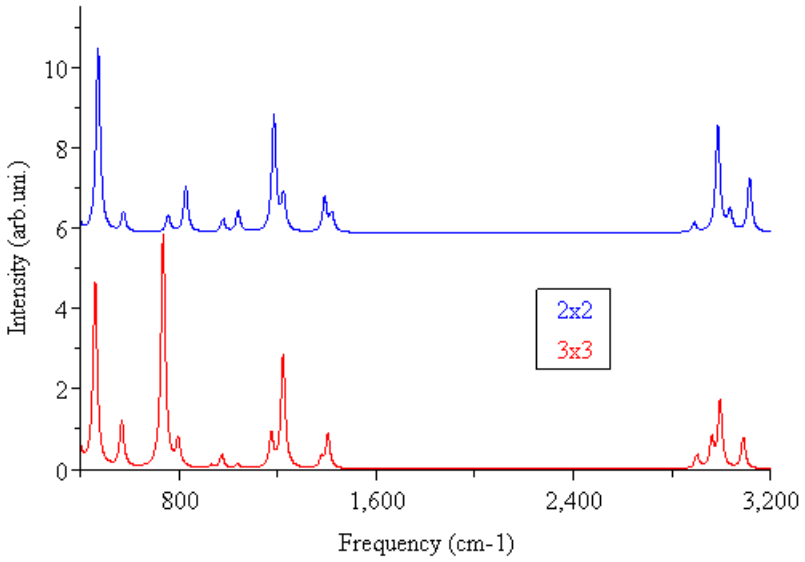

Figure 4.12: Comparison of RAIR spectra of VC adsorbed in C1-fcc-C3-top mode. In red 3×3 unit cell; in blue 2×2 unit cell.

deuterated species.

There are no significant differences between the spectra derived for C1-fcc-C3-top and C1-hcp-C3-top adsorption sites. However, coverage effects influence strongly the spectrum in this case, being a difference with the C1-trans structure. For C1-trans structure 2×2 unit cell is big enough to minimise interactions between two adjacent VC, but for C1-fcc-C3-top this unit cell is too small, and interactions between adjacent VC are large. In the case of 3×3 unit cell these interactions are minimised and RAIR spectrum is different (see Figure 4.12). First, in the ν C−H region the peaks corresponding to ν C2−H and symmetric ν C3H$_2$ interchange their position. Second, in the ν C−C and δ C−H region, the most intense band on the 3×3 unit cell is the less intense one on the 2×2 unit cell for each couple of peaks. Finally, the most intense band of the 3×3 spectrum is a weak peak in the high coverage regime (although it is the most intense between 700-800 cm^{-1}). All these changes can be explained regarding changes in the VNM and in the z-dipole derivatives, specially those of H1 and H2 atoms when they move in the z-direction . For the high coverage regime, there is not significant differences between C1-fcc-C3-top and C1-hcp-C3-top, as expected.

UNIVERSITAT ROVIRA I VIRGILI
ORGANIC MOLECULES ON METAL SURFACES: FORECASTING STRUCTURES AND SPECTRA
Benjamí Martorell Masip
ISBN:978-84-691-9747-9 /DL: T-1259-2008

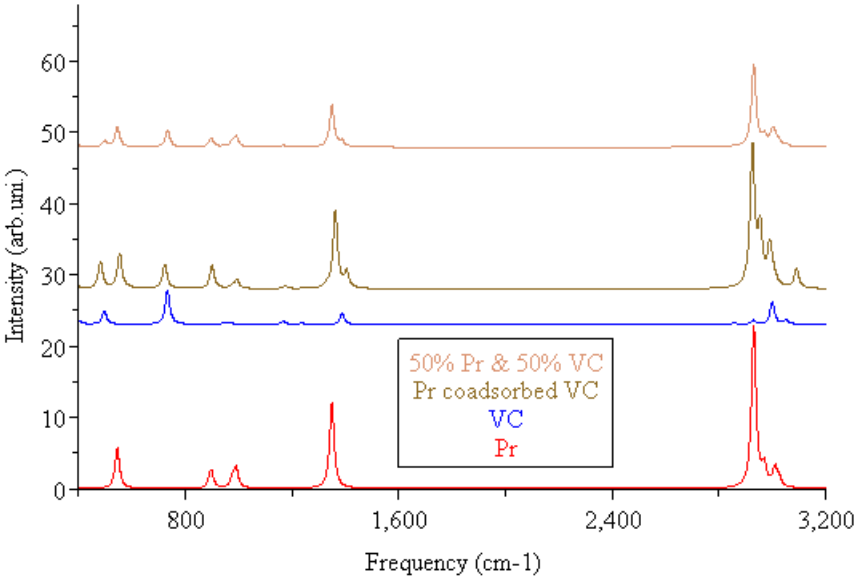

Figure 4.13: RAIR spectra for VC and Pr adsorbed on a $4\times\sqrt{3}$ unit cell. In red propyne (Pr), in blue VC; in sienna coadsorbed Pr and VC and in tan the addition of the spectra of Pr and VC calculated separately.

4.2.3.5 Coadsorption of propyne and VC C3-hollow structure.

In figure 4.13 it is shown the simulated spectra of propyne and VC in a C3-hollow structure adsorbed on the $4\times\sqrt{3}$ unit cell. The spectrum of Pr is similar to the one obtained with two propyne molecules per unit cell [96], being the ν C−H region the most intense one. The spectrum of VC is also similar to that ones obtained with C3-hollow structure adsorbed on the 3×3 unit cell (see figure 4.9). In the later spectrum, the most intense band at 734 cm^{-1} (corresponding to the positive coupling of γ C1−H and γ C2−H) is five times weaker than the most intense band of propyne spectrum (symmetric ν C−H). Moreover, there is no feature in the Pr spectrum around 750 cm^{-1} and the VC spectrum has no intense band around 1350 cm^{-1} (in the Pr spectrum this band corresponds to the negative coupling of ν C1−C2 and δ CH_3). The spectrum labelled 'Pr coadsorbed VC' in figure 4.13 is the one obtained when both molecules are coadsorbed on this unit cell (molecular coverage is 0.25). No couplings between Pr's modes and its isomer's are observed when VNMs are analysed, except in the region between 900 and 1000 cm^{-1} (from 4 to 20%).

It is usual for adsorbed hydrocarbon moieties to simulate spectra of coad-

UNIVERSITAT ROVIRA I VIRGILI
ORGANIC MOLECULES ON METAL SURFACES: FORECASTING STRUCTURES AND SPECTRA
Benjamí Martorell Masip
ISBN:978-84-691-9747-9 /DL: T-1259-2008

sorbed systems from the isolated adsorbed systems as a sum of the spectrum obtained for each system separately (in our case it has been reduced to the half for next discussion) [97]. This procedure avoids not only the expensive whole frequency calculation, but also the simultaneous optimisation process of two (or more) coadsorbed molecules. The spectrum labelled as 50% Pr and 50% VC corresponds to the sum of the spectrum of both systems at coverage 0.125. This spectrum tries to simulate the situation of the coadsorption of Pr and VC. Note the agreement between calculated and simulated spectra is good, but some small differences appear: (1) the ν C3−H3 mode of VC is displaced to higher frequencies ($\sim$40 cm^{-1}) in the coadsorbed calculation, as the motion of H3 atom is in the direction of acetylenic H atom in Pr and due to the position of C3 atom which is between the top and the fcc position; (2) the band just below 1000 cm^{-1} decreases its intensity due to the couplings commented above; (3) the VC band below 500 cm^{-1} presents a major intensity in the coadsorbed spectrum being this fact also related to the position of the C3 atom. Despite these differences, the simulated spectrum using Pr and VC calculated separately should be also useful in order to characterise the presence of both species on the surface.

Now, suppose the presence of both moieties but with a total C_3H_4 coverage of 0.125, where the distance between adsorbed species should be major (so differences coming from couplings between Pr and VC should vanish, and VC could maintain its C3 atom on the fcc site). The calculation of this spectrum is prohibitive as it would require a very large unit cell. However, this spectrum could be useful in the study of the isomerisation surface reaction from Pr to VC. Note that when reaction takes place, the amount of adsorbed Pr will decrease, whereas the quantity of adsorbed VC will increase. So, starting from a Pr coverage of 0.125, the final reaction spectrum could not correspond, obviously, to the spectrum calculated for a coverage of 0.25, the one commented above. If both adsorbates are well separated on the surface (low coverage situation), neither frequencies nor computed intensities of each species should change. However, during the reaction, bands associated with Pr should progressively lose their intensity and the ones of VC should gradually emerge. The change in band intensities should be associated to the population factor. To take this effect into account, one could use to simulate the spectrum the calculated intensities values obtained for the isolated systems but weighted by the corresponding molar fraction. As an example, in figure 4.13 it is shown the spectrum corresponding to a coverage of 0.125 and a fraction of 50% of each isomer. Note the shape of the spectrum is obviously the same as it would be obtained for the sum of Pr and

UNIVERSITAT ROVIRA I VIRGILI
ORGANIC MOLECULES ON METAL SURFACES: FORECASTING STRUCTURES AND SPECTRA
Benjamí Martorell Masip
ISBN:978-84-691-9747-9 /DL: T-1259-2008

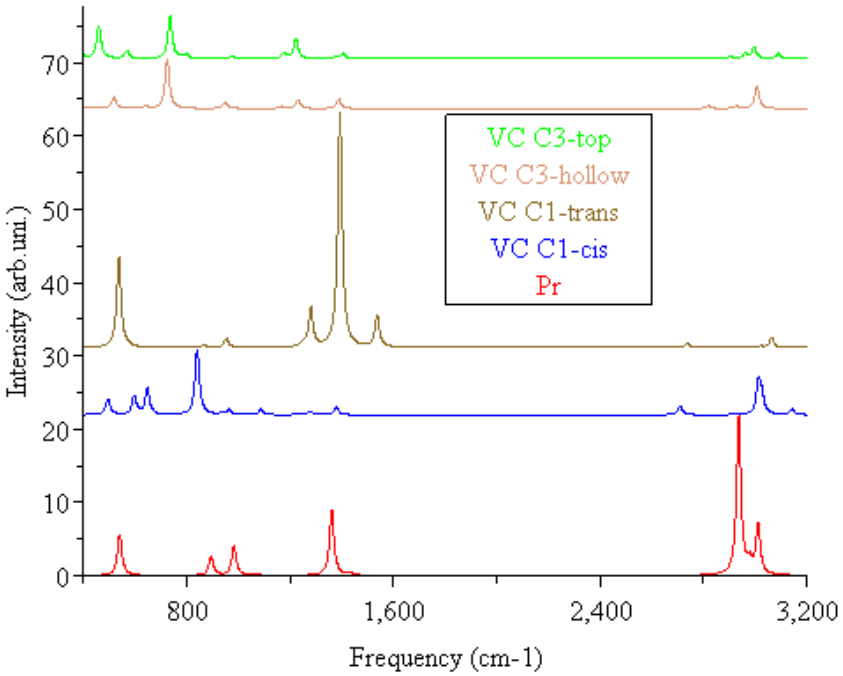

Figure 4.14: RAIR spectra for all VC structures and Pr.

VC, but the comparison with the same coverage regime is easier with the 50% Pr + 50% VC as bands intensities are correlated with the species distribution on the surface. This theoretical strategy could also be applied in the case of more than two species on the surface, for low and medium coverage, when the complete calculation was absolutely prohibitive.

4.2.3.6 Comparison of spectra.

In figure 4.14 the spectra corresponding to C1-cis, C1-trans, C3-hollow and C3-top structures of VC and the one of Pr molecule have been put together, all of them adsorbed on the 3×3 unit cell with C1 atom placed on the fcc site, except for C1-cis structure that has been used a 2×2 unit cell, because of reasons commented before. Although the spectra of VC isomers have been shown in other figures, they have been reproduced together for the purpose of finding the fingerprints of each structure if all them were present on the surface.

The main difference between Pr and all VC isomers spectra is the strong intensity in the ν C−H region for Pr molecule. Between C1-trans and the other

UNIVERSITAT ROVIRA I VIRGILI
ORGANIC MOLECULES ON METAL SURFACES: FORECASTING STRUCTURES AND SPECTRA
Benjamí Martorell Masip
ISBN:978-84-691-9747-9 /DL: T-1259-2008

VC isomers, the key feature is the presence or absence, respectively, of a strong absorption around 1300-1400 cm^{-1}. As the spectrum of Pr molecule presents also a medium band in this region, the relative intensity of the most intense band in this region respect to the most intense band of the ν C−H region, should elucidate the existence of Pr on the surface. The fingerprint for C1-cis structure is a medium band at 840 cm^{-1}, which is a clean zone for the other VC structures, but not for Pr. The key to differentiate between Pr and VC in a C1-cis structure is the relative intensity of the ν C−H region, which in the case of Pr is more intense than for VC in C1-cis structure. The fingerprints of C3-top and C3-hollow structures of VC is a medium band present in the range of 700-750 cm^{-1}. Between C3-top and C3-hollow VC species the difference (previously commented) are scarce, making almost impossible to differentiate these structures using RAIR spectra. On the 3×3 unit cell they are almost degenerated and their geometric differences are small. So, it is easy to recognise Pr, C1-cis and C1-trans structures, but C3-hollow and C3-top structures are too similar between them, and RAIR spectra cannot differentiate between them. Moreover, thermodynamic data show C3-hollow and C3-top structures are almost degenerated, so if one is present on the surface, it is sure the other one to be also present.

4.3 VC adsorbed on Pt(111) and on Pd(111).

4.3.1 Adsorption modes.

The reactivity of propyne on Pt(111) is the total decomposition of the molecule to form a carbidic layer on the metal [100]. On the other hand, on Pd(111) Pr trimerises to yield trimethyl-benzene [99], having the same reactivity as acetylene on Cu(111) [102] and on Pd(111) [103].

Despite behaving very different in the reactivity of Pr, Pt and Pd surfaces behave very similar in the case of the adsorption of VC. This can be attributed to the fact that their electronic valence structure is the same, d^{10}, and that their lattice parameters (both exhibit a crystallographic Fm3m structure) are almost equal due to the effect of lantanid contraction of the third row of transition metals: 3.9242 Å for Pt [152] and 3.8907 Å for Pd [153]. In this section it will be studied the adsorption of VC on Pt(111) and Pd(111) using two different unit cells: 2×2 and 3×3.

UNIVERSITAT ROVIRA I VIRGILI
ORGANIC MOLECULES ON METAL SURFACES: FORECASTING STRUCTURES AND SPECTRA
Benjamí Martorell Masip
ISBN:978-84-691-9747-9 /DL: T-1259-2008

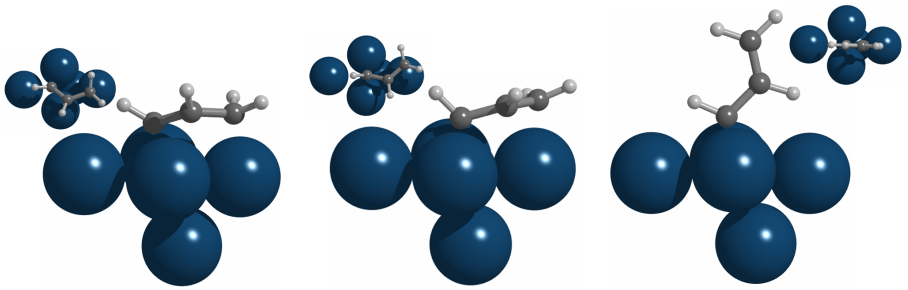

(a) C1-fcc-C3-top (b) C1-b-H1-fcc (c) C1-fcc-trans

Figure 4.15: Different adsorption modes of VC on Pt(111) and Pd(111) on a 2×2 unit cell.

4.3.1.1 2×2 unit cell.

Let's consider first the high coverage regime, like in the case of VC adsorbed on Cu(111). In this case we have used a 2×2 unit cell, that corresponds to the minimum unit cell where VC can be adsorbed. Moreover, 2×2 unit cell has been proposed as the experimental unit cell for the adsorption of Pr on Pt(111) [104] and on Rh(111) [105]. Several adsorption sites and starting geometries have been explored, and six stable minima have been found, three of them have C1 on a fcc site (or displaced to a fcc site as can be observed in figure 4.15), whereas the other have this same atom on a hcp site (or displaced to a hcp site). Like in the case of Cu, only those structures with C1 on a fcc site will be commented, because the other structures are very similar to those ones and energetic differences are small. Two of the structures are the same in adsorption mode as two of the structures found on Cu: C1-trans and C3-top structures. A new structure, not found on Cu is found on Pt and Pd. In this case C1 is placed almost on a bridge site, and the C2=C3 bond is placed on a top site, so we will call them C1-bridge-H1-fcc and C1-bridge-H1-hcp sites (C1-bridge in general).

The adsorption energies respect to propyne in gas phase are shown in table 4.10 for Pt(111) and in table 4.11 for Pd(111). The ZPE corrected and uncorrected values are showed in different columns in order to check ZPE effects in energy differences. For sake of comparison, propyne values are also included. In the case of Pr adsorbed on Pt, Pd and Rh, the most stable structure is that with the adsorption mode di-σ/π [60, 97, 104, 105], where triple bond of Pr can be placed on fcc (tr-fcc) or hcp-site (tr-hcp). First of all, all VC structures are less stable than adsorbed Pr on this unit cell, being the smallest difference

UNIVERSITAT ROVIRA I VIRGILI
ORGANIC MOLECULES ON METAL SURFACES: FORECASTING STRUCTURES AND SPECTRA
Benjamí Martorell Masip
ISBN:978-84-691-9747-9 /DL: T-1259-2008

Table 4.10: Relative adsorption energies of VC adsorbed on Pt(111) on the 2×2 unit cell respect to propyne in gas phase. All values are given in kJ·mol^{-1}.

	E_{ads}				
	No ZPE	ZPE	ZPE-d1	ZPE-d3	ZPE-d4
Propyne tr-fcc	-200.7	-192.5	-193.2	-193.1	-193.8
Propyne tr-hcp	-193.2	-185.5	-186.1	-186.0	-186.7
VC C1-fcc-trans	-123.9	-116.5	-117.3	-116.8	-117.6
VC C1-hcp-trans	-122.1	-114.8	-115.6	-115.1	-115.9
VC C1-b-H1-fcc	-157.3	-148.0	-148.7	-149.0	-149.6
VC C1-b-H1-hcp	-163.5	-154.0	-154.7	-155.0	-155.6
VC C1-fcc-C3-top	-173.0	-163.6	-164.4	-164.5	-165.2
VC C1-hcp-C3-top	-169.3	-159.8	-160.6	-160.7	-161.4

Table 4.11: Relative adsorption energies of VC adsorbed on Pd(111) on the 2×2 unit cell respect to propyne in gas phase. All values are given in kJ·mol^{-1}.

	E_{ads}				
	No ZPE	ZPE	ZPE-d1	ZPE-d3	ZPE-d4
Propyne tr-fcc	-166.4	-161.0	-161.4	-161.5	-161.9
Propyne tr-hcp	-167.4	-162.2	-162.6	-162.7	-163.1
VC C1-fcc-trans	-99.4	-94.5	-94.9	-94.7	-95.1
VC C1-hcp-trans	-98.8	-93.6	-94.1	-93.8	-94.3
VC C1-b-H1-fcc	-138.6	-133.0	-133.4	-133.5	-133.9
VC C1-b-H1-hcp	-141.0	-135.1	-135.5	-135.7	-136.0
VC C1-fcc-C3-top	-142.4	-137.6	-137.9	-138.0	-138.3
VC C1-hcp-C3-top	-138.4	-133.2	-133.7	-133.6	-134.1

between adsorbed Pr and adsorbed VC ∼30 kJ·mol^{-1} for both metals, Pt and Pd. When ZPE correction is included, all E_{ads} for C_3H_4 decrease in a value of ∼10 kJ·mol^{-1} (depends on each particular case), due to the larger correction that suffers Pr in gas phase than C_3H_4 species adsorbed on Pt or on Pd (similar circumstances happened on Cu, section 4.2.1). Another important fact is that for C1-trans and C3-top structures, always the most stable structure is for the structure where C1 is placed on a fcc site, whereas C1-bridge-H1-hcp structure is more stable than C1-bridge-H1-fcc, for Pt and for Pd. VC is ∼20 kJ·mol^{-1} more stable on Pt than on Pd, being this effect also present in the case of Pr adsorbed on these metals, ∼30 kJ·mol^{-1} [60].

C1-trans structure was the most stable one in the case of VC adsorbed on Cu(111). On Pt(111) and Pd(111) this structure becomes the less stable one. This can be easily explained if we take into account the lattice parameter of

UNIVERSITAT ROVIRA I VIRGILI
ORGANIC MOLECULES ON METAL SURFACES: FORECASTING STRUCTURES AND SPECTRA
Benjamí Martorell Masip
ISBN:978-84-691-9747-9 /DL: T-1259-2008

Cu and Pt (or Pd). When we increased the unit cell for Cu, also C1-trans structure became the less stable one, because the other two possible structures were stabilised because of the decrease of the repulsion between adjacent VC molecules. In the case of Pt (and Pd), it is not necessary to increase the unit cell to stabilise the VC structures parallel to surface, because its lattice parameter is larger than the Cu one, and C1-bridge and C3-top structures can be placed on surface without huge interactions with their neighbours. Besides, in the case of Cu, in C1-trans structures, C1 was placed and adsorbed on a hollow site (figure 4.4); in the case of Pt and Pd C1 it is placed almost on a bridge site, and H1 is the one that is placed on a fcc or hcp site (figure 4.15). Despite being C1-trans the less stable structure, the E_{ads} is much larger on Pt (-123.9 kJ·mol^{-1}l) or Pd (-99.4 kJ·mol^{-1}) than on Cu (-25.7 kJ·mol^{-1}).

In the case of Pt, C3-top (-173.0 kJ·mol^{-1}) structure is the most stable one, being ∼15 kJ·mol^{-1} more stable than the C1-bridge one (-163.5 kJ·mol^{-1} for C1-bridge-H1-hcp). This difference is big enough to ensure a small preference of VC being placed on a C3-top site on Pt. In the case of Pd this difference is reduced to ∼1 kJ·mol^{-1}, and C3-top structure (-142.4 kJ·mol^{-1}) and C1-bridge structure (-141.0 kJ·mol^{-1} for C-bridge-H1-hcp) are two degenerated structures on this unit cell.

Finally, all VC structures are more stable than Pr in gas phase. In this case the stabilisation is larger than in the case of Cu. This is a big difference between these two metals respect to Cu, and could be a light source to understand the different reactivity of Cu respect to the other metals.

4.3.1.2 3×3 unit cell.

In order to evaluate coverage effects, the unit cell was increased to a 3×3 dimension, which corresponds to a molecular coverage of 1/9. This unit cell can describe the low (or medium) coverage regime, where situations of repulsion are minimised. Using this unit cell, six stable minima were found for Pt(111) and for Pd(111), which corresponded to the same ones that were found on 2×2 unit cell. The main difference of these structures and the ones obtained for a 2×2 unit cell is the smaller repulsion between adjacent molecules, but in this case the stabilisation of the structures is not as dramatic as on Cu. As on 2×2 unit cell, three minima correspond to the adsorption of C1 on a fcc site (or displaced to a fcc site) and the other three to the hcp site (or displaced to hcp site). The adsorption energies are presented in tables 4.12 for Pt and 4.13 for Pd.

UNIVERSITAT ROVIRA I VIRGILI
ORGANIC MOLECULES ON METAL SURFACES: FORECASTING STRUCTURES AND SPECTRA
Benjamí Martorell Masip
ISBN:978-84-691-9747-9 /DL: T-1259-2008

Table 4.12: Relative adsorption energies of VC adsorbed on Pt(111) on the 3×3 unit cell respect to propyne in gas phase. All values are given in kJ·mol^{-1}.

	E_{ads}				
	No ZPE	ZPE	ZPE-d1	ZPE-d3	ZPE-d4
Propyne tr-fcc	-205.4	-198.2	-198.9	-198.6	-199.3
Propyne tr-hcp	-203.0	-195.9	-196.6	-196.4	-197.1
VC C1-fcc-trans	-131.9	-124.1	-124.9	-124.4	-125.3
VC C1-hcp-trans	-131.7	-124.2	-125.0	-124.5	-125.3
VC C1-b-H1-fcc	-177.1	-167.9	-168.6	-169.0	-169.6
VC C1-b-H1-hcp	-180.5	-171.3	-172.0	-172.3	-173.0
VC C1-fcc-C3-top	-186.1	-177.2	-177.9	-178.1	-178.8
VC C1-hcp-C3-top	-176.2	-167.1	-167.9	-168.0	-168.7

Table 4.13: Relative adsorption energies of VC adsorbed on Pd(111) on the 3×3 unit cell respect to propyne in gas phase. All values are given in kJ·mol^{-1}.

	E_{ads}				
	No ZPE	ZPE	ZPE-d1	ZPE-d3	ZPE-d4
Propyne tr-fcc	-176.0	-171.4	-171.7	-171.8	-172.1
Propyne tr-hcp	-177.4	-173.0	-173.3	-173.3	-173.7
VC C1-fcc-trans	-113.3	-108.4	-108.8	-108.5	-109.0
VC C1-hcp-trans	-113.2	-108.0	-108.4	-108.2	-108.6
VC C1-b-H1-fcc	-156.0	-150.8	-151.1	-150.7	-151.7
VC C1-b-H1-hcp	-157.4	-152.2	-152.5	-152.7	-153.0
VC C1-fcc-C3-top	-155.2	-151.5	-151.8	-151.9	-152.1
VC C1-hcp-C3-top	-151.8	-147.7	-148.0	-148.1	-148.4

C1-trans structure is the less stable one in VC, as in the case of 2×2 unit cell, but in this case is a bit more stabilised (∼10 kJ·mol^{-1} for Pt and ∼15 kJ·mol^{-1} for Pd). This is logic if we imagine that the interaction of this structure with adjacent molecules was already actually small for a 2×2 unit cell, so when we increased the unit cell, coverage effects are almost meaningless. As for 2×2 unit cell, C1-fcc-trans structure is more stable than C1-hcp-trans (and the other structures have the same order than on a 2×2 unit cell, C1-fcc-C3-top more stable than C1-hcp-C3-top and C1-bridge-H1-hcp more stable than C1-bridge-H1-fcc).

In the case of Pt(111), the difference that existed between C3-top and C1-bridge structures decrease to only ∼6 kJ·mol^{-1} (with or without ZPE correction), being their E_{ads} -186.1 and -180.5 kJ·mol^{-1}, respectively. So, in this case they become almost degenerated, still being the most stable structure the C3-top

UNIVERSITAT ROVIRA I VIRGILI
ORGANIC MOLECULES ON METAL SURFACES: FORECASTING STRUCTURES AND SPECTRA
Benjamí Martorell Masip
ISBN:978-84-691-9747-9 /DL: T-1259-2008

one, as on 2×2 unit cell. The stabilisation energy for the 3×3 unit cell is ∼13 kJ·mol^{-1} for C3-top structure and ∼17 kJ·mol^{-1} for C1-bridge structure respect to 2×2 unit cell.

In the case of Pd(111), C3-top and C1-bridge structures only ∼2 kJ·mol^{-1} differentiate them, so they remain being degenerated as in the case of a 2×2 unit cell. Their E_{ads} are -155.2 and -157.4 kJ·mol^{-1}, respectively. This small difference is in the limit of our calculations accuracy, so it is not possible to ensure which of both structures is the most stable one.

All VC structures are less stable than adsorbed Pr, being the difference of the most stable VC structure and Pr ∼20 kJ·mol^{-1} for both Pt and Pd. This difference is a bit smaller than in the case of 2×2 unit cell (it was around ∼30 kJ·mol^{-1}), because Pr is meaningless stabilised when a 3×3 unit cell is used respect to a 2×2 unit cell. Finally, all VC structures are stable respect to Pr in gas phase, being much more stable for Pt and Pd respect to Cu.

4.3.2 Adsorption geometries.

As in the case of VC adsorbed on Cu(111), the position of C1 on the fcc or hcp site does not introduce any relevant change on the adsorption geometries. The comparison of adsorption geometries between fcc and hcp sites for the same adsorption structure indicates that almost all distances do not change more than ±0.02 Å and bond angles do not differ more than ±1°. In table 4.14 geometrical parameters for C1 adsorbed on fcc site on Pt(111) are presented for 3×3 unit cell, and when the parameters for 2×2 unit cell differ more than parameters before commented are also presented in brackets. In table 4.15 values belong to geometrical parameters for C1 adsorbed on fcc site on Pd(111). C−H distances are not presented in these tables because all distances, as in the case of Cu, are in the range 1.09 and 1.12 Å, and no relevant information is obtained.

As commented in section 4.3.1, two of the structures obtained for Pt and Pd correspond to the same obtained for Cu. Although being adsorbed by the same mode, Pt, Pd and Cu are not equal neither in their lattice parameter nor in their electronic structure, so some geometrical differences can be observed.

In C1-trans structure, C1−C2 and C2−C3 distances are 1.46 (1.45 for Pd) and 1.35 Å, respectively, indicating the existence of a single and a double C−C bond respectively, as in the case of Cu. This indicates a carbene-like structure, and C−C distances are very similar to those ones of vinylcarbene in gas phase (1.46 and 1.34 Å respectively). The other important intramolecular parameter,

UNIVERSITAT ROVIRA I VIRGILI
ORGANIC MOLECULES ON METAL SURFACES: FORECASTING STRUCTURES AND SPECTRA
Benjamí Martorell Masip
ISBN:978-84-691-9747-9 /DL: T-1259-2008

Table 4.14: Geometrical parameters of VC adsorbed on Pt(111). A slash ("/") means meaningless value in the case of C1-trans dihedral angle (structure is flat). In brackets changing parameters more than ±0.02 Å or ±1°.

	C1-trans	C3-top	C1-bridge
	3×3 (2×2)	3×3 (2×2)	3×3 (2×2)
[a]d(C1-C2)	1.46	1.43	1.47
d(C2-C3)	1.35	1.48	1.42
[b]α(C1-C2-C3)	122.3	121.2 (119.9)	126.3
α(H1-C1-C2)	111.7	118.3	118.3 (117.1)
α(H2-C2-C1)	118.3	118.0	115.6
α(H2-C2-C3)	119.4	117.6	117.4
α(H3-C3-H4)	117.3	111.8 (110.6)	116.2
α(H3-C3-C2)	121.3	113.9	118.4
α(H4-C3-C2)	121.4	112.6	119.9
[c]tilt	0	62.3	69.1
[d]θ(H1-C1-C2-C3)	/	-143.7	-109.9
θ(H3-C3-C2-C1)	/	178.8	171.7
θ(H4-C3-C2-C1)	/	50.2	19.0
θ(H1-C1-C2-H2)	/	15.6 (14.3)	60.6
θ(H2-C2-C3-H3)	/	19.4 (18.0)	1.4
θ(H2-C2-C3-H4)	/	-109.3	-151.3
[e]d(C1-M)	2.08	2.01	2.08 (2.05)
d(C2-M)	/	2.23	2.24
d(C3-M)	/	2.09	2.18
d(H1-M)	2.66 (2.60)	2.51	2.71
d(H2-M)	2.55 (2.59)	2.76	2.86
d(H3-M)	/	2.68	2.77
d(H4-M)	/	2.57	2.64 (2.71)

[a]d: distances (Å); [b]α: angles (degrees); [c] tilt: angle between C1−C2−C3 plane and the normal vector of surface; [d]θ: dihedral angles (degrees); [e] distances to nearest surface atom.

as commented in the case of C1-trans structure on Cu, is the H1−C1−C2 angle because in gas phase is different for vinylcarbene (107°) and for propene-1,3-diyl (130°). On Pt and Pd it is 111.7° and 112.1°, indicating a sp^3-like hybridisation, the one that vinylcarbene owns.

For C1-trans structure, no important differences appear between fcc or hcp site, but a small difference exists between 2×2 and 3×3 unit cells in the case of Pt and Pd, which did not exist on Cu(111). As can be observed in tables 4.14 and 4.15, M−H1 distances are larger for 3×3 unit cell than for 2×2 unit cell. On the other hand M−H2 distances are shorter for 3×3 unit cell than for 2×2

UNIVERSITAT ROVIRA I VIRGILI
ORGANIC MOLECULES ON METAL SURFACES: FORECASTING STRUCTURES AND SPECTRA
Benjamí Martorell Masip
ISBN:978-84-691-9747-9 /DL: T-1259-2008

Table 4.15: Geometrical parameters of VC adsorbed on Pd(111). A slash ("/") means meaningless value in the case of C1-trans dihedral angle (structure is flat). In brackets changing parameters more than ±0.02 Å or ±1°.

	C1-trans	C3-top	C1-bridge
	3×3 (2×2)	3×3 (2×2)	3×3 (2×2)
[a]d(C1-C2)	1.45	1.43	1.45
d(C2-C3)	1.35	1.45	1.41
[b]α(C1-C2-C3)	122.8	123.1	126.4
α(H1-C1-C2)	112.1	117.9	119.0 (117.5)
α(H2-C2-C1)	118.4	118.2	116.0
α(H2-C2-C3)	118.7	117.2	117.3
α(H3-C3-H4)	117.4	113.8	116.2
α(H3-C3-C2)	121.4	115.6	118.9
α(H4-C3-C2)	121.2	115.1	119.6
[c]tilt	0	60.4 (58.7)	65.8
[d]θ(H1-C1-C2-C3)	/	-139.7 (-142.5)	-117.7 (-114.4)
θ(H3-C3-C2-C1)	/	177.4	173.4
θ(H4-C3-C2-C1)	/	41.5 (42.7)	20.0 (18.2)
θ(H1-C1-C2-H2)	/	26.1 (24.0)	55.3 (57.6)
θ(H2-C2-C3-H3)	/	11.5 (10.2)	0.4
θ(H2-C2-C3-H4)	/	-124.4	-153.0
[e]d(C1-M)	2.04	2.01	2.02
d(C2-M)	/	2.23 (2.26)	2.25
d(C3-M)	/	2.10	2.18
d(H1-M)	2.50 (2.43)	2.26 (2.30)	2.61 (2.67)
d(H2-M)	2.42 (2.49)	2.69 (2.74)	2.88 (2.91)
d(H3-M)	/	2.68	2.79
d(H4-M)	/	2.45 (2.48)	2.47 (2.57)

[a]d: distances (Å); [b]α: angles (degrees); [c] tilt: angle between C1-C2-C3 plane and the normal vector of surface; [d]θ: dihedral angles (degrees); [e] distances to nearest surface atom.

unit cell. Being this the only important difference between 3×3 and 2×2 unit cell, this means that VC tilts different on a 3×3 unit cell respect to a 2×2 unit cell, being the H1 closer to the surface on the 2×2 than on the 3×3, for both metals, Pt and Pd. For Pt, VC is a bit higher than on Pd, being C1−Pt distance 2.08 Å, whereas C1−Pd is a bit shorter, 2.04 Å, but they do not change with coverage. Finally, comparing these values with the ones on Cu (see table 4.5 on page 120), we can observe that H1−M is much shorter than on Pt and Pd, and H2−M is larger. This indicates that VC is even more tilted on Cu. This is coherent because C1-trans structure is adsorbed on a hollow site on Cu, but

UNIVERSITAT ROVIRA I VIRGILI
ORGANIC MOLECULES ON METAL SURFACES: FORECASTING STRUCTURES AND SPECTRA
Benjamí Martorell Masip
ISBN:978-84-691-9747-9 /DL: T-1259-2008

on Pt and Pd, VC is almost adsorbed on a bridge site. This makes the agostic interaction of H1 with metal to be smaller, and H1−M distance is larger on Pt and Pd than on Cu. The same reasoning, but in the opposite way, can be made for H2.

C3-top structure adsorbs on Pt and Pd similar to the ones obtained for Cu, but their geometrical parameters are a bit different. C1−C2 and C2−C3 distances are larger on Pt and Pd than on Cu, being the first one 1.43 Å for Pt and Pd in front of only 1.41 Å on Cu, and the second distance is 1.48 for Pt, 1.45 for Pd, and 1.44 Å for Cu. This seems to be a clear effect of the lattice parameter, because the larger the interatomic metal distance, the larger C−C distance must be to adapt the internal VC structure on the surface. These distances indicate clearly that no double bond exists. H1−C1−C2 angle is more opened in the case of Pd and Pt (∼118°) than on Cu (∼112°). This can be explained because Pd and Pt have a larger radius than Cu, so H1−M distances are bigger in the case of Pt (2.51 Å) and Pd (2.26 Å) than on Cu (2.16 Å). This fact makes the H1−C1−C2 angle must be more opened in the case of Pt and Pd to try to maximise the agostic interaction of H1 with surface.

Another important difference of C3-top structure on Pt/Pd respect to Cu is the tilting angle of C1−C2−C3 plane respect to the normal vector of surface (and associated to this parameter, the distances of C atoms to metal atoms). These angles are bigger in the case of Pt and Pd (62.3° and 60.4°, respectively) than in the case of Cu (46.1°). This means that C3-top structure is more parallel to surface in the case of Pd and Pt than in the case of Cu. C1−M distance does not vary on both metals (2.00 Å for Cu, 2.01 Å for Pt and Pd), C3−M does not either (2.10 Å for Cu and Pd and 2.09 Å for Pt), but C2−M changes (2.27 Å for Cu and 2.23 Å for Pt and Pd), being ∼0.05 Å larger for Cu than for Pt and Pd. This can be explained by the fact that VC interacts stronger on Pd and Pt than on Cu. The E_{ads} is larger for Pt and Pd than for Cu (-155.2, -186.1, and -56.6 $kJ{\cdot}mol^{-1}$, respectively), and this can be partially explained by a major efficiency in the interaction of C2 with the surface. As a consequence of this, H2−M distance is shorter for Pt and Pd (2.76 and 2.69 Å, respectively) than for Cu (2.87 Å).

Finally, in C3-top structure for Pt and Pd neither exist important differences between fcc or hcp sites, nor for 2×2 and 3×3 unit cells.

C1-bridge structure is a new case, which did not exist for Cu. This can be attributed to the different lattice parameter of these metals, much larger for Pt and Pd than for Cu (this also can explain why C3-hollow structure does

UNIVERSITAT ROVIRA I VIRGILI
ORGANIC MOLECULES ON METAL SURFACES: FORECASTING STRUCTURES AND SPECTRA
Benjamí Martorell Masip
ISBN:978-84-691-9747-9 /DL: T-1259-2008

not exist, because VC cannot enlarge enough to adsorb on two hollow sites simultaneously), and making possible the adsorption of C1 on bridge and the double C=C bond on a top site. This structure is similar to the C3-top one in the adsorption mode, because all C atoms interact with the surface (different to C1-trans or C1-cis structures). In this case, the largest C−C distance is not the C2−C3 one (1.42 Å for Pt and 1.41 Å for Pd), but it is the C1−C2 one (1.47 Å for Pt and 1.45 Å for Pd). This is the contrary case as in C3-top structure, where the C1−C2 distance was shorter than the C2−C3 one. This can be explained thinking about the adsorption mode. In the case of C3-top structure, C2 and C3 interact directly with one metal atom each one, so a di-σ bond is created with the surface, and double C=C bond is almost lost. In the case of C1-bridge structure, C2 and C3 atoms do not interact directly with one metal atom each one, but the C2=C3 bond does with one metal atom, so it retains partially a double bond character.

C1-bridge structure is even more parallel to surface than C3-top was, because the angle of C1−C2−C3 plane respect to the normal vector of surface is bigger in this case (69° for Pt and 66° for Pd) than in the case of C3-top structure (62° and 60°, respectively). This fact is related with the larger C1−M and C3−M distances in this case. The unit formed by H3−C3−C2−H2, is almost flat (∼0°), indicating that remains a bit of the sp^2-like hybridisation existing in the gas phase, but H4 tilts ∼30° away this plane, so it is not possible to talk about a real sp^2-like hybridisation. Moreover, in C1-bridge structure all H atoms are less activated than in C3-top structure, because all H−M distances are larger, being much larger H1−M distance (for Pt: H1−M distances are 2.51 (C3-top) and 2.71 Å (C1-bridge); for Pd: 2.26 and 2.61 Å, respectively), and only for the case of H4−Pd the distance remains almost equal (2.45 and 2.47 Å, respectively).

Finally, in C1-bridge structure for Pt and Pd neither exist important differences between fcc or hcp sites, nor for 2×2 and 3×3 unit cell.

4.3.3 IR spectra.

The calculated spectra and assignments of VC structures adsorbed on Pt(111) and Pd(111) are summarised in the tables of next subsections, from 4.16 to 4.20. In these tables only results for the 3×3 unit cell and for C1-fcc structures are displayed. The simulated RAIR spectra are also shown in next subsections, which also include the derived spectra from partial deuteration, VC-d1 and

UNIVERSITAT ROVIRA I VIRGILI
ORGANIC MOLECULES ON METAL SURFACES: FORECASTING STRUCTURES AND SPECTRA
Benjamí Martorell Masip
ISBN:978-84-691-9747-9 /DL: T-1259-2008

Table 4.16: Vibrational frequencies for C1-fcc-trans on the 3×3 unit cell. All frequencies are given in cm^{-1}.

C1-fcc-trans 3×3 unit cell				
Pt (111)		Vibrational mode	Pd (111)	
$\bar{\nu}_e$	I (km/mol)	Pt (111) / Pd(111)	$\bar{\nu}_e$	I (km/mol)
3162	0.1	asym. ν C3H$_2$	3158	0.2
3067	0.8	sym. ν C3H$_2$	3063	0.3
2999	0.1	ν C2−H	2956	0.0
2959	2.5	ν C1−H	2892	2.1
1566	6.5	ν C2=C3 - δ C3H$_2$ + δ C2−H	1552	1.7
1394	68.5	δ C3H$_2$ + δ C2−H	1393	47.9
1270	1.5	δ C2−H - δ C3−H4	1269	1.2
1198	0.4	δ C1−H / δ C1−H + ρ C3H$_2$	1172	0.3
1108	14.6	ν C1−C2 + δ C1−H + δ C2−H	1086	8.2
970	0.0	γ C2−H - τ C3H$_2$	957	0.1
945	5.6	ρ C3H$_2$ + δ C1−H	943	1.2
922	0.2	ω C3H$_2$	908	0.6
834	0.0	γ C1−H	765	0.0
627	9.4	τ C3H$_2$ + γ C2−H - γ C1−H	583	3.7
618	0.5	δ C1−C2−C3 + ρ C3H$_2$ + ν C1−surf.	605	0.0
292	1.1	ν VC−surface	280	0.1

VC-d3, and total deuteration, VC-d4, for each structure. All simulated spectra have been obtained using the same conditions as in the case of Cu(111), i.e., Lorentzian functions, with a bandwidth of 20 cm^{-1} and a resolution of 0.5 cm^{-1}. When significant differences arise from coverage or from the position of C1 atom, those results will be explicitly commented.

In the forthcoming discussion, first the RAIR spectrum of each type of structure and the effect of deuteration will be commented for each region of the spectrum. After that, it will be tried to find out which are the fingerprints of each type of structure necessary to identify their presence on Pt(111) and on Pd(111).

4.3.3.1 C1-trans structure.

In figure 4.16 are presented the spectra of VC in C1-fcc-trans structure adsorbed on Pt(111) and Pd(111) on a 3×3 unit cell (figures a and b, respectively). It can be easily observed that they are really similar, not only for VC spectrum, but also for the deuterated species. Besides, in table 4.16 vibrational frequencies, intensities and assignments are presented. It can be observed that their values

UNIVERSITAT ROVIRA I VIRGILI
ORGANIC MOLECULES ON METAL SURFACES: FORECASTING STRUCTURES AND SPECTRA
Benjamí Martorell Masip
ISBN:978-84-691-9747-9 /DL: T-1259-2008

are very similar in all cases, making spectra to be almost equal. This is the reason why we compare both spectra in the same section.

The spectra for Pt and Pd present very low-intense bands in the ν C−H region. In the case of Pt, four frequencies appear in this region (3162, 3067, 2999, and 2959 cm^{-1}), being the highest one in energy the ν C3H$_2$, in medium lies ν C2−H and the lowest in energy is ν C1−H. This is logic because H1 and H2 are near the surface, so C1−H and C2−H bonds are more activated than the C3−H bonds. In the case of Pd (3158, 3063, 2956, and 2892 cm^{-1}), the same effect happens, but in this case is more intense (frequencies are lower for ν C2−H and ν C1−H) than on Pt, because H1−M (Pt: 2.66 Å; Pd: 2.50 Å) and H2−M (Pt: 2.55 Å; Pd: 2.42 Å) distances are shorter for Pd, so C−H stretching frequency is lower. Besides, C1−H bond is less activated on Pt and Pd than on Cu (2737 cm^{-1}), and in the case of Pt and Pd, this is the most intense band in this region of the spectrum, whereas for Cu the most intense band was the symmetric ν C3H$_2$. This fact can be explained because on Pt and Pd, ν C1−H is not so linked to the surface, so it can create a major change in the z-dipole moment and being a more intense band than on Cu. The deuteration of H1 atom (VC-d1) does not cause any important change in spectrum because this band was very low intense compared with the most intense band of the spectrum (less than 5%). This frequency decreases to 2181 and 2130 cm^{-1} (a decrease of ∼760 cm^{-1}), for Pt and Pd respectively, remaining the other ν C−H in the same region as in VC. In the case of VC-d3 and VC-d4, the behaviour is the same for the three deuterium atoms, because their are decoupled of ν C1−H. When the three H atoms are deuterated, no important changes in spectrum appear, because this region is very low-intense. The asymmetric ν C3D$_2$ decreases its value to 2362 cm^{-1}(Pt) and 2359 cm^{-1} (Pd) (a decrease of ∼800 cm^{-1}), and symmetric ν C3D$_2$ couples with ν C2−D, appearing the positive and the negative coupling at 2252 and 2214 cm^{-1} for Pt and at 2244 and 2189 cm^{-1} for Pd.

Between 1000 and 1600 cm^{-1}, five fundamental transitions are found at 1566, 1394, 1270, 1198, and 1108 cm^{-1} (Pt) and 1552, 1393, 1269, 1172, and 1086 cm^{-1} (Pd). It can be observed that in all cases frequencies for Pd are a bit smaller in value than for Pt. This region, as in the case of Cu, is mainly related to the ν C−C, to the C3H$_2$ scissoringand to the C−H bending in-plane, being all of them extremely coupled (see table 4.16). The band at 1566 cm^{-1} (Pt) and 1552 cm^{-1} (Pd) was also present for Cu (1537 cm^{-1}), and corresponds to the coupling of ν C2=C3 withδ C3H$_2$ and δ C2−H, but it is not very intense. The next band in the spectrum is the most intense one (it was also for Cu at 1393

UNIVERSITAT ROVIRA I VIRGILI
ORGANIC MOLECULES ON METAL SURFACES: FORECASTING STRUCTURES AND SPECTRA
Benjamí Martorell Masip
ISBN:978-84-691-9747-9 /DL: T-1259-2008

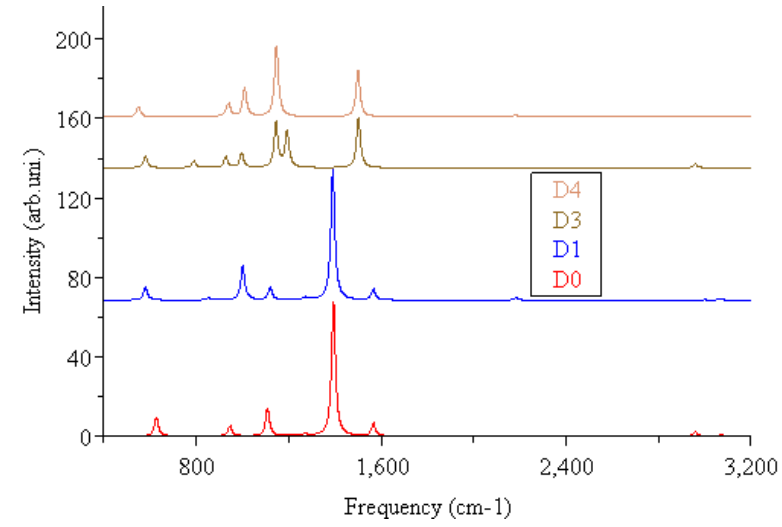

(a) Pt (111)

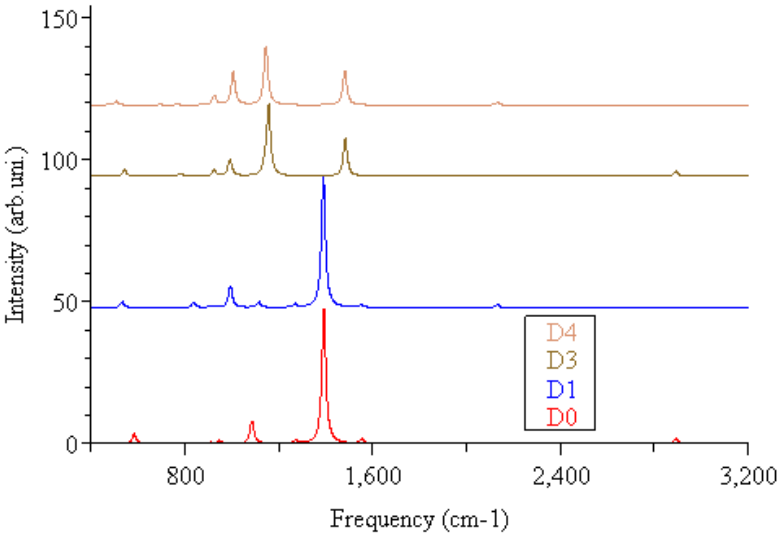

(b) Pd (111)

Figure 4.16: Simulated RAIR spectrum for VC adsorbed in C1-trans structures. a) Spectra for VC adsorbed on Pt(111), b) Pd(111). From bottom to top spectra of VC, VC-d1, VC-d3, and VC-d4.

UNIVERSITAT ROVIRA I VIRGILI
ORGANIC MOLECULES ON METAL SURFACES: FORECASTING STRUCTURES AND SPECTRA
Benjamí Martorell Masip
ISBN:978-84-691-9747-9 /DL: T-1259-2008

cm^{-1}). It appears at 1394 (Pt) and 1393 (Pd) cm^{-1}, so this band is independent of the metal used (so, the frequency of the band is not affected by the small differences in the adsorption modes). This band corresponds to the coupling of the C3H$_2$ scissoring with the C2−H bending in-plane, producing a big change in the dipolar moment of the molecule. The next two bands in the spectrum are very low-intense, lieing at 1270 and 1198 (Pt) cm^{-1} and at 1269 and 1172 (Pd) cm^{-1}. These bands are combinations of bendings in-plane of different C−H bonds (see table 4.16). The last one is the coupling of ν C1−C2with δ C1−H and δ C2−H. The frequency is 1108 (Pt) and 1086 (Pd) cm^{-1}. This is the second most intense band in the spectrum, being this a difference respect to Cu, because this band (1097 cm^{-1} for Cu) was completely inactive in RAIR spectrum, as a consequence of the negative coupling of ν C1−C2 with δ C1−H, whose movements cancelled the variation in z-dipolar moment. For VC-d1, only the bands implying H1 movements change on H1 deuteration. The changing bands have contribution of ν C1−C2. Both changing frequencies decrease from 1198 and 1108 down to 1119 and 1001 cm^{-1} for Pt and from 1172 and 1086 down to 1114 and 994 cm^{-1} for Pd. In the spectrum can be observed the shifting of these bands. For VC-d3 and VC-d4 the situation is different because all couplings change. As VC-d3 and VC-d4 spectra are very similar, only VC-d4 spectrum will be commented. In this case, for both metals, the two first VNMs correspond to ν C−C coupled with δ C−D, and the three lower ones are couplings of δ C−D modes. At 1500 and 1482 cm^{-1} (for Pt and Pd, respectively) appears the coupling of ν C2=C3 withδ C3D$_2$ and δ C2−D, being in this case a very intense band ($\sim$66% of the most intense one), whereas for VC and VC-d1 it was a clean zone. At 1146 and 1147 cm^{-1} (for Pt and Pd, respectively) appears ν C1−C2 coupled with δ C−D, which is the most intense band. Near, at 1009 and 1006 cm^{-1} (for Pt and Pd, respectively) it appears the band corresponding mainly to δ C3D$_2$, which was the most intense band for undeuterated VC, but in this case is less intense than before because it does not couple so strongly with δ C2−D, making the variation in z-dipolar moment to be smaller. Finally, one small peak appears at 939 and 925 cm^{-1} (for Pt and Pd, respectively). It corresponds to the coupling of some C−D bendings in-plane of VC-d4.

Next region in the spectrum, from 600 to 1000 cm^{-1} corresponds to the C−H bonds bendings out-of-plane and the bending in-plane of the carbonated skeleton. Only two of these peaks have a low intensity in the spectrum of Pt, but they are almost no visible in the case of Pd. The first one lies at 945 cm^{-1} for Pt. It is the C3H$_2$ rocking coupled with δ C1−H . The other intense

UNIVERSITAT ROVIRA I VIRGILI
ORGANIC MOLECULES ON METAL SURFACES: FORECASTING STRUCTURES AND SPECTRA
Benjamí Martorell Masip
ISBN:978-84-691-9747-9 /DL: T-1259-2008

Table 4.17: Vibrational frequencies for Pt (111) in a C1-fcc-C3-top structure on the 3×3 unit cell. All frequencies are given in cm^{-1}.

	C1-fcc-C3-top 3×3	
Vibrational mode	$\bar{\nu}_e$	I (km/mol)
asym. ν C3H$_2$	3067	0.10
ν C2−H + ν C1−H	3024	0.25
ν C1−H - ν C2−H	2990	1.12
sym. ν C3H$_2$	2985	0.00
δ C3H$_2$	1402	0.00
(ν C1−C2 - ν C2−C3) - δ C2−H	1348	0.02
ν C1−C2 + δ C2−H + δ C1−H	1195	0.41
ρ C3H$_2$ + δ C2−H - δ C1−H	1134	1.75
ρ C3H$_2$ - δ C2−H + δ C1−H	1048	0.35
ω C3H$_2$	1025	0.10
ν C1−C2 + ν C2−C3 + δ C1−H + δ C3−H3	932	0.37
γ C1−H - γ C2−H	859	1.43
γ C1−H + γ C2−H	783	1.70
τ C3H$_2$	727	0.24
δ C1−C2−C3	585	0.05
ν C1−surf - ν C3−surf	518	0.01
ν VC−surf	449	0.02
ν C2−surf	375	0.21

peak is the C3H$_2$ twisting. In this mode, both H atoms do not move in the same extension, this explains why this movement implies an active fundamental band. Deuteration of H atoms does not find out any other information about this zone in the spectrum. Below 600 cm^{-1} bands corresponding to frustrated translations and rotations are present, but they are very weak.

For this structure no differences exist between C1-fcc and C1-hcp coordination modes. The effect of coverage does not cause significant differences neither on frequency values nor on the normal modes, but intensities calculated are smaller in the case of a 2×2 unit cell.

4.3.3.2 C3-top structure.

This structure has no symmetry, losing its plane when it is adsorbed on the surface, because all H atoms leave the plane defined by C atoms on the adsorption process. The intensities of the overall spectrum are lower than the spectrum of VC adsorbed in a C1-trans structure (see tables 4.17 and 4.18, and then compare intensity values with the corresponding ones in table 4.16). In the case of

UNIVERSITAT ROVIRA I VIRGILI
ORGANIC MOLECULES ON METAL SURFACES: FORECASTING STRUCTURES AND SPECTRA
Benjamí Martorell Masip
ISBN:978-84-691-9747-9 /DL: T-1259-2008

Pt and Pd surfaces, RAIR spectra are similar, but not equal (see figure 4.17). VNMs and frequencies are not strictly the same. This can be explained easily if we take into account that adsorption modes are not strictly equal on both metals (for more details see section 4.3.2).

For Pt, in the C−H stretching region appears one band with a shoulder. In this region four fundamental transitions exist at 3067, 3024, 2990, and 2985 cm^{-1}, being very close one to each other. In this case, the two extreme frequencies correspond to the asymmetric and symmetric ν C3H$_2$, being the two in the middle part the positive and negative coupling of ν C1−H with ν C2−H. In this case, ν C−H are weak, but comparatively, are intense in the spectrum because absolute intensities are all very small in comparison with the C1-trans structure's ones. The most intense peak in this region lies at 2990 cm^{-1}, which has a big contribution of ν C1−H. In VC-d1, ν C1−D is the most intense band in this zone and it shifts down to 2210 cm^{-1}, still being a relatively intense peak in the spectrum, but in the region around 3000 cm^{-1} no important peaks can be observed. In the case of VC-d3, the important peak in this zone of the spectrum corresponds to ν C1−H, which remains at the same position of VC. The other ν C−D frequencies shift down to 2292, 2283, and 2172 cm^{-1}, corresponding to the asymmetric ν C3D$_2$, ν C2−D and symmetric ν C3D$_2$, respectively. In the case of VC-d4, VNMs corresponding to ν C3D$_2$ lie at same frequency as in VC-d3, but ν C1−D couples with ν C2−D (like in VC). For VC-d4 they lie at 2237 and 2205 cm^{-1}, whose intensities are the largest ones in this region for VC-d4.

For Pd, in the C−H stretching region of the spectrum appear four peaks. The vibrational frequencies are at 3078, 3008, 2971, and 2885 cm^{-1} (see table 4.18). In this case they are more separate than in the case of Pt, and no couplings exist among different ν C−H. This different behaviour can be attributed to the short H1−Pd distance (2.26 Å) in comparison with the long H1−Pt distance (2.51 Å). For Pd, the H1 atom is more activated than for Pt (ν C1−H: 2885 vs 2990 cm^{-1}, respectively), even more than on Cu, where vibrational frequency was 2901 cm^{-1}. ν C1−H is the most intense peak in this region, and in VC-d1, it is shifted down to 2129 cm^{-1}, remaining all other frequencies in the same value as undeuterated VC. For VC-d3, ν C1−H stays at 2885 cm^{-1}, and the other frequencies decrease down to 2292, 2220, and 2163 cm^{-1}, corresponding to asymmetric ν C3D$_2$, ν C2−D and symmetric ν C3D$_2$. Finally VC-d4 is a mixture of VC-d1 and VC-d3 for C−D stretching modes.

For Pt, the range from 900 to 1450 cm^{-1} is a very complicated region because of the multiples couplings of the functional groups vibrations. All bands corre-

UNIVERSITAT ROVIRA I VIRGILI
ORGANIC MOLECULES ON METAL SURFACES: FORECASTING STRUCTURES AND SPECTRA
Benjamí Martorell Masip
ISBN:978-84-691-9747-9 /DL: T-1259-2008

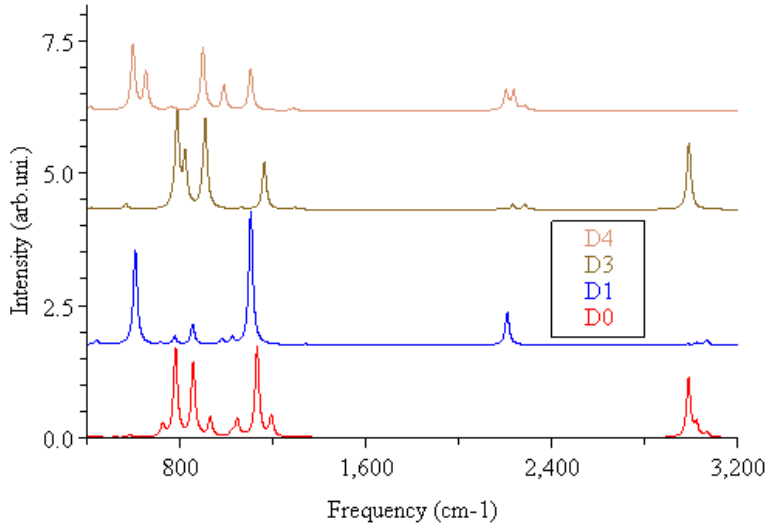

(a) Pt(111)

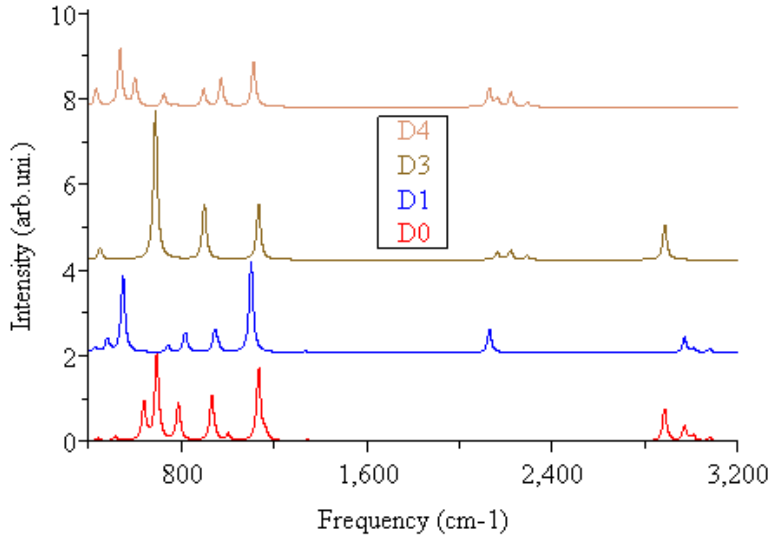

(b) Pd(111)

Figure 4.17: Simulated RAIR spectrum for VC adsorbed in C3-top structures. a) Spectra for VC adsorbed on Pt(111), b) Pd(111). From bottom to top spectra of VC, VC-d1, VC-d3, and VC-d4.

UNIVERSITAT ROVIRA I VIRGILI
ORGANIC MOLECULES ON METAL SURFACES: FORECASTING STRUCTURES AND SPECTRA
Benjamí Martorell Masip
ISBN:978-84-691-9747-9 /DL: T-1259-2008

Table 4.18: Vibrational frequencies for Pd (111) on a C1-fcc-C3-top structure on the 3×3 unit cell. All frequencies are given in cm^{-1}.

	C1-fcc-C3-top 3×3	
Vibrational mode	$\bar{\nu}_e$	I (km/mol)
asym. ν $C3H_2$	3078	0.11
ν C2−H	3008	0.14
sym. ν $C3H_2$	2971	0.38
ν C1−H	2885	0.81
ν C2−C3 + δ $C3H_2$ - δ C2−H	1400	0.01
ν C1−C2 - ν C2−C3 + δ $C3H_2$ - δ C2−H	1344	0.04
ν C1−C2 + δ C1−H + δ C2−H	1163	0.20
ν C1−C2 + ν C2−C3 + ρ $C3H_2$ + δ C2−H	1134	1.74
ρ $C3H_2$ - δ C2−H + δ C1−H	1001	0.16
ω $C3H_2$ - γ C2−H	947	0.06
ν C2−C3 + ω $C3H_2$ - γ C2−H	932	1.09
γ C2−H - γ C1−H	788	0.92
γ C1−H + γ C2−H	695	2.07
τ $C3H_2$ + δ C1−H (ν H1−surf)	639	0.93
δ C1−C2−C3	516	0.12
ν C1−surf - ν C3−surf	441	0.08
ν VC−surf	410	0.01
ν C2−surf	330	0.02

sponding to ν C−C and the C−H bendings in-plane (one bending out-of-plane appear in this region, ω $C3H_2$) are present in this region. The overall spectrum presents three bands of relative intensity. One of them is placed in this region, at 1134 cm^{-1}. Vibrational frequencies appear at 1402, 1348, 1195, 1134, 1048, 1025, and 932 cm^{-1}. First of all it is interesting to observe that vibrational frequency corresponding to double C2=C3 bond does not appear, because in this adsorption mode (see section 4.3.2) C−C distances were too large to maintain a double bond. The first frequency is the $C3H_2$ scissoring, which is not visible in the spectrum. Frequency at 1348 cm^{-1} corresponds to the negative coupling of both ν C−C and δ C2−H, whose intensity is very low. The peak at 1195 cm^{-1} is visible at the spectrum, but weak. It corresponds to the coupling of ν C1−C2 and the bending in-plane of C1−H and C2−H. The most intense peak in the spectrum lies at 1134 cm^{-1}, and the next peak, at 1048 cm^{-1} corresponds to the positive and negative coupling of the $C3H_2$ rockingwith C1−H and C2−H bendings in-plane. The combination of these movements creates an intense peak at 1134 cm^{-1}. At 1025 cm^{-1} already appears one bending out-of-plane, the $C3H_2$

UNIVERSITAT ROVIRA I VIRGILI
ORGANIC MOLECULES ON METAL SURFACES: FORECASTING STRUCTURES AND SPECTRA
Benjamí Martorell Masip
ISBN:978-84-691-9747-9 /DL: T-1259-2008

wagging, which is very weak in the spectrum. Finally, the positive coupling of both ν C−C with δ C1−H, which is visible in the spectrum, lies at 932 cm^{-1}. In VC-d1, the most important change in the spectrum is the shift down of the most intense peak, that corresponds in this case to the coupling of ν C2−C3 and the ω $C3H_2$. In VC-d3, couplings and decouplings change, but two intense peaks remain in this region, one at 1165 cm^{-1}, corresponding to the positive coupling of δ $C3D_2$ with δ C1−H, and the other one at 911 cm^{-1}, which is one of the two most intense peaks in the spectrum and corresponds to the coupling of ν C2−C3 with δ $C3D_2$ and δ C1−H. For VC-d4, three intense peaks appear in this zone, at 1106, 991 and 901 cm^{-1}. The first one corresponds to the negative coupling of both ν C−C and δ $C3D_2$. The second one is the positive coupling of all δ C−H, and finally, the last one (one of the most intense peaks in the spectrum) is the positive coupling of ω $C3D_2$ with δ C2−D.

For Pd, in the range from 1000 to 1400 cm^{-1}, are present all bands corresponding to ν C−C and the C−H bendings in-plane and are strongly coupled among them. Contrary to Pt, mixing with bendings out-of-plane is not observed for Pd. As in the case of Pt, this is a very complicated zone. In this region appears one of the two most intense peaks in spectrum, being the only one visible in this region. Vibrational frequencies lie at 1400, 1344, 1163, 1134, and 1001 cm^{-1}. Only the band at 1134 cm^{-1} has an appreciably intensity (see table 4.18). The assignment of this band is the positive coupling of both ν C−C with δ $C3H_2$ and δ C2−H. This peak lies at the same vibrational frequency as in the case of Pt, but the associated VNM is a bit different (see table 4.17). For VC-d1 only one peak (the most intense one in the spectrum) exists in this region, which corresponds to the positive coupling of both ν C−C with a non-pure movement of $C3D_2$ that could be viewed as a twisting one. In the case of VC-d3 two peaks in this region are visible in the spectrum: one at 1134 cm^{-1}, corresponding to the positive coupling of both ν C−C with δ C1−H and δ $C3D_2$, and the other peak at 900 cm^{-1}, corresponding to the same assignation, but with a negatively coupled δ C1−H. Finally, for VC-d4, three peaks appear at this region, at 1112 (the second most intense peak in the spectrum), 972, and 896 cm^{-1}. The first peak corresponds to the positive coupling of both ν C−C with δ $C3D_2$. The second band corresponds to the positive coupling of δ $C3D_2$ with δ C2−D, and finally, the last one, is the negative coupling of δ $C3D_2$ with δ C1−D and δ C2−D.

For Pt, in the region from 550 to 900 cm^{-1} appear the C−H bendings out-of-plane. Two of the three most intense peaks of the spectrum are in this region.

UNIVERSITAT ROVIRA I VIRGILI
ORGANIC MOLECULES ON METAL SURFACES: FORECASTING STRUCTURES AND SPECTRA
Benjamí Martorell Masip
ISBN:978-84-691-9747-9 /DL: T-1259-2008

They lie at 859 and 783 cm^{-1}, and correspond to the positive and negative coupling of the C1−H and C2−H bendings out-of-plane. Two other frequencies appear in this zone at 727 and 585 cm^{-1}, which correspond to the C3H$_2$ twisting and the bending in-plane of all carbonated skeleton, which are not intense in the RAIR spectrum. For the spectrum in VC-d1, the two most intense peaks in this region disappear, and an intense peak emerges at 610 cm^{-1}, which corresponds to the γ C1−D, like in the case of undeuterated VC. In the case of VC-d3, the most important feature in this region is the presence of two peaks at 824 and 790 cm^{-1} (this last is one of the most intense peaks in spectrum), that correspond to the positive and negative coupling of the C3D$_2$ waggingand the C1−H bending out-of-plane. In the case of VC-d4 these two peaks also appear, but they are shifted down to 600 and 655 cm^{-1}, because they correspond to the C1−D bending out-of-planeand the coupling of γ C1−D with γ C2−D. So we can observe that in all cases the C1−H bending out-of-plane plays an important role, it is always active in the spectrum.

For Pd, the C−H bendings out-of-plane are located mainly in the region from 500 to 950 cm^{-1}. In this region of the spectrum appear the most intense bands and three other peaks that have the half intensity of the most intense one. Vibrational frequencies appear at 947, 932, 788, 695, 639, and 512 cm^{-1}. The most intense peak of the spectrum lies at 695 cm^{-1}, and corresponds to the positive coupling of γ C1−H with γ C2−H. The negative coupling lies at 788 cm^{-1}. The band at 947 cm^{-1} is very weak. At 932 cm^{-1} exists another peak, which corresponds to the coupling of ν C2−C3 with ω C3H$_2$ and γ C2−H. The band at 639 cm^{-1}corresponds to the coupling of the C3H$_2$ twisting with a movement that can be assignated to the stretching of H1 against surface. Finally, at 512 cm^{-1} appears the bending in-plane of the carbonated skeleton. In VC-d1 this region changes a lot, one very intense band appears, and other three less intense exist. At 549 cm^{-1} exists the most intense peak in the spectrum (together with the peak around 1100 cm^{-1}), and it corresponds to the C1−D bending out-of-plane. The weak peaks at 944 and 817 cm^{-1} correspond to the negative and positive coupling of ω C3D$_2$ with γ C2−H. Finally, at 481 cm^{-1} a weak peak appears, corresponding to δ C1−C2−C3. In VC-d3 only one very intense peak exists in this region at 689 cm^{-1}, which is the γ C1−H, and it lies at the same place as in the undeuterated VC. In the case of VC-d4, three bands appear in this region. At 609 cm^{-1} appears a peak corresponding to the coupling of ω C3D$_2$ with γ C2−D and γ C1−D (low intense). The most intense one in the spectrum emerges at 536 cm^{-1} and it corresponds to the positive coupling of

UNIVERSITAT ROVIRA I VIRGILI
ORGANIC MOLECULES ON METAL SURFACES: FORECASTING STRUCTURES AND SPECTRA
Benjamí Martorell Masip
ISBN:978-84-691-9747-9 /DL: T-1259-2008

Table 4.19: Vibrational frequencies for Pt (111) in a C1-bridge-H1-fcc structure on the 3×3 unit cell. All frequencies are given in cm^{-1}.

	C1-bridge-H1-fcc 3×3	
Vibrational mode	$\bar{\nu}_e$	I (km/mol)
asym. ν C3H$_2$	3140	0.07
ν C2−H	3042	0.45
sym. ν C3H$_2$	3036	0.04
ν C1−H	3016	0.45
δ C3H$_2$ + ν C2−C3	1439	0.20
δ C3H$_2$ + δ C2−H + (ν C1−C2 - ν C2−C3)	1349	0.07
δ C2−H + ν C2−C3	1201	0.01
δ C1−H - ν C1−C2	1125	0.48
ρ C3H$_2$ - δ C2−H + δ C1−H	1032	0.01
ω C3H$_2$	952	0.28
γ C2−H + (ν C1−C2 + ν C2−C3) + ρ C3H$_2$	928	0.00
γ C2−H + γ C3−H4	874	1.98
γ C2−H + τ C3H$_2$	771	0.06
γ C1−H	738	0.00
ν C1−surf - γ C2−H	572	0.11
δ C1−C2−C3	516	0.17
ν C2−surf - ν C3−surf	409	0.00
ν C2−surf + ν C3−surf	353	0.20

γ C2−D with γ C1−D. Finally one peak (weak) appears at 433 cm^{-1} associated to the τ C3D$_2$ coupled with γ C2−D and ν C1−surf.

At lower frequencies there are the fundamental transitions corresponding to the stretching movements of C atoms respect to the surface.

Finally, neither exist significant differences between the spectra derived for C1-fcc-C3-top and C1-hcp-C3-top adsorption modes, nor exist important differences in the spectrum due to coverage effects. This is a different aspect respect to Cu, where differences existed for 2×2 and 3×3 unit cells. In the case of Pt and Pd these differences are minima because the repulsion among adjacent molecules is not so important on a 2×2 unit cell.

4.3.3.3 C1-bridge structure.

This system has no symmetry, like in the case of C3-top structure, but H2 and H3 are in the same plane as C2 and C3, conserving the planarity of a double C=C bond. In this structure C1 is adsorbed on a bridge site, forming a sp^3-like structure with the two adjacent metal atoms, and the double C2=C3 bond is

UNIVERSITAT ROVIRA I VIRGILI
ORGANIC MOLECULES ON METAL SURFACES: FORECASTING STRUCTURES AND SPECTRA
Benjamí Martorell Masip
ISBN:978-84-691-9747-9 /DL: T-1259-2008

Table 4.20: Vibrational frequencies for Pd (111) in a C1-bridge-H1-fcc structure on the 3×3 unit cell. All frequencies are given in cm^{-1}.

	C1-bridge-H1-fcc 3×3	
Vibrational mode	$\bar{\nu}_e$	I (km/mol)
asym.ν C3H$_2$	3130	0.03
ν C2−H	3022	0.7
sym. ν C3H$_2$	3012	0.15
ν C1−H	2986	0.52
δ C3H$_2$ + ν C2−C3	1435	0.00
δ C3H$_2$ - δ C2−H + (ν C1−C2 - ν C2−C3)	1348	0.12
δ C2−H - δ C3−H4 + ν C2−C3	1197	0.14
δ C1−H + δ C2−H + ρ C3H$_2$ + ν C1−C2	1103	1.21
δ C1−H - δ C2−H + ρ C3H$_2$	995	0.00
ρ C3H$_2$ + δ C2−H + ν C1−C2 + ν C2−C3	931	0.15
ω C3H$_2$ - γ C2−H	904	0.16
γ C2−H + γ C3−H4	845	1.74
τ C3H$_2$ + γ C2−H + δ C1−H	705	0.00
γ C1−H	640	0.14
τ C3H$_2$ + γ C2−H + ν C1−surf	510	0.02
δ C1−C2−C3	496	0.15
ν C2−surf - ν C3−surf	365	0.03
ν C2−surf + ν C3−surf	304	0.02

placed on a top-site. The intensities in the spectrum of this structure are of the same magnitude as the ones of C3-top structure, and consequently, much less intense than in the case of C1-trans structure (see table 4.19 and 4.20). This structure does not exist for Cu, so no comparison with Cu is possible. RAIR spectra are very similar for Pt and Pd, but they exhibit some differences (see figure 4.18). This can be explained easily if we take into account that adsorption modes are not strictly equal on both metals (for more details see section 4.3.2).

In the C−H stretching region, the asymmetric and symmetric C3H$_2$ stretching mode are bands with no appreciable intensity, which lie at 3140 and 3036 cm^{-1} for Pt and 3130 and 3012 cm^{-1} for Pd. The most intense peak at this region is the C2−H stretching mode, it is of 3042 cm^{-1} and of 3022 cm^{-1} for Pd. The other intense peak in this region is the C1−H stretching mode, being for Pt as intense as the ν C2−H one. It lies at 3016 cm^{-1} for Pt and at 2986 cm^{-1} for Pd. Comparing with values of table 4.16, 4.17 and 4.18, it can be concluded that C1-bridge structure is the one where C1−H is less activated. This is a consequence of the large H1−M distance (in the case of Pd: C3-top:

UNIVERSITAT ROVIRA I VIRGILI
ORGANIC MOLECULES ON METAL SURFACES: FORECASTING STRUCTURES AND SPECTRA
Benjamí Martorell Masip
ISBN:978-84-691-9747-9 /DL: T-1259-2008

2.26 Å, C1-bridge: 2.61 Å) respect to C3-top structure. For VC-d1, the main change is the shift down of ν C1−D mode, at 2224 and 2201 cm^{-1} for Pt and Pd, respectively. For VC-d3 also a peak shifts down (for undeuterated VC, only ν C2−D mode is quite intense to be observed in RAIRS), appearing a band at 2248 and 2232 cm^{-1} for Pt and Pd, respectively. Finally, in VC-d4, the shiftings are the same as in VC-d1 and VC-d3, because no coupling exists among different ν C−D.

In the region from 925 (for Pt and Pd) to 1500 cm^{-1} appear all VNM corresponding to C−C stretching and C−H bending in-plane modes. In the case of Pt one bending out-of-plane appears in this region at 952 cm^{-1}, which corresponds to the ω $C3H_2$. VNM corresponding to the coupling of C2−C3 stretching with $C3H_2$ bending in-plane are at 1439 and 1435 cm^{-1} (Pt and Pd, respectively), being very weak. The next frequency is also very weak and corresponds to the negative coupling of both ν C−C modes with δ $C3H_2$ and δ C2−H (1349 and 1348 cm^{-1} for Pt and Pd, respectively). For Pt, four more VNMs are present at 1201, 1125, 1032 and 928 cm^{-1}. The first, third and fouth frequencis are very weak bands, and they correspond to the coupling of ν C2−C3 with δ C2−H, to the coupling of ρ $C3H_2$ with δ C2−H and δ C1−H and to the positive coupling of both ν C−C with ρ $C3H_2$ and γ C2−H. Finally, the most intense peak in this region (∼25%) lies at 1125 cm^{-1} and corresponds to the coupling of ν C1−C2 with δ C1−H. For Pd, the corresponding frequencies lie at 1197, 1103, 995, and 931 cm^{-1}. The only peak with an appreciable intensity is that one that lies at 1103 cm^{-1} and is the coupling of ν C1−C2 with all C−H bending in-plane modes. The other band is a coupling of different ν C−C with δ C−H (see table 4.20). For VC-d1 no big differences exist with undeuterated VC spectrum, and the most important difference is the shifting down of the most intense peak in this region to ∼1080 cm^{-1} (for both Pt and Pd), due to the decoupling of δ C1−D from the other modes. In the case of VC-d3, for Pt, three weak bands exist in this region at 1332, 1122, and 895 cm^{-1}, corresponding the first one to the negative coupling of both ν C−C with δ C2−D and δ $C3D_2$, the second one to the coupling of ν C1−C2 with δ C1−D and δ $C3D_2$, and finally, the third one to the negative coupling of δ C1−H and δ C2−D. For Pd the number of peaks increase to four in this region, at 1340, 1114, 1036, and 887 cm^{-1}. The first band corresponds to the negative coupling of both ν C−C with δ C2−D and δ $C3D_2$. The second peak, which is the most intense in this region, is the coupling of ν C1−C2 with δ C1−H and δ $C3D_2$. The weak peak at 1036 cm^{-1} corresponds to the coupling of δ C1−H and δ $C3D_2$, and finally, the last one

UNIVERSITAT ROVIRA I VIRGILI
ORGANIC MOLECULES ON METAL SURFACES: FORECASTING STRUCTURES AND SPECTRA
Benjamí Martorell Masip
ISBN:978-84-691-9747-9 /DL: T-1259-2008

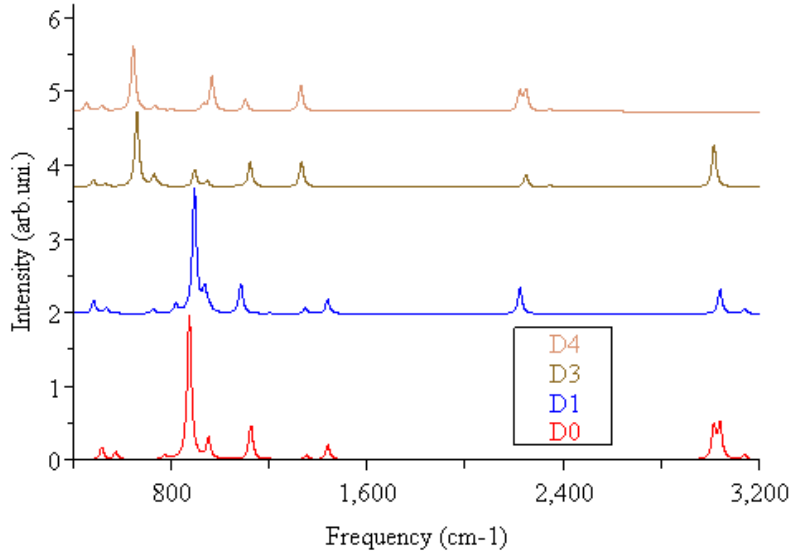

(a) Pt(111)

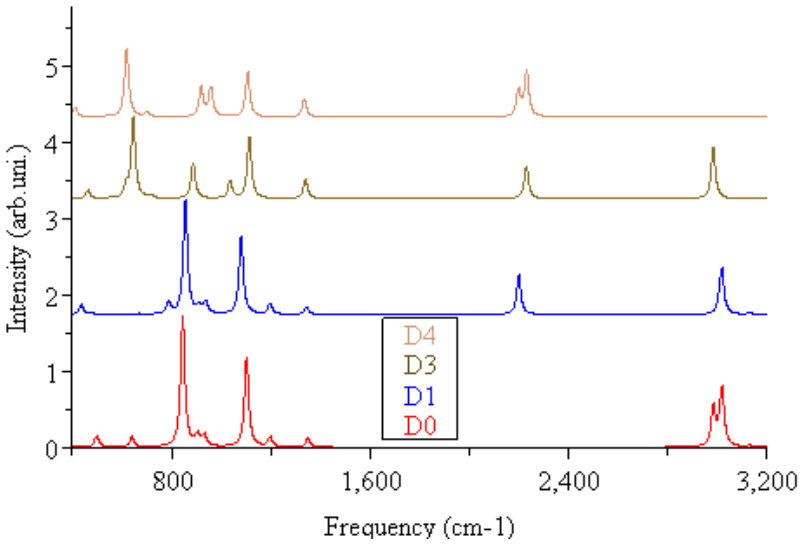

(b) Pd(111)

Figure 4.18: Simulated RAIR spectrum for VC adsorbed in C1-bridge structures. a) Spectra for VC adsorbed on Pt(111), b) Pd(111). From bottom to top spectra of VC, VC-d1, VC-d3, and VC-d4.

UNIVERSITAT ROVIRA I VIRGILI
ORGANIC MOLECULES ON METAL SURFACES: FORECASTING STRUCTURES AND SPECTRA
Benjamí Martorell Masip
ISBN:978-84-691-9747-9 /DL: T-1259-2008

corresponds to the coupling of ν C1−C2 with δ C2−D and δ C1−H. In VC-d4, for Pt, three peaks are present in this region, at 1329, 1102, and 966 cm^{-1}. The first one corresponds to the negative coupling of both ν C−C with δ C2−D and δ $C3D_2$. The second one, the most intense in this region, is the positive coupling of both ν C−C with δ C2−D and δ $C3D_2$. Finally, the last one is also the positive coupling of both ν C−C, but with δ C2−D and δ C1−D. For Pd four bands exist at 1335, 1107, 958, and 919 cm^{-1}. The first and the second one correspond to the same VNMs as in the case of VC-d4 on Pt. The third one is the positive coupling of both ν C−C with δ $C3D_2$, and the last one is the coupling of δ C2−D with δ C3−D4.

In the region from 500 to 960 (Pt) or 920 (Pd) cm^{-1} appear all bands corresponding to the C−H bonds bendings out-of-plane and the C−C−C bending in-plane (see tables 4.19 and 4.20). For both metals this region is quite similar. A small band followed by the most intense band of the spectrum appear at 952 and 874 cm^{-1} for Pt and at 904 and 845 cm^{-1} for Pd. The first feature corresponds mainly to the ω $C3H_2$, but the most intense peak of the spectrum is the positive coupling of both C2−D and C3−D4 bendings out-of-plane. This is the VNM that generates the major variation in the z-dipolar moment of the molecule (although it remains being a weak band). In the case of VC-d1, this region does not change, and the most intense peak remains at 895 and 856 cm^{-1} for Pt and Pd, respectively. For Pt it is the same mode as in the case of VC, and for Pd it changes, corresponding to the coupling of ω $C3H_2$ with γ C2−H. In VC-d3, the most intense peak in the spectrum shifts down to 660 and 646 cm^{-1} for Pt and Pd, respectively. For Pt this mode corresponds to the coupling of ω $C3D_2$ with γ C2−D and for Pd it is the coupling of γ C1−H with γ C2−D. Finally, for VC-d4, the band shifts a bit down to 645 and 619 cm^{-1} for Pt and Pd, respectively. For Pt this VNM corresponds to the coupling of ω $C3D_2$ with γ C2−D and γ C1−D and for Pd is the coupling of γ C1−D with γ C3−D4.

Below these different regions exist the frequencies corresponding to the stretching movements of C atom respect to surface.

Finally, there are not significant differences neither between the spectra derived for C1-bridge-H1-fcc and C1-bridge-H1-hcp adsorption modes, nor between different coverages, as in the case of C3-top structure.

UNIVERSITAT ROVIRA I VIRGILI
ORGANIC MOLECULES ON METAL SURFACES: FORECASTING STRUCTURES AND SPECTRA
Benjamí Martorell Masip
ISBN:978-84-691-9747-9 /DL: T-1259-2008

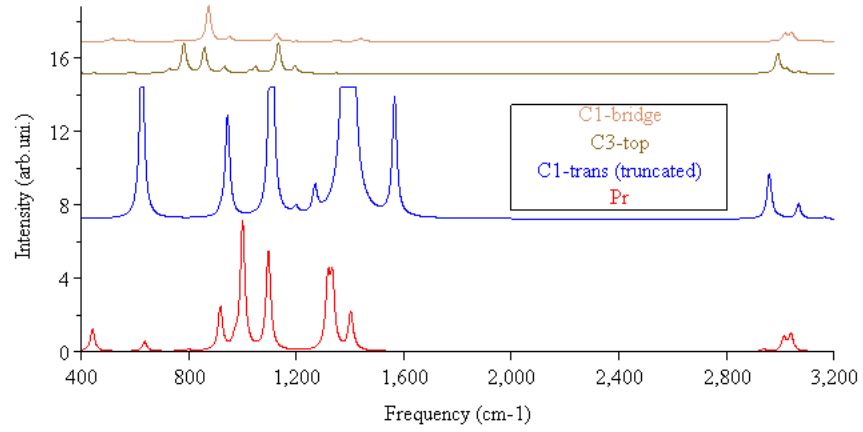

(a) Pt(111)

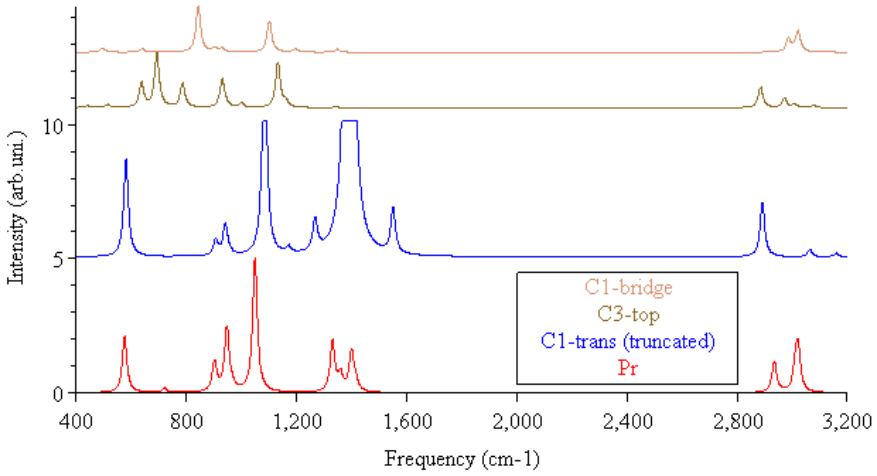

(b) Pd(111)

Figure 4.19: RAIR spectra for all VC structures and Pr on: a) Pt; b) Pd.

4.3.3.4 Comparison of spectra.

In figure 4.19 the spectra corresponding to C1-trans, C3-top and C1-bridge structures of VC and the one of Pr molecule have been put together, all of them adsorbed on the 3×3 unit cell with the C1 atom placed on the fcc site. Although the spectra of VC isomers have been shown in other figures, the spectra have been simulated together for the purpose of finding the fingerprints of each structure when all of them could be present on the surface. In the case of C1-

UNIVERSITAT ROVIRA I VIRGILI
ORGANIC MOLECULES ON METAL SURFACES: FORECASTING STRUCTURES AND SPECTRA
Benjamí Martorell Masip
ISBN:978-84-691-9747-9 /DL: T-1259-2008

trans structure, the absolute intensities were so large in comparison with other spectra that the most intense bands have been truncated. Although the overall spectra seem different for Pt and Pd, fingerprints are very similar in both cases, as will be commented.

For Pt, the Pr spectrum is characterised by the bands at the C−H stretching region and the two intense peaks that lie at 1099 and 1005 cm^{-1}, because these regions are clean for the other species. Also at 1335 cm^{-1} exists one intense band that could be used as a fingerprint for Pr, but in the C1-trans structure the most intense peak appears at 1394 cm^{-1}. This peak is so intense that is the fingerprint for C1-trans structure, existing also bands at 1566, 1108, 954 and 627 cm^{-1}. To differentiate between Pr and C1-trans structure for VC it is only necessary to observe the relative intensity of the band around 1350 cm^{-1}, if it is ten times more intense than the other bands, it is C1-trans structure. In the case of C3-top structure and C1-bridge structure, no intense peaks exist around 1300 cm^{-1}. To differentiate between themselves the easiest way is to count the number of intense peaks that appear in the spectrum in the region from 700 to 1100 cm^{-1}. If only one weak peak appears at ∼874 cm^{-1}, the structure we get is the C1-bridge one. Otherwise, if three weak bands are observed at 1134, 859, and 783 cm^{-1}, what we get is C3-top structure. The problem is, like in the case of Cu with C3-top and C3-hollow structures on Cu, that C1-bridge and C3-top structures are so similar thermodynamically, that it is sure that if we have one structure on the surface, the other one will probably also coexist.

For Pd, the fingerprints are similar. The Pr spectrum owns intense bands at the C−H stretching region, with two intense peaks at 1048 and 945 cm^{-1}. In the region around 1400 cm^{-1} exist two peaks for Pr, but this region is characteristic for C1-trans structure, because it has the most intense peak at 1393 cm^{-1}, which is the main feature of this structure, so the relative intensity in this region will allow us to differentiate between C1-trans structure and Pr. If region around 1400 cm^{-1} is clean, we get C3-top or C1-bridge structure. Once again, the easiest way to differentiate between them is to count the number of intense peaks in the region from 700 to 1100 cm^{-1}. If only two weak peaks are present at 1103 and 845 cm^{-1}, the structure is C1-bridge, but if five weak bands are present (1134, 932, 788, 695, and 639 cm^{-1}) we got the C3-top structure. In this case, C3-top and C1-bridge structures will also coexist on Pd surface.

UNIVERSITAT ROVIRA I VIRGILI
ORGANIC MOLECULES ON METAL SURFACES: FORECASTING STRUCTURES AND SPECTRA
Benjamí Martorell Masip
ISBN:978-84-691-9747-9 /DL: T-1259-2008

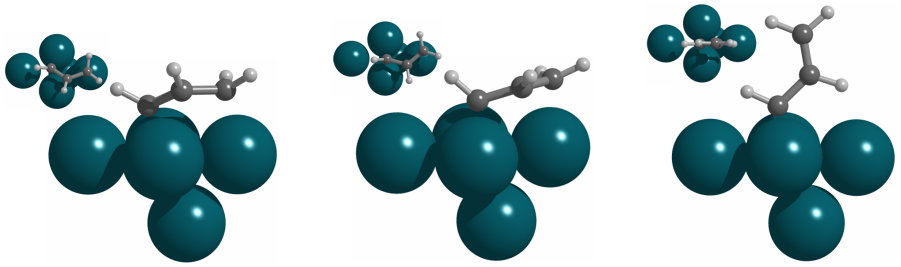

(a) C1-fcc-C3-top (b) C1-bridge-H1-fcc (c) C1-trans-fcc

Figure 4.20: Different adsorption modes of VC on Rh(111) on a 2×2 unit cell.

4.4 VC adsorbed on Rh(111).

4.4.1 Adsorption modes.

The reactivity of propyne on Rh(111) is very similar to the one that exhibits on Pt(111), it dehydrogenates and forms a carbidic layer [105].

Rh (111) behaves very similar to Pt(111) and Pd(111) respect to the adsorption of VC, being the adsorbed VC structures very similar to the ones obtained for Pt(111) and Pd(111). In the case of Pr on Rh(111), Pr could adsorb by different adsorption modes, by the same mode as on Cu (di-σ/di-π, with C1 adsorbed on a hollow-site) and by the same mode as on Pt/Pd (di-σ/π, with the triple bond adsorbed on a hollow-site), being this last structure the preferred one on Rh(111) [97]. This indicates Rh(111) is a metal surface with intermediate features between Cu and Pt/Pd, being closer to the features of Pt/Pd. Rh is a metal with a d^9 valence electronic structure, and its lattice parameter (it exhibits a crystallographic Fm3m structure) is 3.8034 Å [154], which is between the lattice parameter of Cu (∼3.6 Å) and Pt/Pd (∼3.9 Å), being more similar to these ones. In this section the adsorption of VC will be studied using two different unit cells: 2×2 and 3×3.

4.4.1.1 2×2 unit cell.

Let's consider first the high coverage regime, like in the case of VC adsorbed on the other metals. As commented before, 2×2 unit cell has been proposed as the experimental unit cell for the adsorption of propyne on Pt(111) [104] and on Rh(111) [105]. Several adsorption sites and starting geometries have been explored, and six stable minima have been found, three of them have C1 on

UNIVERSITAT ROVIRA I VIRGILI
ORGANIC MOLECULES ON METAL SURFACES: FORECASTING STRUCTURES AND SPECTRA
Benjamí Martorell Masip
ISBN:978-84-691-9747-9 /DL: T-1259-2008

Table 4.21: Relative adsorption energies of VC respect to propyne in gas phase on Rh(111) on the 2×2 unit cell. All values are given in kJ·mol^{-1}.

	E_{ads}				
	No ZPE	ZPE	ZPE-d1	ZPE-d3	ZPE-d4
Propyne C1-fcc	-200.2	-197.8	-198.2	-198.1	-198.5
Propyne C1-hcp	-200.1	-198.0	-198.3	-198.2	-198.5
Propyne tr-fcc	-204.6	-199.2	-199.6	-199.7	-200.1
Propyne tr-hcp	-214.4	-208.7	-209.2	-209.2	-209.7
VC C1-fcc-trans	-131.0	-128.9	-128.6	-129.2	-128.9
VC C1-hcp-trans	-133.5	-132.6	-131.9	-132.9	-132.3
VC C1-b-H1-fcc	-179.6	-173.1	-173.5	-173.8	-174.2
VC C1-b-H1-hcp	-174.2	-168.3	-168.7	-168.9	-169.4
VC C1-fcc-C3-top	-187.5	-182.3	-182.6	-182.7	-183.0
VC C1-hcp-C3-top	-182.9	-177.7	-178.0	-178.1	-178.5

a fcc-site (or displaced to a fcc-site as can be observed in figure 4.20), while the other have this atom on a hcp site (or displaced to a hcp site). Like in the case of the other metals, only those structures with C1 on a fcc-site will be commented, because the structures, whose C1 is adsorbed on a hcp-site, are very similar to those ones and energetic differences are small. The adsorption structures found for Rh are the same structures as on Pd and Pt, i.e., C1-trans, C3-top and C1-bridge structures.

The adsorption energies respect to Pr in gas phase are showed in table 4.21. The ZPE corrected and uncorrected values are shown in different columns in order to check the ZPE effect in energy differences, which in all cases reduces the adsorption energy by ∼5 kJ·mol^{-1}. Gas phase Pr suffers a major correction than C_3H_4 species adsorbed on Rh. For sake of comparison, Pr values are also included (in the case of propyne adsorbed on Rh, four possible adsorption sites are found): the adsorption modes that are similar to Cu (C1-fcc and C1-hcp) and the coordination modes that resembles the case of Pt (tr-fcc and tr-hcp). In all cases, VC structures are less stable than all Pr adsorption modes on this unit cell, being the difference between the most stable adsorbed Pr and the most stable adsorbed VC ∼27 kJ·mol^{-1}. Another important feature of Rh is that it behaves like Pt and Pd, in the sense that the most stable structure is the C3-top structure, the second one is the C1-bridge and finally the C1-trans structure. The relative energy differences between these isomers are also similar, specially with the case case of Pt ($\Delta E_{C3\text{-top/C1-bridge}} \simeq$ 8 (Rh), 16 (Pt), 4 (Pd); $\Delta E_{C3\text{-top/C1-trans}} \simeq$ 57 (Rh), 49 (Pt), 43 (Pd) kJ·mol^{-1} for fcc structures). The

UNIVERSITAT ROVIRA I VIRGILI
ORGANIC MOLECULES ON METAL SURFACES: FORECASTING STRUCTURES AND SPECTRA
Benjamí Martorell Masip
ISBN:978-84-691-9747-9 /DL: T-1259-2008

major stabilisation of Pr respect to the most stable VC structure is also similar ($\Delta E_{C3\text{-}top/Pr} \simeq$ -27 (Rh), -28 (Pt), -14 (Pd) kJ·mol^{-1}).

For C1-trans structure, the most stable adsorption mode is via the C1 atom on a hcp site, being the opposite way than in C1-bridge and C3-top structures, where C1 adsorbed on fcc site is the most stable mode. C1-trans structure is the less stable VC structure, like in the case of Pt and Pd, even more in this case if one consider the differences between C1-trans and C3-top structures. C1 is a bit displaced to a bridge position, indicating that the lattice parameter of Rh is big enough to minimise the repulsion interaction between adjacent molecules. As commented before, VC adsorbs stronger on Rh, and the E_{ads} of C1-trans structure on Rh is -128.9 kJ·mol^{-1}, the largest one of all metals in this structure (Pt: -116.5; Pd: -94.5; Cu: -22.8 kJ·mol^{-1}).

54.0 kJ·mol^{-1} below C1-trans structure lies the C3-top one (-182.3 kJ·mol^{-1}), which is the most stable one on Rh, even 9 kJ·mol^{-1} more stable than C1-bridge structure (-173.1 kJ·mol^{-1}). This difference is big enough to ensure a small preference of VC being placed in a C3-top mode. As in the case of C1-trans structure, the E_{ads} of these structures on Rh are the largest ones for all the studied metals.

Finally, all VC structures become more stable than propyne in gas phase, like in the case of all other metals. This is a real evidence that solid catalysis can stabilise the intermediate structures of a reaction mechanism. In our case, the intermediate is a diradical, which in gas phase is an inaccessible isomer thermically. The surface stabilises largely this diradicalary structures and makes it energetically more favourable.

4.4.1.2 3×3 unit cell.

In order to evaluate coverage effects, the unit cell was increased to a 3×3 dimension, which corresponds to a molecular coverage of 1/9. This unit cell can describe the low (or medium) coverage regime, where situations of repulsion are minimised (as commented before). Using this unit cell, six stable minima were found, which corresponded to the same ones that were found on 2×2 unit cell. The main difference of these structures and the ones obtained for a 2×2 unit cell is the smaller repulsion between adjacent molecules, but like in the case of Pt and Pd, the stabilisation of the structures is not as dramatic as in the case of Cu. As on 2×2 unit cell, three minima corresponds to the adsorption of C1 on fcc site (or displaced to fcc site) and the other three to the hcp site

UNIVERSITAT ROVIRA I VIRGILI
ORGANIC MOLECULES ON METAL SURFACES: FORECASTING STRUCTURES AND SPECTRA
Benjamí Martorell Masip
ISBN:978-84-691-9747-9 /DL: T-1259-2008

Table 4.22: Relative adsorption energies of VC respect to propyne in gas phase on Rh(111) on the 3×3 unit cell. All values are given in kJ·mol^{-1}.

	E_{ads}				
	No ZPE	ZPE	ZPE-d1	ZPE-d3	ZPE-d4
Propyne C1-fcc	-202.0	-199.8	-200.1	-200.2	-200.5
Propyne C1-hcp	-203.2	-200.7	-201.0	-201.1	-201.4
Propyne tr-fcc	-216.8	-211.9	-212.3	-212.3	-212.7
Propyne tr-hcp	-219.2	-214.4	-214.8	214.7	-215.2
VC C1-fcc-trans	-121.8	-118.1	-118.5	-118.2	-118.5
VC C1-hcp-trans	-124.5	-120.2	-120.5	-120.2	-120.6
VC C1-b-H1-fcc	-192.2	-189.6	-189.9	-190.2	-190.5
VC C1-b-H1-hcp	-192.2	-189.5	-189.8	-190.1	-190.4
VC C1-fcc-C3-top	-194.9	-191.3	-191.4	-191.7	-191.8
VC C1-hcp-C3-top	-191.0	-187.0	-187.2	-187.4	-187.6

(or displaced to hcp site). In figure 4.20 are presented the obtained structures and their nomenclature (the same as 2×2 unit cell). The adsorption energies are presented in table 4.22.

C1-trans structure is the less stable VC structure, like on other metals, but a big difference exist for Rh. The E_{ads} for VC on Rh is 10.0 kJ·mol^{-1} higher for 3×3 unit cell than for 2×2 unit cell (-124.5 kJ·mol^{-1} and -133.5 kJ·mol^{-1}, respectively). This structure is also less stable on Rh than on Pt (-131.7 kJ·mol^{-1}), contradicting the argument exposed for 2×2 unit cell that Rh is the most interacting metal (but it is true for the other VC structures on Rh 3×3 unit cell). This is due to the adsorption geometry of VC on Rh (geometrical aspects will be commented in section 4.4.2), but we advance here that on a 2×2 unit cell C1 is adsorbed almost on a hollow site (like on Cu), whereas on a 3×3 unit cell C1 is adsorbed almost on a bridge site (like on Pt and Pd). Besides, on a 2×2 unit cell VC tilts, being H1 very near to surface (see table 4.23) and creating a huge agostic interaction with the surface, otherwise on a 3×3 unit cell VC adsorbs on a bridge site and is more perpendicular to the surface, disappearing the agostic interaction. On the 3×3 unit cell, C1-hcp-trans structure is more stable than C1-fcc-trans structure, which is directly related to the different H1−M distances for both hcp and fcc structures.

C1-bridge and C3-top structures are so close in energy (energy difference of ∼3 kJ·mol^{-1}) that they can be considerated degenerated structures for a 3×3 unit cell, because C1-bridge (-192.2 kJ·mol^{-1}) structure stabilises 12.6 kJ·mol^{-1} respect to 2×2 unit cell, and C3-top (-194.9 kJ·mol^{-1}) only 7.4 kJ·mol^{-1}. This

UNIVERSITAT ROVIRA I VIRGILI
ORGANIC MOLECULES ON METAL SURFACES: FORECASTING STRUCTURES AND SPECTRA
Benjamí Martorell Masip
ISBN:978-84-691-9747-9 /DL: T-1259-2008

is the same case as VC adsorbed on Pd(111) with a 2×2 unit cell, where both structures had the same E_{ads}. This indicates that if one structure is present on surface, the other one also will be present. The E_{ads} is the largest one for all VC adsorption modes on all metals, lieing the E_{ads} only ∼20 kJ·mol^{-1} above Pr on Rh, similar to Pt and Pd surfaces, indicating that Rh stabilises strongly this diradical.

Finally, all VC structures become more stable than Pr in gas phase, being the the E_{ads} very large, indicating the relative stabilisation of VC on Rh(111).

4.4.2 Adsorption geometries.

As in the case of other metals, the adsorption of VC lieing C1 on a fcc site or hcp site does not introduce any relevant change on the adsorption geometry. Only in one case, when VC is adsorbed in a C1-trans structure on a 2×2 unit cell relative differences between C1-fcc and C1-hcp sites exist. The comparison of the rest of adsorption geometries between fcc and hcp for the same adsorption structure indicate that almost all distances do not change more than ±0.02 Å and bond angles do not differ more than ±1°. In table 4.23 geometrical parameters for VC with C1 adsorbed on fcc-site on Rh(111) are presented for a 3×3 unit cell. In the case of C1-trans structure, table 4.23 shows results derived from 2×2 unit cell for both adsorption sites: fcc and hcp. When parameters differ more than the values commented before, values are displaced in brackets. C−H distances are not presented in this table because almost all distances, as in the case of other metals, are in the range 1.09 and 1.12 Å, and no relevant information is obtained (comments about some relevant C−H distances will be made later).

C1-trans structure is present for all metals, and in the case of Rh, important differences exist between 3×3 and 2×2 unit cells, which are more important than the differences found for Pt and Pd. For both cells, C1−C2 and C2−C3 distances are almost equal, ∼1.45 and 1.35 Å, respectively, being these values very similar in all surfaces. What is different is the H1−C1−C2 angle, being the value on a 3×3 unit cell very similar to the one obtained for all other metals (111.3° for Rh and, for instance, 112.1° for Pt), but the value on a 2×2 unit cell differs from all the other H1−C1−C2 angles found until now, being in this case much closer, 104.9° for C1 on fcc site and 101.4° on hcp site. This is a direct consequence of being more tilted on a 2×2 unit cell. Another important feature are the large C1−H distances for this unit cell, 1.17 and 1.21 Å for fcc and hcp sites respectively. These distances are very large if they are compared with the

UNIVERSITAT ROVIRA I VIRGILI
ORGANIC MOLECULES ON METAL SURFACES: FORECASTING STRUCTURES AND SPECTRA
Benjamí Martorell Masip
ISBN:978-84-691-9747-9 /DL: T-1259-2008

Table 4.23: Geometrical parameters of VC adsorbed on Rh(111). A slash means meaningless value in the case of C1-trans dihedral angle (structure is flat). In brackets changing parameters more than ±0.02 Å or ±1°.

	C1-trans		C3-top	C1-bridge
	3×3	2×2 (C1-hcp)	3×3 (2×2)	3×3 (2×2)
[a]d(C1-C2)	1.45	1.46	1.43	1.46
d(C2-C3)	1.35	1.35	1.47	1.42
[b]α(C1-C2-C3)	124.5	125.1	121.3 (120.1)	125.6 (124.4)
α(H1-C1-C2)	111.3	104.9 (101.4)	117.9	118.8
α(H2-C2-C1)	117.6	115.7 (119.6)	118.7	116.5
α(H2-C2-C3)	117.9	119.2 (115.3)	117.9	117.2
α(H3-C3-H4)	117.4	117.3	112.2	115.3
α(H3-C3-C2)	121.3	121.1	114.7	119.2
α(H4-C3-C2)	121.4	121.6	113.9	118.5
[c]tilt	/	/	61.4	68.8
[d]θ(H1-C1-C2-C3)	/	/	-142.7	-114.1 (-110.4)
θ(H3-C3-C2-C1)	/	/	177.2 (176.0)	171.4
θ(H4-C3-C2-C1)	/	/	46.5	22.0
θ(H1-C1-C2-H2)	/	/	20.7 (18.6)	55.9 (58.1)
θ(H2-C2-C3-H3)	/	/	14.2	1.4
θ(H2-C2-C3-H4)	/	/	-117.0 (114.9)	-148.0
[e]d(C1-M)	2.07	2.06	2.02	2.05
d(C2-M)	/	/	2.23	2.20
d(C3-M)	/	/	2.12	2.17
d(H1-M)	2.47	1.88 (1.79)	2.23 (2.28)	2.70 (2.73)
d(H2-M)	2.44	3.02 (3.15)	2.75	2.85 (2.95)
d(H3-M)	/	/	2.71	2.79
d(H4-M)	/	/	2.54 (2.58)	2.55 (2.65)

[a]d: distances (Å); [b]α: angles (degrees); [c] tilt: angle between C1-C2-C3 plane and the normal vector of surface; [d]θ: dihedral angles (degrees); [e] distances to nearest surface atom.

other C−H distances, which are in the range 1.09-1.12 Å. This enlargement is a consequence of the major H1−M interaction, because VC tilts. For 2×2 unit cell, on fcc site H1−M and H2−M distances are 1.88 and 3.02 Å, and on hcp site (where E_{ads} is larger) 1.79 and 3.15 Å indicating a stronger interaction between H1 and M (that causes a minor H1−M distance and a major H2−M distance). These distances are more similar to those obtained for C1-trans structure on Cu, which were 1.97 and 2.72 Å respectively, than to Pt and Pd, which were 2.66 and 2.55 Å and 2.50 and 2.42 Å, respectively for each metal. The distances obtained for Pt and Pd are very similar to those obtained for Rh on the 3×3

UNIVERSITAT ROVIRA I VIRGILI
ORGANIC MOLECULES ON METAL SURFACES: FORECASTING STRUCTURES AND SPECTRA
Benjamí Martorell Masip
ISBN:978-84-691-9747-9 /DL: T-1259-2008

unit cell, which are 2.47 and 2.44 Å. So, it can be concluded that VC adsorbed on Rh on the 2×2 unit cell in C1-trans structure behaves more similar to Cu, and on the 3×3 unit cell to Pt and Pd.

C3-top structure does not present meaningful differences between 3×3 unit cell and 2×2 unit cell, like C1-trans structure did. C1−C2 distance is the same as on Pt and Pd, 1.43 Å, and C2−C3 distance is 1.47 Å, shorter than Pt's value (1.48 Å) and larger than Pd and Cu's values (1.45 and 1.44 Å, respectively), being the structure on Pt the most similar one. These distances indicate clearly that no double C=C bond exist, like on all other metals. This indicates a di-σ bond of C2−C3 unit with two metal surface atoms. Other two parameters that confirm that C3-top structure adsorbs similarly to Pt and Pd are the H1−C1−C2 angle, that has almost the same value (∼118°), and the tilting angle of C1−C2−C3 plane respect to the normal vector of surface, which is 61.4° (similar to the values of Pt and Pd, 62.3° and 60.4°, and different of Cu, 46.1°). This has repercussions on C1−M, C2−M, and C3−M distances (2.02, 2.23, and 2.12 Å, respectively), which are very similar to those found for Pt and Pd (2.01, 2.23 and 2.09 Å). M−H1, M−H2, M−H3 and M−H4 (2.23, 2.75, 2.71, and 2.54 Å, respectively) distances are very similar to those obtained for Pd (2.26, 2.69, 2.68, and 2.45 Å, respectively), being H1 the most activated hydrogen, as in the case of all other metals. Finally, no important differences exist between fcc and hcp sites in this structure.

C1-bridge structure is also present for Rh, like on Pt and Pd. In this structure, C1−C2 and C2−C3 distances are 1.46 and 1.42 Å, respectively, being the C1−C2 distance larger than the C2−C3, on the opposite tendency found for C3-top structure. This effect also happened on Pt and Pd, as commented in section 4.3.2, and it indicates that C2−C3 unit interacts with surface via a π bond with one metal atom. C1−C2−C3 plane forms an angle with the normal vector to surface of 68.8°, being this structure flatter on surface than C3-top (61.4°). This fact is related with the larger C1−M and C3−M distances (2.05 and 2.17 Å) and the shorter C2−M (2.20 Å) one respect to C3-top structure. As in the case of Pt and Pd, H3−C3−C2−H2 unit is almost flat (dihedral angle of ∼1.4°) indicating that in this case remains a degree of sp^2-like hybridisation with the difference that H4 is tilted away ∼30° from this plane in the adsorbed structure. Moreover, for C1-bridge structure all H are less activated than for C3-top structure, like in the case of Pt and Pd. In table 4.23 can be observed that all H−M distances are larger for C1-bridge structure than for C3-top structure. Finally, for C1-bridge structure does not exist important differences, neither

UNIVERSITAT ROVIRA I VIRGILI
ORGANIC MOLECULES ON METAL SURFACES: FORECASTING STRUCTURES AND SPECTRA
Benjamí Martorell Masip
ISBN:978-84-691-9747-9 /DL: T-1259-2008

Table 4.24: Vibrational frequencies of VC for C1-fcc-trans structure on Rh(111) on the 3×3 unit cell. All frequencies are given in cm^{-1}.

	C1-fcc-trans 3×3	
Vibrational mode	$\bar{\nu}_e$	I (km/mol)
asym. ν $C3H_2$	3155	0.1
sym. ν $C3H_2$	3062	0.0
ν C2−H	2925	1.3
ν C1−H	2842	1.5
ν C2=C3 - δ $C3H_2$ + δ C2−H	1556	0.0
δ $C3H_2$ - ν C2=C3+ ν C1−C2 +δ C2−H	1389	39.3
δ C3−H4 - δ C2−H	1276	4.6
δ C1−H + ρ $C3H_2$	1175	0.2
ν C1−C2 + δ C1−H + δ C2−H	1082	1.2
ρ $C3H_2$ - δ C1−H + γ C2−H	935	0.5
ρ $C3H_2$ + ν C1−C2- γ C2−H	935	0.0
ω $C3H_2$	890	0.1
γ C1−H	741	0.0
τ $C3H_2$ + γ C2−H - γ C1−H	600	0.3
δ C1−C2−C3	579	1.3
ν VC−surf	287	0.2

between fcc or hcp-sites, nor between 2×2 and 3×3 unit cells.

4.4.3 IR spectra.

The computted spectra and assignments of VC structures adsorbed on Rh(111) are summarised in the tables of this section. In these tables, for C3-top and C1-bridge structures only results for 3×3 unit cell and for C1-fcc structures are presented, but for C1-trans structure, also 2×2 unit cell is presented because of the important existing differences between two different unit cells. The simulated RAIR spectra are also showed in next sections, which also include the spectra of partial and total deuterated species (VC, VC-d1, VC-d3 and VC-d4). The technical features of spectra are the same used in the preceding sections.

The structure of the analysis will be the same as other metals. First, the RAIR spectrum of each type of structure (the effect of deuteration) will be commented separately. After that, the fingerprints of each structure necessary to identify them on the surface will be tried to find out.

UNIVERSITAT ROVIRA I VIRGILI
ORGANIC MOLECULES ON METAL SURFACES: FORECASTING STRUCTURES AND SPECTRA
Benjamí Martorell Masip
ISBN:978-84-691-9747-9 /DL: T-1259-2008

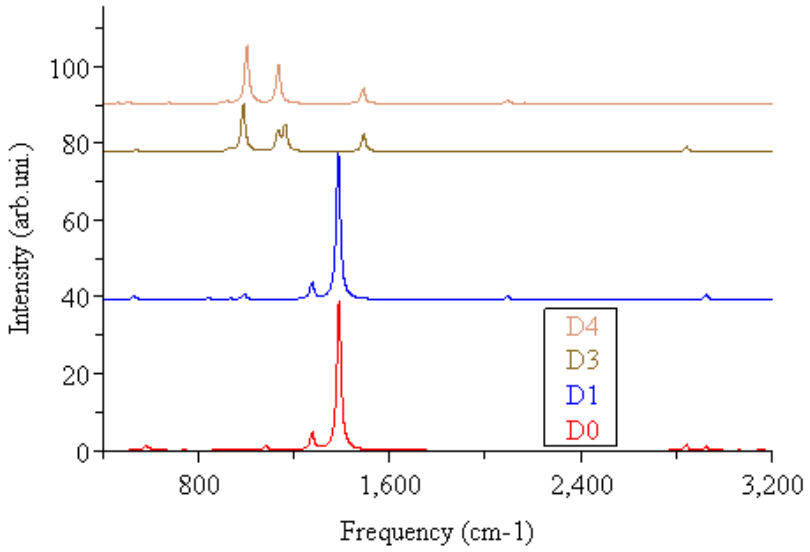

Figure 4.21: Simulated RAIR spectrum for VC adsorbed on C1-trans structures on the 3×3 unit cell. From bottom to top spectra of VC, VC-d1, VC-d3, and VC-d4.

4.4.3.1 C1-trans structure.

In figure 4.21 is presented the spectrum of VC adsorbed on Rh(111) using a 3×3 unit cell for calculations. A very intense band below 1400 cm^{-1} is the most relevant feature of this spectrum. Besides, in table 4.24 frequencies and intensities of each fundamental band are presented. Their values are very similar to the values obtained for Pt and Pd for this same structure (see table 4.16).

In the C−H stretching region four weak frequencies exist at 3155, 3062, 2925, and 2842 cm^{-1}. The two higher frequencies correspond to the asymmetric and symmetric $C3H_2$ group stretching mode. The third one corresponds to the C2−H stretching, and the final one is the C1−H stretching mode, being this the most activated C−H bond. This value is between the one obtained for Cu (2737 cm^{-1}), which is the most activated case for all metals on a 3×3 unit cell, and Pt and Pd (2959 and 2892 cm^{-1} respectively). For VC-d1 no variations appear on the spectrum and only the C1−D stretching mode is affected in this region, shifting down to 2092 cm^{-1}. In the case of VC-d3, frequencies corresponding to asymmetric and symmetric ν $C3D_2$ and ν C2−D shift down to 2356, 2242, and 2162 cm^{-1}, but no other repercussion in the spectrum exists because of the low-intensity of the C−H stretching bands. Finally, VC-d4 case is the addition

UNIVERSITAT ROVIRA I VIRGILI
ORGANIC MOLECULES ON METAL SURFACES: FORECASTING STRUCTURES AND SPECTRA
Benjamí Martorell Masip
ISBN:978-84-691-9747-9 /DL: T-1259-2008

of the deuterated peaks in VC-d1 and VC-d3, indicating that no coupling exist among those modes.

In the region between 1000 and 1600 cm^{-1}, are located the C−C stretching and the C−H bending in-plane modes, being all of them coupled. In this region we found the two most intense bands in the spectrum at 1389 (the most intense one) and at 1276 cm^{-1}. The first one corresponds to the negative coupling of both ν C−C with the $C3H_2$ scissoring and δ C2−H bond. The second one is the negative coupling of bendings in-plane of C2−H and C3−H4. Although their intensity is very weak, three more frequencies are in this zone at 1556, 1175, and 1082 cm^{-1}. The first one corresponds to the coupling of ν C2=C3 with the $C3H_2$ scissoring and δ C2−H bond, the second one is the coupling of δ C1−H with ρ $C3H_2$, and the final one is the coupling of ν C1−C2 with δ C1−H and δ C2−H. Although C2=C3 bond is perpendicular to surface, it is not visible in the spectrum (like in the case of Cu, see section 4.2.3.2).When C1 is deuterated, no changes are present in this region of the spectrum, because the frequencies that change respect to VC are the ones at 1175 and 1082 cm^{-1} to 1104 and 991 cm^{-1}, which are not visible. For VC-d3, important changes exist in this region of the spectrum (see figure 4.21). At 1492, 1163, 1133, and 988 cm^{-1} appear four peaks with relative intensities of ∼33%, ∼50% and ∼50% respect to the band at 988 cm^{-1}. The first band corresponds to the coupling of ν C2=C3 with the $C3D_2$ scissoring, C2−D and C1−H bending in-plane modes. The second is the C1−H bending in-plane. The third one is the ν C1−C2 coupled withδ C1−H, δ C2−D, and δ C3−D3. The last peak corresponds to the coupling of δ $C3D_2$ with δ C1−H. In the case of VC-d4, the spectrum is very similar to the one of VC-d3, but only three bands appear at 1489, 1135, and 1003 cm^{-1} (∼25% and ∼66% respect to the band of 1003 cm^{-1}, respectively). The first one corresponds to the ν C2=C3 coupled with δ $C3D_2$ and δ C2−D, the second one to the coupling of ν C1−C2 with δ $C3D_2$ and δ C2−D, and the last one to the coupling of δ $C3D_2$ and δ C1−D.

The region between 500 and 1000 cm^{-1} is the one corresponding to the C−H bendings out-of-plane and C−C−C bending in-plane. The bands are not visible, because bendings out-of-plane in this structure do not cause variation in z-dipolar moment, being the most intense one in this region the C−C−C bending in-plane at 579 cm^{-1}. In table 4.24 are presented their corresponding assignations. In the case of deuterated species, vibrational frequencies variate and shift down their position, but they are not active in the spectrum, so no comments will be made about them. Finally, below this region lie the frustrated

UNIVERSITAT ROVIRA I VIRGILI
ORGANIC MOLECULES ON METAL SURFACES: FORECASTING STRUCTURES AND SPECTRA
Benjamí Martorell Masip
ISBN:978-84-691-9747-9 /DL: T-1259-2008

Table 4.25: Vibrational frequencies of VC for C1-trans structure on Rh (111) on the 2×2 unit cell. All frequencies are given in cm^{-1}.

$\bar{\nu}_e$	I	Assignation	I	$\bar{\nu}_e$
C1-fcc		C1-fcc / C1-hcp	C1-hcp	
3156	0.0	asym. ν C3H$_2$	0.1	3155
3061	0.4	sym. ν C3H$_2$+ ν C2−H	1.3	3058
3047	0.6	ν C2−H - sym.ν C3H$_2$	1.2	3046
2211	1.0	ν C1−H	0.5	1915
1559	1.5	ν C2=C3 - δ C3H$_2$ + δ C2−H + δ C1−H	0.7	1570
1418	7.0	δ C3H$_2$ + δ C2−H - δ C1−H / δ C1−H- δ C3H$_2$	1.7	1500
1353	3.9	m(ν C1−C2 - ν C2=C3) + δ C3H$_2$ + δ C1−H	5.2	1374
1263	0.0	δ C2−H - δ C3−H4	0.0	1262
1095	0.1	ν C1−C2 + δ C2−H - ρ C3H$_2$	0.0	1096
956	0.0	τ C3H$_2$ - γ C2−H / ρ C3H$_2$ + ν C1−C2 - δ C2−H	0.7	957
955	1.5	ρ C3H$_2$ - γ C2−H / τ C3H$_2$ - γ C2−H	0.2	954
879	0.0	ω C3H$_2$	0.0	883
680	0.1	γ C1−H- γ C2−H- γ C3−H3/ τ C3H$_2$ + γ C1−H	0.0	653
593	0.2	τ C3H$_2$ - γ C1−H / δ C1−C2−C3	2.1	579
576	2.5	δ C1−C2−C3 / τ C3H$_2$ - γ C1−H	0.1	562
282	0.1	ν VC−surf	0.0	281

translations and rotations of the molecule respect to the surface.

No differences exist for RAIR spectra between fcc or hcp-site for the 3×3 unit cell. However, the coverage effect causes significant differences in frequency values and assignments. In figure 4.22 are presented the spectra of VC adsorbed on the 2×2 unit cell on fcc and hcp-sites, and compared with the one of VC adsorbed on the 3×3 unit cell, which was previously commented and it has been truncated because the most intense peak on this unit cell is much larger than on the 2×2 unit cell, although the rest of peaks on the 3×3 unit cell are in the same range of intensity as 2×2 unit cell. In the case of a 2×2 unit cell differences between fcc and hcp-sites are important (see table 4.25). First of all, it is interesting to observe that in the region around 3000 cm^{-1} exist bands on the 2×2 unit cell, which are placed to lower frequencies on the 3×3 unit cell. This peak corresponds to the addition of two close vibrational frequencies, at 3061 and 3047 cm^{-1} for fcc and 3058 and 3046 cm^{-1} for hcp, corresponding to the positive and negative coupling of symmetric ν C3H$_2$ with ν C2−H. But the most important difference respect to 3×3 unit cell is the appearance of a small peak at 2211 cm^{-1} for C1-fcc and at 1915 cm^{-1} for C1-hcp. This corresponds to the C1−H stretching mode. As commented in section 4.4.2 C1−H bond in this

UNIVERSITAT ROVIRA I VIRGILI
ORGANIC MOLECULES ON METAL SURFACES: FORECASTING STRUCTURES AND SPECTRA
Benjamí Martorell Masip
ISBN:978-84-691-9747-9 /DL: T-1259-2008

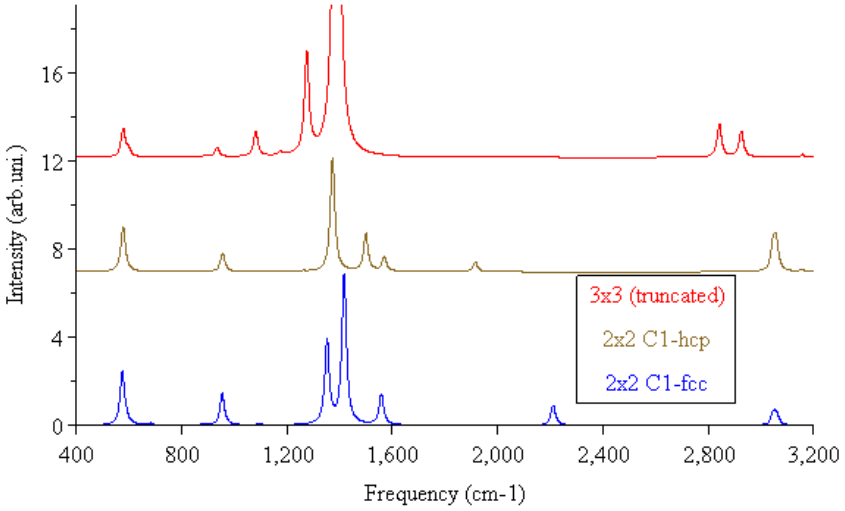

Figure 4.22: RAIR spectra for C1-trans structure on a 3×3 unit cell (blue line, truncated) with the two different adsorption sites on a 2×2 unit cell: C1-fcc (red line) and C1-hcp (green line).

structure for this unit cell is very large compared with the value on the 3×3 unit cell. This indicates that this bond is really activated, and consequently, the vibrational frequency is very low.

At 1559 cm^{-1} for C1-fcc and at 1570 for C1-hcp appears one peak not present on the 3×3 unit cell corresponding to the coupling of ν C2=C3 with all δ C−H. The most intense peak for C1-hcp appears at 1374 cm^{-1}, which corresponds to the negative coupling of both ν C−C with δ $C3H_2$ and δ C1−H, and for C1-fcc appears at 1353 cm^{-1}. But for C1-fcc it is not the most intense peak, the most one lies at 1418 cm^{-1} and corresponds in this case to the coupling of all δ C−H. For C1-hcp one band lies at 1500 cm^{-1} corresponding to the coupling of δ $C3H_2$ with δ C1−H. In the lower region of the spectrum, two new peaks exist at 955 and 576 cm^{-1} for fcc and at 957 and 579 cm^{-1} for hcp-site, but they do not correspond to the same assignation (see table 4.25). So, the RAIR spectrum is different between the case of 3×3 and 2×2 unit cell for the C1-trans structure.

4.4.3.2 C3-top structure.

All preliminary remarks made for other metals for this structure are also valid in this case (see section 4.3.3.2): the loss of VC symmetry respect to the gas phase and the decrease of intensity in the spectrum respect to the C1-trans structure

UNIVERSITAT ROVIRA I VIRGILI
ORGANIC MOLECULES ON METAL SURFACES: FORECASTING STRUCTURES AND SPECTRA
Benjamí Martorell Masip
ISBN:978-84-691-9747-9 /DL: T-1259-2008

Table 4.26: Vibrational frequencies of VC in a C1-fcc-C3-top structure on Rh(111) on the 3×3 unit cell are presented in this table. All frequencies are given in cm^{-1}.

	C1-fcc-C3-top 3×3	
Vibrational mode	$\bar{\nu}_e$	I (km/mol)
asym. ν C3H$_2$	3063	0.09
ν C2−H	3010	0.03
sym. ν C3H$_2$	2971	0.01
ν C1−H	2788	0.98
δ C3H$_2$	1389	0.00
(ν C1−C2 - ν C2−C3) + δ C2−H + δ C3−H3	1332	0.03
δ C2−H + δ C1−H + ν C1−C2	1163	0.08
δ C1−H + ρ C3H$_2$ + ν C2−C3	1124	1.95
δ C1−H - δ C2−H + ρ C3H$_2$	1008	0.17
ω C3H$_2$ - γ C2−H	960	0.13
(ν C1−C2 + ν C2−C3) + δ C1−H	922	1.66
γ C2−H - γ C1−H	807	1.46
γ C2−H + γ C1−H	695	1.58
τ C3H$_2$	623	0.64
δ C1−C2−C3	523	0.08

due to the adsorption mode (compare C1-trans values in table 4.24 and the ones for C3-top in table 4.26). In figure 4.23 VC spectrum and its deuterated derivatives are presented.

In the C−H region four vibrational frequencies exist at 3063, 3010, 2971, and 2788 cm^{-1}. The first and the third ones correspond to the asymmetric and symmetric ν C3H$_2$, the second one to the ν C2−H and the last one to the ν C1−H. The last one presents a intensity around 50% of the most intense one of the overall spectrum. This vibrational frequency is the lowest one for the C3-top structure compared with all other metals (2990 cm^{-1}for Pt, 2901 cm^{-1}for Cu and 2885 for Pd), indicating that on Rh this bond is slightly activated, even more than the C1-trans structure on the 3×3 unit cell (this is the most activated one for Cu and Pt, whereas for Pd it is C3-top structure). This band remains at the same position for VC-d3 and changes for VC-d1 and VC-d4, as logically it can be expected. For VC-d1 this band shifts down to 2056 cm^{-1}, losing part of its poor intensity. For VC-d3, the peak of ν C1−H remains at the same frequency as undeuterated VC, and no changes exist in the spectrum in this region, but frequencies associated to the other C−H stretching modes shift down to 2278, 2223, and 2163 cm^{-1}. The case of VC-d4 is the addition

UNIVERSITAT ROVIRA I VIRGILI
ORGANIC MOLECULES ON METAL SURFACES: FORECASTING STRUCTURES AND SPECTRA
Benjamí Martorell Masip
ISBN:978-84-691-9747-9 /DL: T-1259-2008

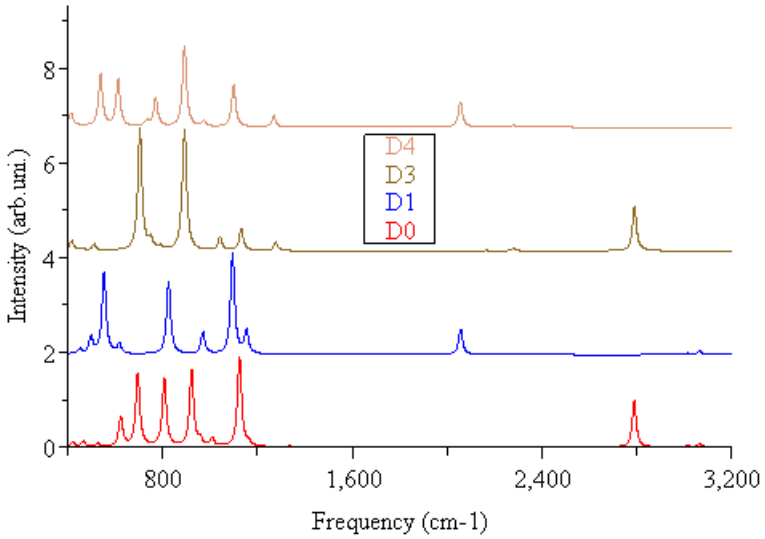

Figure 4.23: Simulated RAIR spectrum for VC adsorbed in C3-top structures on a 3×3 unit cell. From bottom to top spectra of VC, VC-d1, VC-d3, and VC-d4.

of ν C1−D stretching modes of VC-d1 and the other three modes of VC-d3, indicating that no couplings exist among them.

In the region between 1000 and 1400 cm^{-1}, it can be found the bands associated with ν C−C and C−H bendings in-plane. In this region lies the most intense band of the spectrum at 1124 cm^{-1}, corresponding to thecoupling of C3H$_2$ rocking with the C2=C3 stretching mode and the C1−H bending in-plane. Also one very weak peak appears at 1008 cm^{-1}, corresponding to the coupling of all C−H bonds bendings in-plane. In this region three more fundamental frequencies with no significant intensity exist at 1389, 1332, and 1163 cm^{-1}. The first one corresponds to the C3H$_2$ scissoring. The second one to the negative coupling of both ν C−C with δ C2−H and δ C3−H3. The last one corresponds to the coupling of ν C1−C2 with δ C2−H and δ C1−H. In the case of VC-d1 a very intense peak at 1095 cm^{-1} appears in this region, corresponding to the same VNM as in the case of the most intense peak for undeuterated VC, and another weak band at 1153 cm^{-1} that is the coupling of ν C1−C2 with δ C2−H. In the case of VC-d3 the spectrum is quite different. One of the most intense bands, although weak, exists in this region at 893 cm^{-1}, corresponding to the coupling of ν C2=C3 with δ C2−D and δ C3−D4. Three small bands appear also in this region at 1276, 1131, and 1041 cm^{-1}(with very low intensity).

UNIVERSITAT ROVIRA I VIRGILI
ORGANIC MOLECULES ON METAL SURFACES: FORECASTING STRUCTURES AND SPECTRA
Benjamí Martorell Masip
ISBN:978-84-691-9747-9 /DL: T-1259-2008

The first one corresponds to the negative coupling of both ν C−C with δ C2−D and δ $C3D_2$, and the other two are the negative and positive coupling of δ $C3D_2$ with δ C1−H. In the case of VC-d4 those bands move to 1268, 1099, 892 and 770 cm^{-1}. The first peak corresponds to the coupling of the C2=C3 stretching mode with the C1−D bending in-plane and the $C3D_2$ rocking. The second one is the positive coupling of both ν C−C with δ $C3D_2$. The most intense feature is the $C3D_2$ rocking with the C2−D bending in-plane. Finally, the last band corresponds to the coupling of δ C1−D with δ C3−D3.

In the region between 500 and 1000 cm^{-1} six vibrational frequencies can be found (see table 4.26), corresponding all VNM to the C−H bending out-of-plane, except the one at 922 cm^{-1} and the last one, which is the C−C−C bending in-plane (523 cm^{-1}). The first (960 cm^{-1}) and the last (523 cm^{-1}) VNMs are not visible in the spectrum. The weak bands that have more intensity in this region are at 922, 807, and 695 cm^{-1}, corresponding the first one to the positive coupling of both ν C−C with δ C1−H, and the second and third ones to the negative and positive coupling of γ C2−H with γ C1−H. Finally the band that lies at 623 cm^{-1}, corresponds to the $C3H_2$ twisting. In the case of VC-d1 the bands at 825 and 553 cm^{-1} correspond respectively to the coupling of δ C1−D with γ C2−H and to the γ C1−D. However two very weak bands at 617 and at 497 cm^{-1}, corresponding the first one to the coupling of τ $C3H_2$ with δ C1−D and the second one to the C−C−Cbending in-plane. In the case of VC-d3 the most intense peak of the spectrum is the unique visible one in this region, at 704 cm^{-1} (C1−H bending out-of-plane). In VC-d4 bands of equal intensity appear in this region at 612 and 538 cm^{-1}, corresponding the first one to the coupling of $\omega C3D_2$ with δ C1−D and δ C2−D and the second one to the coupling of γ C1−D and the δ C1−C2−C3.

Below 500 cm^{-1} it can be found the VC−surface stretching modes, which are also weak. For this structure no differences exist between C1-fcc and C1-hcp coordination modes. The effect of coverage does not cause significant differences neither in frequency values nor in the normal modes, but computed intensities are smaller in the case of a 2×2 unit cell.

4.4.3.3 C1-bridge structure.

All preliminary remarks made for other metals for this structure are also valid for this case (see section 4.3.3.3): the loss of VC symmetry respect to the gas phase, the sp^3-like hybridisation of C1 and the decrease of intensity in the spectrum

UNIVERSITAT ROVIRA I VIRGILI
ORGANIC MOLECULES ON METAL SURFACES: FORECASTING STRUCTURES AND SPECTRA
Benjamí Martorell Masip
ISBN:978-84-691-9747-9 /DL: T-1259-2008

respect to the C1-trans structure due to the adsorption mode (compare C1-trans values in table 4.24, the ones for C3-top in table 4.26 and the ones for C1-bridge in table 4.27). In figure 4.24 VC spectrum and its deuterated derivatives are presented.

In the C−H stretching region, a band appears in the spectrum. This band is the addition of three very close peaks at 3012, 2995, and 2983 cm^{-1} that correspond, respectively, to the C2−H, symmetric $C3H_2$, and C1−H stretching modes. The fact that these modes are active indicates that C−H bonds are not strictly parallel to surface, as can be observed in figure 4.23(c). The asymmetric $C3H_2$ stretching mode has a frequency of 3113 cm^{-1}, but it is not visible in the spectrum. These frequency values are very similar to those found for Pt and Pd (see tables 4.19 and 4.20 respectively), being in all cases the frequencies above 3000 cm^{-1}or very close to this value. For VC-d1 the band at ∼3000 cm^{-1} decrease in intensity as a consequence of the displacement of the ν C1−D to 2199 cm^{-1}. For VC-d3 something similar happens, decreasing the intensity of the peak around 3000 cm^{-1}. The new features are very close bands (2224 and 2185 cm^{-1}), corresponding to the ν C2−D and the symmetric ν $C3D_2$. The asymmetric ν $C3D_2$ mode shifts also down to 2320 cm^{-1} as expected, but it remains not visible in the spectrum. Finally, VC-d4 is the addition of the deuterated modes of VC-d1 and VC-d3.

In the region from 900 up to 1500 cm^{-1} appear all ν C−C and δ C−H modes. In this region we found two bands in the spectrum at 1105 and at ∼920 cm^{-1} corresponding the first one to the coupling of all δ C−H modes with the ν C1−C2, and the second one includes the coupling of ρ $C3H_2$ with δ C2−H and the frequency associated to the coupling of ρ $C3H_2$ with γ C2−H (920 and 912 cm^{-1}). Four frequencies more lie in this region at 1418, 1336, 1189, and 1009 cm^{-1}, all of them not visible in the spectrum. In the table 4.27 the assignations of these VNMs can be observed. The value of 1418 cm^{-1} indicates that the C2=C3 bond has more double character than in the case of C3-top structure, where vibrational C−C frequencies were lower (see table 4.26). For VC-d1 specie the band at 1078 cm^{-1} is the same mode as for undeuterated VC, but decoupled of δ C1−D. For VC-d3 three very weak peaks are present in this region at 1107, 927, and 886 cm^{-1}. The first one corresponds to the coupling of ν C1−C2 with δ C1−H and δ $C3D_2$, the second one is the positive coupling of both ν C−C with δ C1−H and δ $C3D_2$, and the third one the coupling of ν C1−C2 with δ C2−D. Finally, for VC-d4, two bands are present at 1098 and 955 cm^{-1}. First transition is assignated to the coupling of ν C1−C2 with δ C2−D and δ $C3D_2$

UNIVERSITAT ROVIRA I VIRGILI
ORGANIC MOLECULES ON METAL SURFACES: FORECASTING STRUCTURES AND SPECTRA
Benjamí Martorell Masip
ISBN:978-84-691-9747-9 /DL: T-1259-2008

Table 4.27: Vibrational frequencies of VC in a C1-bridge-H1-fcc structure on Rh(111) on the 3×3 unit cell. All frequencies are given in cm^{-1}.

	C1-bridge-H1-fcc 3×3	
Vibrational mode	$\bar{\nu}_e$	I (km/mol)
asym. ν C3H$_2$	3113	0.07
ν C2−H	3012	0.33
sym. ν C3H$_2$	2995	0.60
ν C1−H	2983	0.29
δ C3H$_2$ + ν C2−C3	1418	0.00
δ C2−H - δ C3H$_2$ - (ν C1−C2 - ν C2−C3)	1336	0.01
δ C2−H - δ C3−H4 + ν C2−C3	1189	0.04
δ C1−H -ν C1−C2 - δ C2−H - ρ C3H$_2$	1105	0.55
δ C1−H - ρ C3H$_2$ + δ C2−H	1009	0.03
ρ C3H$_2$ - δ C2−H	920	0.31
ρ C3H$_2$ - γ C2−H	912	0.21
γ C2−H + γ C3−H4	842	1.63
τ C3H$_2$ + γ C2−H	726	0.02
γ C1−H	629	0.07
ν C1−surf - γ C2−H	533	0.04
δ C1−C2−C3	490	0.20
ν C2−surf - ν C3−surf	400	0.00
ν C2−surf + ν C3−surf	337	0.26

and the second one to the coupling of all δ C−H modes.

The region from 450 to 900 cm^{-1} is mainly associated to C−H bending out-of-plane modes and the C−C−C bending in-plane. In this region appears the most intense band of the spectrum at 842 cm^{-1} (although weak in absolute value), which is the coupling of γ C2−H with γ C3−H4. Below this band, a very weak one (490 cm^{-1}) corresponds to the bending in-plane of the carbonated structure. The other frequencies in this region are not intense (see table 4.27). In the case of VC-d1 five bands appear in the spectrum at 915, 860, 787, 693, and 453 cm^{-1}. The first and second peaks, the two most intense peaks in this region, correspond to the negative and positive coupling of the C3H$_2$ wagging with the C2−H bending out-of-plane. The third and fourth peaks correspond to the negative and positive coupling of the γ C2−H with τ C3H$_2$ and δ C1−D. The last peak is the C1−D bending out-of-plane. For VC-d3 the most intense band of the spectrum is at 641 cm^{-1} corresponding to the ω C3D$_2$ coupled with γ C2−D and γ C1−H. Two very weak bands appear also at 723 and 451 cm^{-1} corresponding the first one to the negative coupling of ω C3D$_2$ with γ C2−D and

UNIVERSITAT ROVIRA I VIRGILI
ORGANIC MOLECULES ON METAL SURFACES: FORECASTING STRUCTURES AND SPECTRA
Benjamí Martorell Masip
ISBN:978-84-691-9747-9 /DL: T-1259-2008

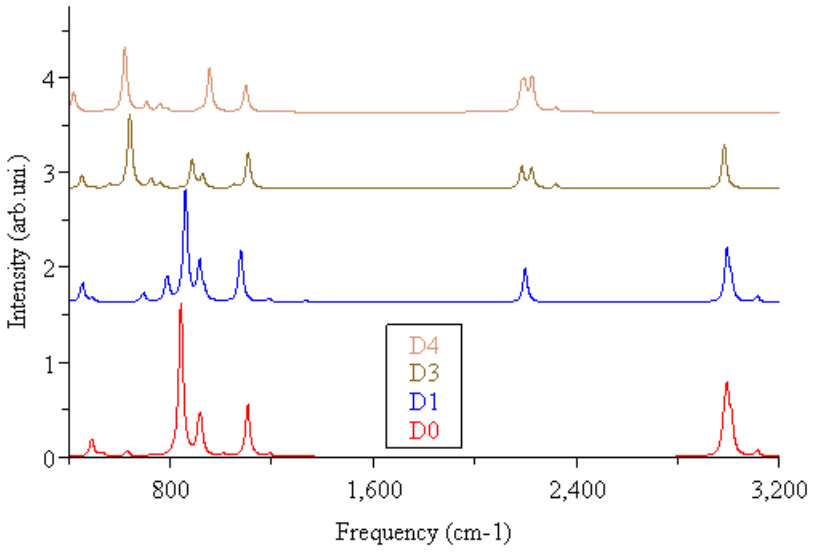

Figure 4.24: Simulated RAIR spectrum for VC adsorbed in C1-bridge structures on a 3×3 unit cell. From bottom to top spectra of VC, VC-d1, VC-d3, and VC-d4.

the second one to the δ C1−C2−C3. Finally, for VC-d4 the most intense band of the spectrum appears at 621 cm^{-1}, corresponding to the positive coupling of ω C3D$_2$ with γ C2−D and γ C1−D. Finally, the δ C1−C2−C3 is at 419 cm^{-1}.

Finally, neither there are significant differences between the spectra derived for C1-bridge-H1-fcc and C1-bridge-H1-hcp adsorption modes, nor exist important differences in the spectrum due to coverage effects, because Rh has a quite large lattice parameter and repulsion between adjacent molecules is not important on the 2×2 unit cell.

4.4.3.4 Comparison of spectra.

In figure 4.25 the spectra corresponding to C1-trans, C3-top and C1-bridge structures of VC and the most stable one of Pr molecule on Rh have been put together, all of them adsorbed on the 3×3 unit cell with C1 atom placed on the fcc site for VC. Despite being the VC spectra already presented in this section, they have been put together in order to find the fingerprints of each structure when all of them could be present on the surface. In the case of C1-trans structure, the absolute intensities were so large in comparison with the other structures, that the most intense band has been truncated.

UNIVERSITAT ROVIRA I VIRGILI
ORGANIC MOLECULES ON METAL SURFACES: FORECASTING STRUCTURES AND SPECTRA
Benjamí Martorell Masip
ISBN:978-84-691-9747-9 /DL: T-1259-2008

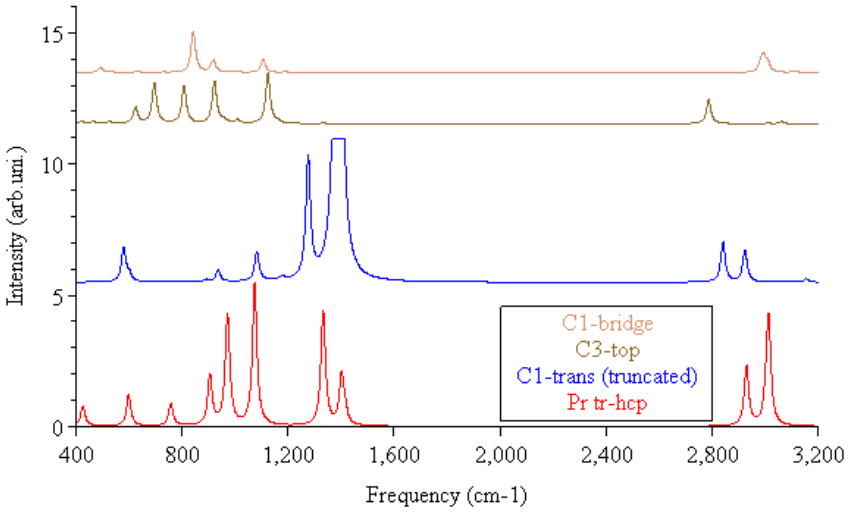

Figure 4.25: RAIR spectra for all VC structures and Pr on Rh(111).

The Pr spectrum is characterised by two intense bands at the C−H stretching region around 3000 and 2900 cm^{-1}, two peaks around 1400 and 1300 cm^{-1}, and finally, three close peaks (among them the most intense one) around 1075, 970, and 905 cm^{-1}. So Pr has three different zones with medium bands. In the case of C1-trans it is easy to distinguish of all other structures, one very intense band around 1400 cm^{-1} is present in the spectrum, so if one band appears at this zone being much more intense than all other bands, C1-trans structure is the one we have (C1-trans structure also presents a medium band around 1250 cm^{-1}). If no strong or medium band is present in this zone, from 1200 to 2800 cm^{-1}, what we have is the C1-bridge or C3-top structure. To differentiate among them, we can observe the C−H stretching region and the region below 1200 cm^{-1}. C1-bridge structure presents one band around 3000 cm^{-1}, whereas C3-top structure presents the most intense band (weak) in this region at lower frequencies (∼2800 cm^{-1}). Besides, C1-bridge structure presents the most intense peak at 840 cm^{-1} with two small peaks at 1105 and 920 cm^{-1}, otherwise C3-top structure presents weak absorptions at 1120, 920, 800, and 700 cm^{-1}. Finally, from the energetic point of view, as C1-bridge and C3-top structure are so close in energy, it is probably they coexist on the surface.

UNIVERSITAT ROVIRA I VIRGILI
ORGANIC MOLECULES ON METAL SURFACES: FORECASTING STRUCTURES AND SPECTRA
Benjamí Martorell Masip
ISBN:978-84-691-9747-9 /DL: T-1259-2008

4.5 Final summary.

In this chapter we have studied the adsorption of VC, the key intermediate in the cyclation reaction of propyne to yield benzene on Cu(111). Moreover, the behaviour of this intermediate has also been analysed on Pt(111), Pd(111) and Rh(111) in order to elucidate why these metals behave so different in the reactivity of propyne. With all that information, we have been capable of answering questions that were raised at the beginning of this chapter:

- Our results for C_3H_4 isomers in gas phase agree with the previously reported ones.
- All VC structures for all metals and all unit cells do not present differences between fcc and hcp-site (only for VC in C1-trans structure on Rh(111) for a 2×2 unit cell differences exist).
- In figure 4.26 is presented a summary of the adsorption energies for all VC structures and metals.
- The adsorption of VC has been studied on Cu(111) using three different unit cells: 2×2, 3×3 and 4×$\sqrt{3}$. This implies three different coverage regimes: 1/4, 1/9 and 1/8:
  - For 2×2 unit cell, six minima have been found: C1-trans , C1-cis and C3-top with C1 placed on fcc or hcp-site.
  - For C1 placed on fcc-site, C1-trans is the most stable structure (-22.8 kJ·mol^{-1}). C1-cis and C3-top (-17.7 and -13.5 kJ·mol^{-1}, respectively) are less stable.
  - For 3×3 unit cell, six minima have been found: C1-trans, C3-top and C3-hollow with C1 placed on fcc or hcp-site (not the same ones as 2×2 unit cell).
  - For C1 placed on fcc-site, C3-hollow and C3-top are isoenergetic (∼-54.0 kJ·mol^{-1}), being C1-trans less stable (-33.4 kJ·mol^{-1}).
  - Coverage effects are visible:
    - For 3×3 unit cell C3-top structure becomes more stabilised than for 2×2 unit cell.
    - C1-cis structure exists only for 2×2 unit cell, and C3-hollow only for 3×3 unit cell.

UNIVERSITAT ROVIRA I VIRGILI
ORGANIC MOLECULES ON METAL SURFACES: FORECASTING STRUCTURES AND SPECTRA
Benjamí Martorell Masip
ISBN:978-84-691-9747-9 /DL: T-1259-2008

    - ∗ All VC structures are more stable on 3×3 than on 2×2 unit cell.
  - For $4\times\sqrt{3}$ unit cell only C3-hollow minimum has been computed (-29.1 kJ·mol^{-1}).
  - ZPE correction has been evaluated, defavouring in all cases the adsorption of VC.
  - In C1-trans structure C1−C2 distance (1.45 Å) is larger than C2−C3 (1.36 Å). In C3-top and C3-hollow C1−C2 distance (1.41 and 1.40 Å) is shorter than C2−C3 (1.44 and 1.45 Å).
  - H1 is more activated for C1-trans and C1-cis structures than in the other structures.

- VC has been studied adsorbed on Pt(111) and Pd(111) using two different unit cells: 2×2 and 3×3.
  - Six adsorption modes have been found for both unit cells: C1-trans, C3-top, and C1-bridge; with C1 placed on fcc or hcp-sites.
  - For 2×2 unit cell the most stable adsorption mode is C3-top (-163.6 (Pt) and -137.6 (Pd) kJ·mol^{-1}), the next C1-bridge (-148.0 (Pt) and -133.0 (Pd) kJ·mol^{-1}) and finally the C1-trans structure (-116.5 (Pt) and -94.5 (Pd) kJ·mol^{-1}).
  - C1-trans structure is not the most stable one like in the case of Cu.
  - For 3×3 unit cell, the relative position of VC structures is the same, being stabilised all of them ∼10 or ∼20 kJ·mol^{-1}.
  - In C1-trans structure C1−C2 (∼1.45 Å for both metals) distance is larger than C2−C3 (∼1.35 Å for both metals), like for C1-bridge. In the C3-top the relative order changes.

- VC adsorbed on Rh(111) has been studied on two different unit cells: 2×2 and 3×3.
  - Three adsorption modes have been found for both unit cells: C1-trans, C3-top and C1-bridge.
  - For 2×2 unit cell, the C3-top structure is the most stable one (-182.3 kJ·mol^{-1}), C1-bridge is less stable (-173.1 kJ·mol^{-1}), and C1-trans is the least one (-128.9 kJ·mol^{-1}).
  - For 3×3 unit cell the relative order is the same.:

UNIVERSITAT ROVIRA I VIRGILI
ORGANIC MOLECULES ON METAL SURFACES: FORECASTING STRUCTURES AND SPECTRA
Benjamí Martorell Masip
ISBN:978-84-691-9747-9 /DL: T-1259-2008

    - ∗ C3-top and C1-bridge structures are ∼15 kJ·mol^{-1} more stable on this unit cell than on the 2×2 unit cell.
    - ∗ C1-trans structure is ∼10 kJ·mol^{-1} less stable on this unit cell than on the 2×2 unit cell.
  - For C1-trans structure on 2×2 unit cell the C1−H distance is relatively large (1.17 Å for fcc-site and 1.21 Å for hcp-site), due to the agostic interaction of H1 with surface.
  - C−C distances are similar to the ones found for Pt and Pd.

- The vibrational frequencies calculation and simulation of RAIR spectra of each structure and the finding of the fingerprints for them:
  - For Cu(111):
    - ∗ C1-trans structure has a very intense band at ∼1400 cm^{-1}, two weak bands at ∼1530 and ∼1280 cm^{-1} and a medium band at ∼530 cm^{-1}.
    - ∗ Adsorbed Pr presents a intense band at the C−H region (∼2950 cm^{-1}), a medium band at ∼1350 cm^{-1}, and three weak bands at ∼500 , ∼900 and ∼1000 cm^{-1}.
    - ∗ C1-cis structure presents two medium features at ∼3050 and ∼850 cm^{-1}. Some other weak bands exist.
    - ∗ C3-top and C3-hollow structures present a medium band at ∼730 cm^{-1}, and other weak peaks, which do not allow to differentiate among them.
  - For Pt and Pd surface:
    - ∗ C1-trans structure presents a very intense band at ∼1400 cm^{-1}, and medium peaks at ∼1100 and ∼600 cm^{-1}. For Pt also medium features exist at ∼1550 and ∼950 cm^{-1}.
    - ∗ For Pt, Pr presents medium bands at ∼1000, ∼1100 and ∼1350 cm^{-1} and also weak bands exist at ∼900 and ∼1400 cm^{-1}.
    - ∗ For Pd, Pr presents medium bands at ∼950 and ∼1050 cm^{-1}. Weak features appear at ∼550, ∼1400 (wide), ∼2950 and ∼3050 cm^{-1}.
    - ∗ For Pt, C3-top structures presents four weak bands at ∼775, ∼850, ∼1125 and ∼3000 cm^{-1}.

UNIVERSITAT ROVIRA I VIRGILI
ORGANIC MOLECULES ON METAL SURFACES: FORECASTING STRUCTURES AND SPECTRA
Benjamí Martorell Masip
ISBN:978-84-691-9747-9 /DL: T-1259-2008

  - ∗ For Pd, six weak bands appear at ∼640, ∼700, ∼790, ∼930, ∼1125 and ∼3000 cm^{-1}.
  - ∗ For Pt, one weak feature exists at ∼875 cm^{-1} for C1-bridge structure.
  - ∗ For Pd, three weak bands exist at ∼850, ∼1100 and ∼3000 cm^{-1}.
- For Rh(111):
  - ∗ C1-trans structure for 3×3 unit cell presents a very intense peak at ∼1400 cm^{-1} and a medium band at ∼1275 cm^{-1}.
  - ∗ C1-trans structure for 2×2 unit cell presents a very low C1−H stretching frequency: ∼2200 and ∼1900 cm^{-1} for C1 placed on fcc and hcp-site. This C−H bond is highly activated.
  - ∗ For C3-top structures, five weak bands exist at ∼700, ∼800, ∼925, ∼1125, and ∼2800 cm^{-1}.
  - ∗ For C1-bridge structures, two weak features appear at ∼850 and ∼3000 cm^{-1}.

- Some important differences in VC adsorption between different metals have been found and commented during this chapter that could give a light in the different reactivity of propyne catalysed on these metal surfaces.

UNIVERSITAT ROVIRA I VIRGILI
ORGANIC MOLECULES ON METAL SURFACES: FORECASTING STRUCTURES AND SPECTRA
Benjamí Martorell Masip
ISBN:978-84-691-9747-9 /DL: T-1259-2008

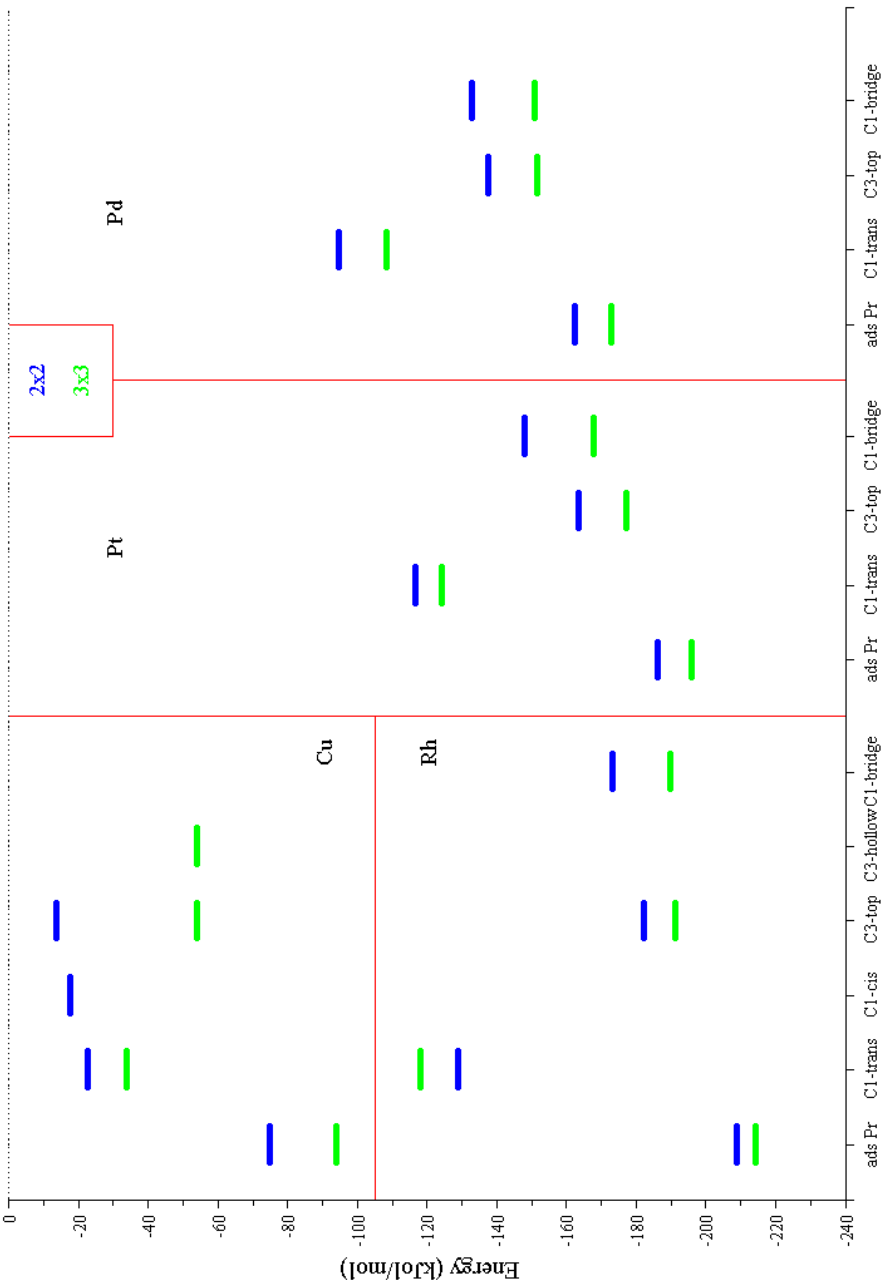

Figure 4.26: Scheme of all VC structures for Cu, Pt, Pd, and Rh (111) surface on 2×2 and 3×3 unit cell.

UNIVERSITAT ROVIRA I VIRGILI
ORGANIC MOLECULES ON METAL SURFACES: FORECASTING STRUCTURES AND SPECTRA
Benjamí Martorell Masip
ISBN:978-84-691-9747-9 /DL: T-1259-2008

Chapter 5

From adsorbed $CHCCH_3$ to $CHCHCH_2$.

kinetic aspects.

In chapter 4 it was studied and explained the interaction between VC and the (111) surface of several metals in order to explain the different behaviour in the reactivity of propyne on those metals. This chapter wants to analyse and explain the kinetic aspects of the isomerisation reaction from Pr to VC and the interconversion of VC adsorption modes.

In the case of the interconversion among VC adsorption modes, the study was only carried on Cu(111) surface. This makes us able to bind all adsorption modes and to explain how the interconversion among them is carried out.

The case of the isomerisation from Pr to VC is a critical point of the reaction, because this step involves the migration of one hydrogen atom, so all carbon atoms will own at least one hydrogen atom, like benzene molecule. The direct transposition of one hydrogen atom from the methylenic group of Pr to the central carbon of VC has been studied on all (111) surfaces (Cu, Pt, Pd, and Rh). This reaction involves the break and simultaneous formation of C−H bonds. Besides, another possible path has been studied in the case of Cu. This is the lost of one hydrogen of the Pr's methylenic group, yielding C_3H_3 plus one H atom coadsorbed on the surface. Finally, the central carbon atom of this specie becomes hydrogenated via the reaction with an hydrogen atom adsorbed on the surface. This step involves the breaking of the new H−M bond, and the

UNIVERSITAT ROVIRA I VIRGILI
ORGANIC MOLECULES ON METAL SURFACES: FORECASTING STRUCTURES AND SPECTRA
Benjamí Martorell Masip
ISBN:978-84-691-9747-9 /DL: T-1259-2008

formation of C−H bond.

So the objectives of this chapter are:

- *To study the interconversion of the different VC adsorption modes on Cu(111) using the transition state theory (TST) [147].*
- *To study the direct transposition of one hydrogen atom from Pr's methylenic group to VC's central carbon atom on the (111) surface of Cu, Pt, Pd, and Rh.*
- *To establish the adsorption modes of C_3H_3 and H atom and their E_{ads} on Cu(111).*
- *To evaluate the coadsorption energy of C_3H_3 and H atom on the several existing possibilities on Cu(111).*
- *To simulate RAIR spectra of isolated C_3H_3 and coadsorbed C_3H_3 + H on Cu(111).*
- *To create reaction profiles to understand how isomerisation is carried out.*

UNIVERSITAT ROVIRA I VIRGILI
ORGANIC MOLECULES ON METAL SURFACES: FORECASTING STRUCTURES AND SPECTRA
Benjamí Martorell Masip
ISBN:978-84-691-9747-9 /DL: T-1259-2008

Table 5.1: ZPE corrected energies for VC structures. C1 is placed on fcc-site. All values are in kJ·mol^{-1}

	Cu 2×2	Cu 3×3	Pt 3×3	Pd 3×3	Rh 3×3
ads Pr	-74.7	-93.9	-195.9	-173.0	-214.4
C1-trans	-22.8	-33.7	-124.1	-108.4	-118.1
C1-cis	-17.7	/	/	/	/
C3-top	-13.5	-54.1	-177.2	-151.5	-191.3
C3-hollow	/	-54.0	/	/	/
C1-bridge	/	/	-167.9	-150.8	-189.6

5.1 Direct isomerisation: H travels from C3 to C2.

The global aim of our group project is to explain the different reactivity of Pr molecule on the (111) surface of different metals: Cu, Pt, Pd, and Rh. The first step of this project was the study of the Pr molecule adsorption. The second one has been the study of the adsorption of the proposed intermediate for this reaction. Now it is time to find out how Pr isomerisates to VC on the metal surface.

In the frame of transition state theory (TST), we desired to find the saddle point that connects the most stable adsorbed Pr structure (only one structure exists for Cu, Pt, and Pd, and two structures exist for Rh) with the most stable adsorbed VC structure, which in most cases is C3-top structure (only for Cu(111) on a 3×3 unit cell it is isoenergetic with C3-hollow structure). This VC structure [90] is the one believed to dimerise yielding benzene, which is the final, desired product.

In order to find the TS that connects Pr and VC, a nudged elastic band (NEB) algorithm was used. In this method, an appropriate number of structures, whose geometry is between adsorbed Pr and VC are generated. The energy of these structures is evaluated, relaxing the atoms of these structures to find the highest energetic image in the reaction pathway. This method is only effective if the connecting TS of these two minima exists, otherwise alternative algorithms must be used.

5.1.1 Reaction profiles.

Unfortunately, the NEB method was not capable of finding the direct isomerisation TS from adsorbed Pr to VC C3-top structure. This forced us to use

UNIVERSITAT ROVIRA I VIRGILI
ORGANIC MOLECULES ON METAL SURFACES: FORECASTING STRUCTURES AND SPECTRA
Benjamí Martorell Masip
ISBN:978-84-691-9747-9 /DL: T-1259-2008

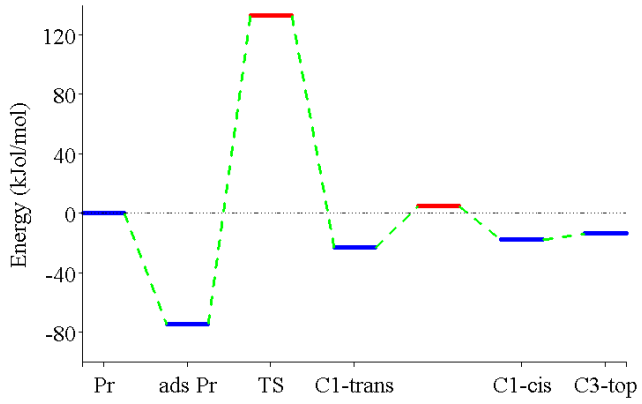

(a) 2x2 unit cell.

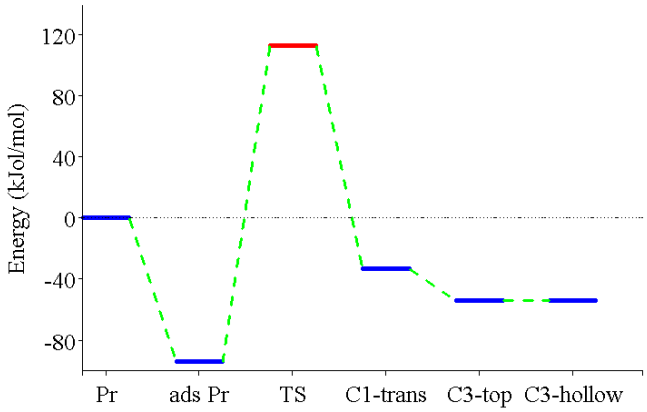

(b) 3x3 unit cell.

Figure 5.1: Reaction profiles for Cu. In blue the minima, in red the transition states and in green the checked reaction pathways.

another algorithm: DIMER method. This method is more "flexible" than NEB, because it is not necessary the two used minima to be connected by a TS, it can search another TS that connects other two minima.

$$Pr_{(ads)} \leftrightarrows [TS]^{\neq} \leftrightarrows VC_{(ads)}^{C1-trans} \tag{5.1}$$

One TS that connects adsorbed Pr and VC was found for all metal surfaces. The VC adsorption mode is not the previously supposed one, but it is the C1-trans structure for all unit cells and for all metals. We can observe this process

UNIVERSITAT ROVIRA I VIRGILI
ORGANIC MOLECULES ON METAL SURFACES: FORECASTING STRUCTURES AND SPECTRA
Benjamí Martorell Masip
ISBN:978-84-691-9747-9 /DL: T-1259-2008

in reaction 5.1. In order to ensure this TS connects Pr and VC C1-trans, we have added positively and negatively the imaginary VNM at the TS equilibrium geometry and those structures have been relaxed. This addition and relaxation brought us to adsorbed Pr and adsorbed VC C1-trans structure.

In figure 5.1 are presented the reaction profiles with ZPE correction for Cu(111) using a 2×2 and a 3×3 unit cell. In figure 5.2 we show the corresponding profiles for Pt, Pd, and Rh on a 3×3 unit cell. In blue are presented the minima (reactants, products and intermediates), in red are presented the transition states, in green the checked pathways and in grey are shown the not checked ones, i.e., where TSs are not determined. For Cu, it can be observed the high energetic barrier that represents the isomerisation TS, indicating that it is easier the desorption of Pr than the isomerisation to VC C1-trans.

In order to obtain benzene, it is necessary C3-top or C3-hollow structures to be present on the surface, as commented before, so C1-trans structure must convert into the other adsorption modes. As can be observed in figure 5.1, C1-trans structure is the most stable VC adsorption mode for 2×2 unit cell, and the less one for 3×3 unit cell. In the case of 2×2 unit cell (where coverage is high and repulsions are important), for the interconversion from C1-cis to C3-top structures no TS has been found (whose energy difference is only ∼5 $kJ{\cdot}mol^{-1}$, so the activation energy corresponds to the thermodynamic energetic difference), but from C1-trans to C1-cis structure one TS exists. Moreover, C1-cis structure was found in the search of the TS that connected C1-trans structure and C3-top. This TS was not found, but it was found C1-cis structure. After finding this minimum, the TS from C1-trans to C1-cis structures was searched and found. This TS is much lower in energy than the one of the isomerisation process, so if the isomerisation can take place, the interconversion among different adsorption modes is highly probable. For the 3×3 unit cell (where coverage is low and no interaction exists between adjacent VC structures, becoming the flat structures stabilised) no TSs have been found in the interconversion among three VC species.

For Pt, Pd and Rh, only the profiles on the 3×3 unit cell are presented, because profiles for 2×2 unit cells are very similar to those ones, but energies are a displaced to higher values, as has been commented in chapter 4. In the case of these metals, due to the large lattice parameters, no important repulsion existed and the coverage effect was not important (except for C1-trans structure for Rh(111)). On these metals, it is supposed that no TS is found among the different VC structures, because as in the case of Cu, when no repulsion existed

UNIVERSITAT ROVIRA I VIRGILI
ORGANIC MOLECULES ON METAL SURFACES: FORECASTING STRUCTURES AND SPECTRA
Benjamí Martorell Masip
ISBN:978-84-691-9747-9 /DL: T-1259-2008

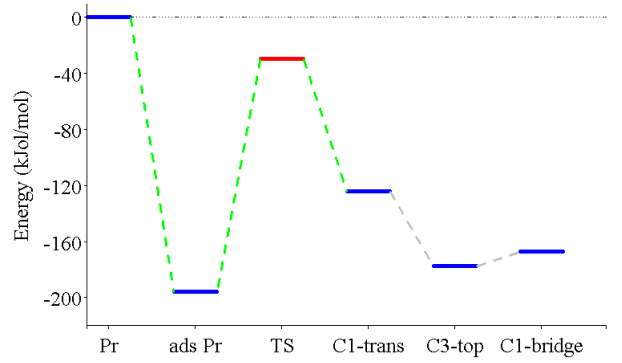

(a) Pt 3x3

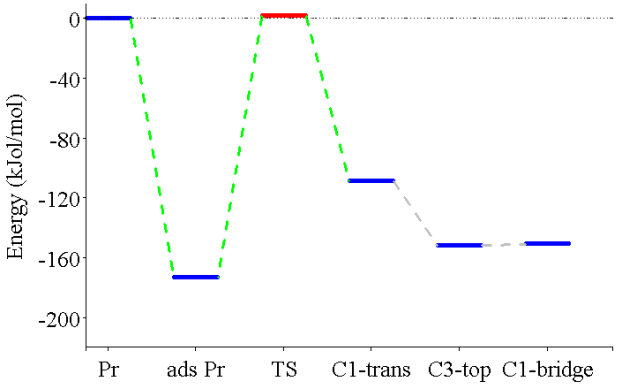

(b) Pd 3x3

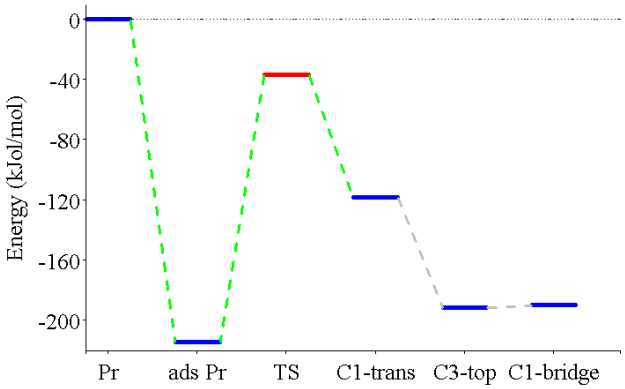

(c) Rh 3x3

Figure 5.2: Reaction profiles for a) Pt, b) Pd, and c) Rh on a 3×3 unit cell. In blue the minima, in red the transition states, in green the checked reaction pathways and in grey the non-checked ones.

UNIVERSITAT ROVIRA I VIRGILI
ORGANIC MOLECULES ON METAL SURFACES: FORECASTING STRUCTURES AND SPECTRA
Benjamí Martorell Masip
ISBN:978-84-691-9747-9 /DL: T-1259-2008

for adjacent molecules, no TS existed (another very important reason why these have not been checked is the high computational cost of the TS search, and in this case we could avoid this effort). In the reaction profile for these structures (figure 5.2), in grey appear the non-checked reaction paths. In the case of Pd, the isomerisation TS is isoenergetic to Pr in gas phase, and the most stable VC structures are the isoenergetic C3-top and C1-bridge ones. In the case of Pt and Rh, the isomerisation TS energy is under the gas phase Pr, indicating that is faster to isomerisate this molecule than to become desorbed, and the most stable VC structure is the C3-top one.

Finally, on Cu one could imagine what would happen if the reaction started from adsorbed VC and not from Pr. This could be done using a VC-dihallide ($XHC{-}CH{-}CH_2X$), because C−X bond is very labile on the surface, and X_2 molecule desorbs easily when temperature raises. With this strategy, the efficiency in the formation of benzene could be higher, because the isomerisation to Pr is a high barrier process. For other metals this strategy would not be so effective because the isomerisation barrier from VC to Pr is not so high. For Pd the isomerisation process from VC to Pr could be competitive to the Pr desorption, because barriers are similar. For Pt and Rh, the desorption of Pr is higher in energy than the isomerisation process.

5.1.2 Adsorption mode of isomerisation TS.

In figure 5.3 are presented the transition states structures in the direct isomerisation process from Pr to VC. All TS structures have been checked with a frequency calculation, and in all cases appeared one imaginary frequency around 1000i cm^{-1}, which is the typical value for the transposition of one H atom in a hydrocarbon molecule [95].

In figure 5.3(a) the TS structure for Cu is presented and in 5.3(b) is for Pt, which is the same as for Pd and Rh (not presented for this reason). For all metals this structure is very similar to the one that adopts Pr molecule adsorbed on the respective metal, with the migrating H atom in the middle from C3 and C2 (closer to this last atom, as can be observed in table 5.4), and the other H atoms place in the molecular plane. In the case of Cu, the carbonated chain adsorbs via a di-σ/di-π structure, like in the case of Pr [96, 106, 108], being placed the C1 on a hollow-site. Otherwise, for Pt, Pd, and Rh, the adsorption mode is di-σ/π [60, 97, 104, 105], and C1−C2 bond is placed on a hollow-site (C1 is placed on a bridge-site). No differences between 2×2 and 3×3 unit cells

UNIVERSITAT ROVIRA I VIRGILI
ORGANIC MOLECULES ON METAL SURFACES: FORECASTING STRUCTURES AND SPECTRA
Benjamí Martorell Masip
ISBN:978-84-691-9747-9 /DL: T-1259-2008

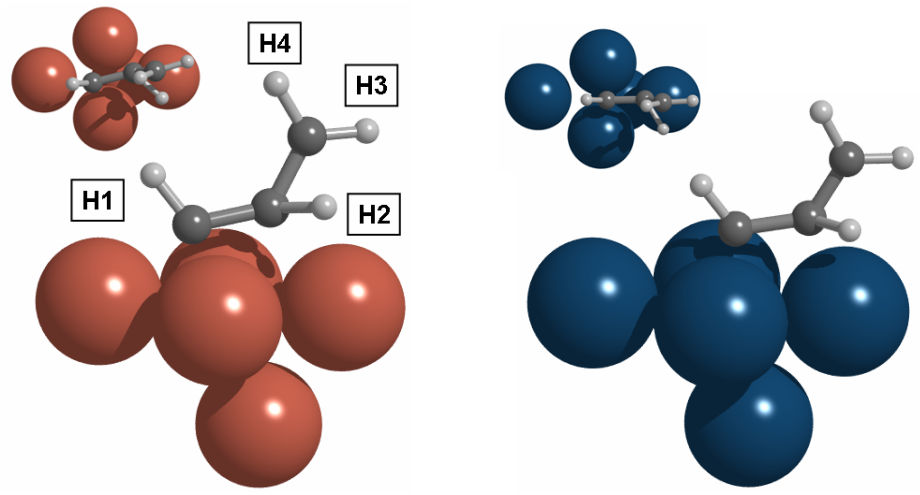

(a) TS on Cu(111) (b) TS on Pt(111), Pd(111) and Rh(111)

Figure 5.3: Transition states from Pr to VC on a) Cu and b) on the other metals.

for each metal exist in the adsorption modes.

5.1.2.1 2×2 unit cells.

In table 5.2 the TS structures energies respect to Pr in gas phase for all metals on the 2×2 unit cell are presented with and without ZPE correction. Besides, for sakes of comparison, it is presented in brackets the energetic barrier of the TS respect to the adsorbed propyne molecule.

The effect of ZPE correction is always favouring the isomerisation reaction, because TS loses one ν C−H vibrational frequency, which is one of the most energetic vibrations, so the transition state always decrease its energy from 7 to 16 kJ·mol^{-1} respect to the non-corrected values. In the case of TS-d3 and TS-d4 this decrease is smaller, because ν C−D vibrational frequency is less energetic than the ν C−H one. This effect is relatively important on Pd, because the TS energy is above the Pr in gas phase, and when ZPE is included this energy shifts down from 30 to only 15 kJ·mol^{-1} for the triple bond placed on a fcc-site.

In the case of Pt and Rh, the energy of the TS is below the energy necessary to desorbe the adsorbed Pr, showing a new difference in reactivity respect to the one observed for Pd, and indicating these two metals can behave similarly. ZPE correction only increases this affinity to isomerisate to VC, disfavouring

UNIVERSITAT ROVIRA I VIRGILI
ORGANIC MOLECULES ON METAL SURFACES: FORECASTING STRUCTURES AND SPECTRA
Benjamí Martorell Masip
ISBN:978-84-691-9747-9 /DL: T-1259-2008

Table 5.2: Relative TS adsorption energies for the direct isomerisation respect to gas phase propyne on the 2×2 unit cell. In brackets respect to adsorbed Pr molecule. All values are given in kJ·mol^{-1}.

	No ZPE	ZPE	ZPE-d1	ZPE-d3	ZPE-d4
Cu C1-fcc	143.3 (222.4)	132.7	132.4	135.9	135.6
Cu C1-hcp	143.9 (223.4)	133.1	132.7	136.3	136.0
Pt tr-fcc	-11.4 (189.5)	-18.7	-19.3	-15.1	-15.7
Pt tr-hcp	-6.3 (187.1)	-13.8	-14.5	-10.2	-10.9
Pd tr-fcc	30.0 (193.5)	14.6	14.3	18.8	18.5
Pd tr-hcp	25.8 (193.4)	13.6	13.3	17.7	17.4
Rh tr-fcc	-15.6 (189.2)	-26.1	-26.5	-22.3	-22.7
Rh tr-hcp	-24.7 (189.8)	-35.2	-35.6	-31.4	-31.8

the desorption of Pr, which remains competitive.

Cu behaves quite different from other metals, and TS energy is higher than Pr in gas phase, so it makes really difficult to overpass this barrier and to get the isomerisation from Pr via a direct transposition of one H atom from C3 to C2. The addition of ZPE correction only reduces ∼10 kJ·mol^{-1} the TS energy, from 143 to 133 kJ·mol^{-1}, but it does not have any relevance in this case.

Another important feature of these transitions states are the energetic barriers from the adsorbed Pr (in brackets in table 5.2). If we compare the values for Pt, Pd, and Rh (∼190 kJ·mol^{-1}), we realise that their values are in a range of ∼5 kJ·mol^{-1}, indicating that not only their structure but also their barrier from adsorbed Pr is almost the same, so the differences that raise in the energy values in TS is due to the differences already present for adsorbed Pr. In the case of Cu, this barrier is 40 kJ·mol^{-1} larger (∼220 kJ·mol^{-1}), due to the different TS adsorption mode. All these barrier values are lower than those found for the H-transposition in gas phase by *Honjou et al.* (334.0 kJ·mol^{-1}) [81] and *Kakkar et al.* (331.5 kJ·mol^{-1}) [82], indicating in some extent the role of the metal as a catalyst.

Finally, for Cu no differences exist between C1-fcc and C1-hcp sites, but for the other metals do. For Pt tr-fcc site is ∼5 kJ·mol^{-1} more stable than tr-hcp, but for Pd and Rh tr-hcp are between ∼5 and ∼10 kJ·mol^{-1} more stable than tr-fcc sites.

UNIVERSITAT ROVIRA I VIRGILI
ORGANIC MOLECULES ON METAL SURFACES: FORECASTING STRUCTURES AND SPECTRA
Benjamí Martorell Masip
ISBN:978-84-691-9747-9 /DL: T-1259-2008

Table 5.3: Relative TS adsorption energies for the direct isomerisation respect to gas phase propyne on the 3×3 unit cell. In brackets respect to adsorbed Pr molecule. All values are given in kJ·mol^{-1}.

	No ZPE	ZPE	ZPE-d1	ZPE-d3	ZPE-d4
Cu C1-fcc	124.2 (221.8)	112.6	112.3	116.0	115.8
Cu C1-hcp	124.8 (223.0)	112.9	112.7	116.4	116.1
Pt tr-fcc	-24.1 (181.4)	-31.9	-32.6	-28.2	28.8
Pt tr-hcp	-21.5 (181.7)	-29.3	-30.0	-25.6	-26.3
Pd tr-fcc	14.0 (190.2)	0.1	-0.2	4.7	4.4
Pd tr-hcp	14.8 (192.4)	2.2	1.8	6.5	6.1
Rh tr-fcc	-26.1 (190.9)	-36.4	-36.7	-32.5	-32.9
Rh tr-hcp	-26.7 (192.7)	-37.2	-37.6	-33.3	-33.7

5.1.2.2 3×3 unit cells.

In table 5.3 the TS structures energy respect to Pr in gas phase for all metals on the 3×3 unit cell are presented with and without ZPE correction. Besides, for sakes of comparison, it is presented in brackets the energetic barrier of the TS from the adsorbed propyne molecule.

When ZPE is taken into account, the isomerisation reaction is favoured, like in the case of 2×2 unit cell, in a range from ∼10 to ∼15 kJ·mol^{-1}, depending on each particular case. Like on the 2×2 unit cell, the most significant effect is on Pd, because the addition of ZPE correction makes isoenergetic the isomerisation TS and the gas phase Pr, indicating that the isomerisation is as easy as the desorption of Pr. This is an important difference respect to 2×2 unit cell, because when coverage decreases, the TS energies are stabilised ∼15 kJ·mol^{-1} for Pd, Cu, and Pt respect to the high coverage regime. For Rh only tr-fcc site stabilises ∼10 kJ·mol^{-1}, tr-hcp site remains as in the case of 2×2 unit cell.

TS adsorbed on Pt and Rh is below the desorption energy of Pr, indicating isomerisation is a more favoured reaction than desorption, once propyne is adsorbed. This is the opposite case to Cu. Despite being stabilised respect to 2×2 unit cell, TS is placed 110 kJ·mol^{-1} above propyne in gas phase, which is a high barrier. So, we can divide our metals in three groups respect to the TS energy, which corresponds to the different reactivity that Pr exhibits when is adsorbed on them:

- Metal with a high H-transposition barrier respect to Pr in gas phase: Cu.
- Metal with an isomerisation barrier similar to the desorption: Pd.

UNIVERSITAT ROVIRA I VIRGILI
ORGANIC MOLECULES ON METAL SURFACES: FORECASTING STRUCTURES AND SPECTRA
Benjamí Martorell Masip
ISBN:978-84-691-9747-9 /DL: T-1259-2008

Table 5.4: Geometrical parameters of TS on the 3×3 unit cell. For Cu C1-fcc values; Pt, Pd, and Rh tr-hcp values. In brackets 2×2 unit cell values.

	Cu	Pt	Pd	Rh
[(a)]d(C1-C2)	1.43	1.46	1.42	1.43
d(C2-C3)	1.41	1.39	1.39	1.40
d(C2-H2)	1.29	1.30	1.36	1.33
d(C3-H2)	1.50	1.57 (1.54)	1.52	1.50
[(b)]α(C1-C2-C3)	127.4	128.0	130.9 (129.1)	130.2
α(H1-C1-C2)	116.4	120.3	121.4	121.2
α(H2-C2-C1)	124.8	118.3 (120.5)	123.0	124.0
α(H2-C2-C3)	67.4	71.6 (69.6)	67.1	66.5
[(c)]θ(H1-C1-C2-H2)	98.0	94.5	103.9	101.1
θ(H2-C2-C3-H3)	66.0	68.1	69.9	68.6
θ(H2-C2-C3-H4)	-117.4	-112.1 (-114.1)	114.8 (-116.1)	-115.9 (-117.0)
[(d)]d(C1-M)	2.01	2.03 (2.06)	2.02	2.06
d(C2-M)	2.15	2.06 (2.03)	2.04	2.03
d(H1-M)	2.42 (2.45)	2.74 (2.77)	2.70 (2.74)	2.77
d(H2-M)	1.97 (2.01)	2.27 (2.20)	2.09 (2.06)	2.10

[(a)]d: distances (Å); [(b)]α: angles (degrees);[(c)]θ: dihedral angles (degrees); [(d)] d: distances to nearest surface atom.

- Metals whose TS is placed below the energy of the Pr desorption: Pt and Rh.

If we compare the values of the barriers respect to adsorbed Pr on the 2×2 and 3×3 unit cells (tables 5.2 and 5.3), we observe that the barrier for Cu is always ∼220 kJ·mol^{-1}, and for Pd, Rh, and Pt it is always ∼190 kJ·mol^{-1} (only for Pt on a 3×3 unit cell this value decreases to ∼180 kJ·mol^{-1}). This fact indicates that the same lateral interactions that existed for Pr, also exist for TS because when the unit cell is increased, the energy difference between both species remains constant.

Finally, for this unit cell it does not exist any difference between both possible adsorption sites for each TS.

5.1.3 Adsorption geometries.

In table 5.4 are presented the geometric parameters of the transition states isomerisation. The first important feature is that the C1−C2 distance is a bit larger than the C2−C3 one. This TS connects adsorbed Pr and VC in C1-trans structure (as was commented in section 5.1.1). In adsorbed Pr, the C1−C2

UNIVERSITAT ROVIRA I VIRGILI
ORGANIC MOLECULES ON METAL SURFACES: FORECASTING STRUCTURES AND SPECTRA
Benjamí Martorell Masip
ISBN:978-84-691-9747-9 /DL: T-1259-2008

distance is shorter (1.37 Å for Cu and Pd, 1.39 Å for Rh, and 1.40 Å for Pt) than the C2−C3 one (1.50 Å for Pt, Pd and Rh, and 1.51 Å for Cu), so the first one can be assigned to a double bond and the second one to a single bond. Otherwise, for VC in a C1-trans structure, the C1−C2 distance is larger than the C2−C3 one (see tables 4.5, 4.14, 4.15, and 4.23), because the position of single and double bonds are commuted respect to Pr. So it is logic to think that in the TS those two C−C distances were similar for Cu, Pd, and Rh (differences $<$0.03 Å), but in the case of Pt this difference is larger, and the C1−C2 distance is 1.46 Å and the C2−C3 one is 1.39 Å.

H atoms not involved in the reaction path (i.e., H1, H3, and H4, see figure 5.3) present C−H distances in the range from 1.09 to 1.12 Å. For the migrating H atom (H2), C2−H distance is ∼1.30 Å (1.36 Å for Pd) and C3−H is ∼1.50 Å (1.57 for Pt). This indicates that H2 is closer to the final VC structure than to the Pr structure. All atoms except the migrating H are almost in the same molecular plane, and C3 presents a typical sp^2-like structure, because all its bond angles are near 120°.

Another important feature of these TS structures is the short H2−M distance, indicating that these TS structures are stabilised by the effect of the surface, because the agostic interaction of H2 with surface allows to break and to create new C−H easier than in the gas phase because of this interaction. The H2−M distance is shorter for all metals than H1−M distance in the TS structures: ∼0.45 Å for Cu and Pt, ∼0.60 Å for Pd, and ∼0.65 Å for Rh.

If we compare H2−M distance with the values obtained for VC, we observe that for Cu this distance is as large as the H1−M one in the C1-trans structure (1.97 Å) and only a bit larger than the same one for C1-cis structure (1.92 Å). For Pt, Pd, and Rh, the H2−M distance (2.27, 2.09, and 2.10 Å, respectively) is shorter than all other H−M distances observed in VC, being the shorter one the H1−M distance in C3-top structure (2.51, 2.26, and 2.23 Å, for Pt, Pd, and Rh, respectively). Only for C1-trans structure on the 2×2 unit cell on Rh, H1−M distance is shorter (1.79 Å) than this distance in TS.

Finally, the relative position of C atoms in the TS structure is very similar to the one that presents adsorbed Pr on the respective metal, as commented in section 5.1.2.

UNIVERSITAT ROVIRA I VIRGILI
ORGANIC MOLECULES ON METAL SURFACES: FORECASTING STRUCTURES AND SPECTRA
Benjamí Martorell Masip
ISBN:978-84-691-9747-9 /DL: T-1259-2008

Table 5.5: Parameters for the adsorption of H atoms on Cu(111). E_{ads} is calculated respect $\frac{1}{2}H_2$ molecule in gas phase, in brackets values respect to H atom in gas phase. For frequencies, in brackets the intensity in km·mol^{-1}.

	d H−Cu	E_{ads}			ν H−surf (z)		ν H−surf (x,y)	
		No ZPE	ZPE	ZPE-d	H (I)	D (I)	H	D
2×2	1.73	-26.4 (-245.9)	-22.5	-23.6	1050 (1.3)	746 (0.6)	875	621
3×3	1.74	-48.0 (-267.5)	-44.1	-45.3	1043 (1.1)	740 (0.5)	868	616

5.2 Isomerisation through the surface on Cu(111): Dehydrogenation and hydrogenation processes.

As commented in section 5.1.1, the barrier that exists in the direct isomerisation process from Pr to VC is really high for Cu(111), being more favoured the desorption of Pr molecule. Although in the reactivity of Pr on Cu(111) it is found a big amount of Pr that desorbs (∼75%), the barrier found in our calculations is too high to explain well the yield of ∼10% of benzene [101]. That is the reason why we tried to find out an alternative reaction pathway via the surface, using a Horiuti-Polanyi mechanism [89], i.e., the steps involved would be:

- Dehydrogenation of one Pr's methylenic H atom.
- Coadsorption of this H atom with C_3H_3 specie on the surface (H2 and H^*, if it is bonded to the carbonated skeleton or if it is adsorbed, respectively).
- Diffusion of this H atom (or another H atom adsorbed on surface) to the correct reaction site (if necessary).
- Hydrogenation of the middle C atom (C2) of C_3H_3 specie, forming the VC specie.

In the next subsections will be studied the adsorption of H atom and C_3H_3 specie, for isolated and coadsorbed specie, and the RAIR spectra will be simulated to find out fingerprints that can help us to identify these species on the surface.

5.2.1 H adsorbed on Cu(111).

The adsorption of molecular and atomic hydrogen on metal surfaces has been largely studied. In particular the adsorption of these species on Cu was studied

UNIVERSITAT ROVIRA I VIRGILI
ORGANIC MOLECULES ON METAL SURFACES: FORECASTING STRUCTURES AND SPECTRA
Benjamí Martorell Masip
ISBN:978-84-691-9747-9 /DL: T-1259-2008

in the last decade [109, 145], because hydrogen molecule (or atom) is the easiest molecule to be calculated, and it served as a starting point for larger and more complicated systems. Not only on Cu was focused this research, but also on other metal surfaces, for example on Ni(111) [114] and on Pd(111) [113]. On both metals, H is adsorbed on a hollow-site, indicating this is the prefered adsorption mode on this metals surface.

In the case of Cu(111) we found fcc hollow-site to be the most stable adsorption site for both 2×2 and 3×3 unit cells. We obtain a H−Cu distance of 1.7 Å (for all Cu atoms directly bonded to H atom) and an adsorption energy of ∼-250 kJ·mol^{-1} respect to H atom in the gas phase and values of -26 and -48 kJ·mol^{-1} respect to $\frac{1}{2}H_2$ molecule in gas phase for 2×2 and 3×3 unit cells (see table 5.5). When the D adsorption is considered, the adsorption energy decreases as expected. Using DFT (VWN exchange-correlation functional) methodology on periodic systems, with a two-layers slab and a coverage of 0.25, *Forni et al.* [111] have evaluated a E_{ads} of -313 kJ·mol^{-1} (the difference of energy respect to our values is due to the use of LDA functional, because they made some tests with GGA and their E_{ads} was reduced a 20%), being the H−Cu distance of 1.70 Å. Using plane-waves method, the exchange-correlation potential of Ceperly-Alder and a 3-layers slab model with a coverage of 1 ML, *Gundersen et al.* calculated the H−Cu to be 1.69 Å on the most stable site: hollow-site [110].

For the frustrated translation of H atom against surface (ν H−surf (z)) we found a value between 1040 and 1050 cm^{-1} (depending on the unit cell and being in both cases weak bands), similar to the value obtained experimentally by *Lamont et al.* (1040 cm^{-1}, weak bands) [112], and below the value determined by *Forni et al.* (1078 cm^{-1}), according with the shorter H−Cu distance they obtained [111].

For the frequencies associated with the H movement parallel to surface (which is non-active in RAIR spectrum and no intensities have been given in table 5.5) we obtained a value of ∼870 cm^{-1}, which is very different to the one determined by *Lamont et al.* [112], 770 cm^{-1}. This difference of ∼100 cm^{-1} can be due to two factors: to the anharmonicity not taken into account in our calculation, and the difficulty of detecting this mode in the experimental spectrum. Although this, our values are more similar to the experimental ones than the values proposed by *Gundersen et al.* [110] of 990 cm^{-1}.

Finally, for both unit cells, we have found also the hcp-site to be a minimum structure (E_{ads}= -25.2 kJ·mol^{-1}, d(H−Cu)= 1.73 Å on 2×2 unit cell; E_{ads}= -48.0 kJ·mol^{-1}, d(H−Cu)= 1.74 Å on 3×3 unit cell). No more minima have been

UNIVERSITAT ROVIRA I VIRGILI
ORGANIC MOLECULES ON METAL SURFACES: FORECASTING STRUCTURES AND SPECTRA
Benjamí Martorell Masip
ISBN:978-84-691-9747-9 /DL: T-1259-2008

Table 5.6: Geometrical parameters of C_3H_3 in gas phase and binding energy of a C3−H bond respect to $\frac{1}{2}H_2$ molecule and H atom in gas phase.

	C_3H_3 gas phase
[a]d(C1-H)	1.07
d(C3-H)	1.09
d(C1-C2)	1.23
d(C2-C3)	1.36
[b]α(H-C3-H)	118.1
α(C2-C3-H)	121.0

[c]BE $C_3H_4 \rightarrow C_3H_3$	kJ·mol^{-1}
respect to H_2 gas phase	171.1
respect to H gas phase	391.0

[a]d: distances (Å); [b]α: angles (degrees); [c]BE: binding energy (kJ·mol^{-1}).

detected. In fact, bridge site has been characterised as the TS ($\bar{\nu}_e$= 451i cm^{-1}) that connects both hollow-sites. The energy difference barrier for the diffusion reaction is only of 13.8 kJ·mol^{-1}, whose small value indicates that the H diffusion is an easy process on this surface.

5.2.2 C_3H_3 adsorbed on Cu(111).

5.2.2.1 C_3H_3 in the gas phase.

The specie that is obtained in the dehydrogenation of propyne's methylenic group is $H\dot{C}$=C=CH_2. This specie is a radical that can be also observed as the product of the dehydrogenation reaction of propadiene. This radical is a very unstable specie in gas phase respect to Pr, as can be observed in the second part of table 5.6, where the energy necessary to break one of the methylenic C−H bonds is presented respect to the H_2 molecule and respect to H atom (171.1 and 391.0 kJ·mol^{-1}, respectively). This is an indicative that isomerisation from Pr to VC in gas phase via a dehydrogenation-hydrogenation pathway is not possible, because even direct isomerisation had a more stable TS structure (334.0 kJ·mol^{-1}) than the two intermediates (C_3H_3 + H) in this case.

The C_3H_3 radical is a flat structure, with a double C=C bond between C2 and C3 and a very strong double C=C bond between C1 and C2 (almost a triple bond), with one unpaired electron placed on the π molecular orbital (MO) perpendicular to the molecular plane (B_2) on C1 and C2. All this can be observed in C−C bond distances. C2−C3 distance is 1.36 Å, the typical double C=C bond distance, the same value as in ethene; C1−C2 distance is shorter, 1.23 Å, indicating that this bond is more similar to a triple bond than to a double, because the triple C≡C bond in Pr is 1.21 Å. This small distance is due

UNIVERSITAT ROVIRA I VIRGILI
ORGANIC MOLECULES ON METAL SURFACES: FORECASTING STRUCTURES AND SPECTRA
Benjamí Martorell Masip
ISBN:978-84-691-9747-9 /DL: T-1259-2008

Table 5.7: Vibrational frequencies for C_3H_3 in gas phase. All frequencies are given in cm^{-1}.

Vibrational mode	$\bar{\nu}_e$	I (km/mol)
ν C1−H	3394	51.6
asym. ν $C3H_2$	3161	4.8
sym. ν $C3H_2$	3075	1.7
ν C1=C2 - ν C2=C3 (m)	1979	0.6
δ $C3H_2$	1404	9.9
ν C2=C3 + ν C1=C2 (m)	1082	3.0
ρ $C3H_2$	991	3.0
ω $C3H_2$	672	49.3
γ C1−H	598	44.9
δ C1−H	430	31.2
γ C1−C2−C3	396	12.3
δ C1−C2−C3	339	6.1

to the presence of the unpaired electron. This effect is also visible in the C1−H distance (1.07 Å), which is the shortest C−H distance found until now. Finally, C3 atom owns a sp^2-like hybridisation because their bond angles are near 120° and it is a flat structure.

The calculation of vibrational frequencies has been carried out to ensure the structure obtained is a minimum. Vibrational frequencies and their assignations are presented in table 5.7. Also the IR spectrum has been simulated for C_3H_3 and the deuterated species, DC=C=CH_2 (C_3H_3-d1), HC=C=CD_2 (C_3H_3-d2) and DC=C=CD_2 (C_3H_3-d3) and they can be observed in figure 5.4. In the C−H stretching region a very intense band appears at 3394 cm^{-1}, followed by two very weak features at 3161 and 3065 cm^{-1}. These values indicate that C−H bonds are very strong. The strongest band corresponds to ν C1−H and the weak bands to asymmetric and symmetric coupling of ν $C3H_2$. In the case of C_3H_3-d1, the most intense peak shifts down to 2598 cm^{-1}, remaining the other two small peaks at the same frequency as for C_3H_3. For C_3H_3-d2, the most intense peak remains at 3394 cm^{-1}, but the two small peaks go down to 2361 and 2239 cm^{-1}. Finally, C_3H_3-d3 behaves as the addition of the deuterated modes in C_3H_3-d1 and C_3H_3-d2.

In the region from 800 to 2000 cm^{-1}, only a band at 1404 cm^{-1} is outstanding, which corresponds to the $C3H_2$ scissoring. In this zone appear all C=C stretching and C−H bending in-plane modes (as a reference, for δ and γ modes for C1−H have been defined respect to the plane perpendicular to the molecular

UNIVERSITAT ROVIRA I VIRGILI
ORGANIC MOLECULES ON METAL SURFACES: FORECASTING STRUCTURES AND SPECTRA
Benjamí Martorell Masip
ISBN:978-84-691-9747-9 /DL: T-1259-2008

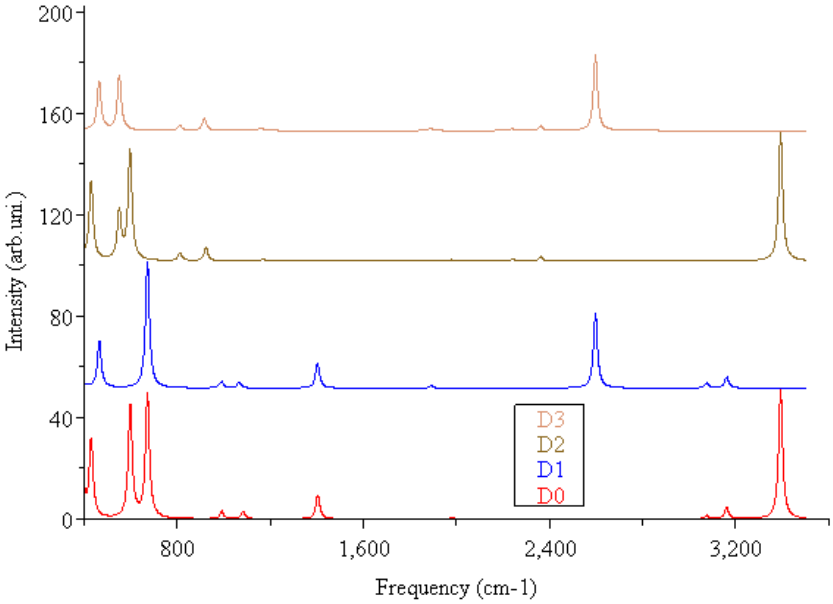

Figure 5.4: Simulated IR spectrum of C_3H_3 in gas phase. D0: C_3H_3; D1: $DC{-}C{-}CH_2$; D2: $HC{-}C{-}CD_2$; D3: C_3D_3.

plane), but in this molecule they are not coupled, as happened in the case of VC. Note that the coupling between ν C=C modes causes two very weak frequencies at 1979 (negative coupling) and at 1082 cm^{-1} (positive coupling, in the zone that usually corresponds to a simple C−C bond). These ν C=C frequencies can be compared with the values for propadiene, which are 1957 and 1073 cm^{-1} [148]. For C_3H_3-d1 the spectrum is the same as for C_3H_3, and only the negative coupling of both ν C=C shifts down to 1891 cm^{-1}, being not observed in the spectrum. In the case of C_3H_3-d2 and C_3H_3-d3 this zone becomes almost flat in the spectrum, because δ $C3D_2$ couples with ν C2=C3 and its intensity decrease a lot, appearing as a weak band at 916 cm^{-1}.

In the region from 300 to 800 cm^{-1} appear all C−H out-of-plane bending modes and the C−C−C bending in and out-of-plane modes. This is a region with a lot of intense peaks. At 672 cm^{-1} appears an intense band corresponding to the $C3H_2$ wagging. At 598 cm^{-1} is present (intense) γ C1−H, and the only bending in-plane in this region at 430 cm^{-1}, δ C1−H. Finally, at 396 and 339 cm^{-1} exist the weak C−C−C bending out-of-plane and in-plane bands respectively. In the case of C_3H_3-d1 four intense peaks appear in this region. At 672 cm^{-1}

UNIVERSITAT ROVIRA I VIRGILI
ORGANIC MOLECULES ON METAL SURFACES: FORECASTING STRUCTURES AND SPECTRA
Benjamí Martorell Masip
ISBN:978-84-691-9747-9 /DL: T-1259-2008

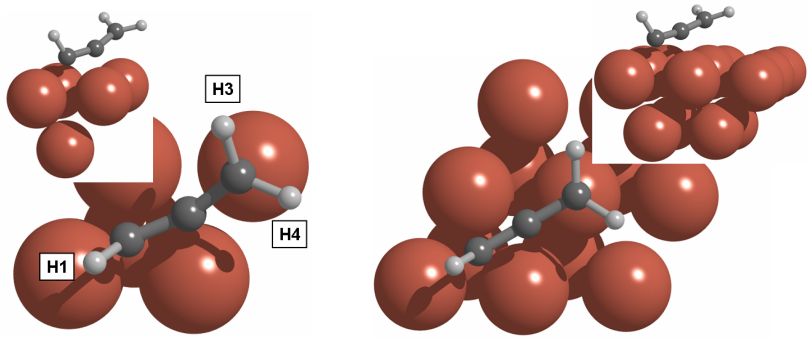

(a) (b)

Figure 5.5: C_3H_3 adsorbed on Cu(111): (a) 2×2 unit cell, (b) 3×3 unit cell.

appears the most intense peak in the spectrum, corresponding to ω C3H_2. A medium band appears at 465 cm^{-1} corresponding to the γ C1−D, and finally at 331 and 318 cm^{-1} exit the medium C−C−C bending out-of-plane and in-plane bands, respectively. In the case of C_3H_3-d2 five peaks appear in this region at 597, 551, 430, 374, and 308 cm^{-1}, corresponding to the γ C1−H, ω C3D_2, δ C1−H, and γ and δ C−C−C. For C_3H_3-d3 only four bands are visible at 551, 464, 317, and 297 cm^{-1}, corresponding to the ω C3D_2, γ C1−D, δ C1−D, and δ C−C−C.

5.2.2.2 Adsorption modes.

As commented in section 5.2.2.1, C_3H_3 specie is a radical with two double bonds perpendicular one to each other and one unpaired electron on the perpendicular π MO of C1−C2 bond respect to the molecular plane. As a chemical exercise, we can speculate how C_3H_3 should interact with the surface. As in the case of VC, this non-paired electron will trend to interact. Besides, the double bond perpendicular to the surface between C2 and C3, will also try to interact with surface, like in the case of propene [94]. So interaction will be made through a non-paired electron on C1 and C2, and through the C2=C3 double bond, which is perpendicular to the surface.

In figure 5.5 are presented the adsorption modes of C_3H_3 on Cu(111) on two different unit cells: 2×2 and 3×3. In both cases C_3H_3 adsorbs via its C1 on a hollow-site, with the C1=C2 unit adsorbed on a bridge site (similar way that ethyne and propyne do on Cu (di-σ/di-π) [92, 106, 108]), but with a large C1=C2

UNIVERSITAT ROVIRA I VIRGILI
ORGANIC MOLECULES ON METAL SURFACES: FORECASTING STRUCTURES AND SPECTRA
Benjamí Martorell Masip
ISBN:978-84-691-9747-9 /DL: T-1259-2008

Table 5.8: ZPE corrected and uncorrected adsorption energies of C_3H_3 on Cu(111) for 2×2 and 3×3 unit cell (values are presented in kJ·mol^{-1}).

	E_{ads} C_3H_3 adsorbed on Cu(111)				
	No ZPE	ZPE	ZPE-d1	ZPE-d2	ZPE-d3
2×2	35.8	21.1	20.8	25.6	25.2
3×3	-0.9	-16.6	-16.8	-12.2	-12.5

distance because the interaction of C2=C3 unit with the surface is strong, being C3 placed on a top position. So C_3H_3 interacts with the surface via the three carbon atoms with a tri-σ/di-π adsorption mode. It is also interesting to point out that for the 2×2 unit cell, C_3H_3 misses its symmetry planes, but on the 3×3 unit cell C_s symmetry remains.

$$E_{\text{ads}} = E_{C_3H_3(\text{ads})} + \frac{1}{2}E_{H_2(g)} - (E_{\text{Pr(g)}} + E_{\text{slab}}) \tag{5.2}$$

In table 5.8 is presented the adsorption energy of C_3H_3 respect to Pr in gas phase. In order to take into account the difference on the number of H atoms, the adsorption energy is evaluated as indicates equation 5.2. A positive value indicates that Pr will not trend to dehydrogenate to C_3H_3 and molecular hydrogen, otherwise if the value is negative, this tendency will exist. On the 2×2 unit cell the E_{ads} is 35.8 kJ·mol^{-1} and on 3×3 unit cell it is almost 0. The difference of energy is ∼35 kJ·mol^{-1}, which is almost the same difference of C3-top structure for VC on the those both unit cells (∼40 kJ·mol^{-1}), indicating an important coverage effect. On the 2×2 unit cell ZPE correction makes to be only ∼25 kJ·mol^{-1}, but it is still above 0, i.e. , adsorbed C_3H_3 and gas phase H_2 are unstable respect to Pr in gas phase. In the case of a 3×3 unit cell, when ZPE correction is taken into account, the adsorption energy becomes negative (-16.6 kJ·mol^{-1}), therefore Pr will trend to be dehydrogenated on the surface (although the adsorption energy of Pr is larger (-95 kJ·mol^{-1}, see table 4.3) than the stabilisation produced by the breaking of this C3−H bond, so it will not be the major reaction product in a first step). So C_3H_3 specie has a different reactivity on the 2×2 respect to the 3×3 unit cell, being a clear coverage effect due to the major interaction between adjacent molecules in the case of a 2×2 unit cell.

Finally, no important differences were found in the case of placing C1 on a fcc or a hcp-site, so only values relatives to C1 on fcc-site have been given.

UNIVERSITAT ROVIRA I VIRGILI
ORGANIC MOLECULES ON METAL SURFACES: FORECASTING STRUCTURES AND SPECTRA
Benjamí Martorell Masip
ISBN:978-84-691-9747-9 /DL: T-1259-2008

Table 5.9: Geometrical parameters of C_3H_3 adsorbed on Cu(111).

	2×2 unit cell	3×3 unit cell
[a]d(C1-C2)	1.34	1.32
d(C2-C3)	1.36	1.37
[b]α(C1-C2-C3)	157.2	172.1
α(H1-C1-C2)	117.2	119.3
α(H3-C3-H4)	116.4	116.9
α(H3-C3-C2)	122.8	119.5
α(H4-C3-C2)	118.9	119.5
[c]tilt	11.4	11.6
[d]d(C1-M)	2.09	2.13
d(C2-M)	2.15	2.33
d(C3-M)	2.28	2.17
d(H1-M)	2.46	2.47
d(H2-M)	2.63	2.68
d(H3-M)	2.94	2.68

[a]d: distances (Å); [b]α: angles (degrees); [c] tilt: angle between C1−C2 bond and the surface plane; [d]d: distances to nearest surface atom.

5.2.2.3 Adsorption geometries.

In table 5.9 are presented the most relevant geometrical parameters of C_3H_3 adsorbed on Cu(111) on both unit cells. Only the values for those structures whose C1 atoms are placed on a fcc-site are presented. C−H distances are not given because all values are in the range between 1.08-1.10 Å. However, note that C1−H distance is larger than the one obtained for gas phase C_3H_3 .

C2−C3 distance does not vary in the adsorption process, remaining at ∼1.36 Å as in the gas phase, but C1−C2 distance enlarge 0.09 Å (up to 1.34 Å) in the case of the 2×2 unit cell and 0.07 Å (up to 1.32 Å) in the case of the 3×3 unit cell, as expected by the adsorption mode.

Another important effect of the adsorption is that C skeleton is not lineal as in the gas phase. This effect is small in the 3×3 unit cell (172°) but it is outstanding on the 2×2 unit cell (157°). The H1 atom was also lined with C atoms in the gas phase, but tilts away in the case of adsorption, forming an angle of 117° (119°) with C1−C2 for the 2×2 (3×3) unit cell. This effect can be observed as the substitution of one H atom in the propadiene molecule by the Cu surface, because the adsorption structure (overall on 3×3 unit cell) is very similar to the one that exhibits propadiene in gas phase, where one H atom has been pulled out and replaced by the surface.

UNIVERSITAT ROVIRA I VIRGILI
ORGANIC MOLECULES ON METAL SURFACES: FORECASTING STRUCTURES AND SPECTRA
Benjamí Martorell Masip
ISBN:978-84-691-9747-9 /DL: T-1259-2008

Table 5.10: Vibrational frequencies, intensities and assignments for C_3H_3 adsorbed on Cu(111) on 2×2 and 3×3 unit cells. All frequencies are given in cm^{-1}.

C_3H_3 adsorbed on Cu(111)				
2×2		Vibrational mode	3×3	
I (km/mol)	$\bar{\nu}_e$	2×2 / 3×3	$\bar{\nu}_e$	I (km/mol)
0.05	3163	asym. ν $C3H_2$	3119	0.17
0.27	3050	sym. ν $C3H_2$	3037	1.11
2.02	3004	ν C1−H	3026	0.03
5.98	1687	ν C1=C2 - ν C2=C3	1741	2.3
2.18	1392	δ $C3H_2$	1385	1.29
2.63	1020	ν C2=C3 + ν C1=C2 + δ C1−H	996	0.79
3.94	983	δ C1−H + ρ $C3H_2$ / ρ $C3H_2$	981	0.03
2.73	938	δ C1−H - ρ $C3H_2$ / δ C1−H	935	8.43
1.43	826	γ C1−H - γ C3−H4/γ C1−H - τ $C3H_2$	772	0.12
5.75	729	ω $C3H_2$	758	10.38
0.21	494	γ C1−H + τ $C3H_2$	525	0.36
1.9	420	ν C1−surf + δ C1−C2−C3	422	0.75
0.32	322	ν C1−surf + γ C1−C2−C3	278	0.21
0.05	283	ν C2−surf + γ C1−C2−C3	243	0.00

The angle between C1−C2 bond and the surface plane is ∼11° for both unit cell, being this bond almost parallel to surface. The difference between the 2×2 and 3×3 unit cell is the position of C2−C3 bond respect to the C1−C2 bond. As commented before, the C−C−C angle was smaller for 2×2 unit cell, and this is a direct consequence of the higher coverage. Consequently on the 2×2 unit cell, C2 atom is placed closer to surface and C3 further than on the 3×3 unit cell, as can be observed in table 5.9. Finally, we want to emphasise that on the 2×2 unit cell, both H atoms in C3 are not placed at the same distance from surface, but this group is a bit tilted, being one of the H atoms further from surface (see figure 5.5).

5.2.2.4 IR spectra.

Table 5.10 shows vibrational frequencies and their assignation for C_3H_3 adsorbed on Cu(111) on both unit cells: 2×2 and 3×3. Besides absolute intensities are also presented for each VNM. We can observe that vibrational frequency on both unit cells are very similar, not differing more than 50 cm^{-1}, although some different couplings in the middle zone of the spectrum appear. In figure 5.6(a) and 5.6(b) are presented the spectra for the 2×2 and the 3×3 unit cell, respectively,

UNIVERSITAT ROVIRA I VIRGILI
ORGANIC MOLECULES ON METAL SURFACES: FORECASTING STRUCTURES AND SPECTRA
Benjamí Martorell Masip
ISBN:978-84-691-9747-9 /DL: T-1259-2008

including the spectra obtained for deuterated species.

In the C−H stretching region all transitions have a weak intensity, so the bands are not visible on the spectra. Only for the 2×2 unit cell have somewhat intensity. For the 2×2 unit cell, vibrational frequencies are 3163, 3050, and 3004 cm^{-1} (the visible band in spectrum), and for the 3×3 unit cell are 3119, 3037, and 3026 cm^{-1}, corresponding to the asymmetric and symmetric $C3H_2$ and C1−H stretching modes, respectively. For C_3H_3-d1 the 3×3 spectrum does not change, because the ν C1−D is not active, shifting down the vibrational frequency to 2221 cm^{-1}. The 2×2's spectrum shows a weak band at 2221 corresponding to the ν C1−D. For C_3H_3-d2, 2×2 spectrum remains equal as the one of C_3H_3, shifting the asymmetric and symmetric ν $C3D_2$ down to 2355 and 2226 cm^{-1}, respectively. For the 3×3 spectrum a weak band is at 2212 cm^{-1}, corresponding to the symmetric ν $C3D_2$, the asymmetric is not visible and lies at 2328 cm^{-1}. The spectra of C_3H_3-d3 behaves like the addition of the deuterated stretching modes of C_3H_3-d1 and C_3H_3-d2 for both unit cells, indicating no coupling among the modes exist.

In the region from 900 to 2000 cm^{-1} appear the vibrational modes associated to C=C stretching and C−H bending in-plane modes. In this zone exists the most intense peak on the 2×2 unit cell.

For the middle-IR region, let's analyse the spectrum on the 2×2 unit cell, where all bands in this region are visible. Five transitions are present at 1687, 1392, 1020, 983, and 938 cm^{-1}, being the last three so close that form a wide band. The first vibrational frequency corresponds to the most intense peak in the spectrum and it is assignated to the negative coupling of both ν C=C. The second one is the $C3H_2$ scissoring mode. The third fundamental band is mainly associated to the positive coupling of both ν C=C, and the two final ones are the positive and negative coupling of δ C1−H with ρ $C3H_2$ (as in the case of C_3H_3 in gas phase, the δ and γ modes for C1−H have been assigned respect to the plane perpendicular to the molecular plane). For C_3H_3-d1 no big differences exist in the spectrum respect to C_3H_3, except the shape of the middle band as δ C1−D decouples from ρ $C3H_2$ (which stays isolated at 969 cm^{-1}). Moreover, δ C1−D couples positively and negatively with ω $C3H_2$ down to 777 and 771 cm^{-1}. The deuteration on C3 (C_3H_3-d2) causes the coupling of δ $C3D_2$ with the positive coupling of both ν C=C, being this band at 1116 cm^{-1}. This coupling causes an increase of the intensity of the band, making this band as intense as the negative coupling of both ν C=C at 1676 cm^{-1}. At 965, 897, 818, and 752 cm^{-1} appear the bands corresponding to the δ C1−H, the coupling of δ C1−H

UNIVERSITAT ROVIRA I VIRGILI
ORGANIC MOLECULES ON METAL SURFACES: FORECASTING STRUCTURES AND SPECTRA
Benjamí Martorell Masip
ISBN:978-84-691-9747-9 /DL: T-1259-2008

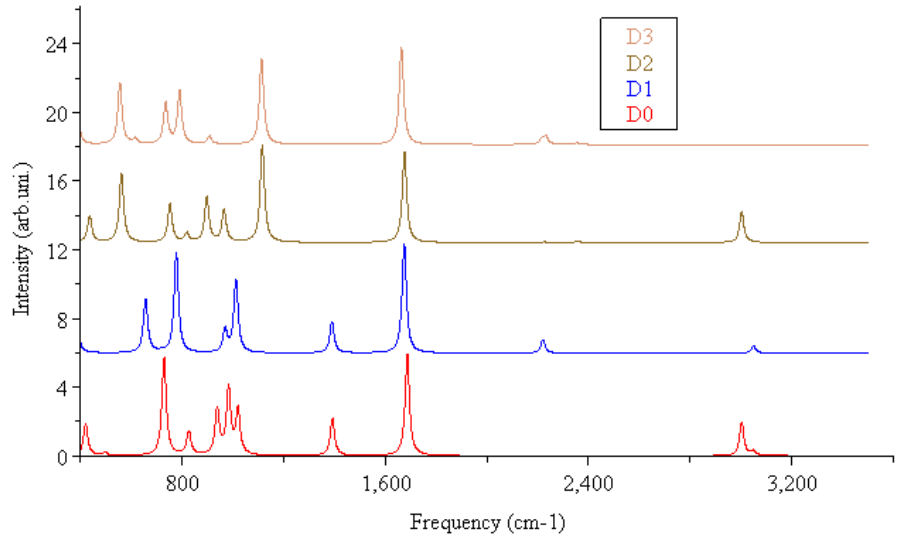

(a) 2x2 unit cell.

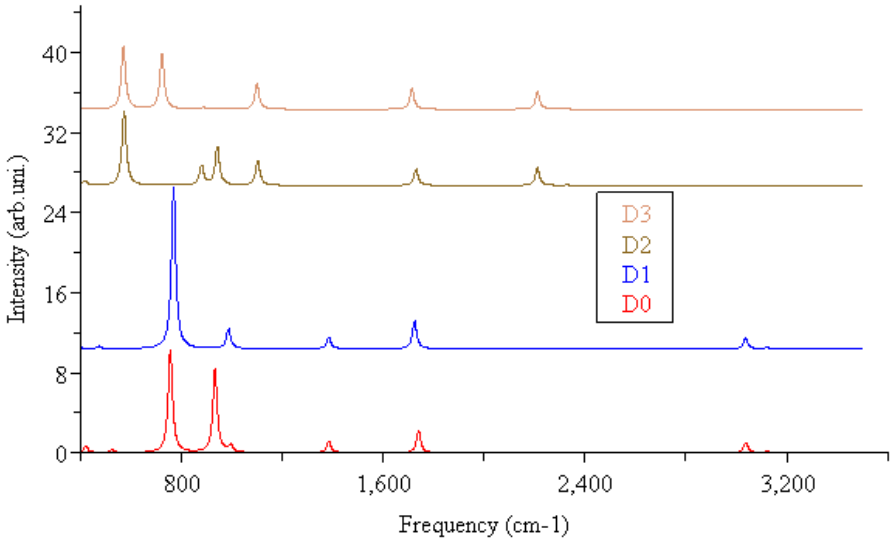

(b) 3x3 unit cell.

Figure 5.6: Simulated RAIR spectrum of C_3H_3 adsorbed on Cu(111), a) 2×2 unit cell, b) 3×3 unit cell. D0: C_3H_3; D1: $DC{-}C{-}CH_2$; D2: $HC{-}C{-}CD_2$; D3: C_3D_3.

with δ $C3D_2$, and the positive and negative coupling of δ $C1{-}H$ with ρ $C3D_2$. For C_3H_3-d3 (similar to the preceding case), the bands at 1113 and 907 cm^{-1}

UNIVERSITAT ROVIRA I VIRGILI
ORGANIC MOLECULES ON METAL SURFACES: FORECASTING STRUCTURES AND SPECTRA
Benjamí Martorell Masip
ISBN:978-84-691-9747-9 /DL: T-1259-2008

(very weak bands) correspond to the positive and negative coupling of δ $C3D_2$ with the positive coupling of both ν C=C. Finally, the features at 790 and 735 cm^{-1} are the positive and negative coupling modes of δ C1−D with ρ $C3D_2$.

In the spectrum of the 3×3 unit cell, the vibrational frequencies and modes are similar to the ones found for the 2×2 unit cell (see table 5.10). However, some band intensities change making the spectrum somewhat different. The most important changes are the increase of the intensity of the ω $C3H_2$ and a decrease of the intensity of the negative coupling of both ν C=C. Moreover, the ρ $C3H_2$ and δ C1−H modes decouple, making the first inactive and more intense the C1−H bending in-plane. Finally, as a minor change, the symmetric ν $C3H_2$ and ν C1−H interchange its intensities, so the weak band on the 3×3 spectrum is now the one related to ν C1−H. The spectrum corresponding to the monodeuterated C_3H_3 (C_3H_3-d1) is quite similar to the undeuterated specie, except that the band below 800 cm^{-1} increases its intensity due to the coupling of ω $C3H_2$ mode with the C1−D bending in-plane mode. The spectrum of C_3H_3-d2 shows three bands between 800 and 1200 cm^{-1}, as a consequence of the decrease of $C3D_2$ scissoring mode when is deuterated. The bands at 1194, 944, and 882 cm^{-1} correspond to the positive coupling of both ν C=C with δ $C3D_2$, to the δ C1−H, and to the ν C=C mode with δ C1−H. The band at 575 cm^{-1} is assigned to the ω $C3H_2$. Finally, the spectrum of the fully deuterated system (C_3D_3) is easy assigned from the partially deuterated and undeuterated systems.

Finally, no important differences were found between the C1 adsorbed on the fcc or hcp-site.

If adsorbed C_3H_3 is compared with the gas phase molecule, we can observe some important changes. First of all, frequency of the negative coupling of both ν C=C decrease from ∼2000 to ∼1700 cm^{-1} due to the interaction of the double C=C bonds with surface, which weakens these bonds. Also the ν C1−H shifts down in the surface from ∼ 3350 to ∼3000 cm^{-1}, due to the enlargement of this bond. The most changing frequency is the C1−H bending, which in-plane shifts to higher frequency, from 430 cm^{-1} in the gas phase to ∼900 or ∼1000 cm^{-1} (depending on the unit cell). No mention about intensities is made because in gas phase variations of dipolar moment are taken into account for all directions.

UNIVERSITAT ROVIRA I VIRGILI
ORGANIC MOLECULES ON METAL SURFACES: FORECASTING STRUCTURES AND SPECTRA
Benjamí Martorell Masip
ISBN:978-84-691-9747-9 /DL: T-1259-2008

Table 5.11: Corrected and uncorrected ZPE adsorption energies for non-interacting, coadsorbed C_3H_3 and H.

	No ZPE	ZPE	ZPE-d1	ZPE-d3	ZPE-d4
2×2	9.4	-1.4	-1.7	2.0	1.6
3×3	-48.9	-60.7	-60.9	-57.5	-57.8

5.2.3 Coadsorption of C_3H_3 and H.

Until now we have studied the adsorption of H and C_3H_3 separately, but if the isomerisation reaction is desired to success, both species must be present on the surface, so we decided to study the coadsorption of both species on the both used unit cells: 2×2 and 3×3 unit cells.

5.2.3.1 Non-interacting system.

As a first step in the coadsorption study, we decided to study the coadsorption of C_3H_3 and H, but without interaction between them. This is the most simple model, because only the adsorption energies for the isolated systems are necessary. The coadsorption energy is calculated as it is indicated in equation 5.3. In table 5.11 the values obtained for the coadsorption of C_3H_3 on C1-fcc-site and H on a fcc-site are presented. The other three possible combinations do not differ more than ∼2 kJ·mol^{-1} of the values here presented.

$$E_{\text{coads}} = E_{\text{ads (H)}} + E_{\text{ads } (C_3H_3)} \tag{5.3}$$

In the case of 2×2 unit cell, the coadsorption energy is 9.4 kJ·mol^{-1}. This value is smaller than the energy necessary to break the C−H bond in gas phase (∼170 kJ·mol^{-1}), favouring the dehydrogenation process on the surface. When ZPE correction is added this value decrease ∼10 kJ·mol^{-1} , down to -1.4 kJ·mol^{-1}. From a thermodynamic point of view, the dehydrogenation process to form the non-interaction system will be competitive with the desorption process, if adsorbed Pr is present on the surface.

For the 3×3 unit cell, the coadsorption energy is lower, -48.9 kJ·mol^{-1}. When ZPE correction is added, the breaking of C−H bond and coadsorption of C_3H_3 and H is even favoured ∼12 kJ·mol^{-1} (-60.7 kJ·mol^{-1}). This value indicates that, from the thermodynamic point of view, when adsorbed Pr is present on the surface, it will trend to dissociate into C_3H_3 and H, and will not trend to desorbe.

UNIVERSITAT ROVIRA I VIRGILI
ORGANIC MOLECULES ON METAL SURFACES: FORECASTING STRUCTURES AND SPECTRA
Benjamí Martorell Masip
ISBN:978-84-691-9747-9 /DL: T-1259-2008

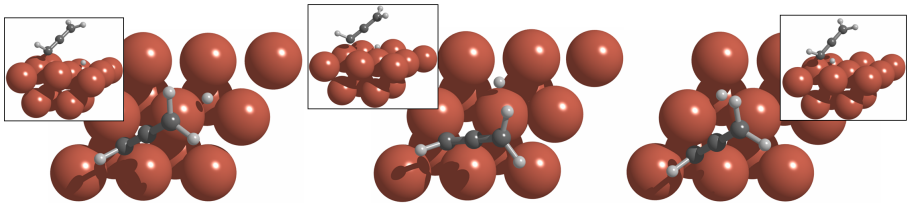

(a) M1. (b) M2. (c) M3.

Figure 5.7: Different coadsorption modes of C_3H_3 with H on Cu(111) 2×2 unit cell, depending on the relative position of adsorbed H.

The small differences in ZPE correction for the 2×2 and 3×3 unit cells are due to small differences in the vibrational frequencies on both unit cells. The ZPE correction of ∼10 kJ·mol^{-1} is smaller than the one found for VC, which was ∼15 kJ·mol^{-1}, due to the minor quantity of frequencies in C_3H_3.

5.2.3.2 Coadsorption modes.

In the coadsorption calculations only have been taken into account the minima where adsorbed H atom and adsorbed C_3H_3 specie are one next to the other one. It means that for 3×3 unit cell only 3 of all possible coadsorption modes have been computed, because these are the minimum steps for the proposed dehydrogenation-hydrogenation process.

With these considerations, three minima have been computed (see figures 5.7 and 5.8):

- M1: H atom is coadsorbed below the $C3H_2$ unit on a hollow site. Coadsorbed H atom and C1 of C_3H_3 are placed on the same hollow-site type.
- M2: H atom is coadsorbed next to the $C3H_2$ unit on a hollow site. Coadsorbed H atom and C1 of C_3H_3 are placed on different hollow-site type.
- M3: H atom is coadsorbed next to the $C3H_2$ unit and near C2 on a hollow site. Coadsorbed H atom and C1 of C_3H_3 are placed on the same hollow-site type.

Actually, if we start from M1 coadsorption mode, the way to arrive M2 is mainly the migration of one H atom to the next hollow-site. Subsequently, to get M3 is once more the diffusion to the next hollow-site.

UNIVERSITAT ROVIRA I VIRGILI
ORGANIC MOLECULES ON METAL SURFACES: FORECASTING STRUCTURES AND SPECTRA
Benjamí Martorell Masip
ISBN:978-84-691-9747-9 /DL: T-1259-2008

Table 5.12: ZPE corrected and uncorrected adsorption energies for the coadsorption of C_3H_3 and H on the three different minima respect to Pr in gas phase on 2×2 unit cell.

	No ZPE	ZPE	ZPE-d1	ZPE-d3	ZPE-d4
M1 C1-fcc + H-fcc	30.7	22.1	21.7	25.4	25.0
M1 C1-hcp + H-hcp	33.6	24.6	24.2	28.0	27.5
M2 C1-fcc + H-hcp	44.1	35.6	35.2	38.7	38.3
M2 C1-hcp + H-fcc	44.5	35.9	35.6	39.1	38.7
M3 C1-fcc + H-fcc	38.8	30.9	30.4	33.9	33.4
M3 C1-hcp + H-hcp	39.3	31.5	31.1	34.5	34.1

2×2 unit cell. In table 5.12 are presented the coadsorption energies for M1, M2 and M3. We can observe that C1 on fcc-site is always more stable than hcp-site, but differences are smaller than 3 kJ·mol^{-1}, so they are almost degenerated.

The adsorption energy for M1 is 31, for M2 44 and for M3 39 kJ·mol^{-1}. When ZPE correction is added these values decrease ∼8 kJ·mol^{-1} in three cases to 22, 36 and 31 kJ·mol^{-1}, respectively. Also the partially and totally deuterated species are taken into account. As the coadsorbed specie is the result of the Pr's methylenic carbon dehydrogenation, D1 is coadsorbed DC−C−CH_2 + H, D3 is coadsorbed HC−C−CD_2 + D, and D4 coadsorbed DC−C−CD_2 + D. As expected, the ZPE correction is larger for the undeuterated coadsorbed species than the deuterated ones. For all coadsorbed modes, the coadsorption energy is larger than in the case of the non-interacting system ∼25-35 kJ·mol^{-1} (∼20-30 kJ·mol^{-1} with no ZPE) due to the repulsion existing between both species on this unit cell (this produces changes in the adsorption mode that will be commented in section 5.2.3.3). This positive value indicates that adsorbed Pr will trend to desorbe and not to break the C−H bond, when temperature is raised.

Coadsorbed M1 structure is the most stable one, followed by the M3 structure and finally M2 is the less stable one, but differences are not larger than ∼15 kJ·mol^{-1}, indicating that the diffusion of the H atom is not difficult. This differences are due mainly to geometric effects that will be commented in section 5.2.3.3.

3×3 unit cell. In table 5.13 are presented the coadsorption energies for M1, M2 and M3. We can observe that C1 on fcc-site is always more stable than hcp-site, but differences are smaller than 1 kJ·mol^{-1}, so they are degenerated in our calculation precision.

In order to study the coverage effects in the coadsorbed structures of C_3H_3

UNIVERSITAT ROVIRA I VIRGILI
ORGANIC MOLECULES ON METAL SURFACES: FORECASTING STRUCTURES AND SPECTRA
Benjamí Martorell Masip
ISBN:978-84-691-9747-9 /DL: T-1259-2008

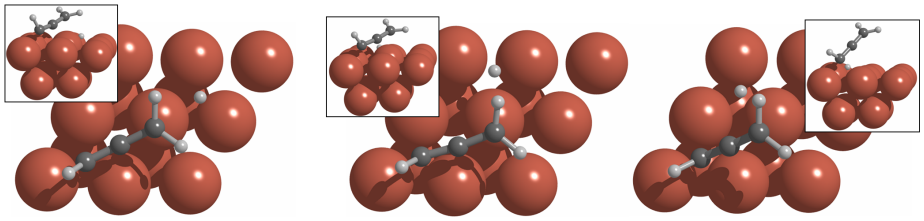

(a) M1. (b) M2. (c) M3.

Figure 5.8: Different coadsorption modes of C_3H_3 with H on the 3×3 unit cell, depending on the relative position of adsorbed H.

with H, we increased the calculation supercell to a 3×3 unit cell. The coverage decreases, and interactions between adjacent molecules also decrease because the separation is larger. In figure 5.8 are presented the minimum necessary coadsorption steps to obtain the intramolecular dehydrogenation-hydrogenation process (although other possibilities of diffusion for H atoms would exist on this unit cell and also other coadsorbed structures could be present), like in the case of 2×2 unit cell.

The adsorption energy for M1 is -11, for M2 -8 and for M3 9 kJ·mol^{-1}. When ZPE correction is added these values decrease ∼11 kJ·mol^{-1} (a value similar to the 2×2 unit cell) in three cases to -21, -19 and -2 kJ·mol^{-1}, respectively. Also the the partially and totally deuterated species are taken into account. As expected, the ZPE correction is larger for the undeuterated coadsorbed species than the deuterated ones. For all coadsorbed modes, the coadsorption energy is higher than in the case of non-interacting system ∼40-60 kJ·mol^{-1} due to the repulsion existing between both species on this unit cell (this produces changes in the adsorption mode that will be commented in section 5.2.3.3). This difference is larger than in the case of 2×2 unit cell, not because the repulsion between C_3H_3 and H is larger on this unit cell, but because on this unit cell the coadsorbed absolute minimum would be a coadsorption mode where H atom and C_3H_3 specie lie more separate than in the calculated positions in order to minimise their repulsion.

For M1 and M2 the coadsorption energy is negative (∼-20 kJ·mol^{-1}) and for M3 it is almost 0. This indicates that the dissociation of the C−H bond is competitive with the Pr desorption when adsorbed Pr is heated. We can observe that the difference between 2×2 and 3×3 unit cell is that in this last case, the dehydrogenation process from Pr is possible, and in the case of the

UNIVERSITAT ROVIRA I VIRGILI
ORGANIC MOLECULES ON METAL SURFACES: FORECASTING STRUCTURES AND SPECTRA
Benjamí Martorell Masip
ISBN:978-84-691-9747-9 /DL: T-1259-2008

Table 5.13: ZPE corrected and uncorrected adsorption energies for the coadsorption of C_3H_3 and H on the three different minima respect to Pr in gas phase on 3×3 unit cell.

	No ZPE	ZPE	ZPE-d1	ZPE-d3	ZPE-d4
M1 C1-fcc	-10.9	-21.3	-21.6	-18.3	-18.6
M1 C1-hcp	-11.3	-21.9	-22.2	-18.9	-19.2
M2 C1-fcc	-8.1	-19.1	-19.4	-16.0	-16.3
M2 C1-hcp	-9.0	-19.8	-20.1	-16.7	-17.0
M3 C1-fcc	9.2	-1.6	-1.8	1.9	1.6
M3 C1-hcp	9.4	-1.6	-1.8	2.0	1.7

2×2 unit cell this process is more difficult to occur. This is due to the repulsion effect on the 2×2 unit cell, because on the 3×3 unit cell C_3H_3 and H are better accommodated. This effect will be seen in geometric parameters (section 5.2.3.3).

M1 is the most stable structure, as in the case of 2×2 unit cell, but only ∼2 kJ·mol^{-1} above lies the M2 structure, so they are almost degenerated. M3 is ∼20 kJ·mol^{-1} above M1. M2 and M3 interchange their relative position respect to 2×2 unit cell. This is due to the coordination mode of C_3H_3 in M2 structure, as will be commented in the section 5.2.3.3.

5.2.3.3 Adsorption geometries.

In table 5.14 are presented the adsorption geometries of the coadsorbed structures on both unit cells, 2×2 and 3×3, because significant differences exist between both unit cells. These geometrical differences are also responsible of the differences in E_{coads}, as commented above.

2×2 unit cell. In this case C_3H_3 sticks into the surface like a javelin, being this effect observed in the angle that forms C1−C2 bond with the surface plane, which is 41°, 42° and 43° for M1, M2, and M3, respectively, which is a different value from the adsorbed, isolated C_3H_3, which is 11°. The interaction with the surface for isolated C_3H_3 was made via the three C atoms, but only C1 interacts with the surface in the coadsorbed system, so the coadsorbed H atom affects strongly the adsorption mode of coadsorbed species. C1−C2 and C2−C3 distances are both equal and are 1.31-1.32 Å, indicating two very strong double C=C bonds exist in this coadsorbed structure. These values are shorter than those of the isolated C_3H_3 (1.34 and 1.36 Å), indicating these bonds interacted

UNIVERSITAT ROVIRA I VIRGILI
ORGANIC MOLECULES ON METAL SURFACES: FORECASTING STRUCTURES AND SPECTRA
Benjamí Martorell Masip
ISBN:978-84-691-9747-9 /DL: T-1259-2008

Table 5.14: Geometrical parameters of coadsorbed C_3H_3 and H on C1-fcc site of both (2×2 and 3×3) unit cells on Cu(111).

	M1		M2		M3	
	2×2	3×3	2×2	3×3	2×2	3×3
[a]d(C1-C2)	1.31	1.33	1.31	1.32	1.32	1.32
d(C2-C3)	1.31	1.36	1.32	1.35	1.31	1.31
[b]α(C1-C2-C3)	179.0	168.0	177.7	171.8	179.3	178.4
α(H1-C1-C2)	115.0	117.0	114.9	118.2	114.1	113.4
α(H3-C3-C2)	121.7	120.3	121.2	120.1	121.3	120.9
α(H4-C3-C2)	121.7	120.2	121.6	120.1	121.9	121.5
α(H4-C3-H3)	116.6	117.3	117.2	117.2	116.7	117.6
[c]tilt	41.1	13.7	41.8	16.2	43.1	41.9
[d]d(C1-M)	2.10	2.06	2.01	2.13	2.12	2.16
d(H1-M)	2.68	2.46	2.55	2.43	2.36	2.15
d(H*-M)	1.68	1.70	1.64	1.69	1.66	1.67

[a]d: distances (Å); [b]α: angles (degrees); [c] tilt: angle between C1−C2 bond and the surface plane; [d]d: distances to nearest surface atom, H* is the adsorbed H atom.

with the surface. All H−C−C angles are around 120°, indicating a sp^2-like hybridisation of both terminal C atoms. So, this structure resembles that of propadiene (gas phase) where a H atom has been replaced by the surface. The C1−M distance is very similar for M1 and M3 structures (2.10 and 2.12 Å), but is shorter for M2 (2.01 Å), because the adsorption mode of this structure is different than the ones of M1 and M3. C1 for M2 is placed close to a Cu atom, because is not placed exactly on a hollow-site but it is a bit displaced to a bridge-site (see figure 5.7). The H1−M distance is 2.68, 2.55 and 2.36 Å, indicating that no large interaction exist between H atom and the metal surface. Finally, the distance of adsorbed H with the nearest metal atom are very similar, from 1.64 (M2) to 1.68 (M1) Å, which are shorter than the distance of isolated, adsorbed H atom on this surface, 1.73 Å. This distance is shorter because H atom is displaced a bit to a bridge site (due to the repulsion with C_3H_3). So, both structures, C_3H_3 and H, are strongly affected by the existence of the other specie on the surface, so from a computational point of view, the explicitly coadsorption must be taken into account and the non-interacting system calculations should be performed *a priori* only for the purposes to deal with good adsorption geometries to start the calculation of the coadsorbed system. They only would have sense for situations of very low coverage.

UNIVERSITAT ROVIRA I VIRGILI
ORGANIC MOLECULES ON METAL SURFACES: FORECASTING STRUCTURES AND SPECTRA
Benjamí Martorell Masip
ISBN:978-84-691-9747-9 /DL: T-1259-2008

3×3 unit cell. In this case, the adsorption mode for M1 and M2 is different from M3. The angle between C1−C2 bond and the surface plane is 14°, 16°, and 42°, respectively, indicating that the adsorption mode is made via the three C atoms for M1 and M2 and only via the C1 for M3. The C1−C2−C3 angle is 168°, 172°, and 178°, in agree with previous values. For both M1 and M2, the adsorption mode is like isolated C_3H_3, whose angle between C1−C2 bond and the surface plane was 12° and the C1−C2−C3 angle was 172°. C1−C2 and C2−C3 distances are also different for M1 and M2 respect to M3. In M3 distances are equal to the case of 2×2 unit cell (1.32 and 1.31 Å, respectively), due to the adsorption mode, which is equal to the 2×2 unit cell. Distances are 1.33 and 1.36 Å for M1 and 1.32 and 1.35 Å for M2, similar to the ones obtained when H atom is not coadsorbed (1.32 and 1.37 Å). C1−M distances are all very similar, 2.06, 2.13, and 2.16 Å for M1, M2, and M3, so no important differences exist in this value. H1−M distance are 2.46, 2.43, and 2.15 Å for M1, M2, and M3, respectively. This indicates that in M3 the H1−M distance is short and this structure is stabilised by an agostic interaction. Finally, the distance between the adsorbed H atom and the surface atom are 1.70, 1.69, and 1.67 Å for M1, M2, and M3, a bit shorter than in the case of an adsorbed H atom (1.74 Å), like for 2×2 unit cell. The H atom is a bit displaced from the centre of the hollow-site, too. So, also in this case, both structures, C_3H_3 and H, are affected by the existence of the other specie on the surface, but in the case of M1 and M2 this effect is less important.

Finally, no important differences exist on placing C1 on fcc or hcp-site, so only values with C1 on fcc-site are presented.

5.2.3.4 RAIR spectra on the 2×2 unit cell.

In table 5.15 are presented vibrational frequencies and vibrational modes for coadsorbed C_3H_3 and H on Cu(111), using a 2×2 unit cell. Also absolute intensities are given for all these modes, and it is interesting that one mode is very intense, having a value around 100 km·mol^{-1}. We also can observe that vibrational frequencies and intensities are similar for three coadsorption modes, indicating that three RAIR spectra will have the same features. In figure 5.9 are presented the RAIR spectra of three coadsorbed structures, and also their corresponding deuterated spectra are presented, being in this case $DC{=}C{=}CH_2$ & H (C_3H_3-d1 + H), $HC{=}C{=}CD_2$ & D (C_3H_3-d2 + D) and $DC{=}C{=}CD_2$ & D (C_3H_3-d3 + D), because they derive from Pr-d1, Pr-d3 and Pr-d4, respectively.

UNIVERSITAT ROVIRA I VIRGILI
ORGANIC MOLECULES ON METAL SURFACES: FORECASTING STRUCTURES AND SPECTRA
Benjamí Martorell Masip
ISBN:978-84-691-9747-9 /DL: T-1259-2008

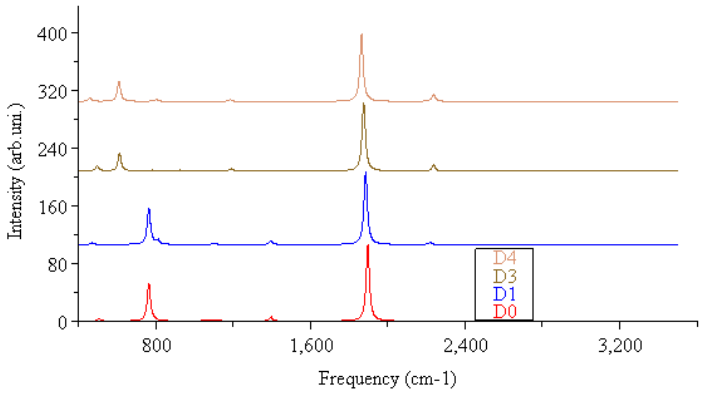

(a) M1.

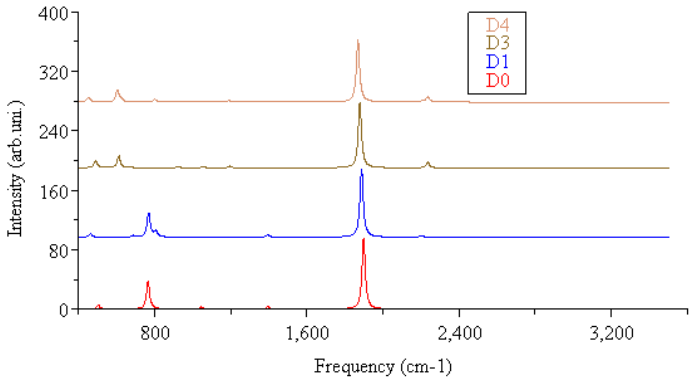

(b) M2.

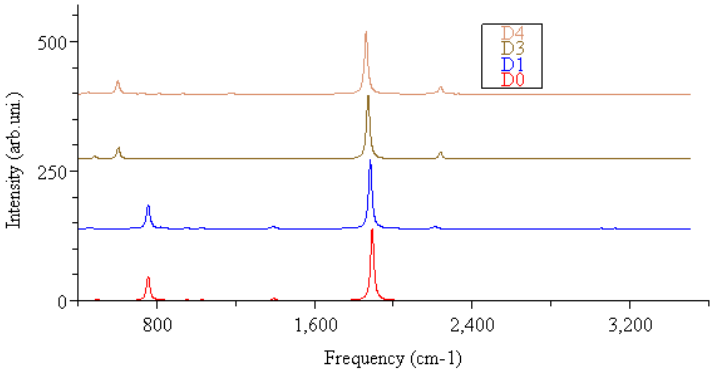

(c) M3.

Figure 5.9: RAIR spectra for coadsorbed C_3H_3 and H for a) M1, b) M2, and c) M3 adsorption modes on Cu(111): 2×2 unit cell. D0: C_3H_3 + H; D1: $DC{-}C{-}CH_2$ + H; D2: $HC{-}C{-}CD_2$ + D; D3: C_3D_3 + D.

UNIVERSITAT ROVIRA I VIRGILI
ORGANIC MOLECULES ON METAL SURFACES: FORECASTING STRUCTURES AND SPECTRA
Benjamí Martorell Masip
ISBN:978-84-691-9747-9 /DL: T-1259-2008

Table 5.15: Vibrational frequencies for C_3H_3 and H coadsorbed on Cu(111) on 2×2 unit cell. Frequencies in cm^{-1}; intensities in $km{\cdot}mol^{-1}$.

	M1		M2		M3	
Assignation (M1 / M2 / M3)	$\bar{\nu}_e$	I	$\bar{\nu}_e$	I	$\bar{\nu}_e$	I
asym. ν $C3H_2$	3118	0.5	3122	0.5	3122	0.9
sym. ν $C3H_2$	3048	0.2	3049	0.1	3051	1.1
ν C1−H	2999	0.2	2980	0.0	2988	0.4
ν C1=C2 - ν C2=C3	1897	106.3	1899	96.9	1893	138.9
δ $C3H_2$	1396	5.9	1393	4.0	1391	4.9
(1) + (2) / (2) / (3)	1125	1.6	1302	0.7	1248	0.2
(2) /(1) / (1)	1096	1.7	1124	0.4	1118	0.0
δ C1−H	1048	2.0	1043	3.4	1061	0.2
(3) / (2) / (2)	999	0.1	966	0.7	1027	2.0
(3) / ρ $C3H_2$ / (3)	961	0.1	960	0.0	956	0.6
ρ $C3H_2$ / (4) / ρ $C3H_2$	954	0.2	837	0.2	949	0.9
(4) / (3) / (4)	840	0.0	782	0.1	837	0.6
ω $C3H_2$	765	54.3	766	37.6	758	48.9
δ C1−C2−C3 - ν C1−M	507	3.2	503	6.0	498	2.7
γ C1−C2−C3	364	0.0	361	0.4	355	0.1
(5) / (6) / (5)	289	6.4	334	0.2	287	7.4
(6) / (5)/ (6)	255	2.2	290	9.0	265	1.3

(1): ν C1=C2 + ν C2=C3 + δ C1−H ; (2): ν H*−M ($\perp$); (3):ν H*−M ($\parallel$); (4): γ C1−H - τ $C3H_2$; (5): δ C1−C2−C3 + ν C1−M ; (6): γ C1−H + τ $C3H_2$.

The C−H stretching region is very similar for all minima, because of two main reasons. The first reason is that the intensity of the associated mode is weak, in all cases less than 1% of the most intense band of the spectrum, so in all spectra there is no band in this region. The second reason is this region is very similar in all cases, vibrational frequencies and their associated vibrational modes are almost equal in three cases. At 3118 cm^{-1} for M1 and 3122 cm^{-1} for M2 and M3 appears the asymmetric ν $C3H_2$, and the symmetric combination at 3048, 3049, and 3051 cm^{-1}, respectively. The C1−H stretching mode appears between ∼2980 and ∼3000 cm^{-1}, indicating this vibrational frequency that this bond is not activated, as the H1−M distances also indicated (see table 5.14). We can compare these values with the obtained ones for the adsorption of isolated C_3H_3 on surface, which were 3136, 3050, and 3004 cm^{-1} for the asymmetric and symmetric ν $C3H_2$ and ν C1−H. These values are very similar to the obtained for coadsorption, although the adsorption mode is a bit different in both cases. For C_3H_3-d1 + H only the ν C1−D is affected by deuteration, indicating no coupling

UNIVERSITAT ROVIRA I VIRGILI
ORGANIC MOLECULES ON METAL SURFACES: FORECASTING STRUCTURES AND SPECTRA
Benjamí Martorell Masip
ISBN:978-84-691-9747-9 /DL: T-1259-2008

between C−H stretching modes exist. In this case the vibrational frequency shifts down to 2217, 2203, and 2209 cm^{-1} for M1, M2, and M3, respectively. In C_3H_3-d2 + D the asymmetric and symmetric ν $C3D_2$ shift down to 2326 and 2236 cm^{-1} for M1, to 2329 and 2235 cm^{-1} for M2, and to 2329 and 2238 cm^{-1} for M3. In the case of C_3H_3-d3 + D, the vibrational frequencies behave like the addition of deuterated vibrational frequencies for C_3H_3-d1 + H and C_3H_3-d2 + D.

The next region of the spectrum is from 900 to 2000 cm^{-1}, where C−H bending in-plane, C=C stretching and H−M stretching modes appear and couplings among them (but in this case they are not as much coupled as in the case of VC). The first band that exists in this region is the most intense one in the spectrum, corresponding mainly to the negative coupling of both ν C=C. Vibrational frequencies are 1897, 1899, and 1893 cm^{-1} for M1, M2, and M3, respectively. This VNM also appeared for isolated C_3H_3, but in that case at 1687 cm^{-1}, indicating that the change in the adsorption mode has affected this value (and also the intensity, because the absolute intensity for the adsorbed, isolated specie was really smaller, spite it was the most intense peak), because the interaction of double C=C bonds with the surface. Next band in this region (medium) corresponds to δ $C3H_2$, which is ∼5% in intensity, and appears at 1396, 1393, and 1391 cm^{-1} for M1, M2, and M3, respectively, and at 1392 cm^{-1} for isolated C_3H_3 (so it does not change). At 1125, 1124, and 1118 for M1, M2, and M3, respectively, appears the positive coupling of both ν C=C coupled with δ C1−H, and only in the case of M1 it is also coupled with the perpendicular H^*−M stretching mode. These frequencies are larger than the one obtained for isolated C_3H_3 at 1020 cm^{-1}, because of the interaction of double C=C bonds with the surface, too. The H^*−M stretching modes are really affected by the coadsorption, and a detailed analysis will be made in the next paragraph. At 1048, 1043, and 1061 cm^{-1} for M1, M2, and M3, respectively, appears the δ C1−H, which is almost not visible in the spectrum (<3%). In the case of isolated C_3H_3 it appeared at 938 cm^{-1} positively and negatively coupled with ρ $C3H_2$, which for M1, M2, and M3 appears at 954, 960, and 949 cm^{-1}, indicating that coadsorption affects also this VNM. For C_3H_3-d1 + H, the spectrum does not suffer any important change, and in this zone only two VNMs are affected by deuteration. The first one happens at the most intense band of the spectrum, because the negative coupling of both ν C=C couples a bit with ν C1−D, but effects on the vibrational frequencies are small, appearing at 1886, 1888, and 1883 cm^{-1} for M1, M2, and M3, respectively. The second change is the shifting

UNIVERSITAT ROVIRA I VIRGILI
ORGANIC MOLECULES ON METAL SURFACES: FORECASTING STRUCTURES AND SPECTRA
Benjamí Martorell Masip
ISBN:978-84-691-9747-9 /DL: T-1259-2008

down of the δ C1−D to 812, 807, and 821 cm^{-1} for M1, M2, and M3, respectively, but this band is not visible in the spectrum. For C_3H_3-d2 + D no important differences appear in the spectrum respect to the non-deuterated species. The negative coupling of both ν C=C, which remains as the most intense band, couples weakly with the symmetric ν $C3D_2$, lieing at 1876, 1879, and 1872 for M1, M2, and M3, respectively, indicating no important effects on this vibrational frequency. Also the positive coupling of both ν C=C changes because it couples with δ $C3D_2$, shifting their values up to 1189, 1193, and 1184 cm^{-1} for M1, M2, and M3, respectively. Also the ρ $C3D_2$ shifts down to 793, 796, and 793 cm^{-1} for different adsorption sites, but it does not affect the spectrum due to its very low intensity. Finally, for the fully deuterated system (C_3H_3-d3 + D) no important differences exist respect to the non-deuterated spectrum. Only the negative coupling of both ν C=C couples with the ν C1−D and the symmetric ν $C3D_2$. This coupling causes a weak decrease of the frequency to 1865, 1869, and 1862 for M1, M2, and M3, respectively.

In the case of adsorbed H on Cu(111), three VNMs appeared at 1050 and 875(2) cm^{-1}, corresponding the first one to the frustrated translation of H atom on the direction perpendicular to the surface (ν H−M $\perp$) and the second ones to the parallel frustrated translations (ν H−M $\parallel$). When C_3H_3 specie is added to this system, the local C_3 symmetry of the system is broken, and vibrational frequencies and modes are strongly affected depending on which place C_3H_3 is adsorbed respect to the position of H atom, i.e., which coadsorption system we obtain. For M1 and M3, the ν H−M $\perp$ appears at 1096 and 1027 cm^{-1}, respectively, but for M2, two ν H−M $\perp$ appear at 1302 and 966 cm^{-1}, because H does not move only in z-direction, but also couples with one of the ν H−M $\parallel$. For M1, two very clear ν H−M $\parallel$ appear at 999 and 961 cm^{-1}, being in a more energetic zone than in the case of isolated H on surface. For M2, only one ν H−M $\parallel$ at 782 cm^{-1} appears. In the case of M3, these VNMs appear at 1248 and 956 cm^{-1}, which are more energetic values than the obtained for isolated H (because H−M distance is shorter for M3, 1.67 Å in front ∼1.70 Å for M1 and M2). All these VNMs do not imply a large variation in dipolar moment and their relative intensity in all cases is small, $<$3% of the most intense band of the spectrum. For C_3H_3-d1 + H no changes exist respect to the non-deuterated species. For C_3H_3-d2 + D and for C_3H_3-d3 + D changes are the same. For M1 and M3 the ν D−M $\perp$ shifts down to 780 and 730 cm^{-1}, respectively, and both ν D−M $\parallel$ go down to 707 and 683 cm^{-1} for M1 and to 885 and 678 cm^{-1} for M3. For M2, like the undeuterated system, ν D−M $\perp$ couples with a ν D−M $\parallel$. For

UNIVERSITAT ROVIRA I VIRGILI
ORGANIC MOLECULES ON METAL SURFACES: FORECASTING STRUCTURES AND SPECTRA
Benjamí Martorell Masip
ISBN:978-84-691-9747-9 /DL: T-1259-2008

the deuterated system they also couple with δ C3D_2. So, these three bands, at 927, 921, and 686 cm^{-1}, are related to ν D−M $\|$. The other ν D−M $\|$ is 555 cm^{-1}.

Below 900 cm^{-1}, there is the region where the C−H bending out-of-plane, the C−C−C bending in-plane and out-of-plane and C−M stretching modes appear. For all coadsorption modes these VNMs are very similar, so they will be commented together. At 840 cm^{-1} for M1 and 837 cm^{-1} for M2 and M3 appears the negative coupling of γ C1−H with τ C3H_2, and the positive coupling at 255, 334, and 265 cm^{-1}, for each coadsorption mode, respectively, but none of them is visible in the spectra. The band that is visible in the spectra is the one corresponding to the ω C3H_2 (in the range from ∼33% to ∼50% respect to the most intense bands, depending on the adsorption mode), which lies at 765, 766, and 758 cm^{-1} for each adsorption site, respectively. Another weak band is visible at 507, 503, and 498 cm^{-1}, which corresponds to the negative coupling of δ C1−C2−C3 with ν C1−M. The positive coupling (not intense) of this last VNM appears at 289, 290, and 287 cm^{-1}. Finally the γ C1−C2−C3 appears at 364, 361, and 355 cm^{-1}. In the case of C_3H_3-d1 + H no visible changes exist in the spectrum in this region, because the only affected VNMs are those that correspond to γ C1−D, which is still coupled with τ C3H_2, appearing the negative coupling at 695, 688, and 690 cm^{-1} for M1, M2, and M3, respectively, and the positive one at 240, 305, and 242 cm^{-1}, respectively. For C_3H_3-d2 + D and for C_3H_3-d3 + D, the most important change is the shifting down of the ω C3D_2 mode to 613, 612 and 606 cm^{-1} for M1, M2, and M3, respectively, which is the main change that can be observed in the spectra in this region. From figure 5.9, it is clear that the major effect of deuteration on the overall spectrum affects only the band just below 800 cm^{-1} (ω C3H_2).

Finally, no important differences were found if C1 was placed on fcc or hcp-sites.

5.2.3.5 RAIR spectra on the 3×3 unit cell.

In the table 5.16 are presented the vibrational frequencies and their assignation for coadsorbed C_3H_3 + H on Cu(111) when a 3×3 unit cell is used. Also absolute intensities are presented in this table, and it can be observed that M1 and M2 behave different that M3 in intensity, because M3 has an adsorption mode similar to the one that has on the 2×2 unit cell, but M1 and M2 are more similar to the one that has isolated C_3H_3 on the 3×3 unit cell. Maximum

UNIVERSITAT ROVIRA I VIRGILI
ORGANIC MOLECULES ON METAL SURFACES: FORECASTING STRUCTURES AND SPECTRA
Benjamí Martorell Masip
ISBN:978-84-691-9747-9 /DL: T-1259-2008

Table 5.16: Vibrational frequencies and intensities for C_3H_3 and H coadsorbed on Cu(111) 3×3 unit cell. Frequencies in cm^{-1}; intensities in $km{\cdot}mol^{-1}$.

Coadsorbed C_3H_3 & H on Cu(111)						
	M1		M2		M3	
Assignation (M1 / M2 / M3)	$\bar{\nu}_e$	I	$\bar{\nu}_e$	I	$\bar{\nu}_e$	I
asym. ν $C3H_2$	3136	0.43	3135	0.06	3130	1.2
sym. ν $C3H_2$	3049	0.88	3052	1.01	3054	2.7
ν C1−H	3009	0.06	3015	0.04	2894	2.3
ν C1=C2 - ν C2=C3	1750	3.91	1775	3.78	1888	120.6
δ $C3H_2$	1391	1.4	1388	1.22	1384	3.0
ν H*−M ($\perp$)	1132	0.13	1150	1.72	1202	1.4
ν C1=C2 + ν C2=C3 + (1)	1016	0.28	1029	0.13	1115	0.3
ρ $C3H_2$ / (2) / (1)	980	0.02	991	0.15	1047	0.3
(1) / ρ $C3H_2$ / ρ $C3H_2$	963	6.55	973	0.43	951	0.2
(2) / (1) / (3)	956	0.01	950	6.07	921	0.3
(3) / (4) / (4)	830	0.66	793	0.44	816	0.3
γ C1−H / $\omega C3H_2$ / (2)	797	0.08	762	14.82	793	0.1
ω $C3H_2$ / (3) /ω $C3H_2$	777	11.83	714	0.94	762	64.6
(5) / (5) / (6)	516	0.67	498	1.62	450	8.1
(6) / (6) / (7)	424	0.38	413	0.10	340	0.0
(7) / (7) / (5)	229	0.27	292	0.95	299	0.0

(1):δ C1−H; (2): ν H*−M ($\parallel$); (3): ν H*−M ($\parallel$) + ν H*−M ($\perp$); (4): γ C1−H - τ $C3H_2$; (5): γ C1−H + τ $C3H_2$; (6): δ C1−C2−C3 - ν C1−M; (7): γ C1−C2−C3.

intensity in M3 (121 $km{\cdot}mol^{-1}$) is ten times the maximum obtained for M1 and M2 (12 and 15 $km{\cdot}mol^{-1}$, respectively). Although the different adsorption modes, the assignations are very similar in all cases, as can be observed in table 5.16, but differences in intensity make spectra really different. In figure 5.10 are presented the RAIR spectra for the three adsorption modes on the 3×3 unit cell. For M3, the most intense bands have been truncated.

Like other hydrocarbons studied in this thesis, bands in the C−H stretching region are very weak. For M2 only the symmetric ν $C3H_2$ band is visible (at 3052 cm^{-1}), whereas for M1 and M3 both asymmetric and symmetric ν $C3H_2$ modes have some intensity (M1: 3136 and 3049; M3: 3130 and 3054 cm^{-1}). Moreover, for the M3 structure C1−H stretching mode is also visible and appears at 2894 cm^{-1}. Among these three minima, ν C1−H band has the lowest frequency value for M3. This frequency variation ($\sim$100 cm^{-1}) is just enough to conclude that C1−H bond on M3 is the most activated one. This fact agree with the minor H1−M distance of this system (2.15 for M3 vs. 2.45 Å for M1 and M2).

UNIVERSITAT ROVIRA I VIRGILI
ORGANIC MOLECULES ON METAL SURFACES: FORECASTING STRUCTURES AND SPECTRA
Benjamí Martorell Masip
ISBN:978-84-691-9747-9 /DL: T-1259-2008

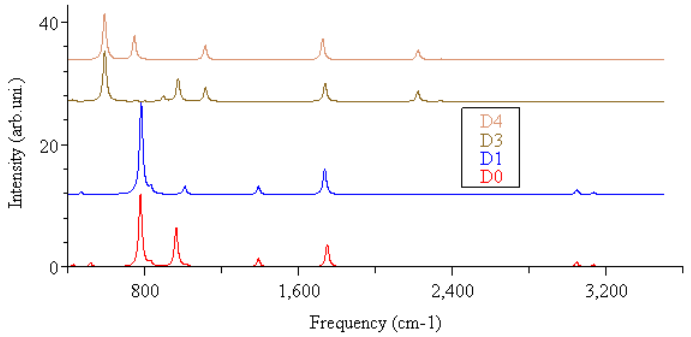

(a) M1.

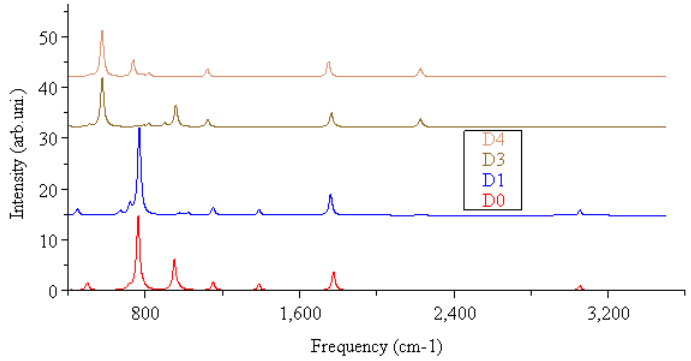

(b) M2.

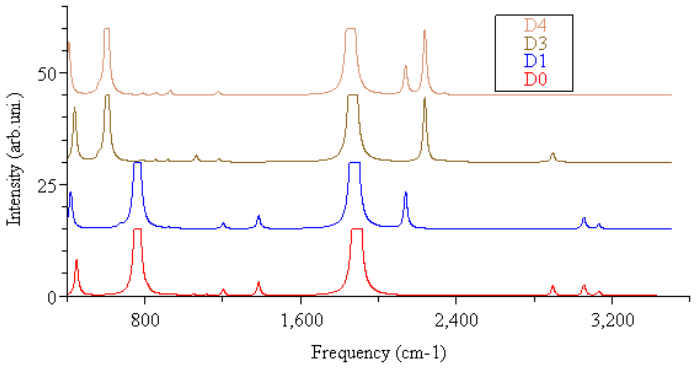

(c) M3.

Figure 5.10: RAIR spectra for coadsorbed C_3H_3 and H for a) M1, b) M2, and c) M3 (truncated) adsorption modes on the 3×3 unit cell of Cu(111). D0: C_3H_3 + H; D1: DC−C−CH_2 + H; D2: HC−C−CD_2 + D; D3: C_3D_3 + D.

UNIVERSITAT ROVIRA I VIRGILI
ORGANIC MOLECULES ON METAL SURFACES: FORECASTING STRUCTURES AND SPECTRA
Benjamí Martorell Masip
ISBN:978-84-691-9747-9 /DL: T-1259-2008

For the monodeuterated system ($DC{-}C{-}CH_2$ + H) only ν C1−D is affected. The frequency value goes down to 2226, 2232, and 2139 cm^{-1} for M1, M2, and M3, respectively. For M3 its intensity increases and becomes a medium band. However, as we comment below, this mode couples with the band between ∼1700 and ∼1900 cm^{-1}, modifying in some extent the intensity of that band, specially for M3. For $HC{-}C{-}CD_2$ + D, asymmetric and symmetric $C3D_2$ stretching mode go down to 2341-2222 for M1, 2340-2225 for M2, and 2235-2238 cm^{-1} for M3. For M3 its intensity increases and becomes a medium band. Like ν C1−D mode of D1, symmetric ν $C3D_2$ couples with the band between ∼1700 and ∼1900 cm^{-1}, decreasing its intensity. Finally, for fully deuterated system (D4) the position of asymmetric ν $C3D_2$ is just the one of D3. However, ν C1−D and symmetric ν $C3D_2$ couple for M1 and M2, increasing the frequency of symmetric ν $C3D_2$ and decreasing the value of ν C1−D (2227-2221 for M1, 2233-2224 cm^{-1} for M2, for the negative and positive coupling, respectively) except for M3 (sym. ν $C3D_2$: 2238; ν C1−D: 2139 cm^{-1}). For M3 two medium bands exist on spectrum, corresponding to ν C1−D and ν $C3D_2$. In this case, symmetric ν $C3D_2$ and ν C1−D couple with the band at ∼1700 -1900 cm^{-1}.

Let's focus now in the RAIR middle-zone, where bands associated toC=C stretching, C−H bending and H−Cu stretching modes are present. The overall spectrum in this region is very different for the tilted structure (M3) respect to the quasi-flat structures (M1 and M2), because the former has a very strong adsorption. The most intense band of this region is always associated with the negative coupling of both ν C=C. Frequency value is 1888 cm^{-1} for M3, whereas for the flat structures, M1 and M2, is at lower frequencies (1750 and 1775 cm^{-1}, respectively). Regarding band intensities, it is important to emphasise that its intensity changes dramatically as a function of the tilt angle of the adsorbate respect to the surface, from 120 to 4 $km{\cdot}mol^{-1}$ for M3 and M1-M2, respectively. Moreover, the intensity of this band for the 2×2 unit cell is between 90-140 $km{\cdot}mol^{-1}$ for all minima (all of them tilted above 40° respect to the surface), whereas for C_3H_3 without coadsorbed H (flat structure) the intensity is <1 $km{\cdot}mol^{-1}$. So, the tilting degree of the whole molecule could be associated to the intensity of this band, following the usual reading of the reduced Metal Surface Selection Rule (reduced-MSSR). This band, as we will show in section 5.2.3.6, will be the fingerprint for the $CHCCH_2$ + H tilted structure. The positive coupling of both ν C=C, which is always coupled with δ C1−H, changes also ∼100 cm^{-1} with the relative tilting of the adsorbate respect to the Cu surface (M1 and M2: 1016 and 1029 cm^{-1}; M3: 1115 cm^{-1}), but all of them are very

UNIVERSITAT ROVIRA I VIRGILI
ORGANIC MOLECULES ON METAL SURFACES: FORECASTING STRUCTURES AND SPECTRA
Benjamí Martorell Masip
ISBN:978-84-691-9747-9 /DL: T-1259-2008

weak bands. $C3H_2$ scissoring frequency has a value between 1380 and 1350 cm^{-1}. Its intensity is somewhat larger for the M3 minimum than for the M1 and M2 bands. Contrarily, the C1−H bending in-plane is more intense for flat-like structures than for the tilted one. Moreover, the frequency value increases also $\sim$100 cm^{-1} when molecule tilts (compare 950-963 cm^{-1} for M1 and M2 with 1047 cm^{-1} for M3). Finally, $C3H_2$ rocking mode is not intense whatever the coordination mode to the surface. The frequency values for this mode are 980, 973 and 954 cm^{-1} for M1, M2, and M3, in this order.

Deuteration causes in the stronger band of this region a decrease of frequency values (between 10-30 cm^{-1}) and intensities. As commented before, this is due to the low coupling of this mode with the corresponding ν C−D modes. Scissoring mode does not change on C1 deuteration, but it couples with the positive coupling of both ν C=C on deuteration of C3. The positive coupling appears at 1116, 1123, and 1181 cm^{-1} (for M1, M2, and M3), and presenting always more intensity than the negative combination at lower frequency (895, 898 and 918 cm^{-1}). Rocking mode remains not visible in all deuterated spectra. C1−H bending in-plane mode does not change its position when this H is not deuterated (D3). When all H atoms are deuterated (D4), this band goes down to 745 and 736 cm^{-1} for M1 and M2. These two bands miss part of their intensity due to the change of the corresponding VNM. However, when $C3H_2$ group is not deuterated (D1), the δ C1−D couples with the wagging mode (around 770 cm^{-1} on undeuterated systems), being the positive coupling at higher frequency and intensity (in fact, reinforcing the ω $C3H_2$ intensity). The negative coupling has zero intensity, so it seems that δ C1−D band disappears (frequencies at 781-743 for M1 and 768-734 cm^{-1} for M2). For the tilted M3 structure, this band is not visible and remains without intensity and uncoupled on C1 deuteration (frequency changes to $\sim$805 cm^{-1}).

$C3H_2$ wagging band (at 777 for M1 and 762 cm^{-1} for M2 and M3) is always visible on the spectra. For M3 it is a very strong band, with an intensity more or less the half than the strongest band. For flat-like structures, M1 and M2, this band has a medium intensity, although it is the strongest band of both spectra. The slightly major value for M1 structure could be associated to the presence of the H atom just below the $C3H_2$ unit. Deuteration on C1 has been commented in the previous paragraph for M1 and M2; for M3, band frequency and intensity do not change. When $C3H_2$ unit is deuterated, for M2 and M3 the band moves down to 575 and 605 cm^{-1}, respectively, losing part of its intensity, as expected. For M1, this band couples with the mode associated to the movement

UNIVERSITAT ROVIRA I VIRGILI
ORGANIC MOLECULES ON METAL SURFACES: FORECASTING STRUCTURES AND SPECTRA
Benjamí Martorell Masip
ISBN:978-84-691-9747-9 /DL: T-1259-2008

of the coadsorbed H atom parallel to the surface (but remaining in the C−C−C direction), causing an additional decrease of its intensity.

The presence of the coadsorbed C_3H_3 unit perturbs also the H*−M modes, in the sense that they are not pure perpendicular and parallel modes. However, on table 5.16 we have kept the same notation in order to make easier the comparison with previous results. The higher frequency associated mainly with ν H*−M ($\perp$) is a very weak band for M2 and M3 (1150 and 1202 cm^{-1}) and it is not visible for M1 (1132 cm^{-1}). When this H atom is deuterated (D3 and D4), this band goes to 804, 817, and 854 cm^{-1} (M1, M2, and M3, respectively) without any coupling with other modes. The other two frequency values are associated mainly to ν H*−M ($\parallel$). One of them is not visible on the spectrum because H atom movement is almost parallel to the surface (956 (M1); 991 (M2); 793 (M3) cm^{-1}). For the other one, H atom also moves in the surface normal direction causing a slight increase of its intensity (830 (M1); 714 (M2); 921 (M3) cm^{-1}). For M1 and M2, this band is like an upper and lower shoulder of the ω $C3H_2$ band. For M3 the increase of intensity is not enough to be appreciated on the spectrum. Frequency values do not change on C1 deuteration. For $C3H_2$ and H* deuteration (D3 and D4), frequency values are 703-509 cm^{-1} for M2 and 654-563 cm^{-1} for M3. In the case of M1, these bands couple with ω $C3D_2$, as commented above. The frequency values are 679, 591, and 589 cm^{-1}, but only the ones below 600 cm^{-1} have an appreciable intensity.

C1−H bending out-of-plane and $C3H_2$ twisting modes are not visible in the spectra. For M2 and M3 these modes are coupled (797 and 516 cm^{-1} for M1; 793 and 498 cm^{-1} for M2; 816 and 450 cm^{-1} for M3).

Finally C−C−C bending in-plane mode is mainly associated with frequency values of 424, 413, and 450 cm^{-1} for M1, M2, and M3, respectively. Only for M3 this band has an appreciable intensity. For all deuterated systems, this M3 band increases slightly its intensity.

Finally, no significant differences exist in the spectrum between the adsorption of C1 on fcc and hcp-sites.

5.2.3.6 Comparison of spectra.

In order to understand the effect on the coadsorption at different coverages, we will focus our attention in some mid-IR bands. Table 5.17 shows the selected bands, which are the fingerprints of $CHCCH_2$ + H systems. These bands are the negative coupling of both C=C stretching modes, the $C3H_2$ scissoring, the

UNIVERSITAT ROVIRA I VIRGILI
ORGANIC MOLECULES ON METAL SURFACES: FORECASTING STRUCTURES AND SPECTRA
Benjamí Martorell Masip
ISBN:978-84-691-9747-9 /DL: T-1259-2008

Table 5.17: Vibrational frequencies (cm^{-1}) and intensities ($km \cdot mol^{-1}$) for most significant fingerprints in coadsorbed C_3H_3 and H.

Group A				
	2×2	3×3		
	C_3H_3	C_3H_3	M1	M2
ν C1=C2 - ν C2=C3	1687 / 6	1741 / 2	1750 / 4	1775 / 4
δ C3H_2	1392 / 2	1385 / 1	1391 / 1	1388 / 1
δ C1−H	Non-pure mode	935 / 8	1048 / 2	1043 / 3
ω C3H_2	729 / 6	758 / 10	762 / 15	777 / 12
δ C1−C2−C3	420 / 2	422 / 1	424 / 0	413 / 0

	Group B			
	2×2			3×3
	M1	M2	M3	M3
ν C1=C2 - ν C2=C3	1897 / 106	1899 / 97	1893 / 140	1888 / 121
δ C3H_2	1396 / 6	1393 / 4	1391 / 5	1384 / 3
δ C1−H	963 / 7	950 / 6	1047 / 0	1061 / 0
ω C3H_2	765 / 54	766 / 38	758 / 49	762 / 64
δ C1−C2−C3	507 / 3	503 / 6	498 / 3	450 / 8

C1−H bending in-plane, the C3H_2 wagging and the δ C1−C2−C3 modes. This table has been organised as a function of the degree of tilting of the whole carbonated structure, which also matches with the C2=C3 distance. First group (A) includes flat-like structures (tilt angle $\backsimeq$ 11-16°), which have C2−C3 distance elongated ($>$ 1.35 Å), without the coadsorbed H atom (at low and high coverage regimes) and those structures with the coadsorbed H atom but keeping a flat structure (M1 and M2 at low coverage regime). The other group (B) includes all H coadsorbed structure of high coverage regime and also the M3 structure of low coverage regime, i.e. the ones with the hydrocarbon fragment tilted (tilt angle $\backsimeq$ 40-43°) and a short C2=C3 distance ($\sim$1.31 Å).

For the first group all frequencies are of lower intensity respect to the second group, except the δ C1−H. The main difference between groups A and B are, of course, the intensity associated to the ν C=C mode and the ω C3H_2 mode. These two bands are very strong for group B and are medium (or even weak) bands for flat-like structures. This rule is also valid for δ C3H_2 mode and C−C−C bending in-plane, although the effect is not so dramatic. C1−H bending in-plane mode has been selected because for H coadsorbed systems only has some intensity for M1 and M2 adsorption structures. Regarding frequency values, the most important change is the variation of ν C=C position. The

UNIVERSITAT ROVIRA I VIRGILI
ORGANIC MOLECULES ON METAL SURFACES: FORECASTING STRUCTURES AND SPECTRA
Benjamí Martorell Masip
ISBN:978-84-691-9747-9 /DL: T-1259-2008

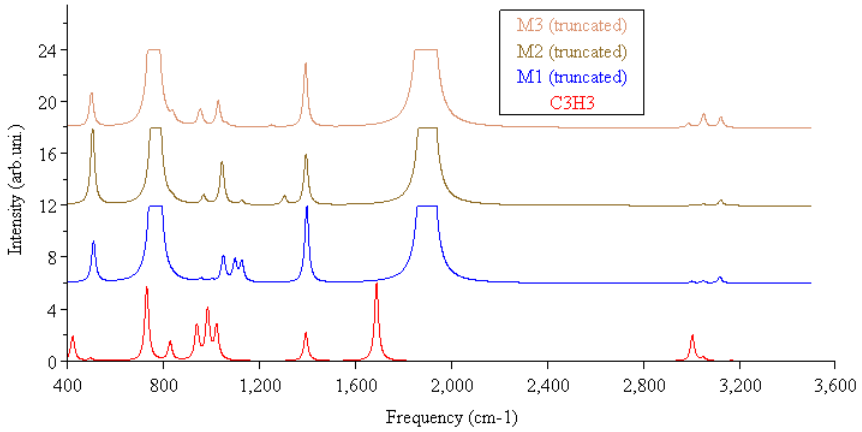

(a) 2x2 unit cell.

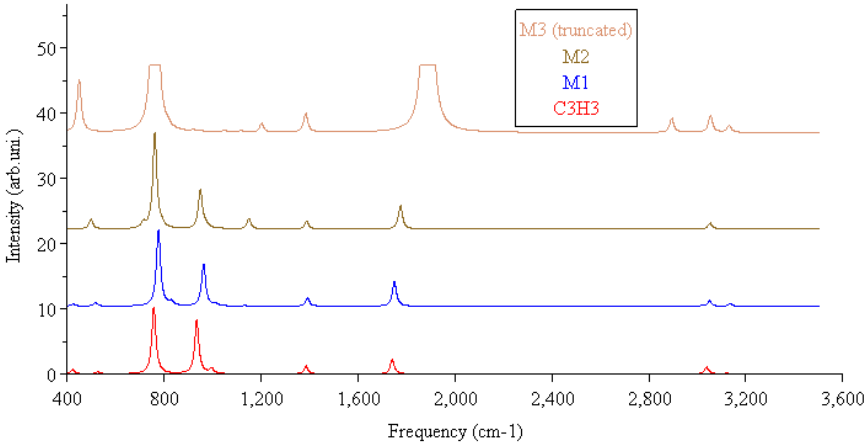

(b) 3x3 unit cell.

Figure 5.11: Comparison of the spectra on every unit cell for all C_3H_3 adsorption modes. From bottom to top: C_3H_3, M1, M2, and M3.

presence of H atom displaces this frequency to higher values. The effect is specially important if the hydrocarbon fragment is tilted away from the surface, with an additional increase of $\sim$100 cm^{-1}. Only the effect of H coadsorption pushes up δ C1$-$H and ω $C3H_2$ modes. Finally, δ $C3H_2$ mode does not change band position neither due H coadsorption nor due to the degree of tilting of the hydrocarbon fragment.

In figure 5.11 are presented together the spectra corresponding to the adsorption of C_3H_3 and the coadsorption modes, M1, M2, and M3 on Cu(111) on

UNIVERSITAT ROVIRA I VIRGILI
ORGANIC MOLECULES ON METAL SURFACES: FORECASTING STRUCTURES AND SPECTRA
Benjamí Martorell Masip
ISBN:978-84-691-9747-9 /DL: T-1259-2008

two different unit cells: 2×2 and 3×3. All of them have already been presented in the last sections, but now are presented in the same image to find out the fingerprints of specie on these unit cells.

Differences between species of group A and B have been commented in last paragraphs and it has been demonstrated to be possible to distinguish them. But between the species of the same group is a more complicated work. In group A is possible to distinguish between adsorbed C_3H_3 specie on the 2×2 unit cell from the species adsorbed on the 3×3 unit cell, because it presents the medium ν C=C band at lower frequencies (1687 cm^{-1} in front ∼1750 cm^{-1} for 3×3 unit cell and weak) and a wide band associated to δ C1−H is present at ∼1000 cm^{-1}. To distinguish the three possible structures of group A on the 3×3 unit cell is not possible because their spectra are almost equal. In the case of group B, only one specie (M3) is present for 3×3 unit cell, which can be easily distinguished from the species on the 2×2 unit cell because the intensity of the δ $C3H_2$ is a bit lower in this case and the δ C1−C2−C3 is ∼50 cm^{-1} to lower frequencies (450 cm^{-1} in front >500 cm^{-1} for 2×2 unit cell). The fingerprint of the three species on the 2×2 unit cells are so similar in three cases that they cannot be distinguished at all.

5.2.4 Dehydrogenation and hydrogenation processes: transition states.

Once we have studied the thermodynamic of the dehydrogenation (dhy) and hydrogenation (hy) process, we could try to find transition states that connect the different minima. In this section we will present these transition states. After that, we will compare the reaction energy profiles of the direct isomerisation reaction from Pr to VC respect to the surface-mediated reaction, i.e. the dhy and subsequent hy, following the Horiuti-Polanyi mechanism.

5.2.4.1 Adsorption modes of TS dhy and TS hy: energetics.

Between adsorbed Pr and adsorbed VC in C1-trans structure we have found two new transition states. One of them connects adsorbed Pr with the dehydrogenated $CHCCH_2$ fragment and coadsorbed H on the same direction that C−C−C skeleton (M1), thereafter dehydrogenation TS or TS dhy. The other one links dehydrogenated $CHCCH_2$ fragment with one coadsorbed H atom near C2 atom (M3) with VC in C1-trans structure (consequently, hydrogenation TS or TS hy). Both TSs are showed in figure 5.12. Like other TS structures of

UNIVERSITAT ROVIRA I VIRGILI
ORGANIC MOLECULES ON METAL SURFACES: FORECASTING STRUCTURES AND SPECTRA
Benjamí Martorell Masip
ISBN:978-84-691-9747-9 /DL: T-1259-2008

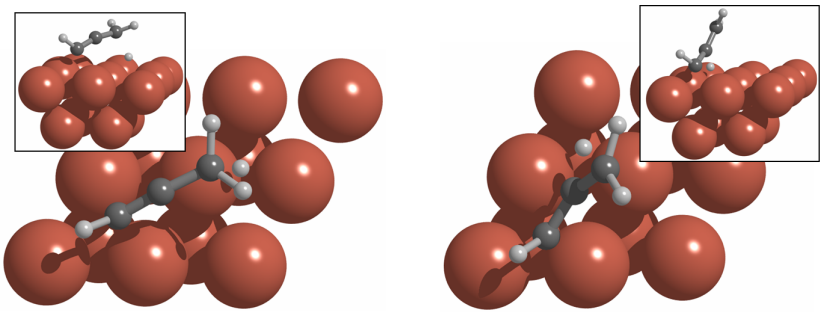

(a) TS dhy from Pr to M1. (b) TS hy from M3 to VC-trans.

Figure 5.12: Transition states involved in dehydrogenation-hydrogenation process on Cu(111).

this chapter, transition states were characterised with a frequency calculation and subsequent optimisation process from the TS geometry following the corresponding imaginary vibrational modes on both senses. The imaginary frequency is in the range from 900 to 1100 cm^{-1}. No important differences in adsorption modes exist between 2×2 and 3×3 unit cells.

Dehydrogenation TS (TS dhy) has structure that is in the middle from Pr and M1, i.e., the migrating H is placed on a bridge-site, the carbonated structure becomes almost linear, and it is a tilted structure (∼25°-30°), which permits the interaction of C3 with a top-site. Hydrogenation TS presents a structure more similar to VC C1-trans than to M3, because the carbonated structure is not linear like in M3, but it is bent, C2 goes down to the surface to make easier the addition of the coadsorbed H atom from surface to C2, and the $C3H_2$ unit is already tilted, because in the case of M3, it is parallel to surface, and in VC-trans it is perpendicular. Despite H atoms number and position, TS hy is similar to the adsorption mode of Pr in other metal surfaces (Pt, Pd and Rh), with C1−C2 bond located on a hollow-site and parallel to a M−M bond [97]. Finally, no differences exist between the TS structures depending on C1 atom position (fcc or hcp-site).

In table 5.18 are presented the ZPE uncorrected and corrected adsorption energies of TS structures respect to Pr in gas phase. For all TS structures, the energy is above the energy to desorbe Pr molecule. We can advance that energy barriers are smaller than in the case of the direct isomerisation from Pr to VC C1-trans. This will be commented in more detail in section 5.2.5.

The addition of ZPE correction makes the barrier to be reduced in ∼15

UNIVERSITAT ROVIRA I VIRGILI
ORGANIC MOLECULES ON METAL SURFACES: FORECASTING STRUCTURES AND SPECTRA
Benjamí Martorell Masip
ISBN:978-84-691-9747-9 /DL: T-1259-2008

Table 5.18: Transition state energies of dehydrogenation and hydrogenation reaction respect to Pr in gas phase (In brackets values respect to adsorbed Pr. All values are given in kJ·mol^{-1}).

E 2×2 unit cell					
	No ZPE	ZPE	ZPE-d1	ZPE-d3	ZPE-d4
TS dhy C1-fcc	95.2 (174.3)	79.9	79.4	84.8	84.4
TS dhy C1-hcp	97.7 (177.2)	82.3	81.8	87.3	86.8
TS hy C1-fcc	90.2 (169.4)	75.6	75.4	80.0	79.8
TS hy C1-hcp	93.1 (172.6)	78.3	78.1	82.7	82.5
E 3×3 unit cell					
	No ZPE	ZPE	ZPE-d1	ZPE-d3	ZPE-d4
TS dhy C1-fcc	68.8 (166.5)	51.2	50.9	56.2	55.8
TS dhy C1-hcp	67.9 (166.0)	50.2	49.9	55.3	54.9
TS hy C1-fcc	64.3 (161.9)	53.8	53.6	58.3	58.1
TS hy C1-hcp	66.1 (164.2)	52.8	52.6	57.2	57.1

kJ·mol^{-1} for dehydrogenation TS for both unit cells and for hydrogenation TS on the 2×2 unit cell, and ∼10 kJ·mol^{-1} for the hydrogenation process on the 3×3 unit cell. This is due to the lost of one vibrational C−H frequency respect to Pr in gas phase, and also to the fact that C−C stretching modes are not so high in energy respect to Pr in gas phase, which owns a triple C≡C bond. So, only ZPE corrected values will be commented. It can be observed that the energy of TSs on the 2×2 unit cell is larger than on the 3×3 unit cell. For the dehydrogenation process, on the 2×2 unit cell the energy is 80 kJ·mol^{-1} and on the 3×3 unit cell is 51 kJ·mol^{-1}, which means an energy difference of 29 kJ·mol^{-1}. For adsorbed Pr this difference is 19 kJ·mol^{-1} and for VC on C3-top structure it is 41 kJ·mol^{-1}. So, high coverages situations pushes up all energy values for the dehydrogenation reactions, indicating an important effect of lateral interactions. For the case of hydrogenation TS, this difference is somewhat smaller, 22 kJ·mol^{-1}, indicating that lateral interactions are not so important, as can be deduced from the different structure of this TS, which is not so flat on the surface. However, its carbonated structure is more similar to the one of adsorbed Pr, so lateral interactions are similar to the ones that Pr suffers.

Another important feature is that dehydrogenation and hydrogenation TSs have almost the same energies, being their difference <5 kJ·mol^{-1}. Note that for both TSs structures the migrating H atom is near the surface, so energy differences are more similar to ones found for the $CHCCH_2$ + H structures than

UNIVERSITAT ROVIRA I VIRGILI
ORGANIC MOLECULES ON METAL SURFACES: FORECASTING STRUCTURES AND SPECTRA
Benjamí Martorell Masip
ISBN:978-84-691-9747-9 /DL: T-1259-2008

to the adsorbed Pr or VC species. If temperature is enough to achieve TSs energy, as both TS lies at similar energy the final amount of adsorbed Pr and VC C1-trans will be related to the different adsorption energy of both isomers (although the Pr desorption will be always a competitive process).

From energy barriers respect to the adsorbed Pr (values in brackets in table 5.18), we can observe a decrease of $\sim$10 kJ·mol^{-1} as coverage is reduced from 1/4 to 1/9. Contrarily, the energy barrier from adsorbed Pr for the direct isomerisation does not change with coverage, although strongly affects the thermodynamics of the reaction. Finally, from an energetic point of view, no important differences exist related to the position of C1 on fcc or hcp-site, being in all cases the fcc-site lower in energy, except for the hydrogenation TS on the 2×2 unit cell.

5.2.4.2 TS dhy and hy: geometric parameters.

In table 5.19 are presented the geometrical parameters for both TSs. In both cases only values for C1 adsorbed on fcc-site are presented, because the differences between them are almost non-existing. Values are given only for the 3×3 unit cell when differences are small, but differences larger than ±0.02 Å in distances and ±1° in angles respect to the 2×2 unit cell are taken into account and are presented in brackets.

For the dehydrogenation TS (from Pr to M1) the C1−C2 distance (1.29 Å) is shorter than the C2−C3 (1.37 Å). The C2−C3 distance has a value similar to the products, M1. However, in the TS structure, the C1−C2 distance is shorter than in the adsorbed Pr and M1 structure, being closer to this last one. Another important parameter is the distance of the migrating H atom (H*) respect to the methylenic carbon (C3), which changes with coverage. For the 3×3 unit cell it is 1.59 Å, whereas for the 2×2 unit cell it is larger (1.67 Å). Two other parameters are related to this fact. First of all, the angle that forms C1−C2 bond with the surface is larger on the 2×2 unit cell (32°) than on the 3×3 unit cell (25°), and besides, the C1−C2−C3 angle is closer on the 2×2 unit cell (161°) than on the 3×3 (167°), so for the 2×2 unit cell, C3 is further from the surface (H atom does not change its position respect to the surface, being in both unit cells 1.72 Å the distance respect to the nearest Cu atom). H1 is almost placed on the same plane than all carbon atoms, and H3 and H4 have very similar dihedral angles (111° and -105°, respectively), making this structure to be almost symmetric respect to the C1−C2−C3 plane. Finally, agostic interaction between H1 and

UNIVERSITAT ROVIRA I VIRGILI
ORGANIC MOLECULES ON METAL SURFACES: FORECASTING STRUCTURES AND SPECTRA
Benjamí Martorell Masip
ISBN:978-84-691-9747-9 /DL: T-1259-2008

Table 5.19: Dehydrogenation and hydrogenation TS geometrical parameters for 3×3 unit cell (2×2 unit cell when values differences are larger than 0.02 Å or 1.0°).

	TS-dhy.	TS-hy.
[a]d(C-H*)	1.59 (1.67)	1.63 (1.67)
d(C1-C2)	1.29	1.38
d(C2-C3)	1.37	1.34
[b]α(C1-C2-C3)	166.9 (161.4)	145.4 (147.9)
α(H1-C1-C2)	124.4	113.7
α(H3-C3-C2)	117.9 (119.5)	123.0
α(H4-C3-C2)	117.3 (119.0)	119.2
α(H3-C3-H4)	114.8 (113.7)	117.8
[c]θ(H1-C1-C2-C3)	173.2 (177.4)	47.1 (48.9)
θ(H3-C3-C2-C1)	111.6 (107.2)	-171.1 (-169.3)
θ(H4-C3-C2-C1)	-104.7	11.2 (13.6)
[d]tilt	24.5 (32.0)	25.4 (27.8)
[e]d(C1-M)	2.15 (2.11)	2.01
d(H1-M)	2.73	2.24
d(H*-M)	1.72	1.71

[a]d: distance, for TS-dhy. it is C3−H* distance, for TS-hy is C2−H* (Å); [b]α: angle (degrees); [c]θ: dihedral angle (degrees); [d]tilt: angle that forms C1−C2 bond with the surface plane; [e]d: distance to nearest surface atom (Å).

Cu atoms does not exist due to the large H1−M distance.

In the TS-hy, from M3 to VC C1-trans, the C1−C2 distance (1.38 Å) is a bit larger than the C2−C3 (1.34 Å). For VC C1-trans structure both distances are 1.45 and 1.36 Å, respectively, whereas for M3 are almost equal and shorter (1.32 and 1.31 Å, respectively) . The C2−H* distance is 1.63 Å, a typical C−H distance of the migrating H for a hydrogenation-dehydrogenation TS [95]. This distance is a bit larger on the 2×2 unit cell (1.67 Å), being the reason the same than for the TS dhy. Another important feature of this structure is that the $C3H_2$ is rotated, among the position of M3 and VC C1-trans. Finally, an agostic interaction between H1 and the surface could exist, because H1−M is shorter (2.24 Å) than the same distance in the TS dhy.

5.2.5 Reaction profiles.

In figures 5.13 are presented the reaction profiles from Pr to adsorbed VC C1-trans on Cu(111) on both unit cells, 2×2 and 3×3. In these profiles it has been

UNIVERSITAT ROVIRA I VIRGILI
ORGANIC MOLECULES ON METAL SURFACES: FORECASTING STRUCTURES AND SPECTRA
Benjamí Martorell Masip
ISBN:978-84-691-9747-9 /DL: T-1259-2008

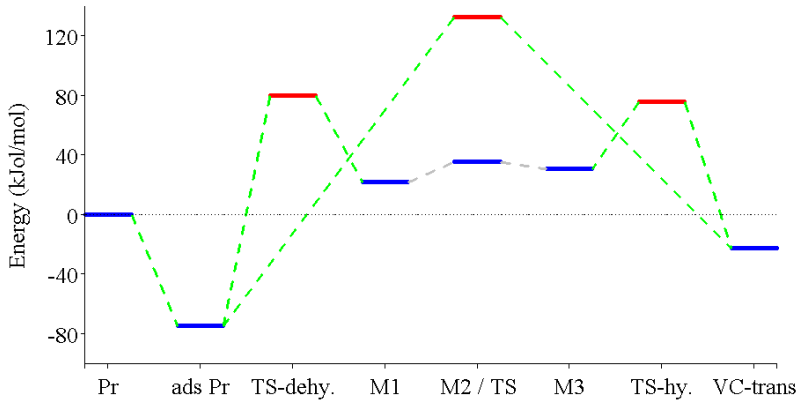

(a) Reaction profile in a 2x2 unit cell.

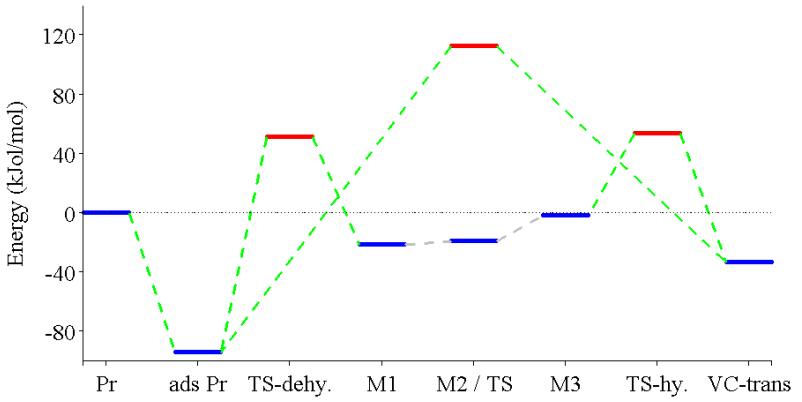

(b) Reaction profile on a 3x3 unit cell.

Figure 5.13: Reaction profiles for the isomerisation from Pr to VC C1-trans: through the direct transposition and through the dhy-hy process.

omitted the interconversion among different VC isomers because it has been already shown in figure 5.1. For both unit cells, the reaction profiles show the path of the TS in the direct isomerisation and the pathway through a dhy-hy process. The direct isomerisation takes place only in one step, but it is the most energetic process (133 kJ·mol^{-1} for 2×2 unit cell and 113 kJ·mol^{-1} for 3×3) becoming the most disfavoured by energetic criterions.

On the other hand, the dehydrogenation-hydrogenation process is, in general, a less costing energetic process, but it involves three intermediates and two transition states (besides the diffusion of H atom on surface), i.e., entropic effects

UNIVERSITAT ROVIRA I VIRGILI
ORGANIC MOLECULES ON METAL SURFACES: FORECASTING STRUCTURES AND SPECTRA
Benjamí Martorell Masip
ISBN:978-84-691-9747-9 /DL: T-1259-2008

could play an important role. However, for the dhy-hy path, both barriers are lower than the direct isomerisation process: ∼80 kJ·mol^{-1} for the 2×2 unit cell and ∼50 kJ·mol^{-1} for the 3×3 unit cell. The large difference between both paths are large enough to rule out the direct isomerisation.

In the interconversion process among different coadsorption sites, the most important factor is supposed to be the diffusion of H atom on surface. It has been evaluated in section 5.2.1 that this diffusion is almost a non-activated when H is adsorbed alone on surface (energy barrier of 13 kJ·mol^{-1}), so it should be supposed that in this case the interconversion from one coadsorption mode to another one will not be a limiting step in the overall process, because the interconversion among them is basically the diffusion of H on surface, which is a very easy process to occur. So in figure 5.13 it has been drawn this process in grey colour because it has not been checked.

Finally, as an opened point of this thesis, it would be interesting to study other possible reaction paths when adsorbed Pr is dehydrogenated. For instance, C_3H_3 could hydrogenate to yield propadiene instead of VC. Or VC could dehydrogenate to yield the specie CHCHCH, which could also dimerise to yield benzene. Possibilities are multiple and this thesis has only been one more step in the global understanding of the dimerisation of Pr.

5.3 Final summary.

In this chapter we have studied the kinetic aspects in the direct interconversion from Pr to VC on the (111) surface of Cu, Pt, Pd and Rh. Moreover, in the case of Cu the direct isomerisation is not a possible pathway and we searched another possible reaction path to yield VC. In this last study, we have characterised a new specie on Cu surface, C_3H_3, and the coadsorption of this specie with H. With all this information, we have been capable of answering the questions that were raised at the beginning of this chapter:

- We have studied the direct isomerisation from Pr to VC C1-trans on two different unit cells: 2×2 and 3×3. Metals can be divided in:
  - Cu: metal with a high H-transposition barrier. 133 kJ·mol^{-1} on the 2×2 unit cell and 113 kJ·mol^{-1} on the 3×3 unit cell.
  - Pd: metal with a barrier similar to the Pr desorption energy: 14 kJ·mol^{-1} on the 2×2 unit cell and 2 kJ·mol^{-1} on the 3×3 unit cell.

UNIVERSITAT ROVIRA I VIRGILI
ORGANIC MOLECULES ON METAL SURFACES: FORECASTING STRUCTURES AND SPECTRA
Benjamí Martorell Masip
ISBN:978-84-691-9747-9 /DL: T-1259-2008

  - Pt and Rh: metals with an isomerisation barrier below the Pr desorption energy: -14 and -35 kJ·mol^{-1} on the 2×2 unit cell and -29 and -27 kJ·mol^{-1} on the 3×3 unit cell (for Pt and Rh, respectively).

- Different VC isomer interconvert differently among them on the different unit cells for Cu(111):

  - On the 2×2 unit cell three VC structures exist. Between C1-cis and C3-top structures no TS was found for the interconversion, but between C1-trans and C1-cis it exists. It has an energy of 5 kJ·mol^{-1}.
  - On the 3×3 unit cell three different VC structures exist. No connecting TS among them was found.
  - On the other metals lateral interactions are small, so it has been supposed to have the same behaviour as on Cu(111) on the 3×3 unit cell: no TS exists among them.

- The direct isomerisation for Cu is a too high demanding process, so we studied an alternative mechanism (dhy-hy).

- H atom adsorbs on a hollow-site. Its E_{ads} depends on the unit cell used: -23 kJ·mol^{-1} for 2×2 and -44 kJ·mol^{-1} for 3×3. Vibrational frequencies are almost the same on both unit cells: ν H*−M ($\perp$) ∼1045 and ν H*−M ($\parallel$) ∼745 cm^{-1}.

- C_3H_3 structure adsorbs via its unpaired electron and the double C2=C3 bond. Its E_{ads} is 21.2 kJ·mol^{-1} on the 2×2 unit cell and -16.6 kJ·mol^{-1} on the 3×3 unit cell.

- The non-interacting coadsorption energy of C_3H_3 + H is -1 kJ·mol^{-1} on the 2×2 unit cell and -61 kJ·mol^{-1} on the 3×3 unit cell, indicating that if no interaction existed between both species, on the 2×2 unit cell the C−H bond break would be competitive to the Pr desorption, and on the 3×3 unit cell the C−H bond break would be the majoritary reaction.

- On the interacting system, three coadsorption modes have been calculated:

  - M1: H* atom is coadsorbed below the $C3H_2$ unit on a hollow site.
    * 2×2 unit cell: E_{ads}= 22 kJ·mol^{-1}; tilt angle = 41°; C2−C3 distance = 1.31 Å.

UNIVERSITAT ROVIRA I VIRGILI
ORGANIC MOLECULES ON METAL SURFACES: FORECASTING STRUCTURES AND SPECTRA
Benjamí Martorell Masip
ISBN:978-84-691-9747-9 /DL: T-1259-2008

    * 3×3 unit cell: E_{ads}= -21 kJ·mol^{-1}; tilt angle = 14°; C2−C3 distance = 1.36 Å.
  - M2: H* atom is coadsorbed next to the $C3H_2$ unit on a hollow site.
    * 2×2 unit cell: E_{ads}= 36 kJ·mol^{-1}; tilt angle = 42°; C2−C3 distance = 1.32 Å.
    * 3×3 unit cell: E_{ads}= -19 kJ·mol^{-1}; tilt angle = 16°; C2−C3 distance = 1.35 Å.
  - M3: H* atom is coadsorbed next to the $C3H_2$ unit and near C2 on a hollow site.
    * 2×2 unit cell: E_{ads}= 31 kJ·mol^{-1}; tilt angle = 43°; C2−C3 distance = 1.31 Å.
    * 3×3 unit cell: E_{ads}= -2 kJ·mol^{-1}; tilt angle = 42°; C2−C3 distance = 1.31 Å.

- The TS from adsorbed Pr to M1 and from M3 to adsorbed VC C1-trans have been calculated and characterised:
  - On the 2×2 unit cell:
    * Dehydrogenation TS energy is 80 kJ·mol^{-1}.
    * Hydrogenation TS energy is 76 kJ·mol^{-1}.
  - On the 3×3 unit cell:
    * Dehydrogenation TS energy is 51 kJ·mol^{-1}.
    * Hydrogenation TS energy is 54 kJ·mol^{-1}.

- The overall process for the Horiuti-Polanyi mechanism is more favourable than for the direct isomerisation process for Cu(111).

- In figure 5.14 are presented the simulated RAIR spectra for all C_3H_4 species on Cu(111) on the 3×3 unit cell.
  - Adsorbed Pr presents a strong band in the ν C−H region and the other structures are very low-intense in this region.
  - The existence of bands between 1600 and 2000 cm^{-1} (negative coupling of both ν C=C) allows us to identify the dehydrogenated structures, because no other structure presents adsorption in this zone. At ∼760 cm^{-1} another important band exists, corresponding to ω

UNIVERSITAT ROVIRA I VIRGILI
ORGANIC MOLECULES ON METAL SURFACES: FORECASTING STRUCTURES AND SPECTRA
Benjamí Martorell Masip
ISBN:978-84-691-9747-9 /DL: T-1259-2008

$C3H_2$. The different tilting degree of the structure makes spectrum very different for M3 respect to M1 and M2.

- M1 and M2 structures are difficult to be distinguished.
- The existence of a strong band at $\sim$1350 cm^{-1} identifies the VC C1-trans structure.
- The flat VC structures (C3-top and C3-hollow) present very weak bands, being the most intense one $\sim$750 cm^{-1}. Both are difficult to be distinguished.

UNIVERSITAT ROVIRA I VIRGILI
ORGANIC MOLECULES ON METAL SURFACES: FORECASTING STRUCTURES AND SPECTRA
Benjamí Martorell Masip
ISBN:978-84-691-9747-9 /DL: T-1259-2008

Figure 5.14: Comparison of RAIR spectra for all calculated species on Cu (111) 3×3 unit cell.

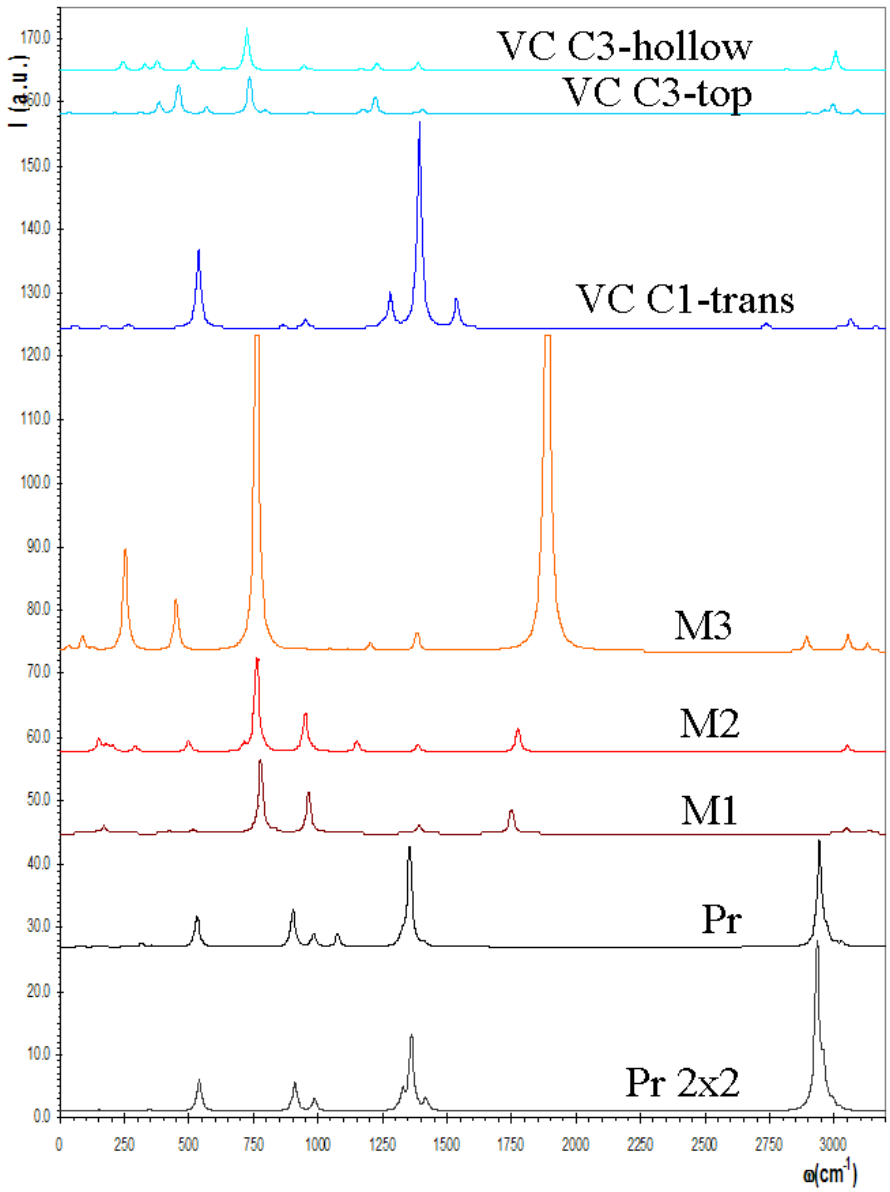

UNIVERSITAT ROVIRA I VIRGILI
ORGANIC MOLECULES ON METAL SURFACES: FORECASTING STRUCTURES AND SPECTRA
Benjamí Martorell Masip
ISBN:978-84-691-9747-9 /DL: T-1259-2008

Chapter 6

NEXAFS spectra for adsorbed molecules.

Following the isomerisation process from Pr to VC using NEXAFS spectroscopy.

Until now we have focused our efforts to simulate RAIR spectra. RAIR spectroscopy is a very powerful tool for experimental chemists and physicists to study the phenomena that occur on a surface, for example, the study of a chemical reaction catalysed by a heterogeneous catalyst [69, 70]. This technique has been used by Toomes et al. *to elucidate the propyne structure on Cu(111) [108]. This technique is based on the interaction of a light source (from 10 to 10000 cm^{-1}) with the system. As a consequence of this interaction, the system can change the vibrational levels, which are associated to the movement of the atomic nuclei. Transitions between different vibrational levels give bands on the IR spectrum, which are mainly related to one (or more) functional group of the molecule. Some of them are the fingerprints of a determined structure and can be used to propose the presence or absence of a concrete structure. Chapters 3, 4, and 5 have been focused to obtain the fingerprints of the RAIR spectra for some organic adsorbates. Moreover, the obtained values could also be used for others IR-band techniques as (HR)EELS.*

Let's focus now in another kind of technique that has also demonstrated to be very sensitive to the chemical environment for adsorbed molecules. In this case, the technique is based on another physical phenomenon and another

UNIVERSITAT ROVIRA I VIRGILI
ORGANIC MOLECULES ON METAL SURFACES: FORECASTING STRUCTURES AND SPECTRA
Benjamí Martorell Masip
ISBN:978-84-691-9747-9 /DL: T-1259-2008

frequency region. NEXAFS spectroscopy is based in the excitation of an inner-shell electron (in our case the 1s electron of C atoms) to the unoccupied orbitals near the ionisation potentials (IP). In the case of C atoms, the IP for 1s electrons is placed around 290 eV, being this value sensitive to the chemical environment. As an example of the sensibility of this technique, Kolzcewsky et al. *were able to differentiate among the three different phenylpropene isomers simulating the NEXAFS spectra at the equilibrium adsorption geometry of these molecules on Cu(111) [36].*

In collaboration with the group of Pr. K. Hermann, who has a large experience in the simulation of NEXAFS spectroscopy [117], we simulated NEXAFS spectra of Pr and VC molecules adsorbed on Cu(111) using the StoBe code. So, the main objectives of this chapter are:

- *To simulate gas phase Pr NEXAFS spectrum and to compare with the experimental one.*
- *To simulate gas phase VC NEXAFS spectrum for two electronic states, the singlet and the triplet state.*
- *To simulate the adsorbed Pr molecule on Cu(111) NEXAFS and to compare it with the spectrum of gas phase Pr molecule.*
- *To simulate the NEXAFS spectrum of adsorbed VC and to compare it with the adsorbed Pr spectrum.*
- *To find out the fingerprints in NEXAFS spectra to follow the isomerisation reaction.*

UNIVERSITAT ROVIRA I VIRGILI
ORGANIC MOLECULES ON METAL SURFACES: FORECASTING STRUCTURES AND SPECTRA
Benjamí Martorell Masip
ISBN:978-84-691-9747-9 /DL: T-1259-2008

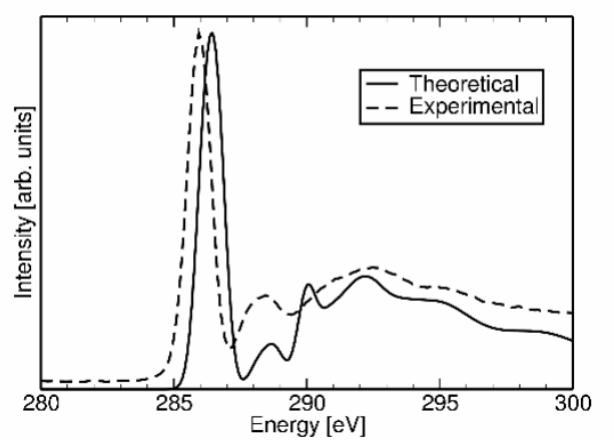

(a) Total spectra.

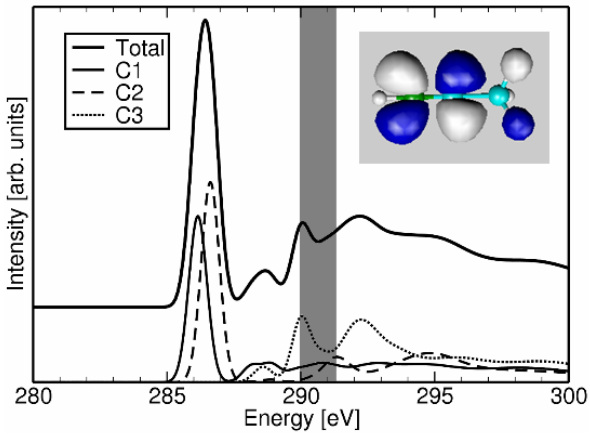

(b) Decomposed spectrum.

Figure 6.1: NEXAFS spectra of gas phase propyne. a) Simulated and experimental NEXAFS spectra. b) Decomposed NEXAFS spectrum and the molecular orbital involved in the most intense transition. The grey strip deals with the range of IP for all carbon atoms.

6.1 Simulation of NEXAFS spectra.

6.1.1 Gas phase propyne.

NEXAFS spectrum of gas phase propyne has been simulated and compared with the experimental one. In figure 6.1(a) it can be observed the good agreement

UNIVERSITAT ROVIRA I VIRGILI
ORGANIC MOLECULES ON METAL SURFACES: FORECASTING STRUCTURES AND SPECTRA
Benjamí Martorell Masip
ISBN:978-84-691-9747-9 /DL: T-1259-2008

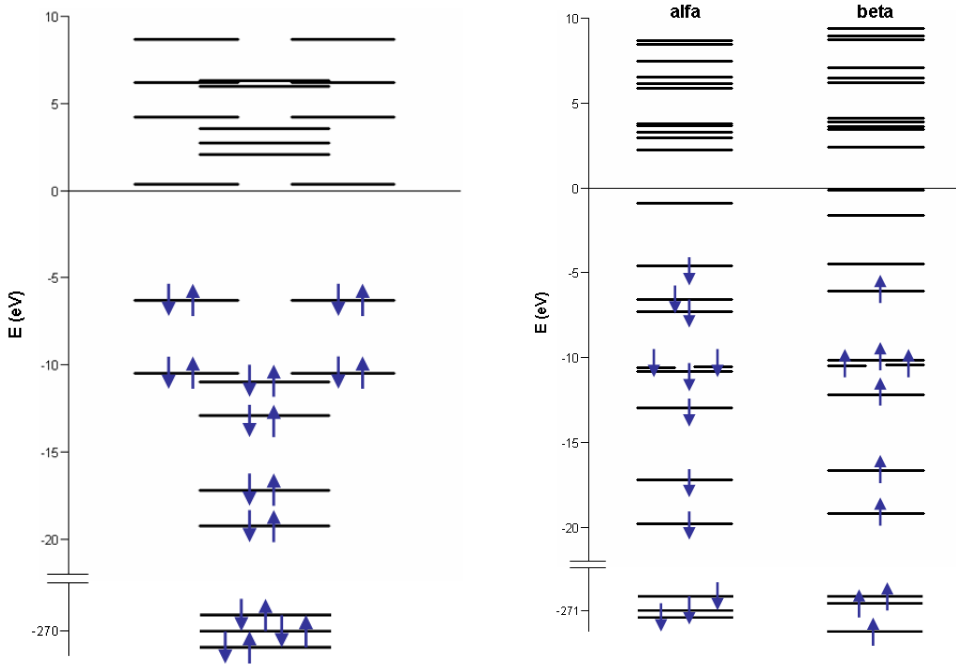

(a) Singlet state. (b) Triplet state.

Figure 6.2: Molecular orbital diagram for gas phase propyne.

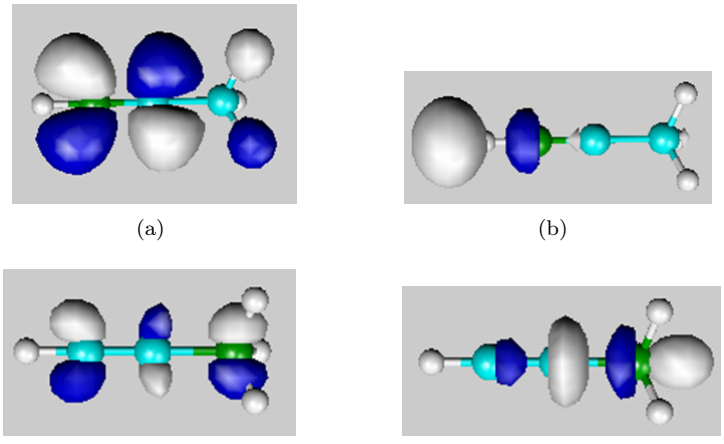

(a) (b)

(c) (d)

Figure 6.3: Final molecular orbitals involved in the transitions of C 1s electrons of propyne.

UNIVERSITAT ROVIRA I VIRGILI
ORGANIC MOLECULES ON METAL SURFACES: FORECASTING STRUCTURES AND SPECTRA
Benjamí Martorell Masip
ISBN:978-84-691-9747-9 /DL: T-1259-2008

between the experimental spectrum and the theoretical one. Only a small shift of 0.5 eV to higher energies is observed for the theoretical spectrum that can be achieved to the NEXAFS calculation method and its approximations. To assign every band to a concrete transition, the individual contributions of each carbon atom of propyne were represented. Moreover, the molecular orbital diagram for gas phase propyne is presented in figure 6.2(a) in order to make easier the discussion of resutls. It can be observed (figure 6.1(b)) that the two atoms that contribute to the triple bond (C1 and C2) are totally different respect to the methylenic one. The acetylenic carbon (C1) has an Ionisation Potential (IP) of 290.0 eV, and it presents a very intense peak at 286.2 eV, due to the excitation of its 1s electron to the π^* C≡C molecular orbital (MO, see figure 6.3(a)). Another less intense peak at 288.2 eV can be assigned to the excitation to the σ^* C1−H MO (see figure 6.3(b)). For the C2 atom the IP is a bit higher, of 290.6 eV. A very intense peak at 286.6 eV corresponds to the excitation of 1s (C2) electron to the π^* C≡C MO. The differences between both carbons could be due to the different charge distribution on these two carbons. The C1 atom presents a Mulliken charge of -0.3 electrons, whereas the C2 is almost neutral, so the 1s (C2) electron is a little bit more stabilised, and more energy is required to take the electron to highest levels. On the other hand, the methylenic carbon (C3) behaves very different from C1 and C2, because it forms a simple C−C bond. The IP of C3 is 291.3 eV, higher than the one of C1 and C2. Besides, C3 has no contribution at the zone of the most intense peak, around 286 eV, but it has contribution in the more energetic peaks. The two most intense peaks of C3 are at 290.1 and 292.3 eV. The peak at 290.1 eV is the excitation to σ^* C3−H MO (see figure 6.3(c)), and the other peak corresponds to the excitation to σ^* C2−C3 bond (see figure 6.3(d)). So, if we compare the experimental spectrum with the theoretical simulation we can conclude that the most intense peak at the experimental spectrum, 285.9 eV, is the excitation of the C1 and C2 1s electron to π^* C≡C, the next peak at 288.4 eV is the excitation of C1 and C3 1s electron to σ^* C−H bond and the broad peak at 292 eV can be assigned to the C3 excitation to σ^* C2−C3 bond.

When propyne is adsorbed on Cu(111), it adopts a bent geometry, similar to the geometry of the gas phase propyne in the low-lying triplet state [60, 36]. So, we decided to simulate the NEXAFS spectrum for gas phase propyne in its triplet state geometry, for both singlet and triplet states. The triplet state geometry presents a C_s symmetry; the acetylenic hydrogen and the methyl group are tilted away in the plane. It can be seen as a propene molecule, where two

UNIVERSITAT ROVIRA I VIRGILI
ORGANIC MOLECULES ON METAL SURFACES: FORECASTING STRUCTURES AND SPECTRA
Benjamí Martorell Masip
ISBN:978-84-691-9747-9 /DL: T-1259-2008

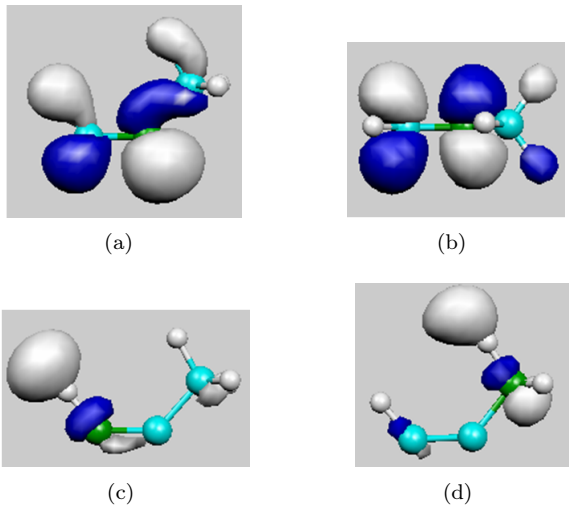

(a) (b) (c) (d)

Figure 6.4: Final molecular orbitals involved in the transitions of C 1s electrons of propyne in C_s geometry (singlet state).

H atoms of the double C=C bond have been removed (one for each carbon). The C1−C2 bond distance is enlarged from the C_{3v} propyne (1.23 Å) to 1.35 Å, typically a double bond distance. The H−C1−C2 angle bends from 180° (^{1}A-C_{3v} state) to 129° in ^{3}A' C_s state, and the C1−C2−C3 angle shifts to 131°. The triplet state is 3.42 eV above the low-lying singlet state for propyne. For the triplet state geometry, the singlet state is 2.14 eV above the C_{3v} propyne (but it is not a minimum).

We have simulated the NEXAFS spectra for the triplet state geometry (C_s geometry) in its triplet state and in singlet state, to be compared with the C_{3v} propyne and the adsorbed Pr. The NEXAFS spectrum of single state Pr with geometry of the triple state is quite different respect to C_{3v} Pr spectrum, as can be observed in figure 6.5(a). The most important difference is the appearance of a very intense peak at 283.2 eV, remaining peaks at 286.0 and around 290.0 eV, decreasing the intensity of the peak at 286.0 eV. The peak at 290.0 eV is due to the methyl carbon of the Pr, like in the C_{3v} Pr. The IP of C3 is in this case 291.5 eV, and the peak at 289.8 eV is due to the excitation of its 1s electron to σ^* C3−H (see figure 6.4(d)). The peak at 286.0 eV is the excitation of the C1 and C2 1s electrons to the π^* C−C MO perpendicular to the plane H−C1−C2 (A" orbital, see figure 6.4(b)), because the other π^* C−C MO, in the plane H−C1−C2 (A' orbital, see figure 6.4(a)), is stabilised because of the

UNIVERSITAT ROVIRA I VIRGILI
ORGANIC MOLECULES ON METAL SURFACES: FORECASTING STRUCTURES AND SPECTRA
Benjamí Martorell Masip
ISBN:978-84-691-9747-9 /DL: T-1259-2008

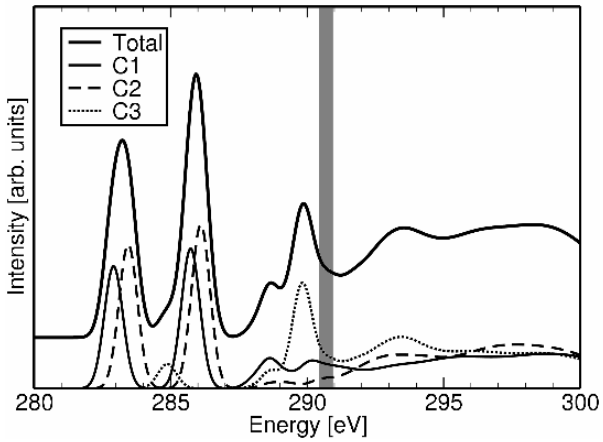

(a) Singulet calculation in triple state geometry.

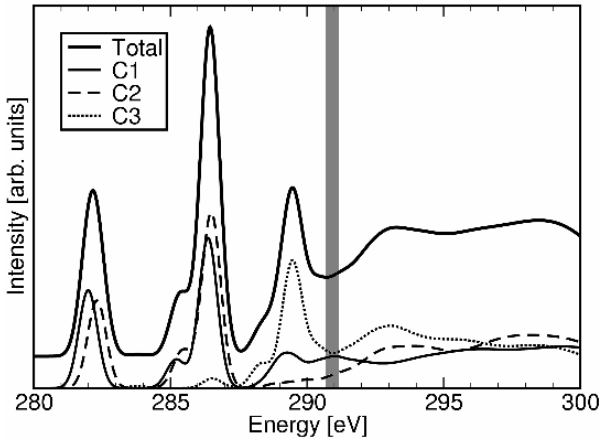

(b) Triple state calculation.

Figure 6.5: NEXAFS spectra for propyne molecule in the triplet state geometry. a) singlet state and b) triplet state.

breaking of the linearity of Pr, and destabilising the bonding MO of the triple bond. This makes to appear a peak at 283.3 eV. Of course the peaks at 286.0 and 283.3 eV only have contribution of C1 and C2, and there is a small shift of 0.4 eV between the contribution of C1 and C2 due to the difference of charge between C1 and C2, like in the C_{3v} Pr. The IP for C1 is in this case 290.4 eV, and for C2 is 290.9 eV.

For Pr in triple state, the excitation for alpha and beta electron is different (due to the unrestricted calculation method used) and they must be taken into

UNIVERSITAT ROVIRA I VIRGILI
ORGANIC MOLECULES ON METAL SURFACES: FORECASTING STRUCTURES AND SPECTRA
Benjamí Martorell Masip
ISBN:978-84-691-9747-9 /DL: T-1259-2008

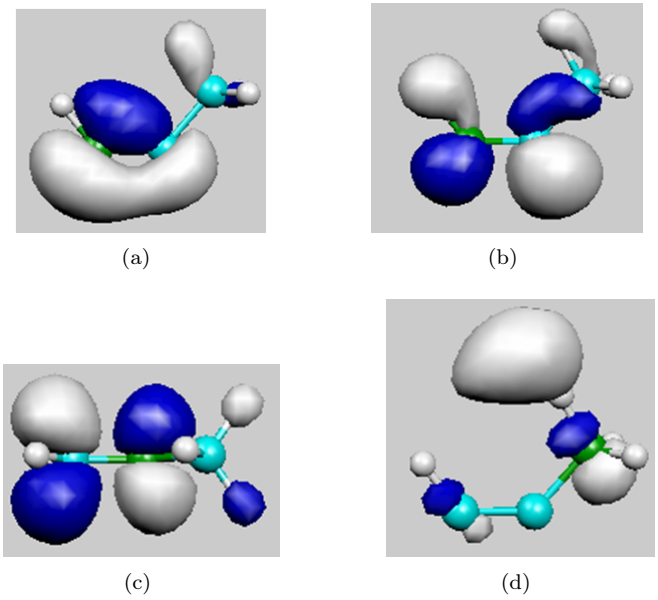

(a) (b)

(c) (d)

Figure 6.6: Final molecular orbitals involved in the transitions of C 1s electrons of propyne in C_s geometry (triplet state).

account. Final NEXAFS spectrum is the addition of both spectra, the alpha and the beta ones. Total NEXAFS of Pr in the triple state can be observed in figure 6.5(b), it is quite similar to the spectrum of the single state with the triplet state geometry NEXAFS spectrum (figure 6.5(a)). The triplet state spectrum of Pr has three mainly peaks with a shoulder the most intense one. The band corresponding to C3 atom remains more o less equal like the case of singlet state. The IP of this carbon is 291.1 eV, independently for both alpha and beta excitations. C3 has an intense peak at 289.5 eV, that belongs to the excitation of the 1s electron to the σ^* C3−H orbital (see figure 6.6(d)). The situation for C1 and C2 is quiet different, because there are two electrons decoupled, with the same spin in the same molecule, and localised on these two carbons. IP for 1s electrons of C1 are 291.5 and 290.7 eV, for alpha (occupied) and beta (unoccupied) electron, respectively. IP for C2 are 291.7 and 291.0 eV. The excitations of 1s alpha electrons for both C1 and C2 atoms give only one very intense peak at 286.4 eV for both carbons. These are the excitations of the 1s electron to A" π^* C−C MO (see figure 6.6(c)). The excitations of beta electrons produce a more complicated NEXAFS spectrum. Like for the alpha electrons, there is a peak at 286.4 and 286.6 eV for C1 and C2 respectively, that

UNIVERSITAT ROVIRA I VIRGILI
ORGANIC MOLECULES ON METAL SURFACES: FORECASTING STRUCTURES AND SPECTRA
Benjamí Martorell Masip
ISBN:978-84-691-9747-9 /DL: T-1259-2008

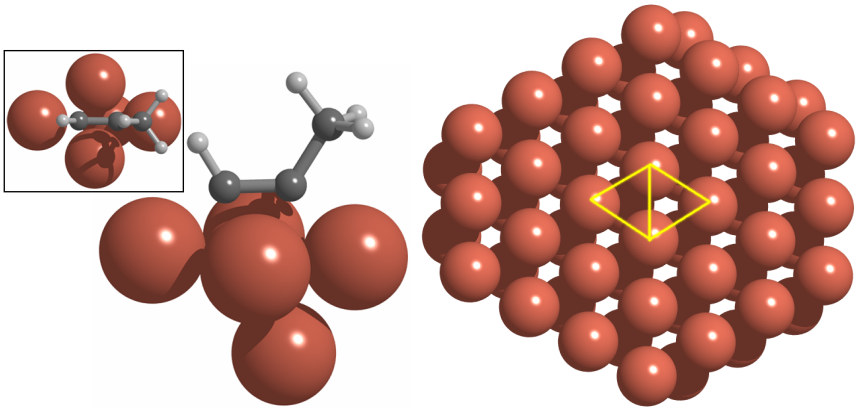

(a) Adsorption mode. (b) Calculation cluster.

Figure 6.7: a) Adsorption mode of Pr on Cu(111). b) The Cu_{59} calculation cluster.

correspond to the excitation to A" π^* C−C MO. Besides a second peak appears near the last one, at 285.3 and 285.5 eV for C1 and C2, corresponding to the shoulder at the total NEXAFS spectrum, and it is the excitation to the A' π^* C−C MO (see figure 6.6(b)). A more intense peak exists at 282.0 and 282.3 eV for C1 and C2, which corresponds to the first intense peak in the total NEXAFS spectrum, and it is the excitation to the A' π C−C (see figure 6.6(a)), which is empty because of the triplet state (it would correspond to the π C−C in the plane of the singlet state).

6.1.2 Propyne adsorbed on Cu(111).

The adsorption of Pr on Cu(111) has already been studied. The adsorption site and geometry, the adsorption energy, and the RAIR spectrum have been already studied by *A. Clotet et al.* [90, 106]. The adsorption mode of Pr on Cu(111) is a di-σ/di-π adsorption mode. In figure 6.7(a) the adsorption site of propyne is presented. The adsorption energy of propyne on Cu(111) has been published to be from 0.22 eV with a cluster model [90] to a highest adsorption energy of 0.86 eV with a periodic model [106]. It has been suggested by LEED experiments that the experimental adsorption energy for the $\sqrt{4}\times3$ unit cell is 0.93 eV . The adsorption energy using the StoBe code with a cluster model of Cu_{59} (see figure 6.7(b), for more computational details see section 2.5) is 0.34 eV, which is between the values before reported. The geometry of adsorbed Pr

UNIVERSITAT ROVIRA I VIRGILI
ORGANIC MOLECULES ON METAL SURFACES: FORECASTING STRUCTURES AND SPECTRA
Benjamí Martorell Masip
ISBN:978-84-691-9747-9 /DL: T-1259-2008

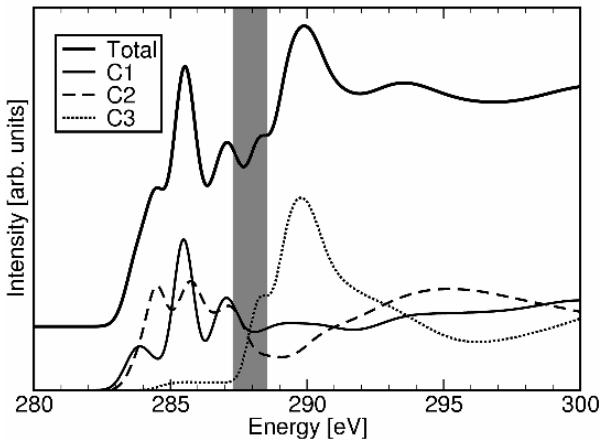

Figure 6.8: Simulated NEXAFS spectrum for adsorbed Pr on Cu(111).

on Cu(111) is similar to the triplet state geometry in the gas phase. In this case, the C1−C2 distance is 1.38 Å, a bit larger than triplet state's distance, and the H−C1−C2 and C1−C2−C3 angles are a bit smaller than triplet state's angles, 119.8° and 121.7°, respectively. This effect is due to the presence of the surface.

As a previous chemical (or physical, where is exactly the frontier?) exercise, we can imagine how the adsorbed Pr NEXAFS spectrum will look from the NEXAFS spectrum of gas phase propyne, with the most adequated geometry, the triplet state geometry, but with the easiest electronic state, the singlet state. We can imagine that the electronic structure remains in the adsorption process, except for the orbitals involved in the bonding with the surface. These are the triple bond π C−C MO. So the biggest changes will occur in these excitations. These MO will interact with the surface, so new more stabilised MO than in the gas phase will appear. This makes the antibonding states to be higher in energy and the excitations to these orbitals will be more energetic than those in gas phase.

NEXAFS spectrum of adsorbed Pr on Cu(111), which is presented in figure 6.8, seems quite different to the gas phase spectra. The decomposition of NEXAFS spectrum was made to understand it. For methylenic carbon, C3, the IP is 288.5 eV, and there is an intense, broad peak centred at 289.8 eV (above IP), with a shoulder at 288.4 eV. This is a band corresponding to the excitations to σ^* C3−H orbitals, being these peaks very similar to those in the gas phase. For C1 and C2, NEXAFS spectra look quite different from the gas phase. The C1

UNIVERSITAT ROVIRA I VIRGILI
ORGANIC MOLECULES ON METAL SURFACES: FORECASTING STRUCTURES AND SPECTRA
Benjamí Martorell Masip
ISBN:978-84-691-9747-9 /DL: T-1259-2008

IP is 287.3 eV. In NEXAFS spectrum of C1 there is an intense peak at 285.5 eV, which corresponds to the excitation to A" π^* C−C MO. Two other less intense peaks are around this one, one at 283.9 and the other one at 287.1 eV. These two peaks are the excitations to orbitals created in the interaction with the surface. The C2 IP is 287.5 eV. In NEXAFS spectrum, the most intense peak is at 285.8 eV and it corresponds to the excitation to A" π^* C−C MO, but there are also two very intense peaks at 284.6 and 287.1 eV, which correspond to the excitations to MO that come from the interaction with the surface. So in the total NEXAFS spectrum, the peak at 285.6 eV corresponds to the excitation to A" π^* C−C, the peak at 289.8 eV corresponds to the excitation to σ^* C3−H orbitals, and the shoulder at 284.5 eV and the peak at 287.1 eV correspond to the excitation to the orbitals coming from the interaction between surface and Pr molecule.

6.1.3 Propene-1,3-diyl and vinylcarbene in the gas phase.

Following section 4.1, where $CHCHCH_2$ molecule was presented extensively, two accessible electronic states exist: singlet state (vinylcarbene) and triplet state (propene-1,3-diyl) [76, 118]. In figure 6.9 are presented the molecular orbitals diagram for both electronic states of VC. This molecule has demonstrated to play an important role in the interconversion of C_3H_4 isomers [80, 81]. Using the StoBe code, we obtained for vinylcarbene a C1−C2 distance of 1.46 Å and a C2−C3 distance of 1.37 Å, being the carbonated structure angle 116°. For propene-1,3-diyl, C1−C2 and C2−C3 distances are 1.39 and 1.40 Å, being the angle among three carbons 126°. All these values are very similar to the ones in table 4.1.

In figure 6.10(a) simulated NEXAFS spectrum for vinylcarbene (singlet state) is presented. C1 IP is 290.6 eV, for C2 is 291.0 eV and for C3 is 290.4 eV. These IP values are in a smaller range (0.6 eV) than propyne's (1.3 eV), indicating these three carbon atoms are chemically more similar than propyne's carbon atoms were among them. The most intense peak in total spectrum lies at 286.8 eV. Analysing the decomposition of the spectrum on three carbon atoms, this peak can be assigned to the resonant π^* orbital over all molecule (see figure 6.11(b)), where all carbon atoms contribute. At 282.4 eV appears another intense peak that corresponds to the excitation of C1 1s electron to the localised p_z orbitals (perpendiculars to molecular plane) on C1 and C3 (see figure 6.11(a)). At 283.5 eV appears the same transition for C3. At 289.1 eV

UNIVERSITAT ROVIRA I VIRGILI
ORGANIC MOLECULES ON METAL SURFACES: FORECASTING STRUCTURES AND SPECTRA
Benjamí Martorell Masip
ISBN:978-84-691-9747-9 /DL: T-1259-2008

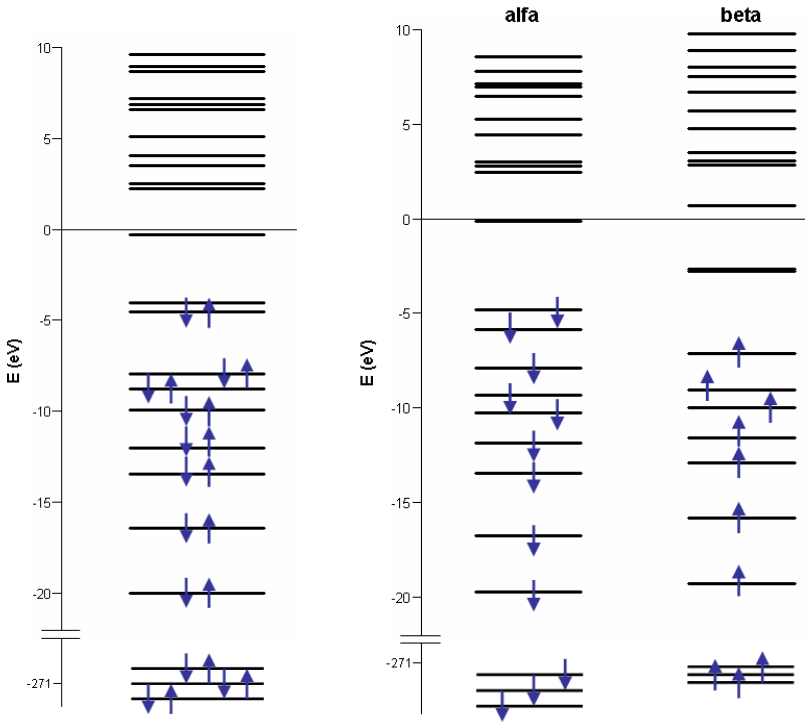

(a) Singlet state. (b) Triplet state.

Figure 6.9: Molecular orbital diagram for gas phase $CHCHCH_2$ molecule.

another intense peak appears. This peak has contribution of all carbon atoms and it is the excitation to σ^* C−H bonds (see figures 6.11(c) and (d)).

In figure 6.10(b) NEXAFS spectrum for propene-1,3-diyl (triplet state) is presented. It can be observed that NEXAFS spectra for vinylcarbene and for propene-1,3-diyl are different, indicating differences in electronic structure. IP for C1 are 291.3 and 290.4 for alpha and beta electrons, respectively (occupied and unoccupied spin-orbitals, see diagram 6.9(b)), for C2 are 290.9 and 291.0 eV and for C3 291.6 and 290.1 eV. In NEXAFS spectrum the most intense peak lies at 283.5 eV and it has contribution from C1 and C3, but only for beta electrons (i.e. the unoccupied states). It is the excitation of C1 and C3 1s electron to p_z^* orbitals localised on C1 and C3 (see figure 6.12(b)). Moreover, C1 has contribution in the excitation to the carbenic orbitals localised on C1 (see figure 6.12(a)). The peak around 286.5 eV has only contribution of alpha electrons, it is the excitation of 1s electrons of C2 and C3 to the resonant π^*

UNIVERSITAT ROVIRA I VIRGILI
ORGANIC MOLECULES ON METAL SURFACES: FORECASTING STRUCTURES AND SPECTRA
Benjamí Martorell Masip
ISBN:978-84-691-9747-9 /DL: T-1259-2008

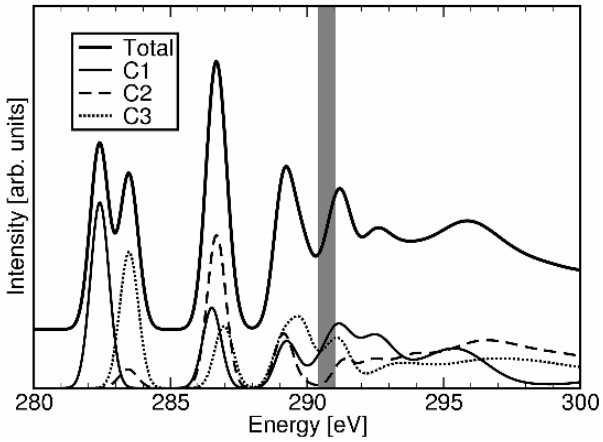

(a) Vinylcabene NEXAFS.

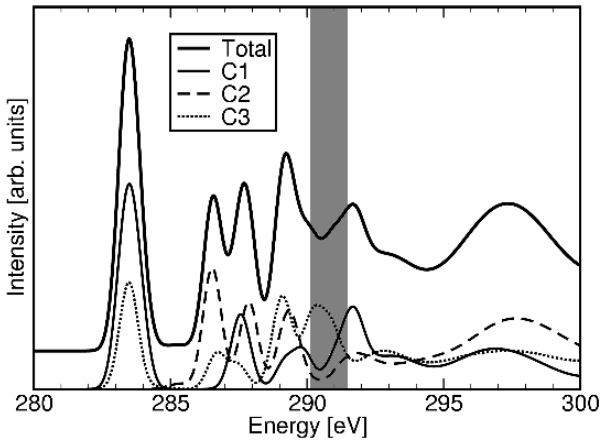

(b) Propene-1,3-diyl NEXAFS.

Figure 6.10: NEXAFS spectra for $CHCHCH_2$ molecule. a) Vinylcarbene (singlet state) and b) propene-1,3-diyl (triplet state).

orbital over all molecule (see figure 6.12(c)). The peak at 287.7 eV corresponds to the excitations of beta electrons to the same orbitals as peak at 286.5 eV, but for this peak it has also a contribution the excitation of C1 alpha electron to the same orbital (resonant π^*). So this excitation is the same for alpha and beta electron of C1, but splits for C2 and C3 in alpha and beta excitations. The peak around 289.2 eV corresponds to the different possible excitations to σ^* C−H, and this value is the same obtained for vinylcarbene.

UNIVERSITAT ROVIRA I VIRGILI
ORGANIC MOLECULES ON METAL SURFACES: FORECASTING STRUCTURES AND SPECTRA
Benjamí Martorell Masip
ISBN:978-84-691-9747-9 /DL: T-1259-2008

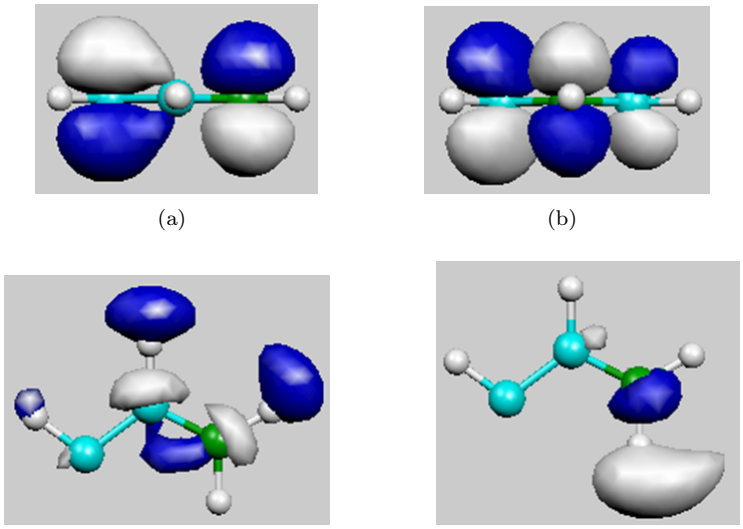

(a) (b) (c) (d)

Figure 6.11: Final molecular orbitals involved in the transitions of C 1s electrons of vinylcarbene (singlet state).

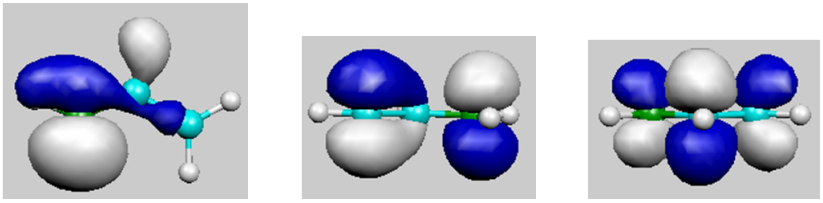

(a) (b) (c)

Figure 6.12: Final molecular orbitals involved in the transitions of C 1s electrons of propene-1,3-diyl (triplet state).

6.1.4 $CHCHCH_2$ adsorbed on Cu(111).

In section 4.2 it has been reported the adsorption modes of VC on Cu(111), being the two most stable modes the C3-top and C3-hollow, being C1-trans structure and C1-cis higher in energy. In figures 4.3 were presented the adsorption modes C3-top, C3-hollow and C1-trans. C3-hollow structure is the most stable one, lieing C3-top 5 kJ·mol^{-1} and C1-trans 25 kJ·mol^{-1} above C3-hollow. So, we decided to simulate NEXAFS spectra for the two most stable minima. Results demonstrated no real differences existed in NEXAFS spectra for C3-hollow and C3-top structures.

UNIVERSITAT ROVIRA I VIRGILI
ORGANIC MOLECULES ON METAL SURFACES: FORECASTING STRUCTURES AND SPECTRA
Benjamí Martorell Masip
ISBN:978-84-691-9747-9 /DL: T-1259-2008

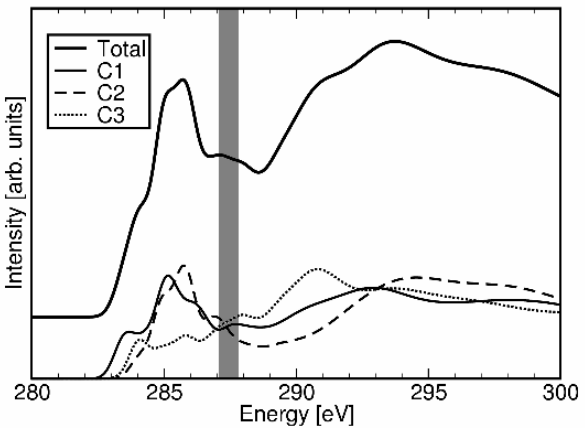

Figure 6.13: NEXAFS spectrum for $CHCHCH_2$ molecule adsorbed on Cu(111) for the C3-hollow adsorption mode.

As those VC structures are present on the 3×3 unit cell (low coverage regime), where repulsion between adjacent molecules is low, we decided to use a large Cu cluster. In this case it is the same one as the used for Pr calculations: Cu_{59} (see figure 6.7(b)).

NEXAFS spectrum for adsorbed VC in the most stable adsorption mode is presented in figure 6.13. This spectrum has a wide band in the range between 283 to 287 eV. This band does not correspond to only one excitation but several excitations. The analysis of all carbon atoms is necessary in order to try to understand this complicated spectrum. C1 IP is 287.1 eV, for C2 this is 287.8 and for C3 is 287.7 eV. The range is small (0.8 eV), indicating these carbons are not very different chemically. This gap is similar to the one obtained for propene-1,3-diyl in gas phase (0.7 eV for alpha electrons and 0.9 eV for beta electrons). The IP values for adsorbed VC are lower than the ones found for free molecule, which were in all cases higher than 290 eV, indicating that 1s electrons are not as stabilised on the cluster as were in gas phase.

The analysis of the excitations is complex because of the interaction between VC and surface. This interaction occurs between the π electrons of VC resonant structure and the sp band of the surface. This makes that a new set of bonding orbitals (and antibonding) with the surface are generated. All these orbitals have p contribution, so the antibonding orbitals generated can be the final state of the excited electrons. This explains why the band before commented in the range 283-287 eV appears in a wide range. For higher energies, around 290 eV

UNIVERSITAT ROVIRA I VIRGILI
ORGANIC MOLECULES ON METAL SURFACES: FORECASTING STRUCTURES AND SPECTRA
Benjamí Martorell Masip
ISBN:978-84-691-9747-9 /DL: T-1259-2008

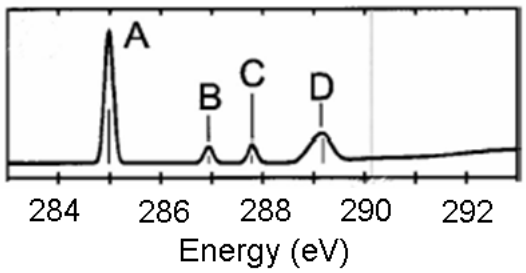

Figure 6.14: NEXAFS spectrum for benzene in gas phase.

(above IP) transitions corresponding to the excitations to σ^* C−H and around 294 eV to σ^* C−C.

6.2 Following the isomerisation reaction via NEXAFS spectra.

As commented in the introduction of this chapter, the aim of this work was to study and to simulate NEXAFS spectra of the species involved in reaction of dimerisation of propyne on Cu(111). Final specie, i.e. benzene in gas phase was already studied by *C. Kolzcewsky et al.* [119, 120]. Theoretical NEXAFS spectrum of benzene in gas phase is presented in figure 6.14, where four peaks can be observed[1]. The most intense one (A) lies at 284.97 eV and it is the first peak in the spectrum. The second one (B) lies at 286.92 eV, the third one (C) at 287.78 eV and the final one (D) around 289.35 eV. All of them have been already assigned.

In the gas phase, the dimerisation of Pr via VC must overpass a large energetic barrier [90]. We have presented here NEXAFS spectra for Pr and VC in gas phase. In figure 6.15 the different NEXAFS spectra for species in gas phase are presented. For Pr, a very intense band at 286.4 eV is present, comparing very well with the experimental NEXAFS that has this band at 285.9 eV. This band corresponds to C 1s electrons excitation to π^* C≡C orbitals. At 288.7 eV excitations to σ^* C−H are present. When Pr changes its geometry to triplet state geometry, but remains in a singlet state, band at 286.4 eV splits in two different bands, one at 286.0 eV and the other at 283.2 eV. This is a clear effect of the symmetry break: the two π^* C−C orbitals are not degenerated. Excitations

[1]This image is taken directly from reference [120]

UNIVERSITAT ROVIRA I VIRGILI
ORGANIC MOLECULES ON METAL SURFACES: FORECASTING STRUCTURES AND SPECTRA
Benjamí Martorell Masip
ISBN:978-84-691-9747-9 /DL: T-1259-2008

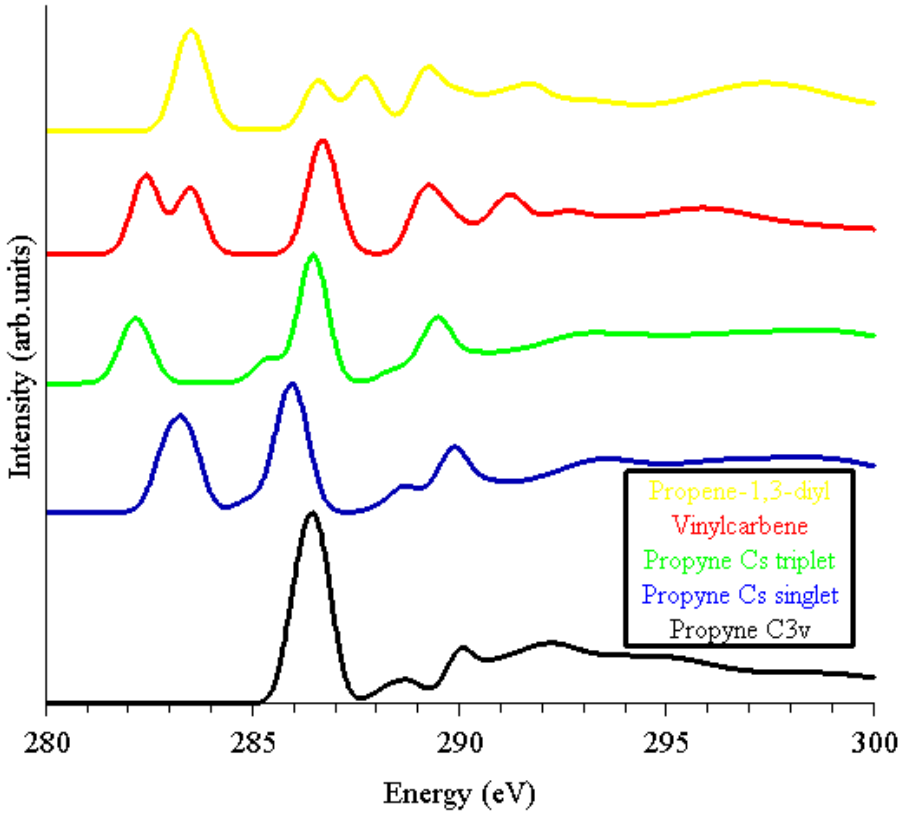

Figure 6.15: NEXAFS spectra for propyne and $CHCHCH_2$ species in gas phase.

to σ^* C−H split also to 288.7 and 289.8 eV. In the triplet state, NEXAFS is very similar to the singlet state C_s geometry. So two bands around 282.1 and 286.4 eV exist, but this one has a little shoulder at 285.3 eV due to different alpha and beta contributions. So if dimerisation reaction took place in gas phase, in the Pr preparing step one should observe in the NEXAFS spectrum the splitting of the band at 286.4 eV.

The next step should be isomerisation to propene-1,3-diyl, which presents a very intense peak at 283.5 eV, being these transitions to carbenic orbitals on C1 and localised orbitals p_z^* on C1 and C3. Two peaks at 286.5 and 287.7 eV appear, these are transitions to resonant π^* system in propene-1,3-diyl, and they are less intense than the first peak. So in the isomerisation step from Pr to propene-1,3-diyl one should realise that peak at 282.1 of Pr disappears, and a couple of new peak appear at 283.5, decreasing the intensity of the peak at

UNIVERSITAT ROVIRA I VIRGILI
ORGANIC MOLECULES ON METAL SURFACES: FORECASTING STRUCTURES AND SPECTRA
Benjamí Martorell Masip
ISBN:978-84-691-9747-9 /DL: T-1259-2008

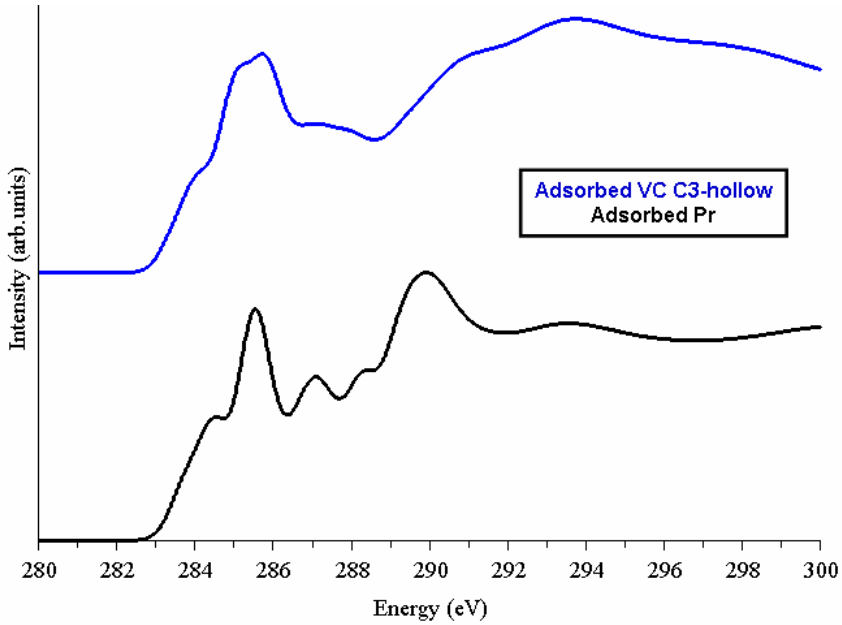

Figure 6.16: NEXAFS spectra for adsorbed propyne and adsorbed $CHCHCH_2$.

286.5 eV and a new peak at 287.7 eV appears. Peak around 289.5 eV for Pr in its triplet state does not change because for propene-1,3-diyl also exists a peak at 289.2 eV.

Now two VC molecules should react to yield benzene and hydrogen. As commented before, benzene presents the most intense peak at 284.97 eV. So the peak of propene-1,3-diyl around 283.4 eV disappears and appears benzene's one. Propene-1,3-diyl's peak at 286.4 would disappear, but very near, at 286.92 benzene presents a peak. At 287.7 eV both molecules present a peak, so no changes would exist in this zone. Peak at 289.2 eV in propene-1,3-diyl molecule does not change significantly because benzene has a peak at 289.35 eV.

Another step could be the transition from propene-1,3-diyl to vinylcarbene. Vinylcarbene has two peaks at 282.4 and 283.5 eV, and propene-1,3-diyl only one at 283.5 eV, so one should observe a splitting of the peak in this transition from propene-1,3-diyl to vinylcarbene. Another important feature is that vinylcarbene only has one peak at 286.8 eV, but propene-1,3-diyl has two peaks, one at 286.5 and the other one at 287.7 eV, so in this zone of the spectrum, from two peaks we obtain only one in this step.

Let's go with the dimerisation process of propyne on Cu(111). In this case,

UNIVERSITAT ROVIRA I VIRGILI
ORGANIC MOLECULES ON METAL SURFACES: FORECASTING STRUCTURES AND SPECTRA
Benjamí Martorell Masip
ISBN:978-84-691-9747-9 /DL: T-1259-2008

the first step is the adsorption of Pr on the surface, the second is the isomerisation from Pr to VC, and finally two molecules of VC couple to yield benzene. In figure 6.16 the NEXAFS spectra for adsorbed propyne and $CHCHCH_2$ are presented. Gas phase Pr has an intense peak at 286.4 eV, but when it is adsorbed, this peak becomes a wide band centred at 285.6 eV. Besides a shoulder at 284.5 and a new peak at 287.1 eV appear due to interaction with the surface. These two new peaks are transitions to unoccupied orbitals, which come from the formation of the Pr–surface bond. Gas phase Pr presents a peak at 290.1 eV, which are transitions to σ^* C−H, and in adsorbed Pr this peak lies at 289.9 eV, becoming the most intense peak of the spectrum. Peak at 292.3 eV in gas phase are transitions to σ^* C−C orbitals, but for adsorbed Pr on Cu(111), this is the continuous region and no well-defined peaks appear. So, to study the adsorption of propyne on Cu(111) one could use NEXAFS spectroscopy.

The next step is the isomerisation from adsorbed Pr to VC on Cu(111). A wide band centred at 285.8 eV appears at VC spectrum. This band is assigned to the excitations to orbitals coming from the interaction of resonant π^* MO of VC with the surface. Then a very wide band centred at 293.7 eV appears. This band (excitations to σ^* C−C orbitals), hides the band around 290.7 eV, which are excitations to σ^* C−H orbitals. So the main difference between adsorbed Pr and VC is that the band at 285.6 eV wides and centres at 285.8 eV. The clear propyne peak at 287.1 eV becomes part of the band centred at 285.8 eV in VC spectrum, and the band around 289.8 eV due to σ^* C−H is hidden by the excitations to σ^* C−C MO. Although this, the differences between NEXAFS of Pr and VC spectra are not large enough to differentiate both species.

Final step is the coupling of two VC molecules and the formation of desorbed benzene. The wide band centred at 285.3 eV in the case of VC disappears. Gas phase benzene presents peaks at 284.97, 286.92, 287.78, and at 289.35 eV. So, if desorbed benzene is produced the wide bands will disappear in the final spectrum.

Finally, we can conclude that NEXAFS is an appropriate tool in order to follow dimerisation reaction of Pr in gas phase, and all species can be identified with no problems, because peaks are clear for every specie. In the case of the catalysed reaction by Cu(111), adsorbed Pr and adsorbed VC cannot be distinguished so clearly because of the presence of wide bands in NEXAFS spectra. Interaction between surface and molecules is really strong and new sets of orbitals, which are actives by selection rules, are generated. Therefore, in cases like the present one, where a lot of π^* MO come from the interac-

UNIVERSITAT ROVIRA I VIRGILI
ORGANIC MOLECULES ON METAL SURFACES: FORECASTING STRUCTURES AND SPECTRA
Benjamí Martorell Masip
ISBN:978-84-691-9747-9 /DL: T-1259-2008

tion adsorbate-surface, NEXAFS technique could not distinguish easily among different adsorption structures (in our case between adsorbed Pr and VC on Cu(111)).

6.3 Final summary.

In this chapter we have simulated NEXAFS spectra of Pr and VC in gas phase and also adsorbed on Cu(111). The aim of this work was to search an experimental tool to observe the isomerisation reaction. In this case we have demonstrated NEXAFS spectrum to be a powerful tool to distinguish between Pr and VC, and even the different electronic states of these molecules can be distinguished. In the case of adsorbed Pr and VC, the existence of the new orbitals that bind the adsorbate and the metal surface makes that bands in NEXAFS spectrum to be wide and both molecules are difficultly distinguished. With all this information, we have been capable of answering the question that were raised at the beginning of this chapter:

- We have simulated Pr NEXAFS spectrum and compared with the experimental one. The agreement between them is really good and only a small shift of +0.5 eV for the simulated spectrum is observed.
- The NEXAFS spectrum of gas phase propyne has been calculated for three different cases:
  - C_{3v} propyne: it presents peaks at:
    - 286.4 eV, strong, corresponds to the excitation of 1s electrons of C1 and C2 to the π^* C≡C MO.
    - 288.2 eV, weak, corresponds to the excitation of 1s electron of C1 to the σ^* C1−H MO.
    - 290.1 eV, medium, corresponds to the excitation of 1s electron of C3 to the σ^* C3−H MO.
    - 292.3 eV, medium, corresponds to the excitation of 1s electron of C3 to the σ^* C2−C3 MO.
  - C_s propyne in singlet state: it presents peaks at:
    - 283.2 eV, strong, corresponds to the excitation of 1s electrons of C1 and C2 to the A' π^* C≡C MO.

UNIVERSITAT ROVIRA I VIRGILI
ORGANIC MOLECULES ON METAL SURFACES: FORECASTING STRUCTURES AND SPECTRA
Benjamí Martorell Masip
ISBN:978-84-691-9747-9 /DL: T-1259-2008

  - 286.0 eV, strong, corresponds to the excitation of 1s electrons of C1 and C2 to the A" π^* C≡C MO.
  - 288.5 eV, weak, corresponds to the excitation of 1s electron of C1 to the σ^* C1−H MO.
  - 289.5 eV, medium, corresponds to the excitation of 1s electron of C3 to the σ^* C3−H MO.

- C_s propyne in triplet state: it presents peaks at:
  - 282.2 eV, medium, corresponds to the excitation of 1s beta electrons of C1 and C2 to the A" π C≡C MO.
  - 286.4 eV, strong, corresponds to the excitation of 1s electrons of C1 and C2 to the A" π^* C≡C MO.
  - 289.5 eV, medium, corresponds to the excitation of 1s electrons of C1 and C3 to the σ^* C−H MO.

- The NEXAFS spectrum of gas phase VC has been simulated for both different cases:
  - Vinylcarbene (singlet state): it presents peaks at:
    - 282.4 and 283.5 eV, medium, correspond to the excitation of 1s electrons of C1 and C3, respectively, to the p_z^* on C1 and C3.
    - 286.8 eV, strong, corresponds to the excitation of 1s electrons of all carbon atoms to the resonant π^* MO.
    - 281.9 eV, medium, corresponds to the excitation of 1s electrons of all carbon atoms to the σ^* C−H MO.
  - Propene-1,3-diyl (triplet state): it presents peaks at:
    - 283.5 eV, strong, corresponds to the excitation of 1s beta electrons of C1 and C3 to the p_z^* on C1 and C3.
    - 286.5 and 287.7 eV, correspond to the excitation of 1s electrons (alpha and beta, respectively) of C2 and C3 to the resonant π^* MO.
    - 289.5 eV, medium, corresponds to the excitation of 1s electrons of all carbon atoms to the σ^* C−H MO.

- The NEXAFS spectrum of adsorbed propyne has been simulated and it presents peaks at:

UNIVERSITAT ROVIRA I VIRGILI
ORGANIC MOLECULES ON METAL SURFACES: FORECASTING STRUCTURES AND SPECTRA
Benjamí Martorell Masip
ISBN:978-84-691-9747-9 /DL: T-1259-2008

  - 284.1 and 287.1 eV, medium, correspond to the excitation of 1s electrons of C1 and C2 to the orbitals that come from the interaction of the A' π C≡C MO with the surface.
  - 285.5 eV, strong, corresponds to the excitation of 1s electron of C1 and C2 to the A" π^* C≡C MO.
  - 289.8 eV, strong, corresponds to the excitation of 1s electron of C3 to the σ^* C3−H MO.

- The NEXAFS spectrum of adsorbed VC has been simulated in the C3-hollow adsorption mode. Its features are:
  - A wide band is present from 283 to 287 eV. It corresponds to the excitations of 1s electron of all carbon atoms to the orbitals that come from the interaction of the resonant π MO with the surface.
  - Around 290 eV exist the transitions to the σ^* C−H MO.
  - Around 294 eV exist the transitions to the σ^* C−C MO.

- IP of 1s electrons have been calculated for all molecules. The most important cases are:
  - C_{3v} gas phase propyne: C1 and C2 values are similar (290.0 and 290.6 eV), indicating they are chemically similar. C3 value is higher (291.3 eV), indicating its chemical environment is different from C1 and C2.
  - Adsorbed propyne: C1 and C2 values are similar (287.3 and 287.5 eV), indicating they are chemically similar, but C3 is not (288.5 eV). All this values are lower than in the case of gas phase propyne, consequently the 1s electron are less stable in the adsorbed structure.
  - Propene-1,3-diyl: The IP values are double for every carbon atom, because of the triplet state calculation. Alpha values are 291.3, 290.9, and 291.6 eV for C1, C2, and C3, respectively. For beta electrons values are 290.4, 291.0, and 290.1 eV. In the case of beta electrons these are less stabilised than the alpha ones. Differences between carbon atoms are not big, being the most different one C3 (because it binds to two H atoms).

UNIVERSITAT ROVIRA I VIRGILI
ORGANIC MOLECULES ON METAL SURFACES: FORECASTING STRUCTURES AND SPECTRA
Benjamí Martorell Masip
ISBN:978-84-691-9747-9 /DL: T-1259-2008

  - Adsorbed VC: IP values are 287.1, 287.8, and 287.7 eV for C1, C2, and C3, respectively. They are very similar, being the most different C1 because its H atom tilts away the molecular plane. All these values are lower than in the gas phase, indicating it is easier to take out the 1s electrons.

- We have discussed about the fingerprints that we can find out in every spectra to follow the isomerisation reaction. It has been demonstrated to be useful for the isomerisation in gas phase, but differences in the NEXAFS spectra of adsorbed molecules are too small to be able to distinguish between them.

UNIVERSITAT ROVIRA I VIRGILI
ORGANIC MOLECULES ON METAL SURFACES: FORECASTING STRUCTURES AND SPECTRA
Benjamí Martorell Masip
ISBN:978-84-691-9747-9 /DL: T-1259-2008

Chapter 7

Final summary and conclusions.

7.1 Summary and conclusions.

In this thesis we performed a strict and deep study of the adsorption of some organic molecules on metal surfaces. The use of periodical-DFT methods has allowed us to predict structures, adsorption energies, vibrational spectra and reaction pathways. Moreover, with the use of DFT method with cluster model we could forecast the NEXAFS spectra of some adsorbed species on metal surfaces. Our work is a clear example how computational chemistry can provide information about still not studied systems, because they are very new materials (TTF) or because they are intermediates difficult to be detected experimentally (VC and C_3H_3).

We focused our efforts in three different systems: TTF and TSF adsorbed on the (110) surface of Ag and Au (chapter 3), VC on the (111) surface of Cu, Pt, Pd and Rh (chapter 4 and 6) and C_3H_3 on Cu(111) (chapter 5).

Chapter 3. The adsorption of two typical organic charge donors on two metallic substrates has been studied in chapter 3. TTF and TSF interact with the (110) surface of Ag and Au via the lone-pair electrons of their sulphur or selenium atoms. These heteroatoms transfer a part of their charge density to the sp band of the surface in most cases (from $\sim$0 e^- in the case of TTF on Ag(110) 1×4 unit cell up to 0.7 e^- in the case of TSF on Ag(110) 2×4 unit cell).

UNIVERSITAT ROVIRA I VIRGILI
ORGANIC MOLECULES ON METAL SURFACES: FORECASTING STRUCTURES AND SPECTRA
Benjamí Martorell Masip
ISBN:978-84-691-9747-9 /DL: T-1259-2008

On the 2×4 unit cell the four heteroatoms interact and TTF or TSF is parallel to the surface, but on the 1×4 unit cell, only two heteroatoms can interact and the molecule lies tilted (30° respect to the normal) to the surface. As a consequence, on the 2×4 unit cell TTF is more stable (-21 kcal·mol^{-1} on Ag) than on the 1×4 (-11 and -8 kcal·mol^{-1} on Ag for both minima found).

We found differences in E_{ads} when the substrate was changed. On Au the interaction was stronger than on Ag, being -35 kcal·mol^{-1} for 2×4 unit cell and -18 kcal·mol^{-1} for the only minimum found on the 1×4 unit cell. Otherwise, if the other interacting actor (i.e., the heteroatom) were substituted, the changes in E_{ads} were not so large and only due to its more "external" lone-pair electrons TSF presents a bit larger E_{ads} (-25 kcal·mol^{-1}).

Finally, geometrical differences allowed us to differentiate 2×4 and 1×4 unit cell structures in the RAIR spectra.

Chapter 4. Computational chemistry is a powerful tool in the study of the reaction intermediates. In chapter 4 we have studied the proposed intermediate for the dimerisation reaction of propyne to benzene on Cu(111): VC. Moreover, VC has also been studied on Pt, Pd and Rh, where propyne presents different reactivity (trimerises on Pd and decomposes on Pt and Rh).

On Cu(111) three different unit cells have been studied: 2×2, 3×3 and $4\times\sqrt{3}$. On the 2×2 unit cell three different adsorption modes were found: VC C1-trans, VC C1-cis and VC C3-top, being this the stability order. C1-trans and C1-cis are not flat respect to the surface, and only C1 atom interacts with metal, whereas C3-top is parallel to the surface and three carbon atoms interact. On the 3×3 unit cell also three adsorption modes were discovered, but only two of them were common with 2×2 unit cell: VC C1-trans and VC C3-top; the new structure is C3-hollow, and in this case the order of stability is C3-hollow$\simeq$C3-top$>>$C1-trans. C3-hollow structure is flat respect to the surface and all carbon atoms interact with the metal. All the structures on the 3×3 unit cell are highly stabilised respect to 2×2 unit cell. Finally, on the $4\times\sqrt{3}$ unit cell only the C3-hollow structure has been evaluated.

On the (111) surface of Pt, Pd and Rh two different unit cells have been investigated: 2×2 and 3×3. On these metals three adsorption modes existed: VC C1-trans, VC C3-top and VC C1-bridge. The relative stabilities of the adsorption modes on both unit cells are always: C1-bridge$\simeq$C3-top$>>$C1-trans. The adsorption on the 3×3 unit cell is always $\sim$10 or $\sim$20 kJ·mol^{-1} more favourable than on the 2×2 unit cell. Although this, VC C1-trans on Rh(111) is more

UNIVERSITAT ROVIRA I VIRGILI
ORGANIC MOLECULES ON METAL SURFACES: FORECASTING STRUCTURES AND SPECTRA
Benjamí Martorell Masip
ISBN:978-84-691-9747-9 /DL: T-1259-2008

stable on the 2×2 unit cell than 3×3 unit cell due to a major agostic H1−M interaction, making the C1−H bond to be very large and activated (its vibrational frequency decrease from ∼2950 down to ∼1900 cm^{-1}).

Finally, the differences in the structures allow us to differentiate the possible VC isomers in RAIR spectra, because the flat structures are characterised by their low intensity bands, whereas the C1-trans isomer presents in all cases a very strong band at ∼1400 cm^{-1} (for more details see the summary of chapter 4).

Chapter 5. The barriers of the isomerisation from Pr to VC have been evaluated in chapter 5, for two possible pathways: the direct transposition of one methylenic hydrogen atom to the middle C atom and via the dehydrogenation-hydrogenation process (only for Cu). In the direct isomerisation three different situations are found. For Cu the barrier is very high >100 $kJ{\cdot}mol^{-1}$ respect to the desorption process; for Pd the barrier is around or a bit high than the desorption process, so desorption and isomerisation are competitive processes; for Pt and Rh this barrier is lower than the desorption process and the isomerisation will be the most favoured process.

In the case of Cu the barrier was so high that another pathway for isomerisation was studied: the dehydrogenation of one methylenic hydrogen atom and the later isomerisation of the middle carbon atom. A new specie appears for this process: $CHCCH_2$. When $CHCCH_2$ is adsorbed on the surface, all three carbons interact with the surface. When one H atom is added and the coadsorption process is evaluated, two possible situations exist. If the repulsion between C_3H_3 and H is large, C_3H_3 interacts only via C1 and it looks like a javelin stuck on the surface. Otherwise, if the repulsion is not large, C_3H_3 remains in the position of the non-interacting system, bonded to surface via its three C atoms.

For the dehydrogenation-hydrogenation mechanism, three coadsorption minima are necessary: M1, M2, and M3, which have been evaluated on the 2×2 and 3×3 unit cells. On the 3×3 unit cell the stabilisation is larger than on the 2×2 unit cell, because the repulsion is not so important. The barriers of the dehydrogenation and the hydrogenation steps are not as expensive energetically as the direct isomerisation, making this to be possible via the Horiuti-Polanyi mechanism.

Finally, the RAIR spectra of M1, M2, and M3 are different for the two possible groups of C_3H_3. In the case of the flat structures all bands are very weak, being difficult to be distinguished. In the case of the "javelin" structure,

UNIVERSITAT ROVIRA I VIRGILI
ORGANIC MOLECULES ON METAL SURFACES: FORECASTING STRUCTURES AND SPECTRA
Benjamí Martorell Masip
ISBN:978-84-691-9747-9 /DL: T-1259-2008

two strong bands at ∼1900 and ∼800 cm^{-1} allow us to identify these structures.

Chapter 6. NEXAFS spectra are a powerful tool to study the geometry and adsorption of molecules on surfaces. In chapter 6 we present the simulated NEXAFS spectra for the most important species in the isomerisation reaction of Pr to VC on Cu(111). Pr and VC NEXAFS spectra in gas phase have been simulated to study the excitations of the free molecule and how they change during the adsorption. Adsorbed Pr and VC NEXAFS spectra have also been simulated to certify if this is an adequated technique to follow this reaction. However, we did not find important differences between the adsorbed spectra due to the excitations to the orbitals of the adsorbate-metal interaction.

7.2 General aspects.

The study of organic compounds on metal surfaces is a very knotty topic. The multiple possible adsorption modes and the dependence of this adsorption modes on the surface model used increases its difficulty. Moreover, in the slab model (the most used in this thesis), the choice of the unit cell is a crucial parameter.

So, the general aspects studied in this thesis are:

- The adsorption modes and relatives energies of the organic molecules on the different metal surfaces.

The periodical-DFT methods allowed us to evaluate the energy and the adsorption modes of several organic molecules on metal surfaces for two different cases: one charge donor on its support and the intermediates in an isomerisation reaction.

The addition of ZPE correction in the adsorption energies allowed us to evaluate with a major precision the processes on the surface.

- The geometrical parameters of adsorbates.

The structures of adsorbates and the relaxation of surface have been evaluated. The used methods have demonstrated the capability to predict the structures of intermediates and other species before the experimental characterisation.

Geometrical parameters also helped us to lucubrate how the interaction between adsorbate and surface is carried out.

- The evaluation of the charge transfer.

UNIVERSITAT ROVIRA I VIRGILI
ORGANIC MOLECULES ON METAL SURFACES: FORECASTING STRUCTURES AND SPECTRA
Benjamí Martorell Masip
ISBN:978-84-691-9747-9 /DL: T-1259-2008

In the case of TTF and TSF on the metallic substrate, PDOS has allowed us to describe how the interaction adsorbate-metal is carried out. Moreover, with the integration of charge density we have have evaluated the donor capacity of these molecules on the metals.

- The simulation of RAIR and NEXAFS spectra.

The calculation of vibrational frequencies and dipolar moments made possible to simulate the RAIR spectra. Also the assignment of the bands and the discussion of the spectra have been made in this thesis. Moreover, the partially and totally deuterated species have been taken into account. The simulation of these spectra is a powerful tool for the detection of these species on the experimental conditions. What is more, the simulation of deuterated spectra give more information about the species that can be present on the surface.

Another kind of spectra have been simulated. NEXAFS spectra have demonstrated to be a powerful tool to study the adsorbates on surfaces.

- The study of reaction intermediates and transition states.

The study of transition states has permitted us to suggest some possible reaction pathways for the isomerisation reaction from Pr to VC.

Two possible pathways have been proposed for Cu, the direct isomerisation (whose barrier is very high) or the Horiuti-Polanyi process (the dhy-hy barriers are lower). Unfortunately the global study of the reaction is still at half-way and more efforts must be made to obtain a complete understanding.

7.3 Which questions are still opened?

As always, when a thesis is finished, exist more opened questions than the closed ones. In the last sections we have summarised and explained which questions have been closed. Now we want to make some questions that are still opened and that could be the starting point for other studies:

- In the case of OMM:
  - The adsorption of two charge donors (the smallest ones) have been made, but what happens with the other ones that are bigger (TMTTF, BEDT-TTF...?

UNIVERSITAT ROVIRA I VIRGILI
ORGANIC MOLECULES ON METAL SURFACES: FORECASTING STRUCTURES AND SPECTRA
Benjamí Martorell Masip
ISBN:978-84-691-9747-9 /DL: T-1259-2008

  - And the charge acceptors? One could study how TCNQ and other derivatives interact with surfaces.
  - The transfer charge salts require the cations and anions and we have studied them independently. What about the coadsorption of both?
  - And more other questions...

- In the case of the cyclation of propyne:
  - We have studied the adsorption of one intermediate for the (111) metal surface of four metals. So, what happens on the other surfaces? and on other metals?
  - Other possible reaction pathways could exist. The dehydrogenation of VC or Pr could exist, so one should study those other pathways.
  - Moreover, the $CHCCH_2$ has only been studied on Cu. What happens on the other metals?
  - The different reactivity of Pr on those metals has been yet not clarified, so other structures should be studied for the other metals.
  - And other questions that everyone can imagine...

UNIVERSITAT ROVIRA I VIRGILI
ORGANIC MOLECULES ON METAL SURFACES: FORECASTING STRUCTURES AND SPECTRA
Benjamí Martorell Masip
ISBN:978-84-691-9747-9 /DL: T-1259-2008

Apendix

In this final appendix we want to give some information about the calculation procediments used in VASP calculations. An accurate strategy of computation makes possible to save a lot of time in the geometry optimisation and in the transition states search.

In the VASP code, the parameters file is called INCAR. In the INCAR file we write the geometric and electronic convergence criterion, the DFT functional used, the geometric and electronic optimisation algorithm, the number of maximum geometric optimisation cycles, and if the calculation is closed or opened shell or the electronic state.

Another important file is the KPOINTS file, where the number of KPOINTS computed in the Brillouin zone are marked.

Geometry optimisation.

All geometries and energies presented in this thesis have been obtained using the following parameters in the INCAR file:

PREC=high This is the calculation precision of the system. This tag controls the cut-off of the plane-waves basis set and the integration zone. The cut-off is 500 eV if C atoms are presents in the calculations, otherwise the tag ENCUT=500 must be present in the INCAR file in order to compare results.

GGA=91 DFT functional used for calculation.

ALGO=fast Electronic optimisation algorithm.

EDIFF=1e-6 Electronic convergence parameter.

IBRION=2 Geometry optimisation algorithm (conjugated-gradients).

UNIVERSITAT ROVIRA I VIRGILI
ORGANIC MOLECULES ON METAL SURFACES: FORECASTING STRUCTURES AND SPECTRA
Benjamí Martorell Masip
ISBN:978-84-691-9747-9 /DL: T-1259-2008

EDIFFG=-0.02 Geometry convergence parameter (A negative value means that forces on the atoms must be lower than this value, a positive value means differences in energies).

NSW=99 Number of maximum optimisation cycles.

These are the parameters in the INCAR file for final results.

In the case of VC calculations on the 2×2 unit cell, this INCAR final is combined with a 7×7×1 k-points mesh.

But if one started the geometry optimisation with these parameters, the computation time would be huge. In order to optimise the calculation time, one can start with a 3×3×1 k-points mesh, with PREC=low, EDIFF=1e-4 and EDIFFG=1e-3, only optimising the adsorbate geometry, but not the surface. Once this calculation is finished, the surface and the adsorbate can be optimised with a 5×5×1 k-points mesh, with PREC=medium, EDIFF=1e-6 and EDIFFG=-0.02.

Finally, when this calculation has converged, the final parameters above commented can be used for a higher quality of the results.

Also the **ISPIN**-tag can be 1 or 2 for closed or open-shell calculations, respectively. Even more, **NELEC** and **NUPDOWN**-tags allow us to control the total number of electrons and the difference between alpha and beta electrons in the calculation.

Projected density of states.

On the optimised geometry, the projection of the density of states on the atomic orbitals of the system atoms can be carried out via the Wigner-Seitz radii procedure (**RWIGS**-tag must be added in INCAR file). The projection is made with a single-point calculation (**NSW**=0 and **IBRION**=2 or **IBRION**=-1). This single-point calculation can be carried out with the presence of the charge density obtained in the geometry optimisation (**ICHARG**=11). The number of bands projected can be increased to obtain a larger description of the conduction zone (for instance **NBANDS**=150). Finally, the range of the projected bands energy can be controlled by the **EMIN** and **EMAX**-tags.

UNIVERSITAT ROVIRA I VIRGILI
ORGANIC MOLECULES ON METAL SURFACES: FORECASTING STRUCTURES AND SPECTRA
Benjamí Martorell Masip
ISBN:978-84-691-9747-9 /DL: T-1259-2008

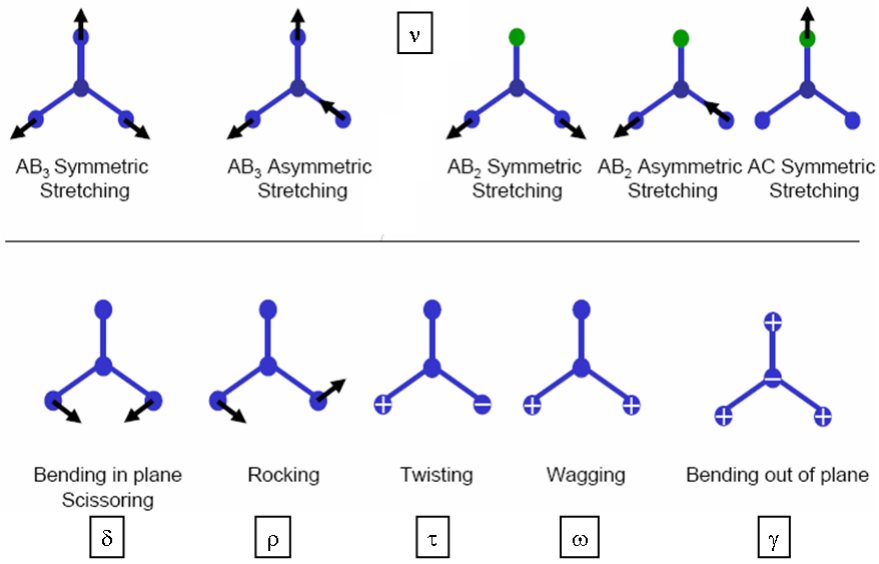

Figure 7.1: Vibrational modes nomenclature [72].

Vibrational calculation.

Once the geometry optimisation is finished, it is possible to make the vibrational calculation on this geometry, changing only a pair of parameters in the INCAR file. The **IBRION**-tag must be 5 for the evaluation of the numerical differences in the energy gradients with finite displacements (**POTIM**=0.02). Also the **IDIPOL**-tag must be present with a value of 3 in order to calculate the dipole moment on the normal direction respect to the surface. Finally, it is also interesting to take into account that the symmetry of calculation is broken when the small displacements of the atoms are made, so it is extremily recommended to break the symmetry in the calculation (**ISYM**=0).

For people not used to the vibrational modes nomenclature, in figure 7.1 are presented the vibrational modes. This makes easier to imagine how atoms moves in the VNM.

Transition states search.

VASP allows several strategies to search transition states (TS). We have used three of them:

UNIVERSITAT ROVIRA I VIRGILI
ORGANIC MOLECULES ON METAL SURFACES: FORECASTING STRUCTURES AND SPECTRA
Benjamí Martorell Masip
ISBN:978-84-691-9747-9 /DL: T-1259-2008

- A geometry optimisation using the quasi-newton algorithm (**IBRION**=1). This algorithm searches points on the potential surface, whose first derivatives are zero. So, we can find a transition state with this method if the starting geometry is near the transition state.

- The NEB (nudged-elastic band) method. In this method it is necessary to have obtained previously the two minima that are connected by the searched TS. In this method **n** intermediate images are generated from the two minima. In a root directory are created **n**+2 directories, labelled from 00 to **n**+1. In 00 and **n**+1 directories are placed the two minima geometries, and in the rest of directories the intermediate images. In the root directory are placed all auxiliary files (INCAR, KPOINTS, POTCAR and the job). In the INCAR, the algorithm used for the relaxation is the quasi-newton one (**IBRION**=**1**), and the **IMAGES**-tag must be present indicating the **n** number of intermediate images. As the work is divided in n processors (or a multiple of this number), the calculation is slow. In order to decrease the calculation time, it is interesting to start with low quality parameters in the INCAR file, as was made in the geometry optimisation, even erasing some layers of the surface. Once this calculation has finished, the quality of calculation parameters can be increased, and in the INCAR file we can add the climbing tag (**LCLIMB**=.TRUE.) to search the maximum of the surface.

- The DIMER method. In this method it is also necessary to have two minima, but it is not necessary they to be two consecutive minima connected by one TS. Even more, one can start a dimer calculation with only one minimum, but results are completely unpredictable. In a root directory are created to directories, where the geometry of this two minima are located. In the root directory are placed all auxiliary files (INCAR, KPOINTS, POTCAR and the job). In the INCAR file, the relaxation algorithm is the molecular dynamics one (**IBRION**=3), which combined with the tags **IMAGES**=2, **POTIM**=0.0 and **ICHAIN**=2 allows us to make the dimer calculation. In this case the number of processors is the half of the total ones for each image, so the calculation is quite fast.

The most efficient strategy we have found to find TSs is the combination of methods as follows. First of all the NEB method is used. Although being the most expensive method, if it converges, results in the first cycles are near the

UNIVERSITAT ROVIRA I VIRGILI
ORGANIC MOLECULES ON METAL SURFACES: FORECASTING STRUCTURES AND SPECTRA
Benjamí Martorell Masip
ISBN:978-84-691-9747-9 /DL: T-1259-2008

final TS geometry. At this point one can stop the NEB calculation and to start a quasi-newton geometry optimisation in order to make the calculation faster. Finally, when it is converged, one must calculate the frequencies to ensure it is a TS.

On the other hand, if NEB does not converge, it means that does not exist one TS between the two used minima. In order to find one TS (which we do not know *a priori* which minima will connect), we can make a dimer calculation. When dimer calculation converges, we can make a quasi-newton optimisation and a frequency calculation. When frequency calculation has finished, we can add the imaginary vibrational mode to the TS structure in order to find which minima connects this TS.

UNIVERSITAT ROVIRA I VIRGILI
ORGANIC MOLECULES ON METAL SURFACES: FORECASTING STRUCTURES AND SPECTRA
Benjamí Martorell Masip
ISBN:978-84-691-9747-9 /DL: T-1259-2008

Bibliography

[1] P.W. Atkins, *"Química Física"*, Ed. Omega, Barcelona (1999).

[2] M. Born, J.R. Oppenheimer, *Ann. Phys.,* 84 (1927) 457.

[3] W.J. Hehre, L. Radom, P.V.R. Schleyer, J.A. Pople, *"Ab initio Molecular Orbital Theory"*, Ed. John Wiley, New York (1986).

[4] J. Andres, J. Beltran, *"Química Teórica y Computacional"*, Ed. Universitat Jaume I, Castelló (2000).

[5] L.H. Thomas, *Proc. Camb. Phil. Soc.,* 23 (1927) 542; E. Fermi, *Rend. Accad. Lincei.* 6 (1927) 602.

[6] H. Hohenberg, W. Koh, *Phys. Rev.,* 136 (1964) B864.

[7] W. Kohn, L.J. Sham, *Phys. Rev.,* 140 (1965) A1133.

[8] S.H. Vosko, L. Wilk, M. Nusair, *Can. J. Phys.,* 58 (1980) 1200.

[9] A.D. Becke, *J. Chem. Phys.,* 84 (1986) 4524.

[10] A.D. Becke, *J. Chem. Phys.,* 98 (1993) 5648.

[11] http://cms.mpi.univie.ac.at/vasp/vasp/vasp.html[1].

[12] J. Sauer, *Chem. Rev.,* 89 (1989) 199.

[13] G. Sun, J. Kürti, P. Rajczy, M. Kertesz, J. Hafner, G. Kresse, *J. Molec. Struc. Theochem.,* 624 (2003) 37.

[14] C. Cohen-Tannoudji, B. Diu, F. Lalöe, *"Mechanique quantique"*, Hermann, Paris (1994).

[1] All webpages were checked on March, 25th 2008.

UNIVERSITAT ROVIRA I VIRGILI
ORGANIC MOLECULES ON METAL SURFACES: FORECASTING STRUCTURES AND SPECTRA
Benjamí Martorell Masip
ISBN:978-84-691-9747-9 /DL: T-1259-2008

[15] H.J. Monkhorst, J.D. Pack, *Phys. Rev. B,* 13 (1976) 5188.

[16] D.R. Hamann, M. Schluter, C. Chiang, *Phys. Rev. Lett.,* 43 (1979) 1494.

[17] D. Vanderbilt, *Phys. Rev. B,* 41 (1990) 7892.

[18] P.E. Blöchl, *Phys. Rev. B,* 50 (1994) 17953.

[19] G. Kresse, J. Hafner, *Phys. Rev B,* 47 (1993) 558.

[20] D.D. Johnson, *Phys. Rev. B,* 38 (1988) 12087.

[21] P. Pulay, *Chem. Phys. Lett.,* 73 (1980) 393.

[22] G. Kresse, J. Furthmüller, *Comp. Mat. Sci.,* 6 (1996) 15.

[23] M.E. Pemble, *"Vibrational Spectroscopy from Surfaces in Surface analysis-The principal Techniques".,* Ed. John Wiley and Sons Ltd. New York (1997) 267.

[24] J.E. Marsden, A.J. Tromba, *"Cálculo Vectorial*", Ed. Adison Wesley, Madrid (2004).

[25] J.W. McIver, A. Komornicki, *J. Am. Chem. Soc.,* 94 (1972) 2625.

[26] H. Johnson, G. Mills, K.W. Jacobsen, *"Nudged Elastic Band Method for finding Minimum Energy path of Transitions, Classical and Quantum Dynamics in Condensed Phase Simulations.",* World Scientific Ed. Singapore (1998) 385.

[27] G. Henkelman, H. Jónsson, *J. Chem. Phys.,* 111 (1999) 7010.

[28] R.G. Par, W. Yang, *"Density Funcitonal Theory of Atoms and Molecules*", Oxford University Press, New York (1989).

[29] W. Koch, M.C. Holthausen, *"A Chemist's Guide to Density Functional Theory*", Wiley-VCH, Weinheim, 2000.

[30] A.D. Becke, *J. Chem. Phys.,* 98 (1993) 1372.

[31] G. Kresse, D. Joubert, *Phys. Rev. B,* 59 (1999) 1758.

[32] W.H. Press, B.P. Flannery, S.A. Teukolsky, W.T. Vetterling, *"Numerical Recipes in C: the art of scientific computing."*, Cambridge University Press, New York, (1986).

UNIVERSITAT ROVIRA I VIRGILI
ORGANIC MOLECULES ON METAL SURFACES: FORECASTING STRUCTURES AND SPECTRA
Benjamí Martorell Masip
ISBN:978-84-691-9747-9 /DL: T-1259-2008

[33] K. Hermann, L.G.M. Pettersson, M.E. Casida, C. Daul, A. Goursot, A. Koester, E. Proynov, A. St-Amant, D.R. Salahub, V. Carravetta, H. Duarte, C. Friedrich, N. Godbout, J. Guan, C. Jamorski, M. Leboeuf, M. Leetmaa, M. Nydberg, L. Pedocchi, F. Sim, L. Triguero, A. Vela, *"StoBe Software"*, 2005.

[34] A.Gil, A. Clotet, J.M. Ricart, G. Kresse, M. Garcia-Hernández, N. Rösch, P. Sautet, *Surf. Scien.,* 530 (2003) 71.

[35] J. Stöhr, *"NEXAFS sprectroscopy"*, Springer Verlag, Berlin, 1992.

[36] F.J. Williams, R.L. Cropley, O.P.H. Vaughan, A.J. Urquhart, M.S. Tikhov, C. Kolczewski, K. Hermann, R.M. Lambert, *J. Am. Chem. Soc.,* 127 (2005) 17007.

[37] J.C. Slater, *Adv. Quant. Chem.*, 6 (1972) 1; J.C. Slater, K.H. Johnson, *Phys. Rev. B*, 5 (1972) 844.

[38] L. Triguero, L.G.M. Pettersson, H. Ågren, *J. Phys. Chem. A*, 102 (1998) 10599; L. Triguero, L.G.M. Pettersson, H. Ågren, *Phys. Rev. B*, 58 (1998) 8097.

[39] A. Nilsson, N. Martensson, *Physica B,* 208&209 (1995) 19.

[40] L. Triguero, L.G.M. Pettersson, H. Agren, *Phys. Rev. B,* 58 (1998) 8097.

[41] O. Takahashi, L.G.M. Pettersson, *J. Chem. Phys.,* 121 (2004) 10339.

[42] C. Adamo, R. Arnaud, G. Scalmani, H. Müller, F. Sahli, V. Barone, *J. Pys. Chem. B,* 103 (1999) 6863.

[43] R. Liu, X. Zhou, H. Kasmai, *Spec. Act. Part A,* 53 (1997) 1241.

[44] R. Pou-Amérigo, E. Ortí, M. Merchán, M. Rubio, P.M. Viruela, *J. Phys. Chem. A,* 106 (2002) 631.

[45] C. Katan, *J. Phys. Chem. A,* 103 (1999) 1407.

[46] E. Demiralp, S. Dasgupta, W.A. Goddard III, *J. Am. Chem. Soc.,* 117 (1995) 8154.

[47] E. Demiralp, W.A. Goddard III, *J. Phys. Chem. A,* 101 (1997) 8128.

UNIVERSITAT ROVIRA I VIRGILI
ORGANIC MOLECULES ON METAL SURFACES: FORECASTING STRUCTURES AND SPECTRA
Benjamí Martorell Masip
ISBN:978-84-691-9747-9 /DL: T-1259-2008

[48] J.J. Ritsko, A.J. Epstein, W.R. Salaneck, D.J. Sandman, *Phys. Rev. B,* 17 (1978) 1506.

[49] R. Bozio, I. Zanon, A. Girlando, C. Pecile, *J. Chem. Phys.,* 71 (1979) 2282.

[50] A. Girlando, F. Marzola, C. Pecile, J.B. Torrance, *J. Chem. Phys.,* 79 (1983) 1075.

[51] O.R. Inderwildi, S.J. Jenkins, D.A. King, *J. Am. Chem. Soc.*, on press.

[52] Y. Yu, St. J. Dixon-Warren, N. Astle, *Chem. Phys. Let.,* 312 (1999) 455.

[53] B. Frühberger, M. Grunze, D.J. Dwyer, *J. Phys. Chem.,* 98 (1994) 609.

[54] D.M. Jaffey, R.J. Madix, *Surf. Scie.,* 258 (1991) 359.

[55] K.T. Leung, X.S. Zhang, D.A. Shirley, *J. Phys. Chem.,* 93 (1989) 6164.

[56] J-G. Lee, J. Lee, J.T. Yates Jr., *J. Phys. Chem. B,* 108 (2004) 1686.

[57] V.T. Joy, T.K.K. Srinivasan, *Chem. Phys. Let.,* 328 (2000) 221.

[58] A. Valcàrcel, A. Clotet, J.M. Ricart, F. Delbecq, P. Sautet, *Surf. Scie.,* 549 (2004) 121.

[59] F. Ample, A. Clotet, J.M. Ricart, *Surf. Sci.,* 558 (2004) 111.

[60] A. Valcarcel, A. Clotet, J.M. Ricart, F. Illas, *Chem. Phys.* 309 (2005) 33.

[61] http://www.webelements.com/webelements/elements/text/Ag/xtal.html.

[62] B. Soulé de Bas, M.J. Ford, M.B. Cortie, *J. Mol. Struct (Teochem),* 686 (2004) 193.

[63] F.A. Cotton, *"La teoría de grupos aplicada a la química"*, Ed. Limusa, México (1983).

[64] C.G. Bernardo, J.A. Gomes, *J. Mol. Struct (Theochem),* 582 (2002) 159.

[65] R.M. Lambert, F.J. Williams, R.L. Cropley, A. Palermo, *J. Mol. Cat. A,* 228 (2005) 27.

[66] D.L.S. Nieskens, A.P. Van Bavel, D. Curulla Ferré, J.W. Niemantsverdriet, *J. Phys. Chem. B,* 108 (2004) 14541.

UNIVERSITAT ROVIRA I VIRGILI
ORGANIC MOLECULES ON METAL SURFACES: FORECASTING STRUCTURES AND SPECTRA
Benjamí Martorell Masip
ISBN:978-84-691-9747-9 /DL: T-1259-2008

[67] T.G. Rucker, M.A. Logan, T.M. Gentle, E.L. Muetterties, G.A. Somorjai, *J. Phys. Chem.,* 90 (1986) 2703.

[68] J.A. Rodríguez, S. Chaturvedi, T. Jirsak, J.Hrbek, *J. Chem. Phys.,* 109 (1998) 4052.

[69] K. Mudiyanselage, M. Trenary, R.J. Meyer, *J. Phys. Chem. C*, 111 (2007) 7127.

[70] R.P. Deng, M. Trenary, *J. Phys. Chem. C*, 111 (2007) 17088.

[71] M. Kuhn, J.A. Rodriguez, *J. Cat.*, 154 (1995) 355.

[72] http://www.quimica.urv.es/~w3qf/DOCENCIA/DEM/DMATDOC/em4_07.pdf

[73] J.A. Rodriguez, M.Kuhn, J. Hrbek, *J. Phys. Chem.,* 10 (1996) 15494.

[74] Y. Yu, St. J. DixonWarren, N. Astle, *Chem. Phys. Let.,* 312 (1999) 455.

[75] http://riodb01.ibase.aist.go.jp/sdbs/cgi-bin/direct_frame_top.cgi.

[76] N. Honjou, J. Pacansky, M.Yoshimine, *J. Am. Chem. Soc.,* 107 (1985) 5332.

[77] D. Feller, W.T. Borden, E.R. Davidson, *J. Phys. Chem.,* 87 (1983) 4833.

[78] J.H. Davis, W.A. Goddard III, R.G. Bergman, *J. Am. Chem. Soc.,* 99 (1977) 2427.

[79] T.N. Le, H. Lee, A.M. Mebel, R.I. Kaiser, *J. Phys. Chem.* A, 105 (2001) 1847.

[80] N. Honjou, J. Pacansky, M. Yoshimine, *J. Am. Chem. Soc.,* 106 (1984) 5361.

[81] N. Honjou, J. Pacansky, M. Yoshimine, *J. Am. Chem. Soc.,* 111 (1989) 4198.

[82] R. Kakkar, R. Garg, P. Chadha, *J. Mol. Struct (Theochem),* 617 (2002) 141.

[83] R. Kakkar, *Int. J. Quant. Chem.,* 94 (2003) 93.

[84] J.A. Miller, S.J. Klippenstein, *J. Phys. Chem. A,* 107 (2003) 2680.

UNIVERSITAT ROVIRA I VIRGILI
ORGANIC MOLECULES ON METAL SURFACES: FORECASTING STRUCTURES AND SPECTRA
Benjamí Martorell Masip
ISBN:978-84-691-9747-9 /DL: T-1259-2008

[85] G. Maier, C. Lautz, S. Senger, *Chem. Eur. J.,* 6 (2000) 1467.

[86] J.H. Wang, C.M. Chiang, *J. Am. Chem. Soc.* 122 (2000) 11521.

[87] F. Zaera, *J. Phys. Chem. B,* 106 (2002) 4043.

[88] Z. Ma, F. Zaera, *Surf. Scien. Rep.,* 61 (2006) 229.

[89] J. Horiuti, M. Polanyi, *J. Mol. Catal. A-Chem.,* 199 (2003) 185.

[90] A. Clotet, J.M. Ricart, F. Illas, G. Pacchioni, R.M. Lambert, *J. Am. Chem. Soc.,* 122 (2000) 7573.

[91] C.M. Fehrenbach, H. Bross, *Phys. Rev. B,* 48 (1993) 17703.

[92] S. Bao, K.M. Schindler, Ph. Hofmann, V. Fritzsche, A.M. Bradshaw, D.P. Woodruff, *Surf. Sci.,* 291 (1993) 295.

[93] N. Sheppard, *Ann. Rev. Phys. Chem.,* 39 (1988) 589.

[94] A. Valcàrcel, J.M. Ricart, A. Clotet, A. Markovits, C. Minot, F. Illas, *Surf. Sci.,* 519 (2002) 250.

[95] A. Valcàrcel, J.M. Ricart, A. Clotet, F. Illas, A. Markovits, C. Minot, *J. Cat.,* 241 (2006) 115.

[96] A. Valcàrcel, J.M. Ricart, A. Clotet, F. Illas, *J. Phys. Chem., B,* 108 (2004) 1827.

[97] A. Valcàrcel, A. Clotet, F. Illas, J.M. Ricart, *Phys. Chem. Chem. Phys.,* 9 (2007) 311.

[98] A. Valcàrcel, G. Novell-Leruth, A. Clotet, J. Pérez-Ramírez, J.M. Ricart, "*Spectroscopy and reactivity of molecules on metal surfaces from DFT calcuations*", (2007).

[99] T.M. Gentle, E.L. Muetterties, *J. Phys. Chem.,* 87 (1983) 2469.

[100] J.W. Peck, D.I. Mahon, B.E. Koel, *Surf. Sci.*, 410 (1998) 200.

[101] R.L. Middleton, R.M. Lambert, *Cat. Let.,* 59 (1999) 15.

[102] J.R. Lomas, C.J. Baddeley, M.S. Tikhov, R.M. Lambert, *Langmuir,* 11 (1995) 3048.

UNIVERSITAT ROVIRA I VIRGILI
ORGANIC MOLECULES ON METAL SURFACES: FORECASTING STRUCTURES AND SPECTRA
Benjamí Martorell Masip
ISBN:978-84-691-9747-9 /DL: T-1259-2008

[103] C.H. Patterson, R.M. Lambert, *J. Phys. Chem.,* 92 (1988) 1266.

[104] R.J. Koestner, J.C. Frost, P.C. Stair, M.A. van Hove, G.A. Somorjai, *Surf. Sci.,* 116 (1982) 85.

[105] B.E. Bent, C.M. Mate, J.E. Crowell, B.E. Koel, G.A. Somorjai, *J. Phys. Chem.,* 91 (1987) 1493.

[106] A. Valcàrcel, J.M. Ricart, A. Clotet, A. Markovits, C. Minot, F. Illas, *J. Chem. Phys.,* 116 (2002) 1165.

[107] A. Valcàrcel Ortí, Ph.D. Thesis: "*Modelling unsaturated hydrocarbons on metals: towards understanding catalytic processes*" (2005) Dpt. Química Física i Inorgànica. Universitat Rovira i Virgili. Tarragona. Spain.

[108] R. L. Toomes, R. Lindsay, P. Baumgärtel, R. Terborg, J.-T. Hoeft, A. Koebbel, O. Schaff, M. Polcik, J. Robinson, D. P. Woodruff, A. M. Bradshaw, R. M. Lambert, *J. Chem. Phys.,* 112 (2000) 7591.

[109] P. Sandl, U. Bischler, E. Bertel, *Surf. Scien.,* 291 (1993) 29.

[110] K. Gundersen, B. Hammer, K.W. Jacobsen, J.K. Norskov, J.S. Lin, V. Milman, *Surf. Scien.,* 285 (1993) 27.

[111] A. Forni, G. Wiesenekker, E.J. Baerends, G.F. Tantardini, *Int. J. Quant. Chem.,* 42 (1994) 1167.

[112] C.L.A. Lamont, B.N.J. Persson, G.P. Williams, *Chem. Phys. Let.,* 243 (1995) 429.

[113] W. Dong, G. Kresse, J. Furthmüller, J. Hafner, *Phys. Rev. B*, 54 (1996) 2157.

[114] H. Yang, J.L Whitten, *J. Chem. Phys.,* 89 (1988) 5329.

[115] H. Lüth, *"Solid surfaces, interfaces and thin films"*, Springer Verlag, Berlin (2001).

[116] C. Kolczewski, F.J. Williams, R.L. Cropley, O.P.H. Vaughan, A. J. Urquhart, M.S. Tikhov, R.M. Lambert, K. Hermann, *J. Chem. Phys.,* 125 (2006) 34701.

[117] http://www.fhi-berlin.mpg.de/th/cms/index.php?option=com_wrapper&Itemid=176.

UNIVERSITAT ROVIRA I VIRGILI
ORGANIC MOLECULES ON METAL SURFACES: FORECASTING STRUCTURES AND SPECTRA
Benjamí Martorell Masip
ISBN:978-84-691-9747-9 /DL: T-1259-2008

[118] N. Honjou, J. Pacansky, M. Yoshimine, *J. Am. Chem. Soc.,* 111 (1989) 2785.

[119] R. Püttner, C. Kolczewski, M. Martins, A.S. Schlachter, G. Snell, M. Sant'Anna, J. Viefhaus, K.Hermann, G. Kaindl, *Chem. Phys. Let.,* 393 (2004) 361.

[120] C. Kolczewski, R. Püttner, M. Martins, A.S. Schlachter, G. Snell, M.M. Sant'Anna, K.Hermann, G. Kaindl, *J. Chem. Phys.,* 124 (2006) 34302.

[121] A. Clotet, *IRIAN program*, Universitat Rovira i Virgili, 2003. (http://www.quimica.urv.cat/~w3qf/soft.html).

[122] J. Almlöf, R. Ahlrichs, *"Notes on Hartree-Fock theory and related topics in European Summer School in quantum Chemistry 2003"*, book I. B.O. Roos, P.-O. Widmark Eds., Lund University, Lund (2003) 169; B.O. Roos *"Multiconfigurational (MC) Self-Consistent (SCF) Theory in European Summer School in quantum Chemisry 2003"*, book II. B.O. Roos, P.-O. Widmark Eds., Lund University, Lund (2003) 285; P.R. Taylor, *"Coupled-Cluster Methods in quantum Chemistry in quantum Chemisry 2003"*, book II. B.O. Roos, P.-O. Widmark Eds., Lund University, Lund (2003) 361; N.C. Handy, *"Density functional theory in quantum Chemistry in quantum Chemisry 2003"*, book II. B.O. Roos, P.-O. Widmark Eds., Lund University, Lund (2003) 503.

[123] J.P. Perdew, *Phys. Rev. B,* 33 (1986) 8822.

[124] J.P. Perdew, Y. Wang, *Phys. Rev. B,* 33 (1986) 8800.

[125] C. Lee, W. Yang, R.G. Parr, *Phys. Rev. B,* 37 (1988) 785.

[126] J.P. Perdew, K. Burke, M. Ernzerhof, *Phys. Rev. Lett.,* 77 (1996) 3865.

[127] J.P. Perdew, *Phys. Rev. B,* 34 (1986) 7406.

[128] N.W. Ashcroft, N.O. Mermin, *"Solid State Physics"*, W.B. Saunders Company, New York (1976).

[129] G.B. Bachelet, D.R. Hamann, M. Schluter, *Phys. Rev. B,* 26 (1982) 4199.

[130] G. Kresse, J. Hafner, *Phys. Rev. B,* 48 (1993) 13115.

[131] G. Kresse, J. Hafner *Phys. Rev. B,* 49 (1994) 14251.

UNIVERSITAT ROVIRA I VIRGILI
ORGANIC MOLECULES ON METAL SURFACES: FORECASTING STRUCTURES AND SPECTRA
Benjamí Martorell Masip
ISBN:978-84-691-9747-9 /DL: T-1259-2008

[132] G. Kresse, J. Furthmüller, *Phys. Rev. B,* 54 (1996) 11169.

[133] E.M. McCash, *"Surface Chemistry*", Oxford University Press, Oxford (2001).

[134] G. Coudurier, F. Lefebvre, *"Infrared Spectroscopy in Catalyst Characterisation. Physcial Techniques for Solid Materials*", Ed. Plenum Press, New York (1994) 11.

[135] K.W. Kolasinski, *S"urface Science, Foundations of Catalysis and Nanoscience*", John Wiley and Sons Ltd, West Sussex (2002).

[136] A.D. Becke, *Phys. Rev. A,* 38 (1988) 3098.

[137] F. Ample, A. Clotet, J.M. Ricart, *Surf. Scien.,* 558 (2004) 111.

[138] A. Nilsson, L.G.M. Pettersson, *Surf. Sci. Reports,* 55 (2004) 49.

[139] U. von Barth, G. Grossmann, *Phys. Rev. B,* 25 (1982) 5150.

[140] V.I. Grebennikov, Y.A. Babanov, O.B. Sokolov, *Phys. Stat. Sol.,* 79 (1977) 423.

[141] C. Kolczewski, R. Püttner, O. Plashkevych, H. Agren, V. Staemmler, M. Martins, G. Snell, A.S. Schlachter, M. Sant'Anna, G. Kaindl, L.G.M. Pettersson, *J. Chem. Phys.,* 115 (2001) 6426.

[142] Y. Negishi, Y. Takasugi, S. Sato, H. Yao, K. Kimura, T. Tsukuda, *J. Am. Chem. Soc.,* 126 (2004) 6518.

[143] I.A. Solov'yov, A.V. Solov'yov, W. Greiner, *Phys. Rev. Let.,* 90 (2003) 53401.

[144] R. Jin, S. Egusa, N.F. Scherer, *J. Am. Chem. Soc.,* 126 (200) 9900.

[145] J. Dai, Z.H. Zhang, *J Chem. Phys.,* 102 (1995) 6280.

[146] D. Farrely, R.D. Levine, *J. Chem. Phys.,* 97 (1992) 2139.

[147] K. Klier, *Top. Cat.,* 18 (2002) 141.

[148] http://webbook.nist.gov/cgi/cbook.cgi?ID=C463490&Units=SI&Mask=800#Electronic-Spec.

UNIVERSITAT ROVIRA I VIRGILI
ORGANIC MOLECULES ON METAL SURFACES: FORECASTING STRUCTURES AND SPECTRA
Benjamí Martorell Masip
ISBN:978-84-691-9747-9 /DL: T-1259-2008

[149] J. W. Niemantsverdriet, "*Spectroscopy in Catalysis: An introduction*". Wiley-VCH Verlag (2000) Winheim, Germany.

[150] http://www.webelements.com/webelements/elements/text/Au/xtal.html.

[151] http://www.webelements.com/webelements/elements/text/Cu/xtal.html.

[152] http://www.webelements.com/webelements/elements/text/Pt/xtal.html.

[153] http://www.webelements.com/webelements/elements/text/Pd/xtal.html.

[154] http://www.webelements.com/webelements/elements/text/Ag/xtal.html.

[155] http://www.webelements.com/webelements/elements/text/Rg/key.html.

[156] L.B. Coleman, M.J. Cohen, D.J. Sandman, F.F. Yamagishi, A.F. Garito, A.J. Heeger, *Sol. state com.*, 12 (1973) 1125.

[157] S. Molas Busquets, Ph.D. Thesis: "*Preparació i caracterització de capes fines de materials orgànics derivats del tetratiafulvalè"* Universitat de Barcelona. Barcelona. Spain.

[158] D. Jerome, A. Mazaud, M. Ribault, K. Bechgaard, *J. Phys. Chem.,* 41 (1980) L95.

[159] J.R. Ferraro, J.M. Williams, *"Introduction to synthetic electrical conductors*", Academic Press, (1987) Orlando.

[160] S.R. Forrest, P.E. Burrows, E.I. Haskal, Y. Zhang, *Mat. Res.*, 328 (1994) 37.

[161] W. Xu, G.R. Chen, R.J. Li, Z.Y. Hua, *Appl. Phys. Let.*, 67 (1995) 2241.

[162] Z.Y. Hua, G.R. Chen, W. Xu, D.Y. Chen, *Appl. Surf. Sci.*, 169-170 (2001) 447.

[163] Y. Itoh, S. Yoshiura, *J. Electrochem. Soc.*, 124 (1979) 1128.

[164] C.D. Dimitraskopoulos, P.R.I. Malenfant, *Adv. Mat.*, 14 (2002) 99.

[165] J.H. Schön, C. Kloc, B. Batlogg, *Org. Elect.*, 1 (2000) 57.

[166] G. Kyriakou, J. Kim, M.S. Tikhov, N. Maecleod, R.M. Lambert, *J. Phys. Chem. B*, 109 (2005) 10952.

UNIVERSITAT ROVIRA I VIRGILI
ORGANIC MOLECULES ON METAL SURFACES: FORECASTING STRUCTURES AND SPECTRA
Benjamí Martorell Masip
ISBN:978-84-691-9747-9 /DL: T-1259-2008

[167] J. Storm, R.M. Lambert, N. Memmel, J. Onsgaard, E. Taglauer, *Surf. Sci.*, 436 (1999) 259.

[168] http://www.rpi.edu/dept/phys/ScIT/InformationTransfer/waves/waves.html.

[169] T.H. Dunning, *J. Chem. Phys.,* 55 (1971) 716.

[170] W. Kutzelnigg, U. Fleischer, M. Schindler, "*NMR-Basic principles and progress*", Springer Verlag, Heidelberg, Germany (1990).

[171] H. Ågren, V. Carravetta, O. Vahtras, L.G.M. Pettersson, *Theor. Chem. Acc.*, 97 (1997) 14.

[172] N. Godbout, D.R. Salahub, J. Andzelm, E. Wimmer, *Can. J. Chem.*, 70 (1992) 560.

[173] A. Mattsson, I. Panas, P. Siegbahn, U. Wahlgren, H. Akeby, *Phys. Rev. B*, 36 (1987) 7689.

UNIVERSITAT ROVIRA I VIRGILI
ORGANIC MOLECULES ON METAL SURFACES: FORECASTING STRUCTURES AND SPECTRA
Benjamí Martorell Masip
ISBN:978-84-691-9747-9 /DL: T-1259-2008

REFLEXIÓ FINAL.

"Només hi ha dues coses infinites: l'univers i l'estupidesa humana.
I de la primera no n'estic del tot segur".

Albert Einstein